Provenance of the Upper Jurassic Norphlet and Surrounding Formations from U-Pb Detrital Zircon Geochronology

Andrea Frances Lisi

Thesis submitted to the
Department of Geology and Geography
at West Virginia University
in partial fulfillment of the requirements
for the degree of

Master of Science
in
Geology

Amy Weislogel, Ph.D., Chair
Tim Carr, Ph.D.
Jaime Toro, Ph.D.

Department of Geology and Geography

Morgantown, West Virginia
2013

Keywords: Norphlet Formation; Haynesville Formation; Eastern Gulf of Mexico; U-Pb detrital zircon geochronology; Suwannee Terrane

Abstract

Provenance of the Upper Jurassic Norphlet and Surrounding Formations from U-Pb Detrital Zircon Geochronology

Andrea Frances Lisi

U-Pb detrital zircon geochronology supplemented by thin-section petrography, dense mineral analysis of samples, and well log analysis from onshore Florida (western panhandle and western peninsula) as well as from the offshore federal lease blocks, Mobile Bay, Pensacola, Destin Dome, St. Petersburg, and Florida Middle Ground are used to constrain the provenance of the Upper Jurassic Norphlet and surrounding formations. Using LA-ICPMS, 867 U-Pb ages from 10 samples, core and cuttings, were determined. Results show an influence of both Laurentian and Gondwanan (Suwannee Terrane) derived sediments. Four major U-Pb age populations exist in the samples which include 250-500 Ma, 500-700 Ma, 900-1400 Ma, and 1950-2250 Ma. These age populations are coeval with several known tectonic events in the source terranes: Laurentian Appalachian mountain building (Alleghanian, 280-325 Ma, Acadian, 384-425 Ma, Taconic, 430-480 Ma) and Grenville orogenies (900-1300 Ma) and the Gondwanan, Pan-African (500-680 Ma) and Trans-Amazonian/Eburnean (1900-2250 Ma) events.

To understand sediment distribution in the study area, four geochronologic source areas, based on suites of U-Pb age distributions, were identified: Appalachian hinterland, Appalachian foreland basin, Mesozoic rift basin, and the Suwannee Terranne. Only the Mobile Bay sample showed an almost entirely Laurentian suite of U-Pb ages. The three samples from the Florida Panhandle showed some mixing of Laurentian and Gondwanan sediments. While the U-Pb age distribution of the Florida Panhandle samples showed a more abundant Laurentian population (250-500 Ma and 900-1300 Ma), a Gondwanan population is also present (500-700 Ma and 1900-2250 Ma). The two samples within the Apalachicola Embayment (i.e., Destin Dome and Pensacola federal lease blocks) have a stronger Gondwanan influence but the Laurentian-aged zircon are still present. The samples from southeastern Gulf of Mexico are past the updip limit of the Norphlet Formation and consist of Paleozoic Basement, the Haynesville Formation, and the Cotton Valley Group. Their U-Pb age distribution shows an entirely Gondwanan source with most ages between 500-700 Ma (Pan-African).

The U-Pb detrital zircon data along with thin-section petrography and dense mineral analysis support previous paleogeographic models that consist of a proximal paleo-high source in which alluvial and wadi facies carry sediment into the eolian system. Point-counting of five samples showed the Norphlet to increase in compositional maturity away from the paleo-high source areas. The Norphlet consists of subarkose in the Florida Panhandle with an average modal abundance of $Q_{64}F_{33}L_3$ and arkose in the Apalachicola Embayment with an average modal abundance of $Q_{79}F_{15}L_6$. Dense mineral analysis showed that detrital samples closer to the paleo-high source area have more of the less resistant phyllosilicate material (Florida Panhandle and Mobile Bay) than those more distal (Apalachicola Embayment).

The provenance data also supports the hypothesis of two major fluvial and eolian sediment transport pathways, one to the south in southwestern Alabama and Mobile Bay and

another to the west in the Apalachicola Embayment. Where these two converging winds meet, deposition of eolian sands occurred in thick deposits along the eastern Mobile Bay and western Destin Dome and Pensacola offshore lease blocks. This sediment distribution pattern is supported through log analysis. These results suggest that major Norphlet discoveries in the deep offshore eastern Gulf of Mexico such as Appomattox, Shiloh, and Vicksburg are predominantly Suwannee-sourced sediments forming along the trend of thick eolian reservoir sandstone.

Acknowledgements

I would like to thanks Murphy Oil Corporation for their generous support for whom this project could not have been possible without. I would also like to thank the Oklahoma Geological Survey and Florida Geological Survey for their help with the tedious nature of tracking down and collecting samples. Special thanks to my advisor, Dr. Amy Weislogel, who gave me endless guidance on the project as well as my committee members Drs. Tim Carr and Jaime Toro.

A large amount of assistance was received from within the WVU Geology and Geography Department from several peers who helped with sample preparation, collection, and analysis for which I am ever so grateful; Marcus Jessee, Matt McKay, Fei Shang, Asa Mullenex, Evan Knight, and Katie Flowers. A special thanks to Evan Knight for his work on detrital zircon grain size distribution.

I would also like to thank the folks at the University of Alabama including Dr. Delores Robinson, Thomas Lovell, Lance Wilson, and Bryan Hunt. Their work was paramount to my own. Lastly, I would like to thank my family for their support, especially my husband for all the encouragement and long drives.

Contents

List of Figures

List of Tables

1. Introduction

Currently, the Norphlet Formation is a very important reservoir in the eastern Gulf of Mexico (EGOM) in areas including the Florida Panhandle, southern Alabama, and central Mississippi as well as the offshore federal lease blocks Mobile Bay (MO), Destin Dome (DD), Mississippi Canyon (MC), and De Soto Canyon (DC; Fig. 1). The Jurassic Norphlet Formation first became a major drilling target in the onshore EGOM in 1968 when condensates were discovered in the Flomaton Field in Escambia County, Alabama. In 1979, gas was discovered in offshore Norphlet Formation reservoirs showing an increased potential of the reservoir with technological advances in offshore drilling and better understanding of the depositional environment (Mancini et al., 1985). Shell recently discovered 215 million BOE in the Mississippi Canyon offshore lease block in 7,257 ft (2,212 m) of water (Oil & Gas Journal, 2012).

Other Jurassic formations have also proven to be important EGOM reservoirs including the Smackover and Haynesville formations. The Smackover Formation, an organic-rich carbonate unit conformably overlying the Norphlet Formation, likely sourced hydrocarbons both to itself and the Norphlet below (Claypool and Mancinl, 1989). The Haynesville Formation, which overlies the Smackover Formation, has an organic-rich shale unit that is thought to have sourced some of its overlying sandstone units and is a potential reservoir in areas of proper facies (DOI, 2008).

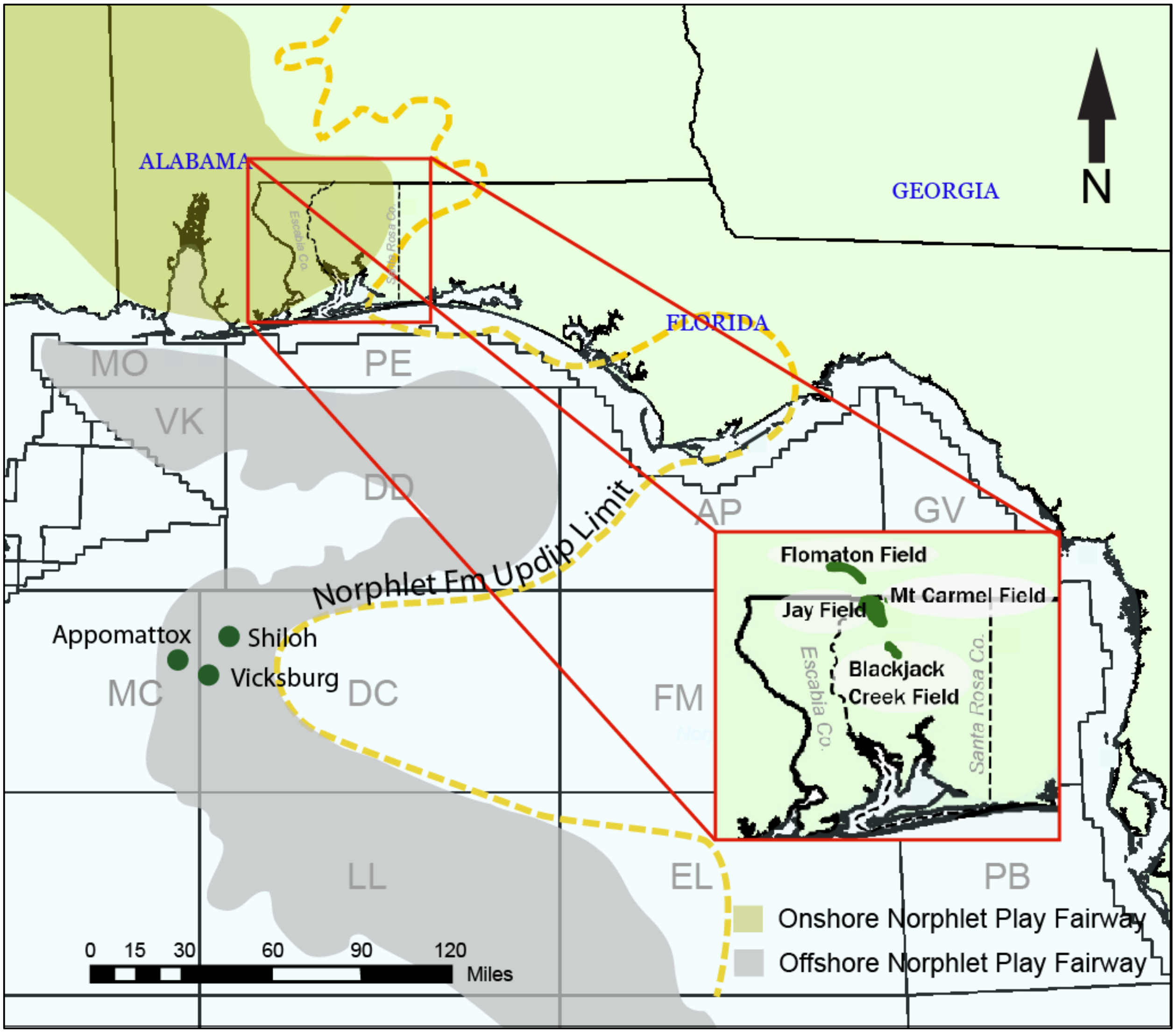

Figure 1. Major Norphlet producing fields in the Florida Panhandle highlighted in Green (Lloyd, 1991) including the Flomaton Field, just north of Florida, the first major Norphlet drilling target (Mancini et al., 1985). Gray area is the offshore Norphlet play fairway (BOEM, 2012a). Yellow region is the onshore Norphlet play fairway (Tew et al., 1991). Approximate location of the Shiloh, Vicksburg, and Appomattox prospects in the Mississippi Canyon and De Soto Canyon lease blocks marked by green circles. The Appomattox prospect contains at least 215 million BOE (Oil & Gas Journal, 2012).

The Norphlet and Smackover formations have been heavily produced in Alabama and the Florida Panhandle. These formations in the Santa Rosa County of the Florida Panhandle currently produce from three fields: the Jay, Mt. Carmel, and Blackjack Creek fields. The Jay field is a major producing field in Florida, accounting for 83% of gas production and 60% of oil produced in Florida in 2008 (Fig. 1; DOI, 2008). The Norphlet also produces in the deep offshore

Gulf of Mexico. As of 2001, all producing offshore wells deeper than 15,000 feet (4,572 m) were estimated to have 10 Tcf of recoverable gas, 2.5 Tcf of which is from the Norphlet Formation (MMS, 2001). The recent Shell discovery of 215 million BOE includes 150 ft (45.7 m) of oil pay in the Appomattox fault block structure in the Mississippi Canyon and De Soto Canyon lease blocks (Fig. 1; Oil & Gas Journal, 2012).

1.2 Research Problem and Significance

Drilling of the Norphlet Formation in the central Gulf of Mexico began in 1979 and has continued and expanded in the Mobile Bay, DeSoto Canyon, and Mississippi Canyon offshore lease blocks. However, the EGOM is relatively unexplored and currently under a drilling moratorium. The GOM Energy Security Act (2006) leasing and drilling moratorium covers most of the EGOM. While the Obama administration has allowed for drilling in the EGOM in the 2010-2015 leasing plan, it is still under the Energy Security Act moratorium until 2022 unless Congress decides to open the area. The Norphlet Formation within offshore Florida and the EGOM is a prospective target for future exploration upon expiration of the moratorium. A primary concern for exploration in this region is sparse well data, making reservoir distribution and quality difficult to predict. An improved paleogeographic model is needed to help understand reservoir distribution in this relatively unexplored area.

Previous paleogeographic models of the Norphlet deposystem in southwestern Alabama identified a northern Appalachian and Talladega slate belt source area (Fig. 2; Mancini et al., 1985; Walls, 1985). However, recent work has shown that the Gondwanan Suwannee terrane, which makes up the northern Florida basement, also sourced sand to the Norphlet Formation in southeastern Alabama and federal lease blocks offshore of the Florida Panhandle (Fig. 3; Lovell and Weislogel, 2010; Lovell, 2013) suggesting a more complex paleogeography and depositional pattern. Sediment lithology being a function of the source material from which it is derived and can vary significantly across source areas. Scott (1991) noted the difference between the Norphlet Formation framework grain abundances in the Florida Panhandle and those identified by Mancini et al. (1985) in southwestern Alabama (Figs. 4 and 9). The Norphlet Formation in southwestern Alabama is more compositionally mature, a difference that could be due to varying source lithology as well as distance from the source. These differences in provenance could also control reservoir quality. In order to create an improved paleogeographic model for the EGOM, the origin of the Norphlet and surrounding sediments and dispersal patterns require additional constraints.

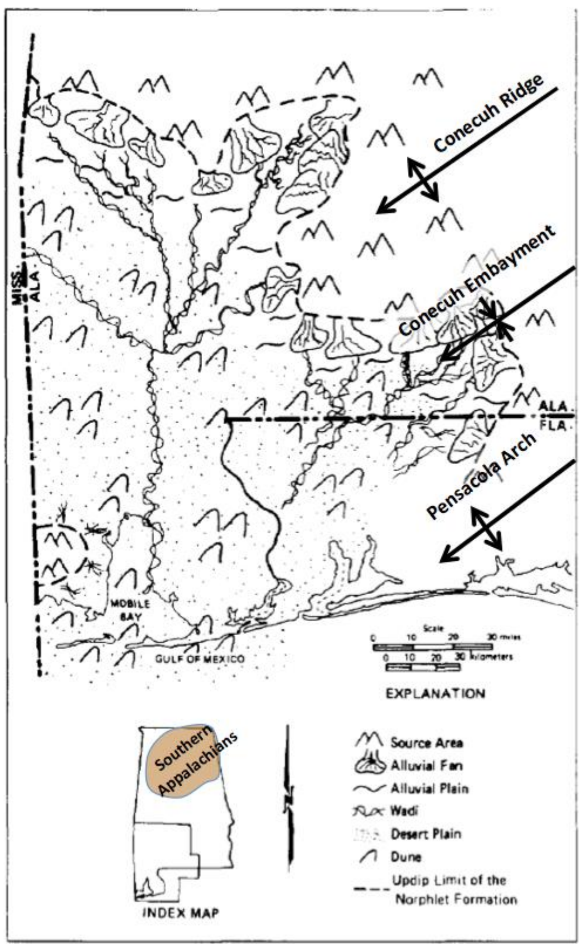

Figure 2. Paleogeographic model of the Norphlet Formation in southwest Alabama and the western Florida Panhandle (Modified from Mancini et al., 1985).

This study tests and expands upon previous paleogeographic models to aid in future exploration of the Norphlet Formation in the EGOM. Provenance scenarios determined from the U-Pb detrital zircon geochronology will help constrain sediment dispersal pathways and ultimately reservoir distribution, reservoir facies and reservoir quality in the EGOM. Knowing the source of sediments can help identify structural barriers and pathways for sediment dispersal that existed during the Late Jurassic.

1.3 Goals and Research

This study focuses on the Norphlet and surrounding formations in the EGOM including the Florida Panhandle, offshore Florida Peninsula, and offshore federal lease blocks Mobile Bay, Pensacola, Destin Dome, Florida Middle Ground, and St. Petersburg (Fig. 3). In order to create an improved paleogeographic model for the EGOM, the origin of the Norphlet and surrounding sediments will be constrained using U-Pb detrital zircon geochronology. U-Pb detrital zircon geochronology is an excellent tool commonly used for determining provenance due to the robust nature of zircon. They are very resistant to weathering, both mechanically and chemically which allows for likely retention of all zircon populations within a sediment package. They also usually have high U and Th concentrations

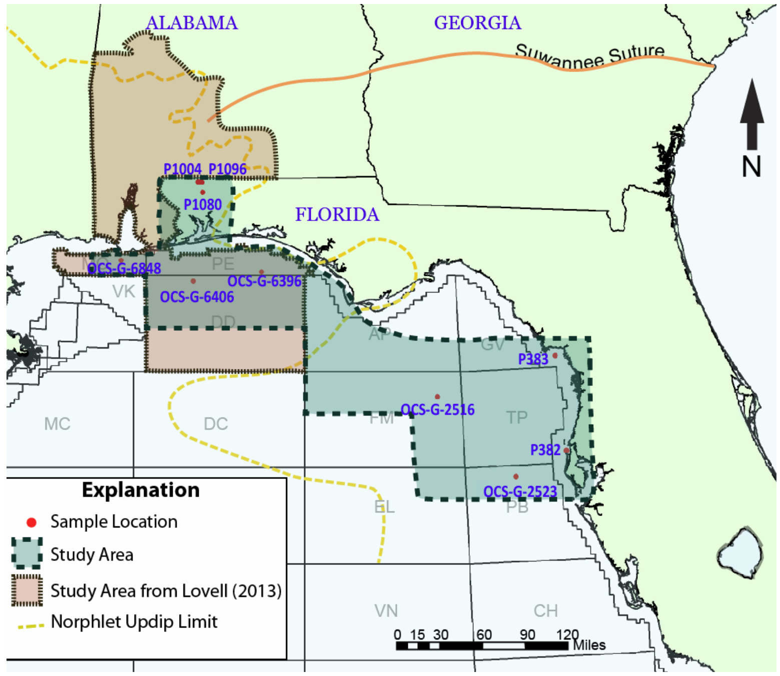

Figure 3. Study area highlighted in green. Lovell (2013) study area highlighted in brown.

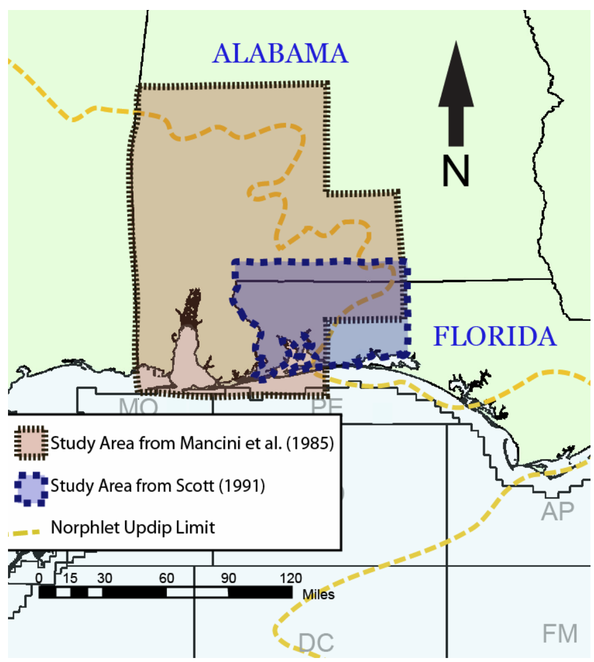

Figure 4. Study area of Norphlet Formation from Mancini et al. (1985) and Scott (1991).

(10-100 ppm) with low common lead, are commonly found in felsic and intermediate rocks, and can retain lead up to the zircon's melting point at ~1300°C therefore recording crystallization age (Fedo et al., 2003; Hoskin and Schaltegger, 2003).

Provenance, determined from U-Pb detrital zircon ages, is supplemented by thin-section petrography and dense mineral analysis. Thin-section petrography is another useful tool for determining provenance. Dickinson and Suczek (1979) have shown that the relationship between sandstone composition and plate tectonics can be used to assess the origin and potential source terranes of a sandstone through the quantitative evaluation of framework modal abundances. Along with a qualitative assessment of dense mineral abundances, U-Pb detrital zircon geochronology and thin-section petrology will provide a robust method for constraining the source terranes for the Norphlet and surrounding formations. The provenance work as well as large-scale distributional trends identified through well log analysis and previous studies regarding Norphlet distribution will be used to generate paleogeographic models.

2. Background

2.1 Tectonic Setting

The deposition of Jurassic sediments in the Gulf of Mexico basin were predominantly controlled by rifting that accompanied the breakup of the supercontinent Pangea (Salvador, 1987; Dobson and Buffler, 1997). Rifting began during the Late Triassic about 204 Ma until the late Callovian at 160 Ma (Marton and Buffler, 1999) due to mantle upwelling which possibly created thinned transitional crust (Fig. 5; Salvador, 1987). The NW-SE trending rifts lead to the development of alternating paleo-highs, consisting of thicker transitional crust of 20-35 km, and paleo-lows produced from thinner transitional crust about 8-15 km thick (Dobson and Buffler, 1997). The paleo-highs and lows were regionally extensive, up to 240 km long and creating up to 2 km of offset (Lance, 2011). Prominent paleo-highs in the study area include the Wiggins Arch, Pensacola Arch, Southern Platform, Middle Ground Arch, and the Sarasota Arch and paleo-lows include the Mississippi Interior Salt Basin, Apalachicola Embayment, DeSoto Canyon Salt Basin, Tampa Embayment, and the South Florida Basin. Figure 6 illustrates these highs and lows created in the basement rock as well as locations where volcanism was occurring during the Triassic and Jurassic. The rhyolitic and basaltic volcanism in Georgia (Chowns and Williams, 1983) and basaltic volcanism (basalt, diabase, and diacitic tuff) in the Florida Panhandle are thought to be rift-related occurring along the Triassic Tallahassee graben, which coincides with the Apalachicola Embayment (Arthur, 1988; Heatherington and Mueller, 2003). However, basalt flows and rhyolites in southern Florida have been related to a hot spot below due to their difference in geochemistry (Heatherington and Mueller, 2003).

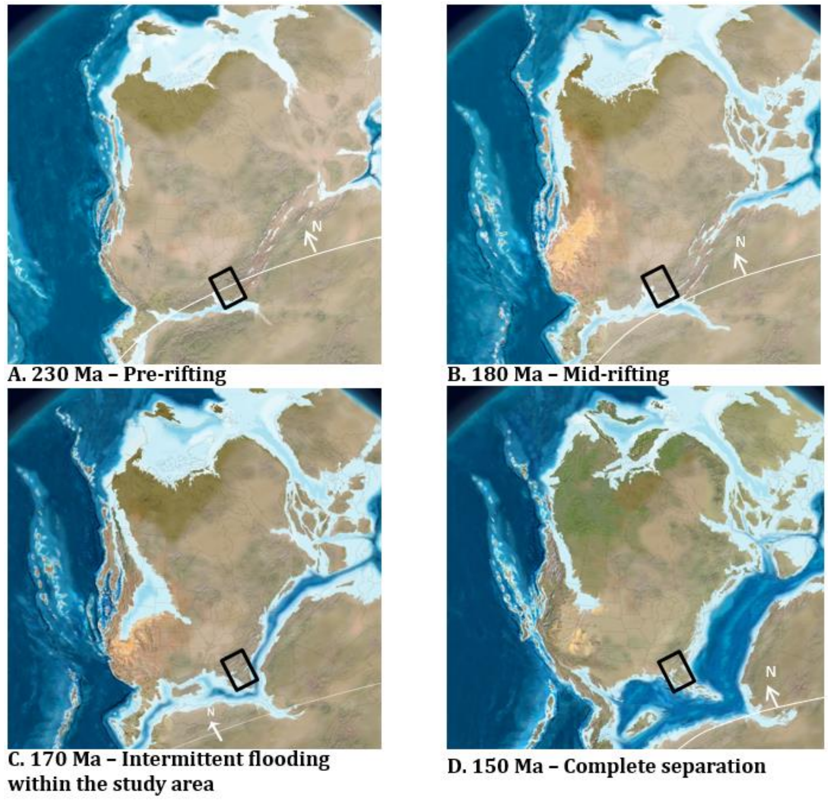

Figure 5. Paleogeographic maps. A) Middle Triassic, B) Early Jurassic, C) Middle Jurassic, and D) Late Jurassic. (Modified from Blakey, 2011 <jan.ucc.nau.edu/~rcb7/nam.html>). Equator and north arrow in A., B., and D inferred from Parrish and Peterson (1988).

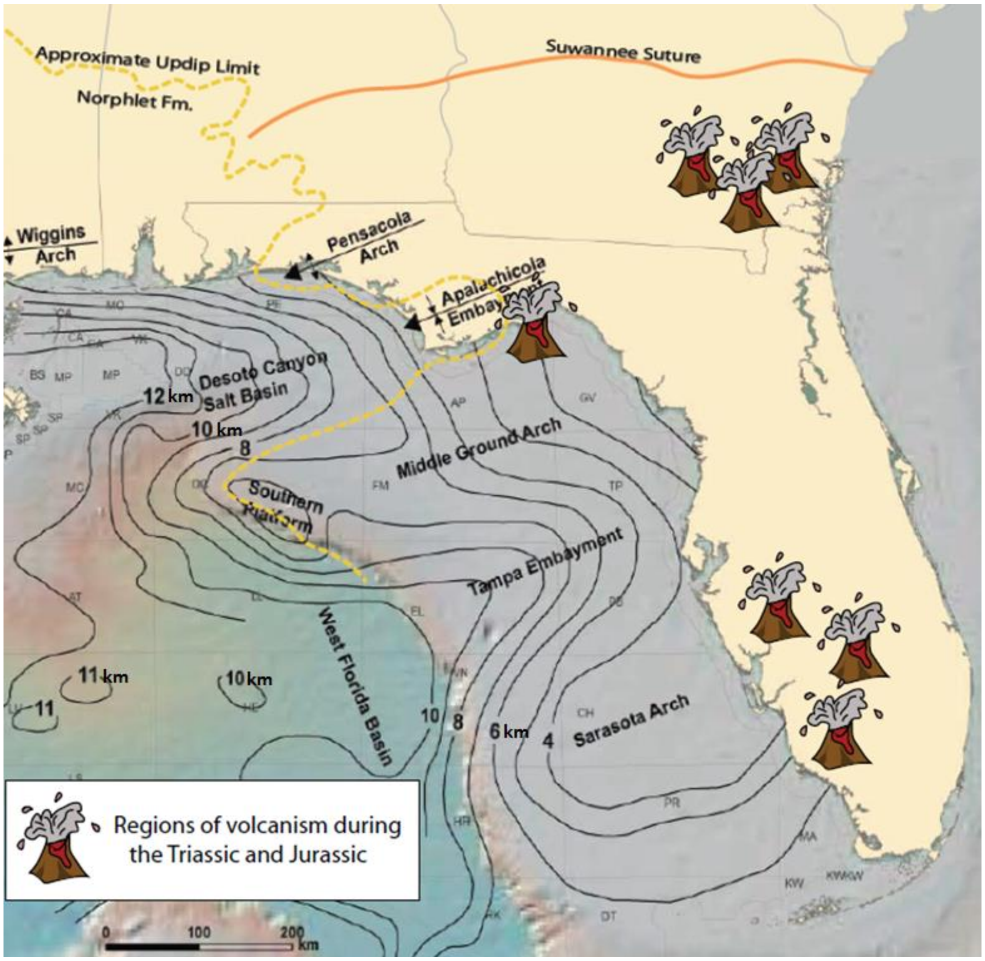

Figure 6. Paleo-highs and lows in the eastern Gulf of Mexico (modified from Wilson, 2011). Contours are depth to the basement in 2 km intervals. Approximate updip limit of the Norphlet Formation from Mancini et al. (1990) and Hunt (2012), and Suwannee Suture from Steltenpohl et al. (2008). Volcanism from Arthur (1988); Chowns and Williams (1983); and Heatherington and Mueller (2003).

By the late Jurassic (Oxfordian), extension had waned leading to a period of tectonic stability and thermal subsidence. This caused development of deposits that were more widespread and uniform which was quite different from the lower and mid dle Jurassic sediments which accumulated in the paleolows and onlapped onto rift grabens and half-grabens (Salvador, 1987).

2.2 Depositional Environment and Stratigraphy

The Upper Triassic syn-rift sediments are terrestrial red bed sandstones and volcanics of the Eagle Mills Formation. The sediments of the Eagle Mills Formation were derived from the horst blocks and were deposited at the same time basalt dikes and sills were forming in the southeastern US from the rifting events (Salvador, 1987; Tew et al., 1991). This formation contains the oldest Mesozoic strata and is preserved in the paleo-lows (Fig. 7). However, very few wells penetrate this formation and it is only known from a few locations. From paleontological data (BOEM, 2012), only one EGOM well located in the Gainesville lease block identifies this formation. Presence of it in the western Florida Panhandle has been inferred in previous studies (Scott, 1991).

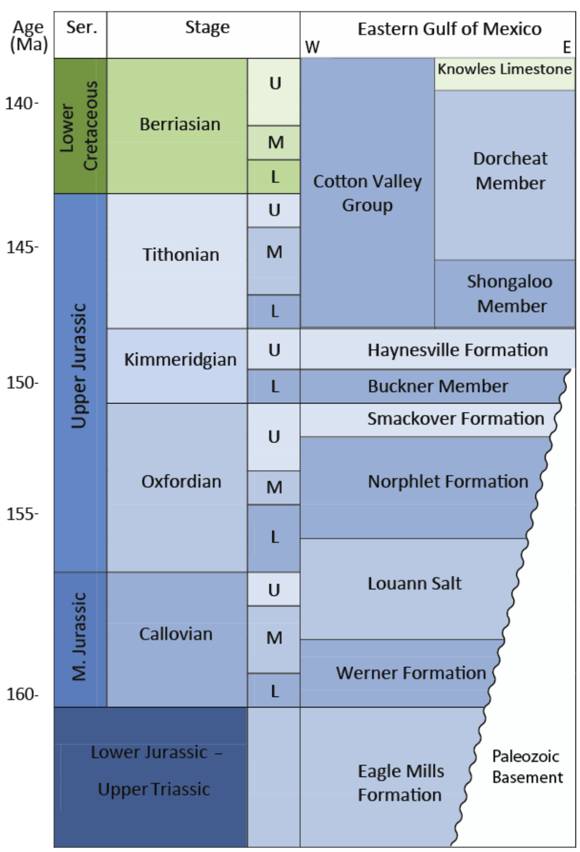

Figure 7. Generalized stratigraphic column of the Eastern Gulf of Mexico. Modified from Mancini et al., 2008 and Mancini et al., 1985.

Intermittent flooding of marine waters into the eastern Gulf of Mexico began during late Bathonian and Callovian from a small opening to the Pacific to the southwest of the study area (Salvador, 1987; Dobson and Buffler, 1997; Ajdukiewicz et al., 2010). During the Middle Jurassic, an arid climate prevailed which (Mancini et al., 1985) led to the evaporative concentration of hyper-saline marine water resulting in widespread deposition of the Callovian Werner Formation and the Callovian to earliest Oxfordian Louann Salt in the topographic lows. The minor amount of shale that occurs at the base of the Werner Formation represents the initial transgression of normal marine water into the Gulf of Mexico. However, most of the Werner Formation consists of the overlying anhydrite. This formation is discontinuously distributed and was preferentially deposited in the loci of subsiding grabens (Tew et al., 1991). The distribution of the Louann Salt was also primarily controlled by paleotopography as well as the regional peripheral fault system which rims the northern Gulf of Mexico continental rift margin and roughly controlled the updip limit of thick Louann Salt deposits (Tew et al., 1991). The thickest onshore accumulations in the EGOM occur in the Mississippi Interior Salt Basin. The Louann Salt is absent from Chocotaw, Conecuh, and Pensacola-Decator ridges (Tew et al., 1991). A basinward increase in salt thickness occurs offshore where as much as 2,000 feet (610 m) of salt may have accumulated. On the western Florida shelf the Louann Salt began during the Oxfordian, syn- and post-Norphlet deposition (determined through seismic data), and is continuing through the present creating several important hydrocarbon-capturing structures such as diapirs and domes (Dobson and Buffler, 1997).

With continued arid conditions, alluvial, fluvial, and eolian sands of the Norphlet Formation were deposited conformably on top of the Louann Salt or unconformably above the Werner, Eagle Mills, or Basement depending on the updip limit of these formations. A broad desert existed in southwestern Alabama and western Florida that was rimmed to the north and east by the Appalachians and to the south by a developing shallow Oxfordian Sea (Mancini et al., 1985; Dobson and Buffler, 1997). The paleo-highs likely acted as the source areas for sediment deposited in the adjacent lows, sourcing the proximal deposition of the alluvial conglomerate facies (Fig. 2). Downdip, the conglomerates grade into red bed sandstones and intermittent wadi complexes, which then transition into eolian desert plain sediments (Mancini et al., 1985). The wadi complexes, which most frequently occur adjacent to the conglomerate facies, were responsible for moving sediment from the paleo-highs into the eolian system where the sediments were reworked into dunes (Hunt, 2012).

The Norphlet Formation in the eastern Gulf of Mexico can be up to 450 m thick (Salvador, 1987) and is made up of four major facies (Pearson, 2011). The lower Norphlet is a discontinuous black shale deposited in a bay/lagoonal setting. The conglomeritic sandstone facies represents a wadi and proximal alluvial fan setting with poorly-sorted clasts that are composed of phyllite, chert, quartzite, granite and rhyolite rock fragments. Red bed sandstone facies of the Norphlet Formation represent more distal alluvial fan deposition as well as wadi and fluvial environments. This facies consists predominately subarkose sandstones, siltstones, and mudstones. The eolian sandstone facies, known as the Denkman Member, can be greater than 180 m thick and can range from lithic arkose to mature, well-sorted quartz arenites depending on location (Mancini et al., 1985; Scott, 1991; Pearson, 2011).

In the late Oxfordian, the Gulf of Mexico opened up to the Atlantic, flooding the Norphlet (Mancini et al., 1990; Ajdukiewicz et al., 2010). Due to the transgression of the Oxfordian Sea, the upper Norphlet is composed of marine facies with finer clastics and more carbonate and/or quartz cement (Mancini et al., 1985). The transgression is thought to have been low energy and fairly rapid due to the lack of large-scale reworking of the upper Norphlet (Ajdukiewicz et al., 2010), high preservation of fossils, and lack of bioturbation (Mancini et al., 1985).

The Smackover carbonates were deposited above the Norphlet in the Oxfordian Sea (Mancini et al., 1990; Ajdukiewicz et al., 2010) and consist of three distinct facies. The lower Smackover was deposited in an anoxic, low energy, marine environment and is an excellent hydrocarbon source rock (Pearson, 2011). While the mean TOC of the entire lower Smackover is only 0.5%, isolated stylolites can have up to 10% TOC (Sassen et al., 1987). The lower Smackover is interpreted to be intertidal to subtidal and consists of laminated lime mudstone. Above this is a subtidal argillaceous limestone that shows burrows indicating more oxic conditions. The upper part of the Smackover Formation was deposited in a high-energy intertidal to subtidal environment and consists of oolitic and peloidal grainstone and packstone (Mancini et al., 1990; Pearson, 2011).

During the Kimmeridgian, sabkha and saline lagoon environments lead to the deposition of the Haynesville Formation (Salvador, 1987; Mancini et al., 1990). The lowest unit of the Haynesville Formation is the Buckner Anhydrite Member, consisting primarily of massive anhydrite. The middle unit of the Haynesville Formation consists of sandstone, shale, and anhydrite and is overlain by a lithologically similar upper unit that also includes lime mudstone. This formation has been interpreted to illustrate upward shallowing from subaqueous to subaerial terrestrial deposits (Mancini et al., 1990). In the eastern Gulf of Mexico, the Haynesville Formation consists of updip conglomerate and sandstone which grades into to sandstone and shale downdip (Dobson and Buffler, 1997).

2.3 Norphlet Formation Petrology

Most of the Florida Panhandle sits between the Conecuh Ridge and Pensacola Arch within the Conecuh Embayment. The Norphlet Formation in the Florida Panhandle is thought to be sourced from both of these paleo-highs (Fig. 2). Scott (1991) studied the sandstone petrology of the upper Norphlet, Denkman Member in several counties in the Florida Panhandle, his results summarized below.

In the Florida Panhandle, the Denkman Member is a lithic arkose (e.g., Folk, 1980). The average framework grain modal composition consists of 61% quartz (90% monocrystalline), 26% feldspar, and 12% rock fragments. Lithic fragment modal abundances are 80% metamorphic, 15% volcanic, and 5% sedimentary rock fragments (Scott, 1991). The most common rock fragment is a finely crystalline grain type which bears resemblance to chert but is classified as a metamorphic rock fragment due to occasional phyllosilicate inclusions and microlayers of some grains (Scott, 1991). This varies somewhat from what is seen in southwestern Alabama, where the framework grains of the Denkman Member is on average composed of 79% quartz, 16% feldspar, and 5% rock fragments. The rock fragment types include chert, slate, phyllite, schist,

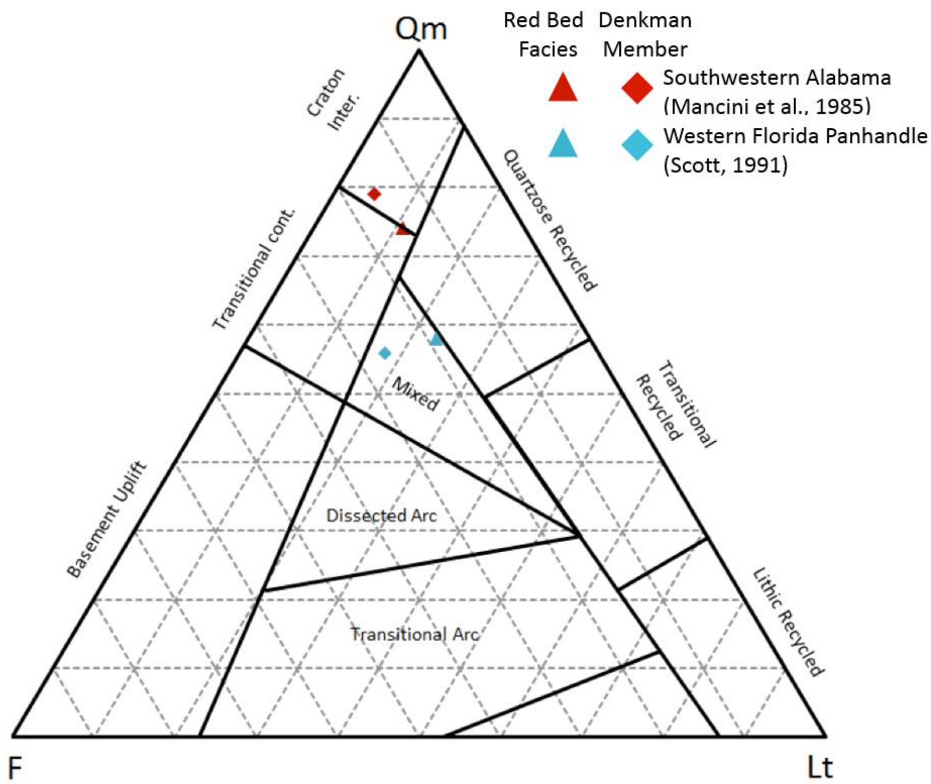

Figure 8. QmFLt plot of the average framework grain modal composition of the Norphlet Formation in southwestern Alabama (Red; Mancini et al., 1985) and the western Florida Panhandle (Blue; Scott, 1991). Triangles represent the red bed facies and the diamonds represent the Denkman Member.

and quartzite (Mancini et al., 1985). The Florida Panhandle has a much higher percentage of rock fragments and less quartz than southwestern Alabama.

Below the Denkman Member is the red sandstone and mudstone lithofacies. In the Florida Panhandle, the red bed sandstone composition is feldspathic litharenite with the average framework grains consisting of 61% quartz (92% monocrystalline), 15% feldspar, and 23% rock fragments. Lithic grain variety abundance is 74% metamorphic and 24% volcanic rock fragments (Scott, 1991). In southwestern Alabama, the average framework grain composition of the red bed sandstone is 74% quartz, 14% feldspar, and 11% rock fragment. Rock fragment types in the southwestern Alabama red bed sandstone include chert, phyllite, quartzite, schist, and basic to felsic igneous rock (Mancini et al., 1985).

Toward the updip limit of the Norphlet Formation the conglomeritic lithofacies is present. The conglomeritic lithofacies in the Florida Panhandle consists of pebble to cobble-sized, angular to rounded clasts of plutonic and metamorphic rocks (Scott, 1991). In southwestern Alabama the conglomeritic lithofacies consist of granule- to cobble-size, angular to subangular, fragments of chert, shale, quartzite, granite, and rhyolite (Mancini et al., 1985). These variations in lithofacies from southwestern Alabama and the Florida Panhandle (Fig. 8) are likely caused by their proximity to the paleo-high source as well as the type of source material. Figure 6 shows a proposed suture zone between the Laurentian (Grenville) crust and the Gondwanan, Suwannee Terrane. The approximate location of the suture suggests that the Conecuh Ridge basement likely consists of both Laurentian and Suwannee terrane while the Pensacola Arch is underlain solely by the Gondwanan, Suwannee Terrane.

3. Methodology

3.1 Sampling

A total of ten detrital zircon samples, six from the Norphlet Formation (samples P1004, P1096, P1080, OCS-G-6848, OCS-G-6406, and OCS-G-6396), one from the Haynesville Formation and Paleozoic basement (OCS-G-2513), one from the Cotton Valley Group, Haynesville Formation and Paleozoic basement (OCS-G-2523), and two from the Paleozoic basement (P383 and P382), came from 10 different well locations from onshore Florida and the offshore lease blocks Mobile Bay, Destin Dome, Pensacola, Florida Middle Ground, and St. Petersburg (Fig. 9). Florida samples were provided by the Florida Geological Survey and chosen based on location, depth, and availability. Identification of the sampled formations came from physical observation of sample lithology as well as from well log data, paleontological data from BOEM (2012b), and previous studies.

Sandstone samples from 3 onshore and 2 offshore Florida State wells were taken from the Norphlet or surrounding formations. Onshore samples P1080, P1004, and P1096 were taken from core chips directly from the Norphlet Formation sampling each foot available, accumulating 150-200 grams for each sample. Because wells P382 and P383 are east of the updip limit of the Norphlet Formation, the Paleozoic basement was sampled. Well P382 was sampled for all available core chips over 11 feet of basement resulting in ~400 grams of sample. Well P383 had core chips available for 13 feet of basement which were sampled and supplemented with cuttings from above (~300 grams of sample). Table 1 summarizes the pertinent information regarding samples used in this study.

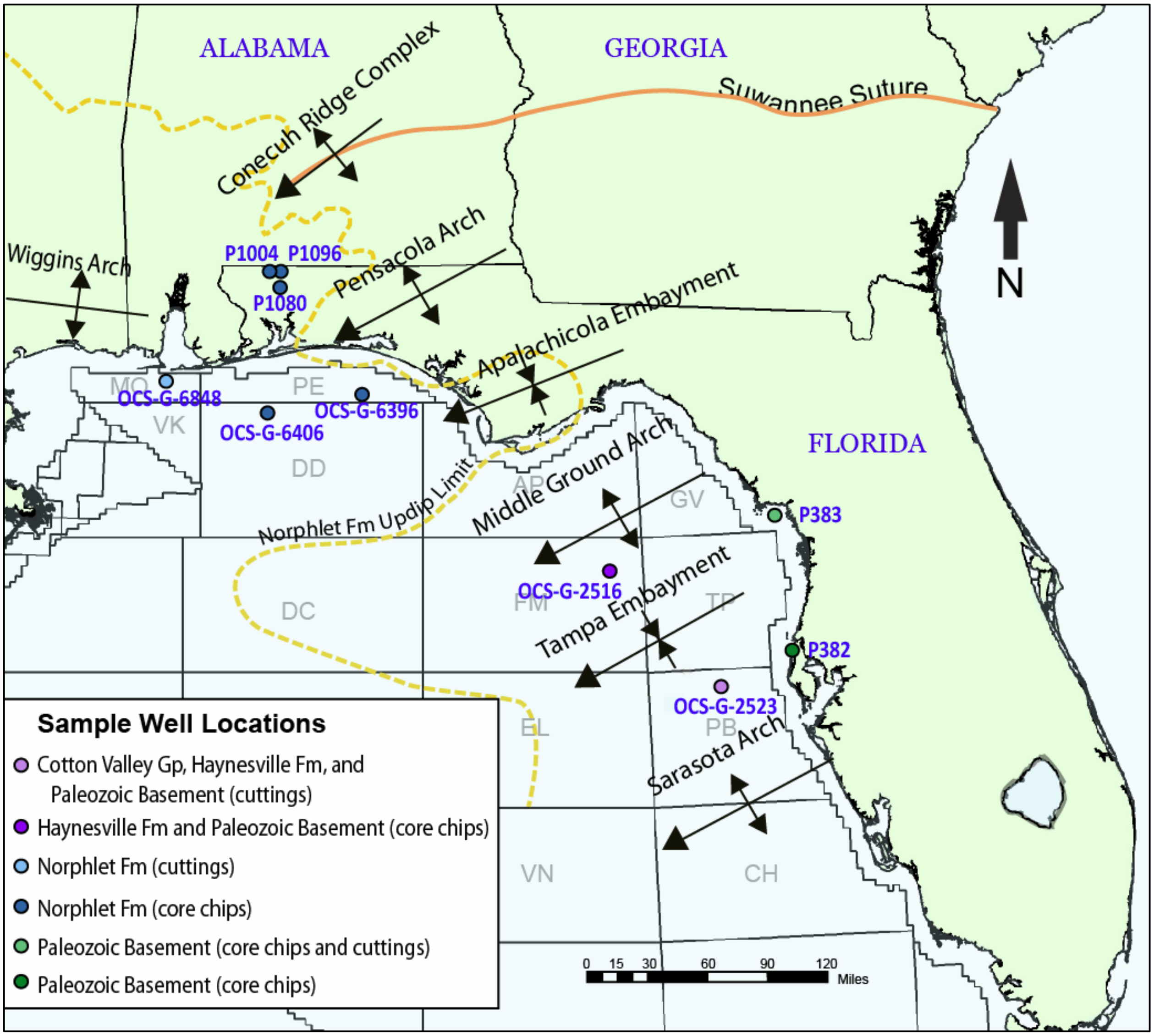

Figure 9. Location of samples used for U-Pb detrital zircon geochronology. Arrows indicate structural highs and lows created from the rifting of Pangea. Suwannee suture from Steltenpohl et al. (2008). Norphlet updip limit from Mancini et al. (1990).

The Oklahoma Geological Survey provided four offshore samples from the Mobile Bay, Pensacola, Florida Middle Ground, and St. Petersburg federal lease blocks. Eighteen non-consecutive feet of core was available for the Pensacola well (OCS-G-6396) in which each foot was sampled, accumulating 2 kilograms of sample. The remaining wells did not have available core and thus cuttings were utilized. The Mobile Bay well (OCS-G-6848) contained an apparent Norphlet interval identified for sampling. Identification of Norphlet in this well was based on the sandstone lithology immediately following a thick limestone section as well as from mud log descriptions. Two grams of cuttings were sampled from every ten feet for 50 feet (~100 grams of sample). The Florida Middle Ground and St. Petersburg wells are east of the Norphlet updip limit. In this case, clastics within and above the Paleozoic basement were sampled and identified based on BOEM paleontological data (2012) and seismic observations of Dobson and Buffler (1997). The Florida Middle Ground well (OSC-G-2516) was sampled for the Haynesville Formation and Paleozoic basement with 2 grams sampled every ten feet (~200 grams of sample). The St. Petersburg well (OSC-G-2523) was sampled for the Cotton Valley Group, Haynesville Formation and Paleozoic basement with 2 grams sampled every ten feet (~300 grams of sample). Lastly, Murphy Oil Corporation supplied core plugs from a well within the Destin Dome lease block (OCS-G-6406). Core plugs were sampled every three feet for 180 feet (~1.2 kg of sample).

Table 1. Information for samples used for U-Pb detrital zircon geochronology.

Sample name	API	Location Lease block	Latitude/ Longitude	Origin of sample:	Sample Formation	Sample type (cuttings/core)	Approx. Sample Size (grams)	Lithology/ Composition	Depth	Operator of well	Production
P1004	0911320188	Santa Rosa County, FL	30°57'34" N 87°9'21.92" W	Florida Geological Survey	Norphlet Formation	Core Chips	150	Sandstone	15,765-15,787	Exxon	1981 Test Gas: 1358 MCFPD Test Oil: 1104 BOPD
P1096	0911320207	Santa Rosa County, FL	30°57'15.48" N 87°6'32" W	Florida Geological Survey	Norphlet Formation	Core Chips	200	Sandstone	15,160-15,239	Smackco Ltd	Dry Hole
P1080	0911320203	Santa Rosa County, FL	30°51'13" N 87°6'12" W	Florida Geological Survey	Norphlet Formation	Core Chips	200	Sandstone	16,099-16,153	Exxon	1982 Test Gas: 302 MCFPD Test Oil: 984 BOPD
OCS-G-6848	60815400990000	Mobile Bay	30°8'21.7" N 88°4'43.68" W	Oklahoma Geological Survey	Norphlet Formation	Cuttings	100	Sandstone	20,090-22,140	Mobile Oil E&P Southeast	Gas show
OCS-G-6406	60822400357000	Destin Dome	29° 56' 16.21" N 87°11'9.86" W	Murphy Oil Corporation	Norphlet Formation	Core Chips	1,200	Sandstone	22,560-22,740	Murphy E&P Company	Gas show
OCS-G-6396	60821400030000	Pensacola	30°1'10.62" N 86°23"45.57" W	Oklahoma Geological Survey	Norphlet Formation	Core	2,000	Sandstone	17,501-17,504 17,528-17,532 17,558-17,567 17, 584-17,587	Texaco	Dry Hole
OCS-G-2516	60828400000000	Florida Middle Ground	28°41'44.12" N 84°19'50.16" W	Oklahoma Geological Survey	Haynesville Formation and Paleozoic Basement	Cuttings	200	Sandstone/Shale	14,713-15,658	Texaco	Dry Hole
OCS-G-2523	60835400010000	Saint Petersburg	27°50'32.23" N 83°25'48.66" W	Oklahoma Geological Survey	Cotton Valley Group, Haynesville Formation, and Paleozoic Basement	Cuttings	300	Sandstone/Shale	15,810-16,900	Texaco	Dry Hole
P382	0921720001	Citrus County, FL	28°5'59" N 82°49'41" W	Florida Geological Survey	Paleozoic Basement	Core Chips	400	Shale Siltstone Quartzite	6,035-6,044 6045 6046	Mobil Oil Corp	Dry Hole
P383	0927520002	Levy County, FL	29°5'24" N 82°55'16" W	Florida Geological Survey	Paleozoic Basement	Core Chips Cuttings	300	Chips-Quartzite	Chips: 4722-4735 Cuttings: 4500-4720	Mobil Oil Corp	Dry Hole

3.2 U-Pb detrital zircon geochronology

Separation of zircon grains from the samples involved crushing, milling, hydrodynamic separation using a Gemini table, magnetic separation using a Frantz magnetic separator, dense liquid separation using lithium polytungstate (LPT) and methylene iodide (MEI), and nitric acid to remove pyrite. Most of the samples were small, ranging from 100 to 500 grams, with the exception of the larger Pensacola and Destin Dome samples; these two wells were the only samples run through the Gemini table before magnetic and liquid separation.

After the samples were soaked in 20% nitric acid to dissolve pyrite, they remained fairly impure ranging from only 20-50% zircon. To concentrate the zircons without bias to size or shape, other grains (predominately barite) were mostly removed by hand picking with tweezers. The zircons were then mounted in epoxy disks of an inch in diameter, polished, and imaged. Cathodoluminescence (CL) imaging was done at WVU using a JEOL scanning electron microscope. Both backscatter and CL detectors were used to attain SEM and CL images of the mounts. The mounts were also imaged using a Nikon Eclipse polarizing microscope.

Ultimately, over 100 zircons were concentrated for each sample. Vermeesch (2004) recommends 117 grains be dated to achieve a 95% certainty that no populations are missing. While several hundred grains would be necessary to represent all age populations, Andersen (2005) recommends practical work to require 35-70 grains in order to achieve a detection limit of 1-2% at a 0.5 probability (where populations less than 1-2% in abundance may fail to be detected 50% of the time). However, with the range of 35-70 grains, a 10% population abundance has a probability of 0.95 and will fail detection less than 5% of the time. For this study, a target of 100 grains per mount were analyzed giving a detection limit of >1% at a 0.5 probability and a detection limit of ~3% at a probability of 0.95.

Samples were analyzed at the Arizona LaserChron Center (ALC) at the University of Arizona using Laser Ablation-Multicollector (ICP-MS). The GVI Isoprobe uses a 193 nm wavelength laser to produce stable elemental analysis. The detrital zircon analysis used a beam diameter of 30 microns and a pit depth of approximately 15 microns (Gehrels et al., 2006). Samples are analyzed using comparison to a standard zircon. The in-house standard used at the ALC is a Sri Lanka zircon that dates 563.5 +/- 2.3 Ma. R-33 was used as a secondary standard, which has an age 419.3+/- 0.4 Ma. Each sample began with five standard analyses. Then a standard was analyzed every five grains until 100 hundred of the sample grains were analyzed. At the end, three Sri Lanka standards and one R-33 standard were analyzed. The ratios of $^{206}Pb/^{238}U$, $^{207}Pb/^{235}U$, and $^{206}Pb/^{207}Pb$ were obtained in order to determine the zircon age with an error of 2-sigma.

Data was extracted and reduced using the Isoplot 4 software (Ludwig, 2012). All samples had some removal of grain analyses based on several factors including poor precision due to high errors (>10% uncertainty) of the $^{206}Pb/^{207}Pb$ and $^{206}Pb/^{238}U$ isotope ratios, high ^{204}Pb, low $^{206}Pb/^{204}Pb$, high discordance (>20%), or reverse discordance (>5%). Isoplot 4 was then used to create various plots of the data.

Age vs. U/Th plots were made in order to identify metamorphic detrital zircon populations within each sample. The U/Th ratio of metamorphic zircons is generally much higher than igneous zircons due to the larger ionic radius of Th^{4+} than U^{4+} and is thus preferentially purged during metamorphism. The U/Th ratio of igneous zircons is typically less than 2 but more rarely can reach up to 5 or greater (Hoskin and Schaltegger, 2003). Because of this, a cut off of 4 is used to distinguish metamorphic zircons.

3.3 Thin-section Petrography

Thin-section petrography was used in this study to supplement the U-Pb detrital zircon data as a provenance indicator. Eleven thin-sections were point counted from five wells, one of which had conventional core and four of which had sets of sidewall core chips, within the eolian facies of the Norphlet Formation. The Gazzi-Dickinson method of point counting was used in order to avoid grain size biases such as those based on breakage of lithic grains. Where other methods would classify a granite lithic clast in the lithic mode, the Gazzi-Dickinson method classifies it by the individual sand-sized mineral components such as quartz, feldspar, biotite, etc. (Ingersoll et al., 1984). For each thin-section 400 points were counted to attain a maximum error of 5% at 2σ (Van Der Plas and Tobi, 1965). The data was then plotted on various ternary diagrams to help constrain the tectonic setting from which the sandstones were derived (Dickinson and Suczek, 1979).

3.4 Dense Mineral Analysis

Due to the small sample sizes available, traditional methods for dense mineral analysis were not possible to be used. Instead, a more qualitative analysis was performed for all ten samples. The portion of disaggregated rock used for the dense mineral analysis included the magnetic fraction of the sample, the light fraction of the MEI that had settled through the LPT, and the heavy fraction of the MEI following the removal of pyrite by 20% nitric and removal of zircons for mounting. Due to nitric acid soak some dense minerals were dissolved such as apatite and were not considered in the analysis. These grains were then mixed back together and made into pressed grain mounts. The grain mounts included a large amount of quartz and rock fragments making point counting of dense minerals using a grid futile. Therefore, to count dense minerals, all dense minerals in a 10x microscope frame were counted before moving to the next frame. This process was repeated until 50 grains were counted for each sample.

3.5 Log Analysis

Well log analysis was used to better understand facies distribution within the Norphlet and done using GeoGraphix 10.2. Logs from 32 wells were used to correlate the Norphlet Formation in the offshore federal lease blocks Mobile Bay, Pensacola, and Destin Dome and the western Florida Panhandle. Beyond the updip limit of the Norphlet, logs from four wells that reach Paleozoic basement in the Florida Middle Ground and St. Petersburg federal lease blocks and offshore Florida were used to analyze overlying Jurassic sediments (Fig. 10). Offshore wells that hit the Norphlet Formation were provided from the BOEM while offshore wells east of the Norphlet

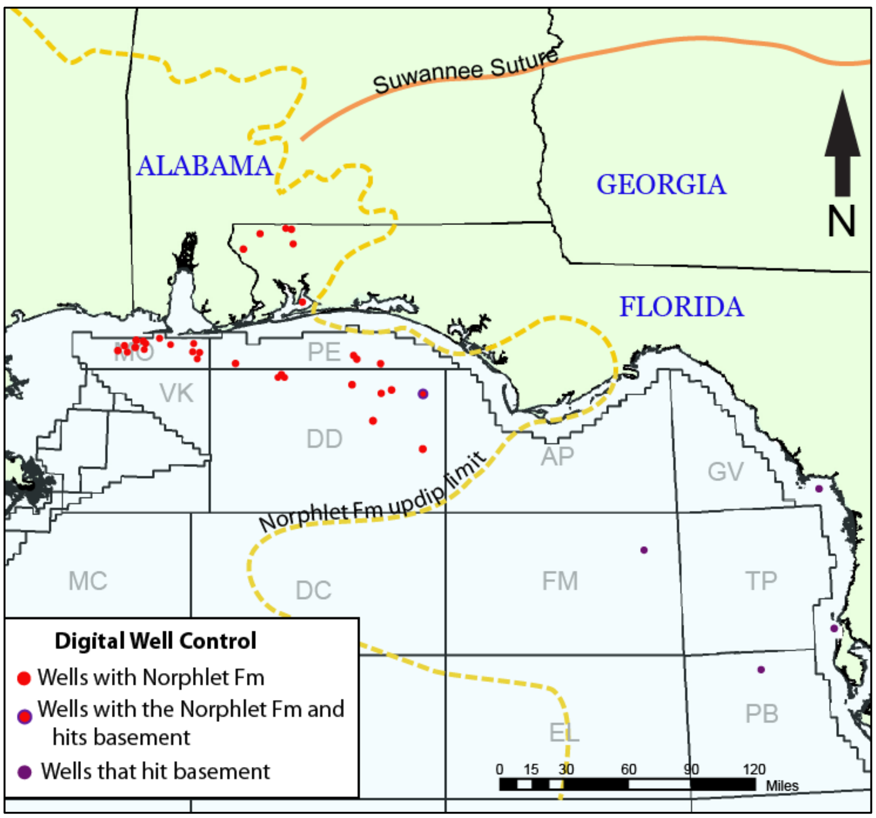

Figure 10. Well control for log analysis in the eastern Gulf of Mexico.

updip limit, Florida Middle Ground and St. Petersburg, were proved by TGS. The Florida Geological Survey provided six Florida State well logs.

The distribution of eolian facies in the study area was interpreted based on the average shale volume of the Norphlet Formation. Many of the offshore wells do not penetrate the entirety of the Norphlet therefore, v-shale was calculated from the upper portion of Norphlet that was penetrated. Excluded from the average shale volume calculation was the Norphlet basal shale which was only identified in one Destin Dome well, 608224002100. V-shale calculations were done using Eq. 1 where clean sandstone gamma ray was defined as 20 API and shale gamma ray was defined as 100 API. Calculations were then compared to previous extensive studies on well log facies identified in the Norphlet Formation (Ridgway, 2010; Hunt, 2012) as well as previous paleogeogaphic models (Mancini et al., 1985; Tew et al., 1991; Lovell and Weislogel, 2010). Shale volume calculations were also compared to core obtained from the Oklahoma Geological Survey from the Pensacola well, 608214000300, to ensure accurate estimation.

Eq. 1: Shale Volume: Vshl[] = min(1, max(0, (GR[]-GRcln) / (GRshl-GRcln)))

3.6 Detrital Zircon Grain Size Analysis

Undergraduate research was undertaken by Evan Knight to see if any correlation existed between grain size of the detrital zircon and age. To do this, each grain that was analyzed at the Arizona LaserChron lab was measured using a Nikon Eclipse polarizing microscope using reflected light and the NIS Elements image analysis software. Grains with U-Pb ages that were removed from the data due to poor precision etc. were not included in the grain size analysis either.

4. Results

4.1 Sample Descriptions and U-Pb Detrital Zircon Age Distributions

A total of 867 detrital zircon U-Pb ages from the 10 prepared samples were determined to be reliable. Figure 11 shows the concordia plots of the 10 samples. The following discussion includes relative probability plots for each individual sample where the red curve shows the relative probability distribution of U-Pb ages including a 2-sigma error. The plots also include a histogram where the number of grains per age are binned in 50 Ma bins. Black bars above the curves represent distinct age groups present in the sample.

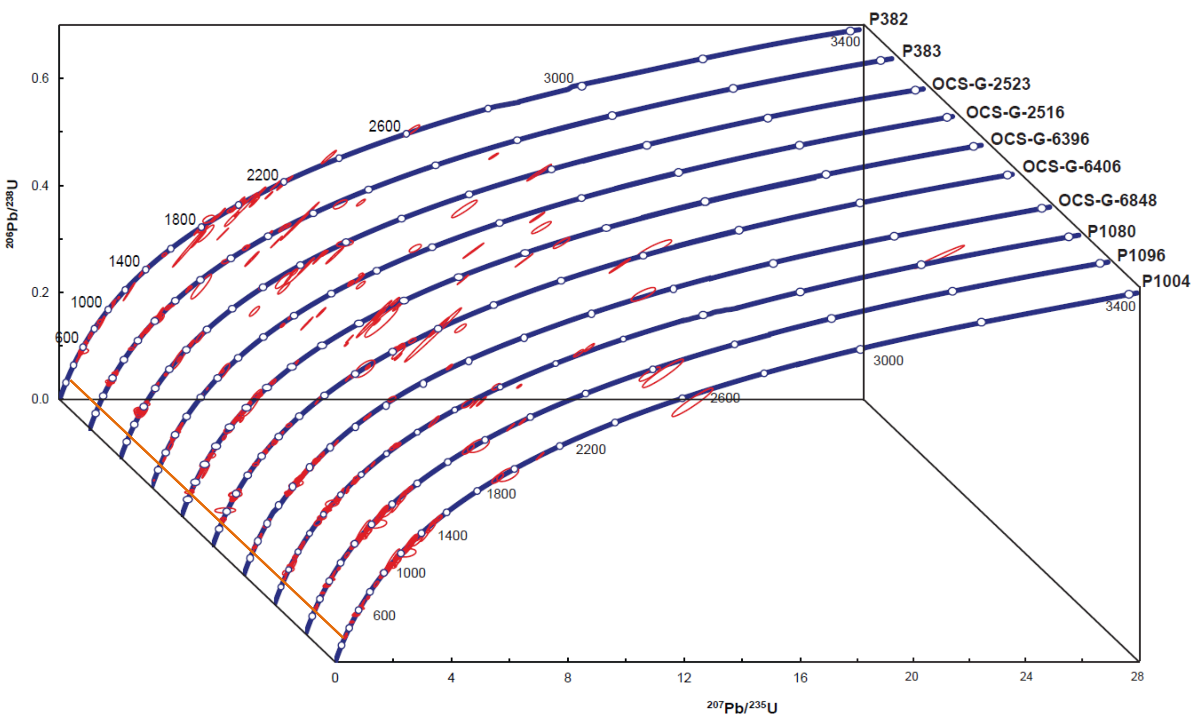

Figure 11. Wetherill concordia plot of all 10 samples. Red ellipses represent single detrital zircon U-Pb analysis with an error of 2-sigma. Orange line indicates deposition age of the Norphlet Formation (~157 Ma)

4.1.1 Sample P1004 – Norphet Formation

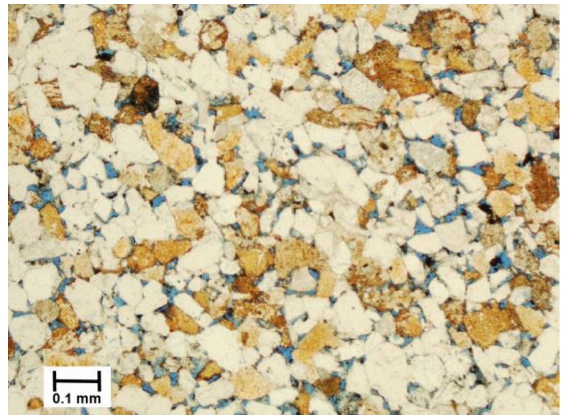

Figure 12. Thin-section image of sample P1004 which consists of moderately to well sorted, angular to subrounded, medium- to very fine-grained sand in plane polarized light.

Sample P1004 came from the western Florida Panhandle and was sampled from core chips within the Denkman Member of the Norphlet Formation over a 22 foot-thick interval. It consisted of light gray, moderately to well sorted, angular to sub-rounded, medium- to very fine-grained sand. No distinct bedding or laminae were observed in the chips or thin-section (Figure 12).

Analysis of sample P1004 provided 95 reliable U-Pb ages; four were removed due to reverse discordance and one removed for discordance. The age range of this sample is from 283.5 Ma (+/- 4.2 Ma) to 2673.2 Ma (+/- 19.5 Ma) (Fig. 13A). The majority of the U-Pb ages

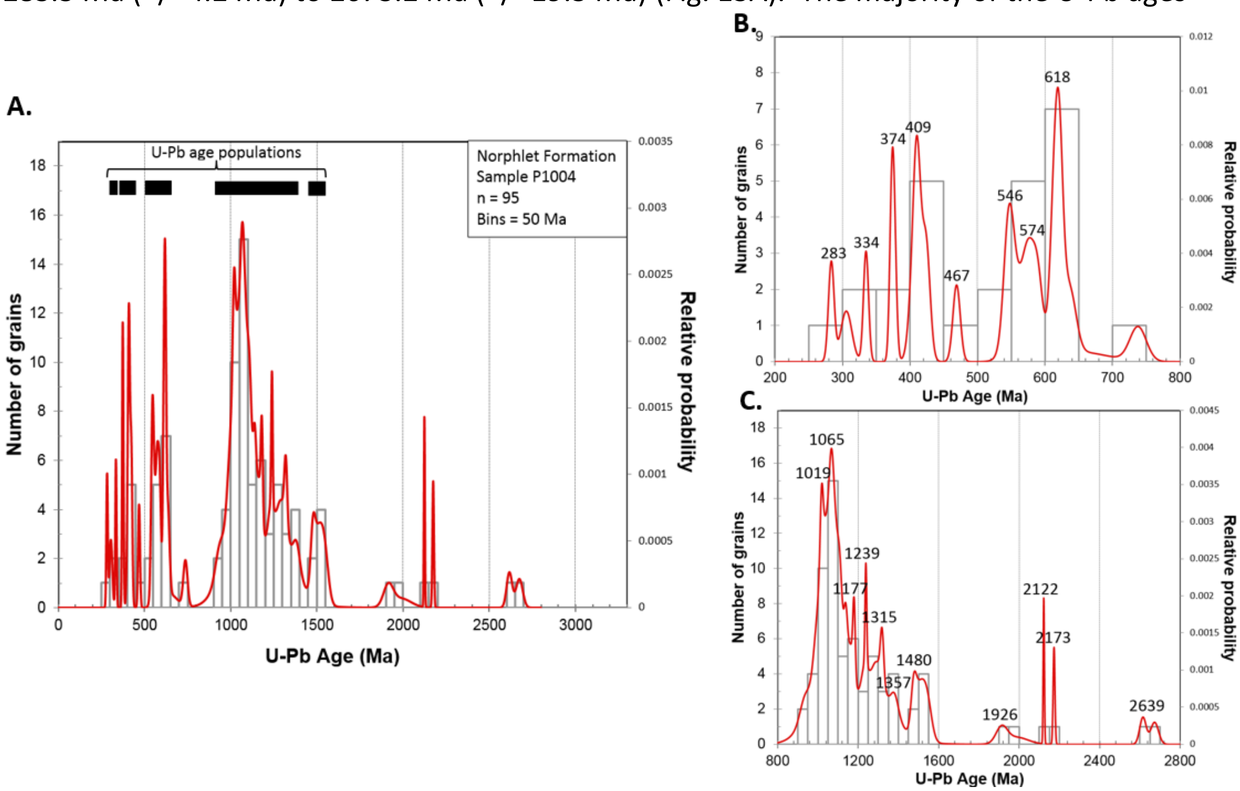

Figure 13. A) Relative probability density curve (red) and histogram in 50 Ma bins showing results of the Norphlet Formation from sample P1004. B) 200-800 Ma age range. C) 800-2800 Ma age range.

range between 250-650 Ma (26%; Fig. 12B) and 900-1550 Ma (66% grains; Fig. 13C). Four U-Pb age populations were identified in this sample; 283-450 Ma (two major peaks at 374 and 409 Ma), 500-650 Ma (peaks at 546, 574, and 618 Ma; Fig. 13B), 900-1400 Ma (peaks throughout including 1019,1065, 1177, 1239, 1315, and 1357 Ma), and 1450-1550 Ma (peak at 1480 Ma; Fig. 13C).

4.1.2 Sample 1096

Sample P1096 came from a well in the western Florida Panhandle and was sampled from core chips within the Denkman Member of the Norphlet Formation over a 79 foot interval and is very lithologically similar to sample P1004. It also consists of light gray, moderately to well sorted, angular to sub-rounded, medium- to very fine-grained sand. No distinct bedding or laminae were observed in the chips or thin-section (Fig. 14).

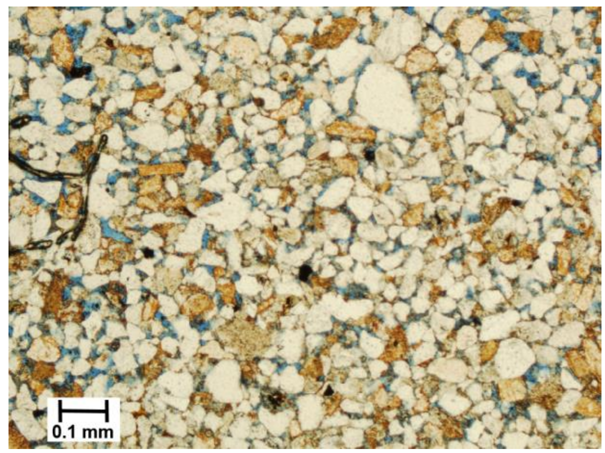

Figure 14. Thin-section image of sample P1096 which consists of moderately to well sorted, angular to sub-rounded, medium- to very fine-grained sand in plane polarized light.

Analysis of sample P1096 provided 80 reliable U-Pb ages; three were removed due to high $^{206}Pb/^{238}U$ error, two for high $^{206}Pb/^{207}Pb$ error, one for high ^{204}Pb, three for discordance and 11 for reverse discordance. The age range of this sample is from 330.9 Ma (+/- 6.9 Ma) to 2137.4 Ma (+/- 10.1 Ma) (Fig. 15A). Similar to zircon ages of sample P1004, most U-Pb ages range between 300-650 Ma (38%; Fig. 15B) and 900-1550 Ma (56%; Fig. 15C). Four main U-Pb age populations were identified; 330-500 Ma (peaks at 374, 431, 463, and 484 Ma), 500-650 Ma (peaks at 535, 583, and 633 Ma; Fig. 15B), 900-1250 Ma (peaks at 1011, 1050, 1086, and 1152 Ma), and 1250-1400 Ma (peaks at 1320 and 1390 Ma; Fig 15C).

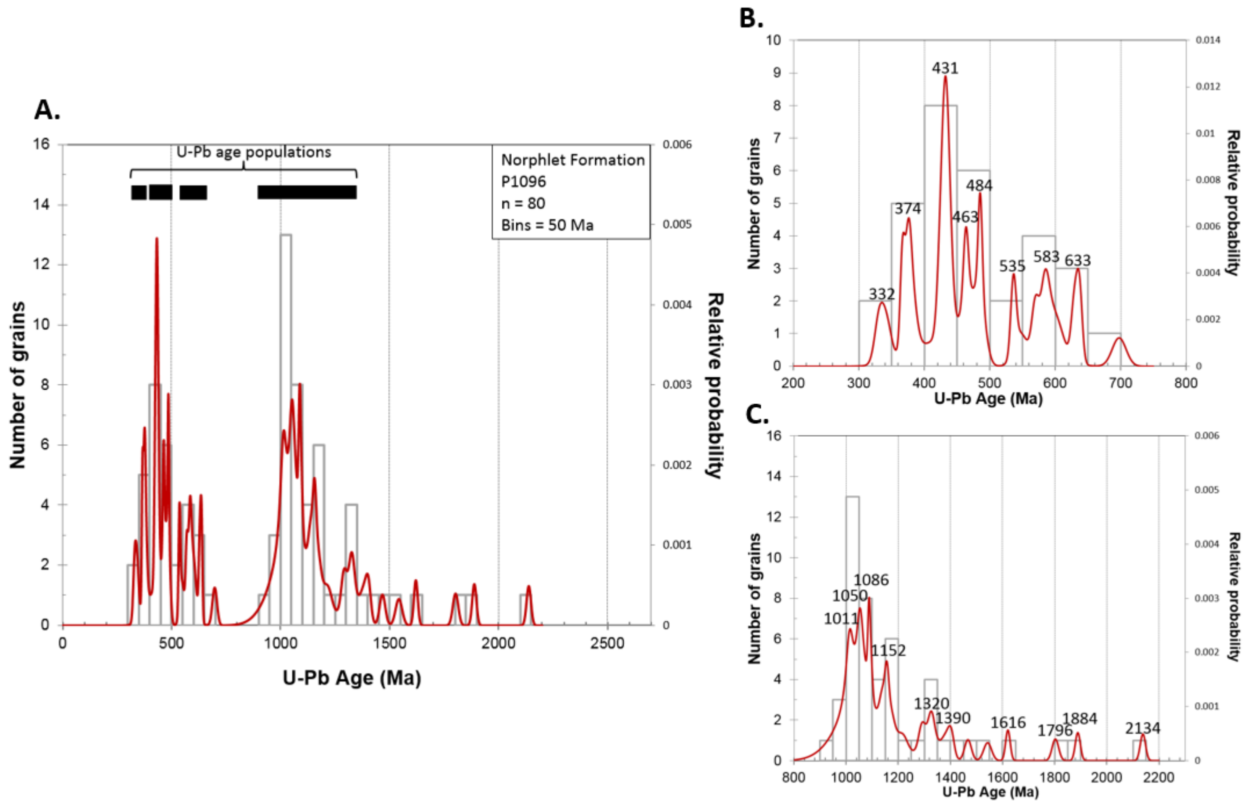

Figure 15. A) Relative probability density curve (red) and histogram in 50 Ma bins showing results of the Norphlet Formation of sample P1096. B) 200-800 Ma age range. C) 800-2200 Ma age range.

4.1.3 Sample P1080 – Norphlet Formation

Sample P1080 came from a well in the western Florida Panhandle and was sampled from core chips within the Denkman Member of the Norphlet Formation over a 54 foot thick interval. This sample is lithologically similar to P1004 and P1096 except texturally it shows more angular and larger grains with poorer sorting, which coincides with the sample's more proximal location to the source. It consists of light gray, moderately sorted, angular to sub-rounded, coarse- to very fine-grained sand. No distinct bedding or laminae were observed in the chips or thin-section (Fig. 16).

Analysis of sample P1080 provided of 89 reliable U-Pb ages; two were removed due to high $^{206}Pb/^{238}U$ error, one for high ^{204}Pb, three for discordance and five for reverse discordance. The age range of this sample is from 295.7 Ma (+/- 3.8 Ma) to 2481.5 Ma (+/- 6.2 Ma) (Fig 17A). The majority of U-Pb ages range between 295-650 Ma (45%; Fig. 17B) and 900-1550 Ma (40%; Fig. 17C).

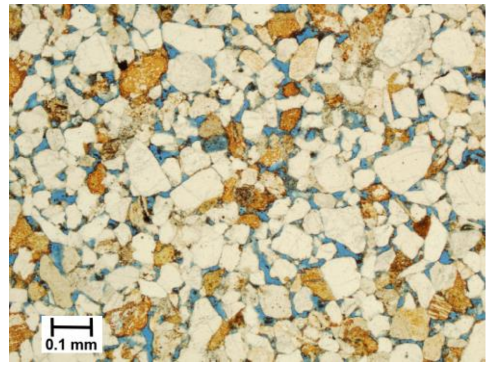

Figure 16. Thin-section image of sample P1080 which consists of moderately sorted, angular to sub-rounded, coarse- to very fine-grained sand in plane polarized light.

These two predominant U-Pb age groups are similar to those of samples P1004 and P1096. However, samples P1004 and P1096 have a larger percentage of grains between 250-650 Ma where sample P1080 has a larger percentage of grains between 900-1550 Ma. Sample P1080

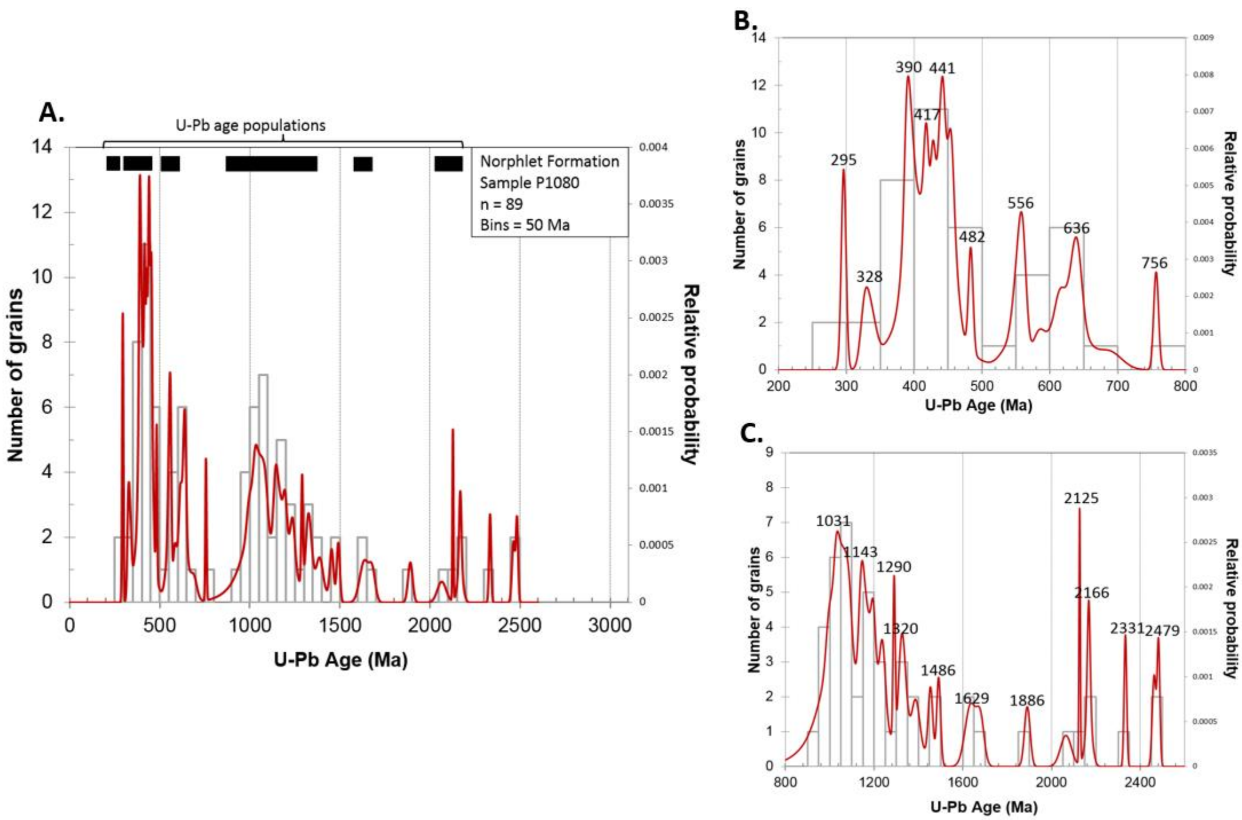

Figure 17. A) Relative probability density curve (red) and histogram in 50 Ma bins showing results of the Norphlet Formation from sample P1080. B) 200-800 Ma age range. C) 800-2600 Ma age range.

has three major U-Pb age populations and two minor ones; 295-500 Ma (peaks at 295, 390, 417, 441, and 482 Ma), 500-650 Ma (two peaks at 556 and 636 Ma; Fig. 17B), 900-1400 Ma (peaks at 1031, 1143, 1290, and 1320 Ma), and the two smaller U-Pb age populations 1600-1700 Ma (peak at 1629 Ma) and 2050-2200 Ma (peaks at 2125 and 2166 Ma; Fig. 17C).

4.1.4 Sample OCS-G-6848 – Norphlet Formation

Sample OCS-G-6848 (MO) came from the Mobile Bay offshore lease block and was sampled from cuttings within the Denkman Member of the Norphlet Formation over a 50 foot thick interval. The cuttings contained of a large amount of limestone from the overlying Smackover Formation, which were removed with dilute acid. The Norphlet cuttings consisted of fragments of medium gray, medium- to very fine-grained sand. Due to the small size of the sample, none was spared to make a thin-section.

Analysis of sample OCS-G-6848 provided 90 reliable U-Pb ages; one was removed due to high $^{206}Pb/^{238}U$ error, four for discordance, and four for reverse discordance. The age range of this sample is from 293.6 Ma (+/- 4.2 Ma) to 3401 Ma (+/- 6.7 Ma) (Fig. 18A). The majority of U-Pb ages range between 293-650 Ma (37%; Fig. 18B) and 900-1400 Ma (56%; Fig. 18C). There are two prominent age populations which include 300-500 Ma (peaks at 369, 388, 421, and 455 Ma; Fig. 18B) and 900-1400 Ma (peaks at 1013, 1060, 1154 and 1301 Ma; Fig. 18C). Another smaller age population present is 550-650 Ma (peaks at 570, 589, and 624 Ma; Fig. 18B).

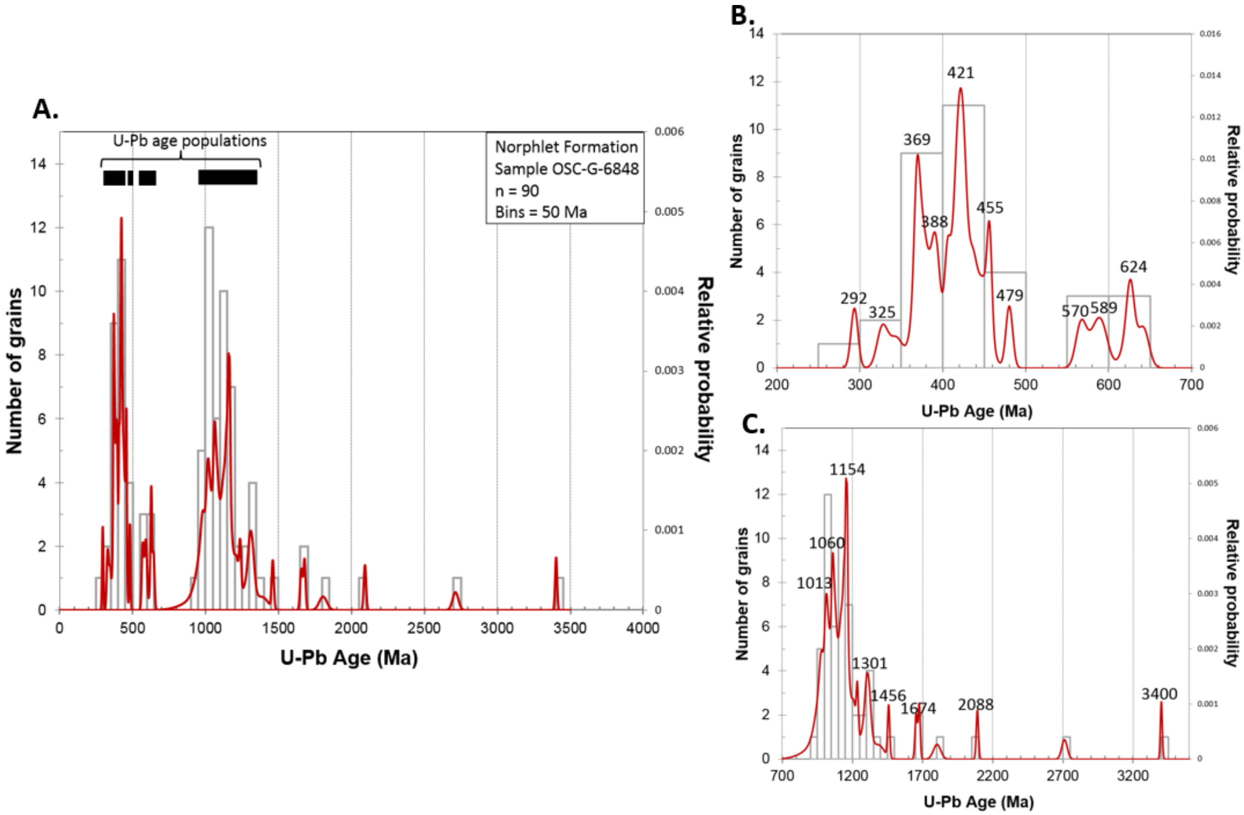

Figure 18. A) Relative probability density curve (red) and histogram in 50 Ma bins showing results of the Norphlet Formation from sample OCS-G-6848. B) 200-700 Ma age range. C) 700-3700 Ma age range.

4.1.5 Sample OCS-G-6406 – Norphlet Formation

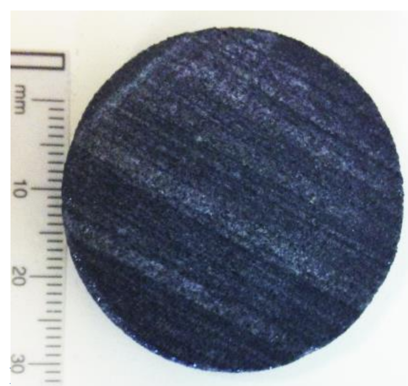

OCS-G-6406. Norphlet is eolian facies with very thin laminae and alternating coarse- and very fine grained sand lamina (22, 606 ft).

Sample OCS-G-6406 (DD) came from the Destin Dome offshore lease block and was sampled from core chips within the Denkman Member of the Norphlet Formation over a 180 foot thick interval. It consisted of very thin laminae of alternating coarse- and very fine-grained sand lamina that showed both reverse and normal grading. The grains within the laminae are well sorted and are sub-angular to well-rounded. The top of the Norphlet Formation is dark gray/black with hydrocarbon staining which decreases with depth becoming a light gray/beige at the bottom (Fig. 19).

Analysis of sample OCS-G-6406 provided 88 reliable U-Pb ages; two were removed due to high $^{206}Pb/^{238}U$ error, one for high ^{204}Pb, three for discordance, and six for reverse discordance. The age range of this sample is from 199.1 Ma (+/- 10.7 Ma) to 3093.2 Ma (+/- 16.6 Ma) (Fig. 20A). This sample has the youngest zircons out of the 10 samples with two Triassic-aged zircon (199.1 and 212.1 Ma). The majority of U-Pb ages range between 273-700 Ma (52%; Fig. 20B), 1000-1400 Ma (23%; Fig. 20B), and 2050-2200 Ma (13%; Fig. 20C). The two largest age populations include 500-700 Ma ages (high peaks at 542 Ma and 602 Ma) and 1000-1350 Ma ages (peaks at 1045 Ma and 1117 Ma; Fig. 20B). Two less abundant age populations include 250-500 Ma (peaks at 302 Ma and 423 Ma; Fig. 20B) and 2050-2200 Ma (peaks at 2050, 2094, and 2122 Ma; Fig. 20C).

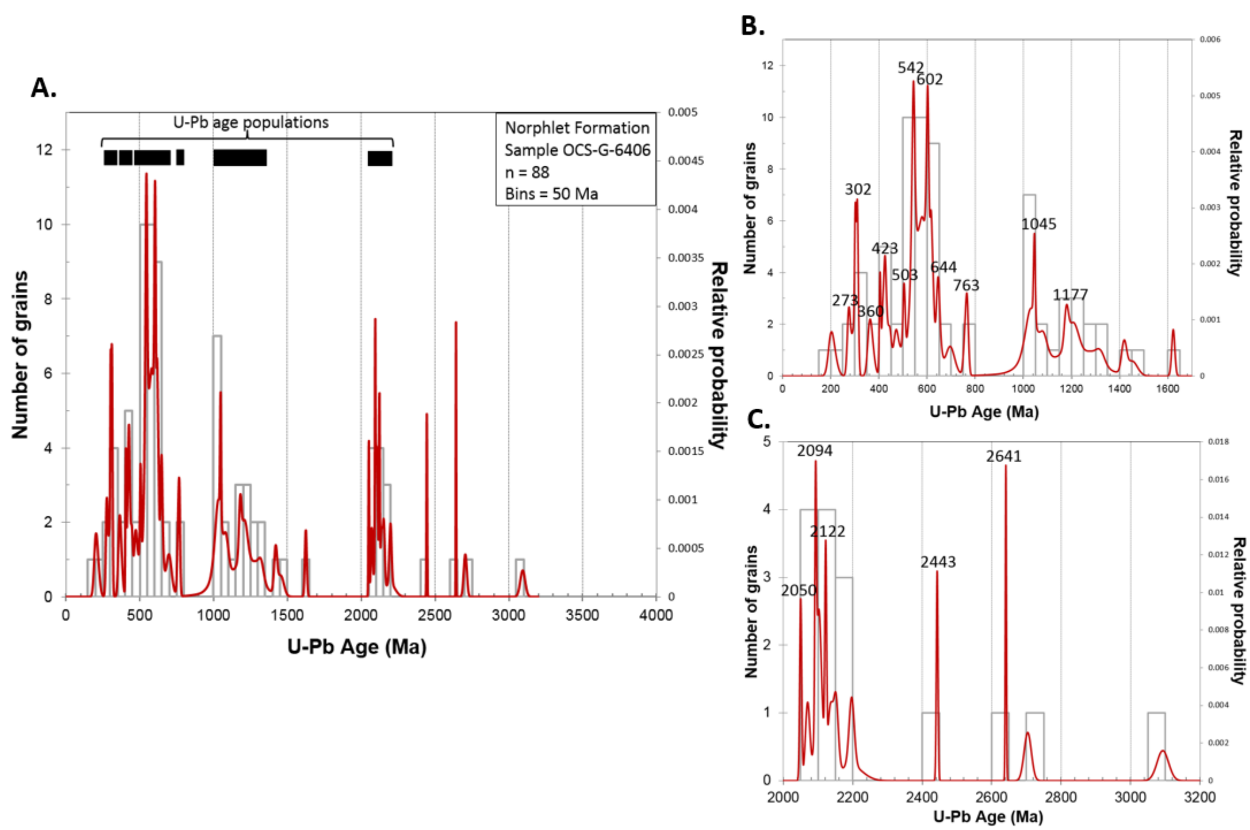

Figure 20. A) Relative probability density curve (red) and histogram in 50 Ma bins showing results of the Norphlet Formation from sample OCS-G-6406. B) 0-1700 Ma age range. C) 2000-3200 Ma age range.

4.1.6 Sample OCS-G-6396 – Norphlet Formation

Sample OCS-G-6396 came from the Pensacola offshore lease block and was sampled from core within the Denkman Member of the Norphlet Formation over a 19 foot interval. Similar to sample OCS-G-6406, it consisted of very thin laminae of alternating coarse- and very fine-grained sand lamina that showed both reverse and normal grading. The grains within the laminae are well sorted and are sub-angular to well-rounded. The top of the core contained carbonate cement which decreased rapidly with depth and was absent below four feet. There is some hydrocarbon staining causing a medium-gray color which decreases with depth turning to light gray. The core also showed scours within some laminae as well as a burrowed section (Fig. 21).

Analysis of the sample OCS-G-6396 provided 89 reliable U-Pb ages; two were removed due to high $^{206}Pb/^{238}U$ error, one for high ^{204}Pb, three for discordance, and five for reverse discordance. The age range of this sample is from 202.1 Ma (+/- 16.7 Ma) to 2766.6 Ma (+/- 3.7 Ma) (Fig. 22A). Similar to the Destin Dome sample, this sample also has a single young, Triassic-aged zircon. Unlike the other samples, the U-Pb ages are more evenly distributed with less clustering. The majority of U-Pb ages range between 250-700 Ma (56%; Fig 22B), 900-1300 Ma (22%; Fig. 22B), and 1700-2250 Ma (15%; Fig. 22C). The two largest age populations include 500-700 Ma (peaks at 551 Ma and 623 Ma) and 900-1300 Ma (age peaks at 977, 1030, and 1221 Ma; Fig. 22B). Three less abundant age populations include 250-350 Ma (age peaks at 293 Ma and 318 Ma), 400-450 Ma (age peaks at 412 Ma and 430 Ma; Fig 22B), and 1950-2250 Ma (age peaks at 2032, 2092, and 2192 Ma; Fig. 22C).

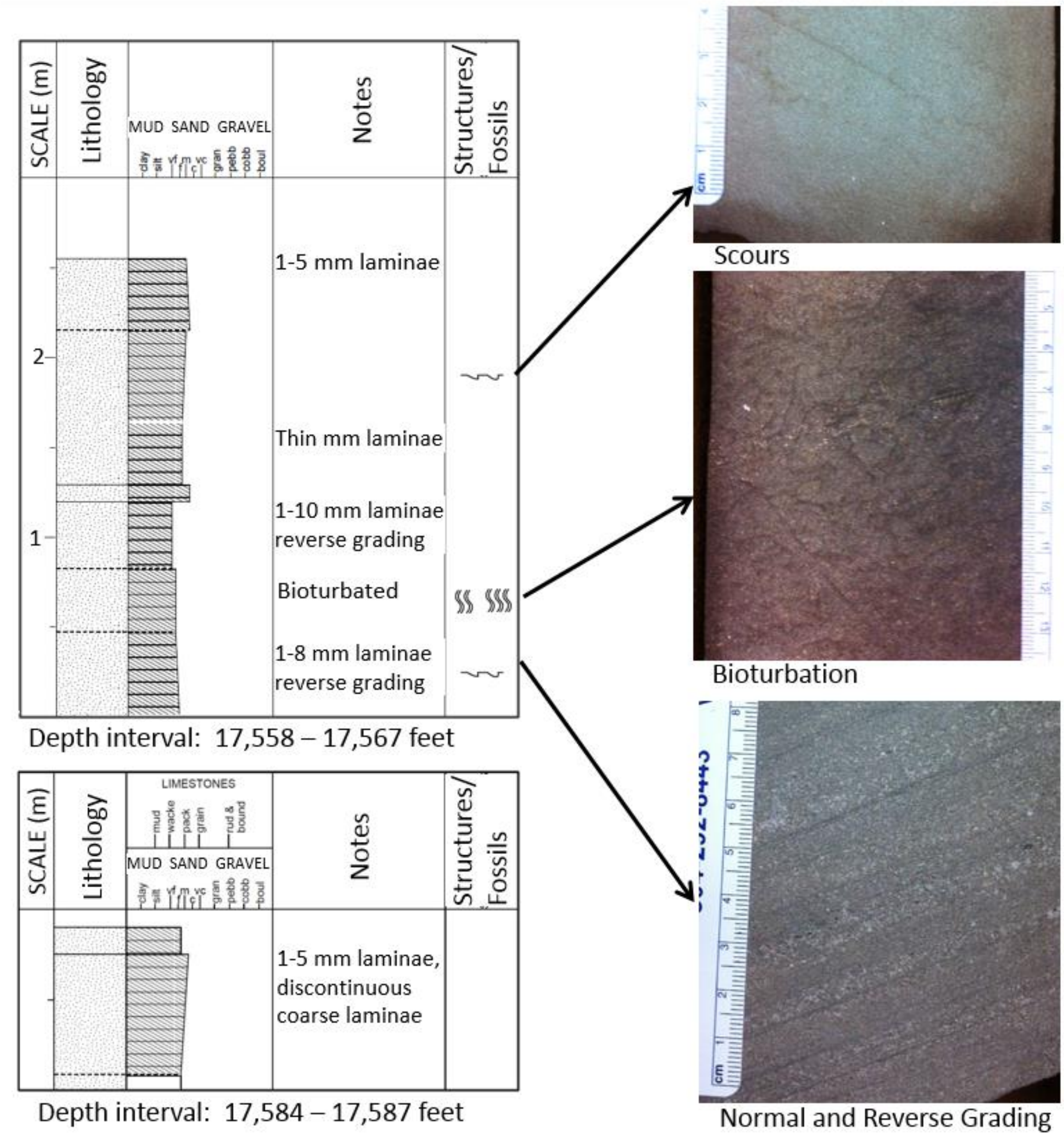

Figure 21. Core description and images of the Norphlet Formation from sample OCS-G-6396. The sample consisted of very thin laminae of alternating coarse- and very fine-grained sand lamina that showed both reverse and normal grading. Sedimentary structures include scours, bioturbation and normal and reverse graded beds.

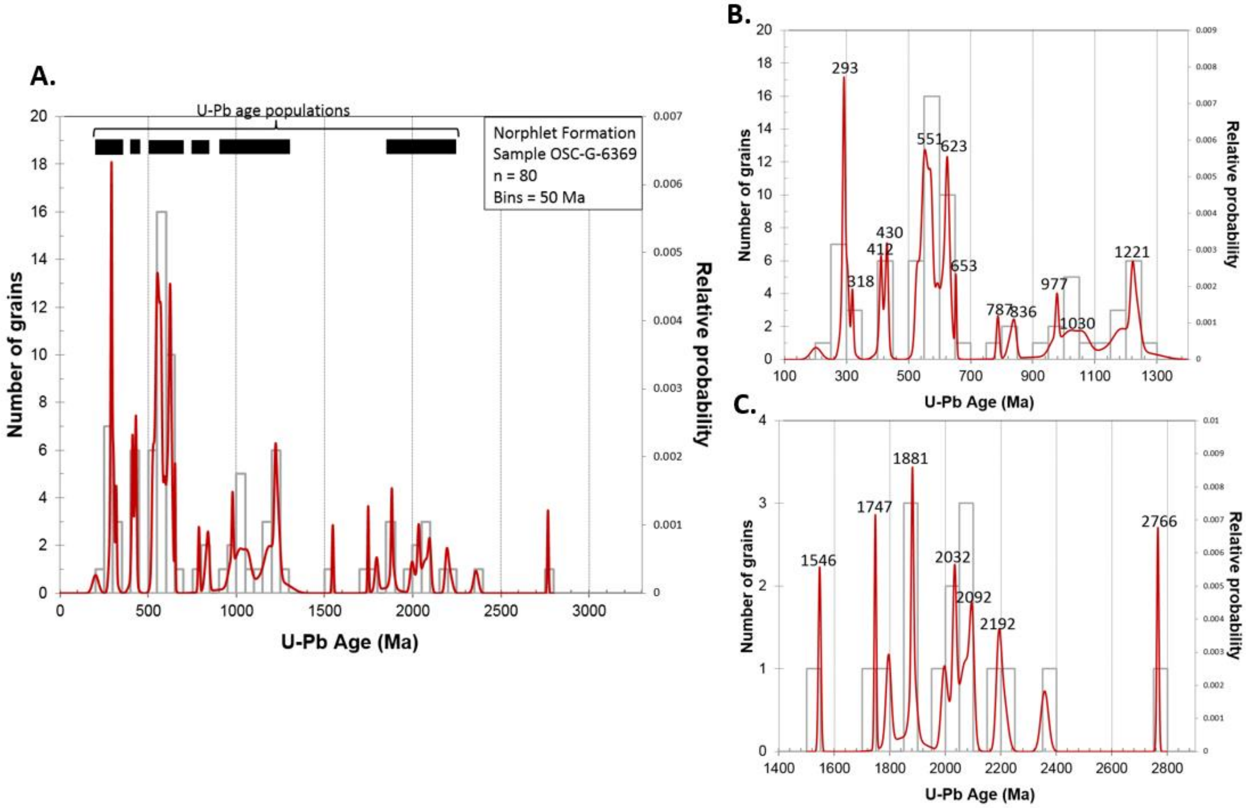

4.1.7 Sample OCS-G-2516 – Haynesville Formation and Paleozoic Basement

Figure 22. A) Relative probability density curve (red) and histogram in 50 Ma bins showing results of the Norphlet Formation from sample OCS-G-6396. B) 100-1400 Ma age range. C) 1400-2900 Ma age range.

Sample OCS-G-2516 (FMG) came from the Florida Middle Ground offshore lease block and was sampled from cuttings recovered from the Haynesville Formation and Paleozoic basement over a 55 foot interval. The cuttings consisted of pieces of shale, siltstone, sandstone, and quartzite (Fig 23).

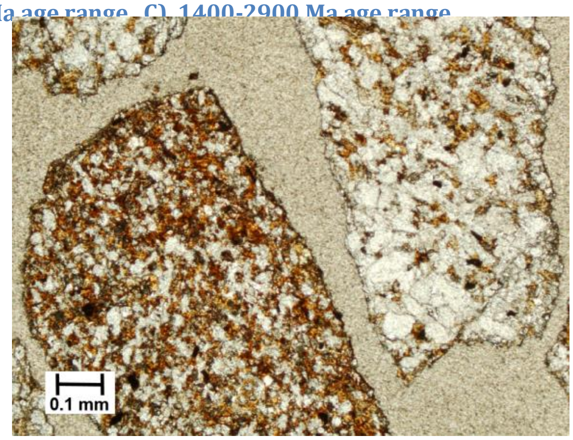

Figure 23. Thin-section image of cuttings from sample OCS-G-2516 which consists of shale, siltstone, sandstone, and quartzite in plane polarized light.

Analysis of sample OCS-G-2516 provided of 75 reliable U-Pb ages; two were removed due to high $^{206}Pb/^{238}U$ error, one due to high

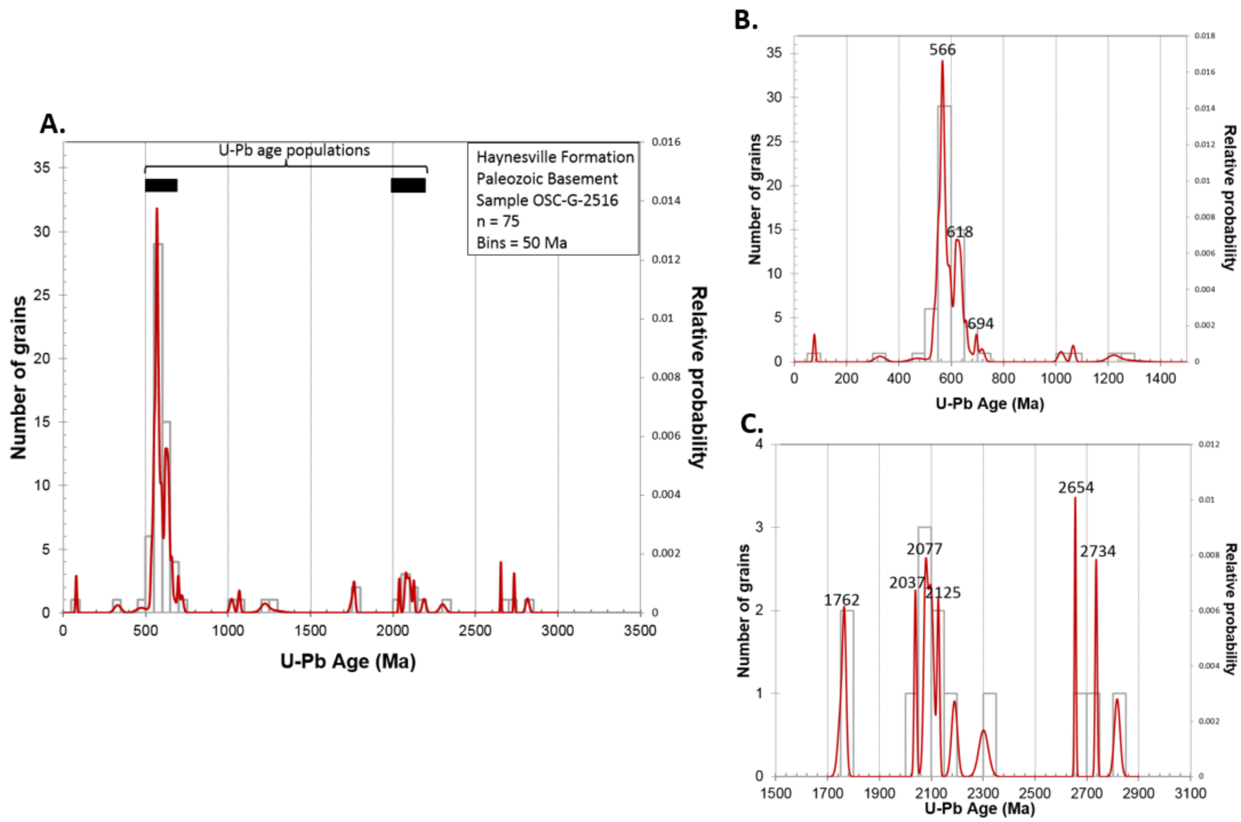

Figure 24. A) Relative probability density curve (red) and histogram in 50 Ma bins showing results of the Haynesville Formation and Paleozoic basement from sample OCS-G-2516. B) 0-1500 Ma age range. C) 1500-3100 Ma age range.

$^{206}Pb/^{207}Pb$ error, one for high ^{204}Pb, ten for discordance, and eleven for reverse discordance. The youngest zircon examined was 77.4 Ma (+/- 4.2), much younger than the formation age and is considered to be a result of contamination due to the sampling of cuttings and mixing of younger sediments via well bore circulation during drilling. The detrital zircon age range of this sample is from 328.8 Ma (+/- 20.3 Ma) to 2815.9 Ma (+/- 10.9 Ma) (Fig. 24A). The majority of U-Pb ages range between 450-750 Ma (75%; Fig. 24A) and 2000-2350 Ma (11%; Fig. 24B). There are only two prominent age populations for this sample which include 500-700 Ma (peaks at 566 Ma and 618 Ma; Fig. 24B) and 2000-2200 Ma (age peaks at 2037, 2077, and 2125 Ma; Fig. 24C).

4.1.8 Sample OCS-G-2523 – Cotton Valley Group, Haynesville Formation, and Paleozoic Basement

Sample OCS-G-2523 (STPB) came from the St. Petersburg offshore lease block and was sampled from cuttings within the Cotton Valley Group, Haynesville Formation, and Paleozoic basement over a 90 foot thick interval. The cuttings consisted of pieces of shale, siltstone, sandstone, and quartzite (Fig. 25).

Figure 25. Cuttings from sample OCS-G-2523 consisting of shale, siltstone, sandstone and quartzite.

Analysis of sample OCS-G-2523 provided 88 reliable U-Pb ages; one was removed for high ^{204}Pb, six for discordance, and eight for reverse discordance. The age range of this sample is from 516.0 Ma (+/- 4.3 Ma) to 2771.1 Ma (+/- 4.8 Ma) (Fig. 26A). The majority of U-Pb ages fall between 500-650 Ma (72%; Fig, 26B), 800-1400 Ma (11%; Fig. 26B), and 1950-2250 Ma (13%; Fig. 26B). Similar to the Florida Middle Ground sample, only two prominent age populations occur; 500-650 Ma (peaks at 556 Ma and 637 Ma; Fig. 26B) and 1950-2250 Ma (age peaks at 1995, 2061, 2105, and 2218 Ma; Fig. 26C).

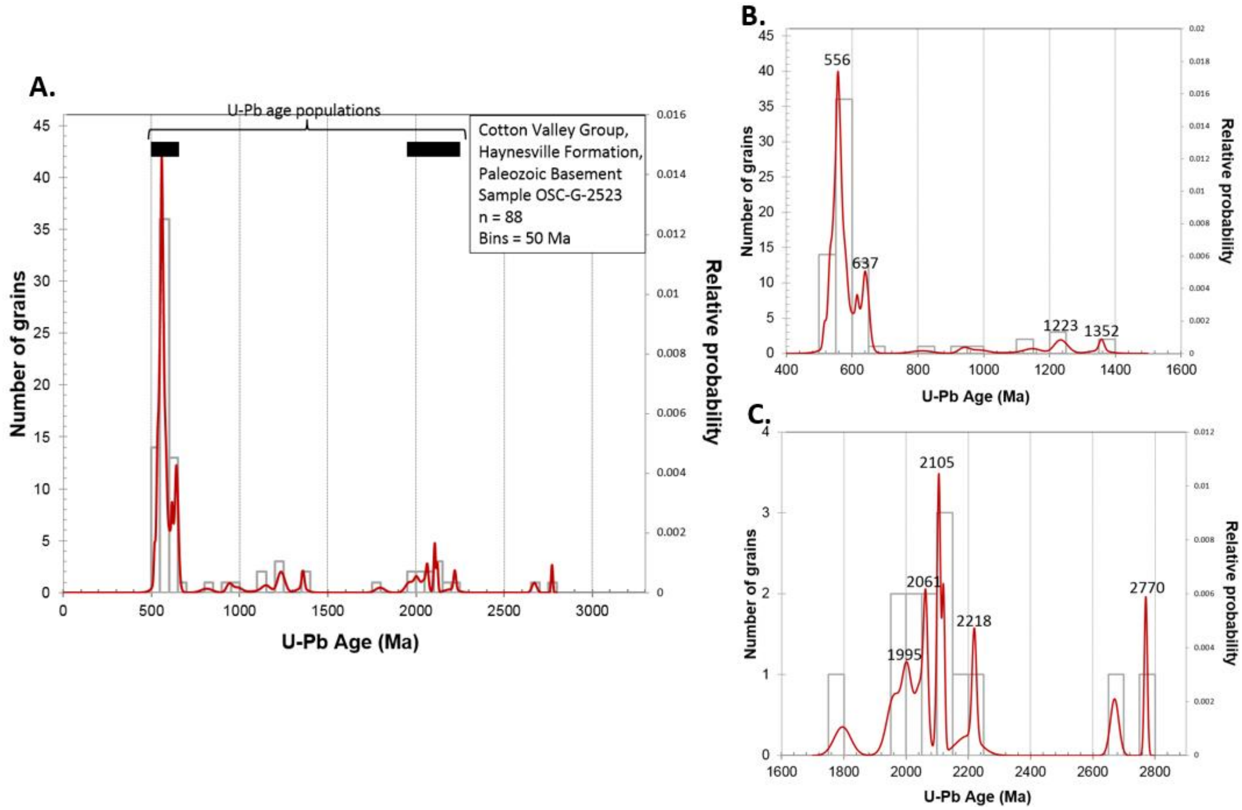

Figure 26. A) Relative probability density curve (red) and histogram in 50 Ma bins showing results of the Cotton Valley Group, Haynesville Formation, and Paleozoic basement from sample OCS-G-2523. B) 400-1600 Ma age range. C) 1600-2900 Ma age range.

4.1.9 Sample P383 – Paleozoic Basement

Sample P383 came from the Florida State offshore waters east of the Gainesville offshore lease block and was sampled from core chips and cuttings within the Paleozoic basement over a 220 foot thick interval. The core chips consisted of sandstone and quartzite and the cuttings consisted of quartzite, shale, and siltstone (Fig. 27).

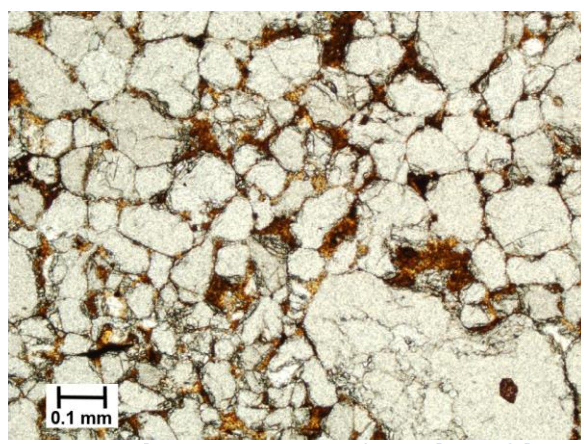

Figure 27. Thin-section image of core chips of the Paleozoic basement from sample P383 consisting of sandstone in plane polarized light.

Analysis of sample P383 provided 88 reliable U-Pb ages; one was removed for high ^{204}Pb, one for discordance, and ten for reverse discordance. The age range of this sample is from 526.2 Ma (+/- 4.9 Ma) to 2799.8 Ma (+/- 3.7 Ma) (Fig. 28A). The majority of U-Pb ages range between 500-700 Ma (50%; Fig. 28B), 800-1900 Ma (40%; Fig. 28B), and 1950-2200 Ma (7%; Fig. 28C). Unlike the Florida Middle Ground and St. Petersburg sample, P383 has three prominent age populations; 500-700 Ma (peaks at 550, 626 and 652 Ma), 950-1350 Ma (two peaks at 1013 Ma and 1214 Ma; Fig. 28B), and 1950-2200 Ma (peaks at 1990, 2050, 2133, and 2155 Ma; Fig. 28C).

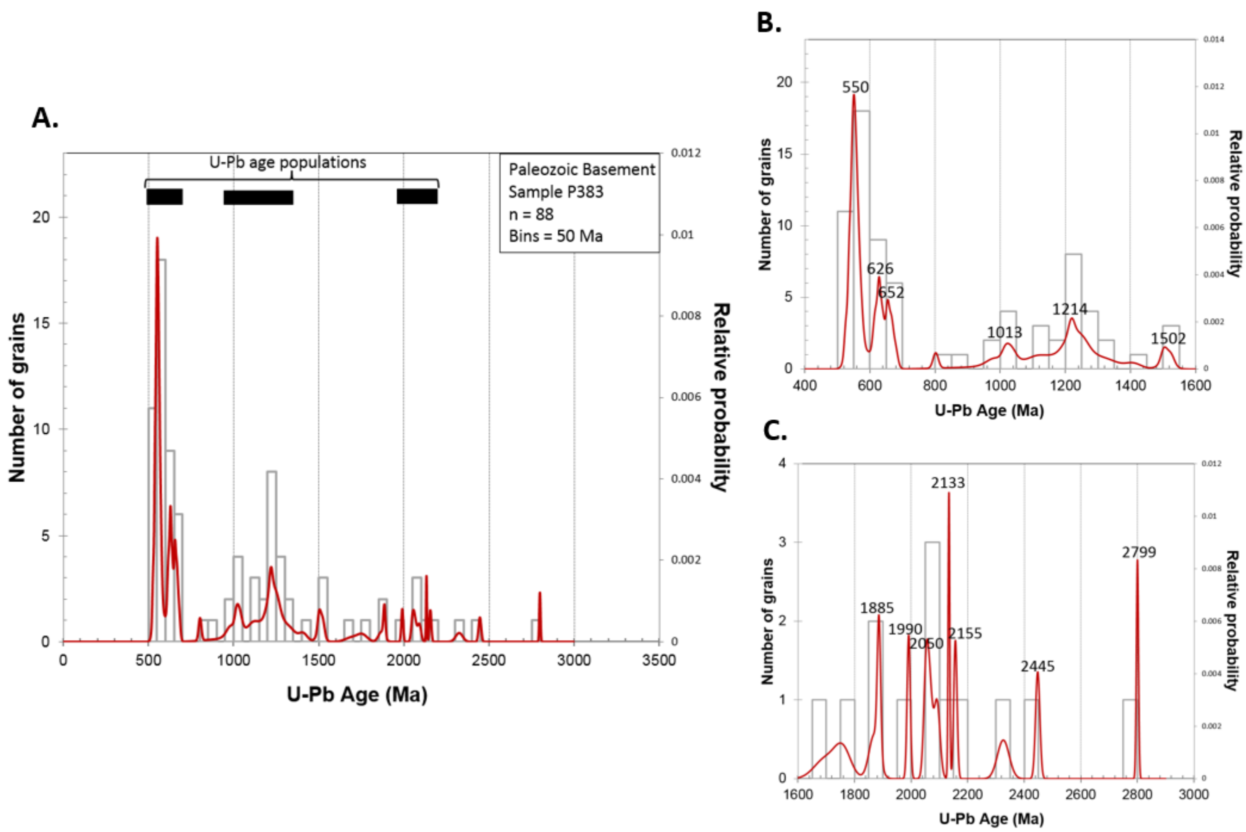

Figure 28. A) Relative probability density curve (red) and histogram in 50 Ma bins showing results of the Paleozoic basement from sample P383. B) 400-1600 Ma age range. C) 1600-3000 Ma age range.

4.1.10 Sample P382 – Paleozoic Basement

Sample P382 came from the Florida State offshore waters east of the Tarpon Springs offshore lease block and was sampled from core chips within the Paleozoic basement over an 11 foot thick interval. The core chips consisted of quartzite, shale, and siltstone (Fig. 29).

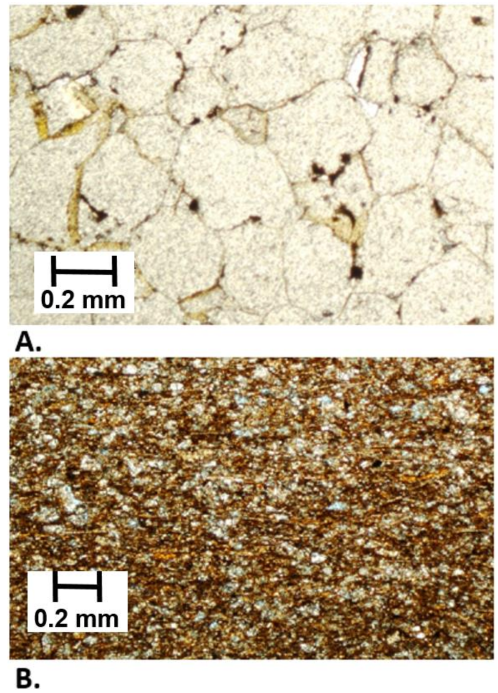

Figure 29. Thin-section images of the Paleozoic basement from sample P382 in plane polarized light. A) Quartzite from 6,046 ft. B) Shale from 6,044 ft.

Analysis of the sample P382 provided 85 reliable U-Pb ages, one was removed due to high $^{206}Pb/^{207}Pb$ error, six for high ^{204}Pb, one for discordance, and seven for reverse discordance. The age range of this sample is from 456.4 Ma (+/- 18.1 Ma) to 2605.5 Ma (+/- 9.8 Ma) (Fig. 30A). The majority of U-Pb ages range between 450-650 Ma (51%; Fig. 30B), 800-1600 Ma (16%; Fig. 30B), and 1750-2350 Ma (28%; Fig. 30C). Similar to sample P383 to the north, P382 has three prominent age populations; 450-650 Ma (peaks at 493, 553 and 620 Ma), 950-1200 Ma (two peaks at 983 Ma and 1067 Ma; Fig. 30B), and 2050-2250 Ma (age peaks at 2095, 2121, 2160, 2188, and 2218 Ma; Fig, 30C). However, P382 has a small age population from 1750-1900 Ma with peaks at 1785 Ma and 1889 Ma that is not present in any of the other samples.

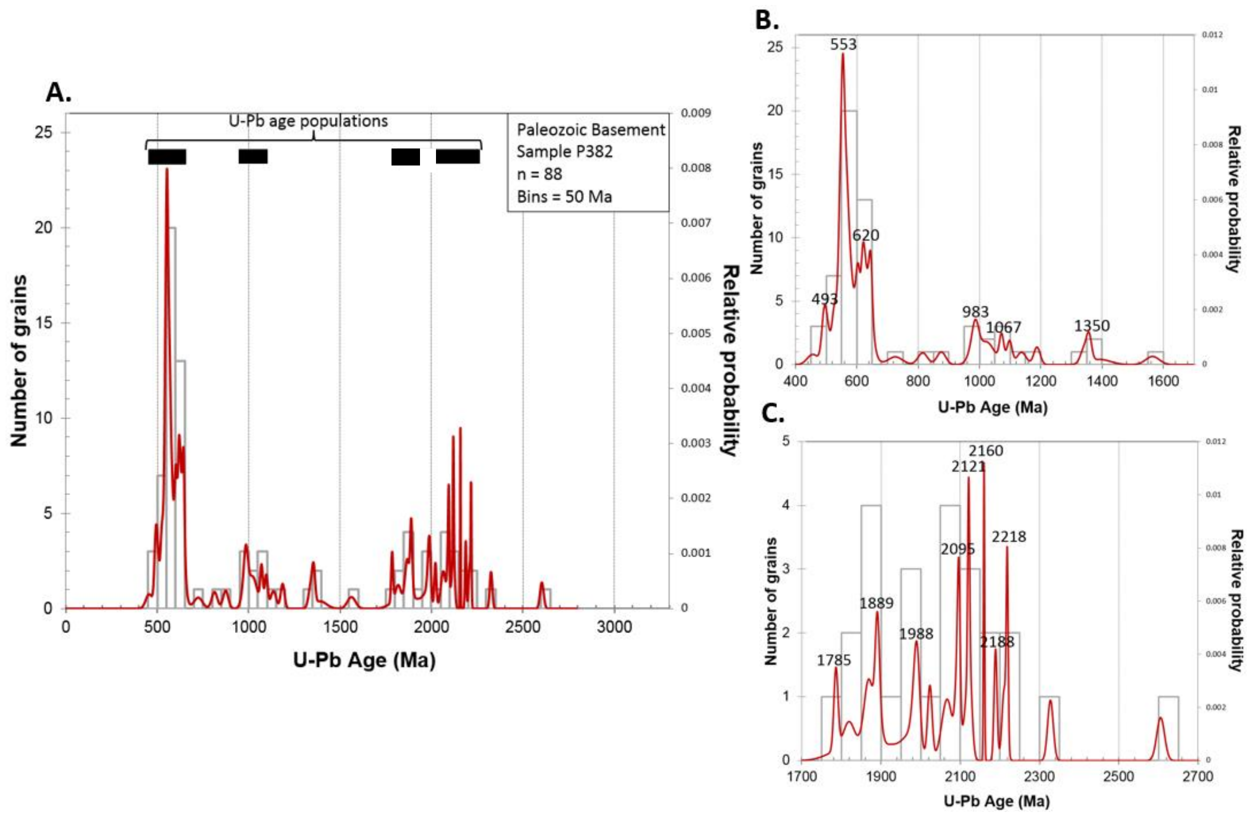

Figure 30. A) Relative probability density curve (red) and histogram in 50 Ma bins showing results the Paleozoic basement from sample P382. B) 400-1700 Ma age range. C) 1700-2700 Ma age range.

4.2 Shared Age Populations and Peak Age Correlation

The ten samples show several major and overlapping U-Pb age populations. Figure 31 shows normalized relative probability plots of the ten samples. This figure highlights the similarity of the four southeastern samples OCS-G-2516, OCS-G-2523, P383 and P382 and their overall difference from the other six samples. Figure 32 shows the cumulative age populations (as black boxes) from figures 11-15, 17-20, and 22 for comparison. The predominant age groups include 250-500 Ma, 500-700 Ma, 900-1400 Ma, and 1950-2250 Ma. The youngest age group from 250-500 Ma is shared between the Florida Panhandle wells (P1004, P1096, and P1080), Mobile Bay (MO, OCS-G-6848), Destin Dome (DD, OCS-G-6406), and Pensacola (PE, OCS-G-6396) samples. The 500-700 Ma zircon age population is shared between all samples

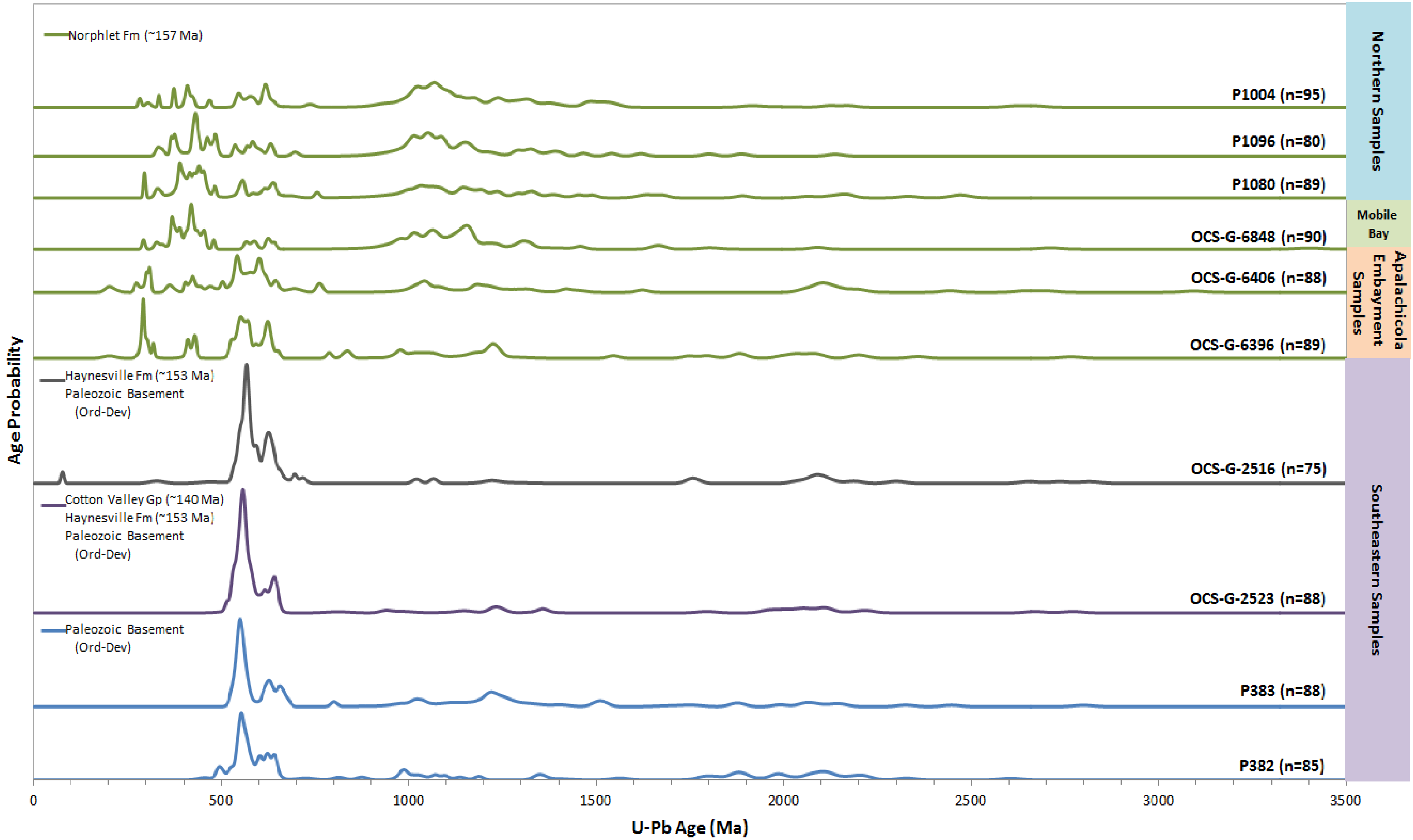

Figure 31. Cumulative relative probability plots for all 10 detrital zircon samples. Green line indicates a Norphlet Formation samples, gray indicates Haynesville Formation and basement, purple indicates Cotton Valley Group, Haynesville Formation, and basement, and blue indicates Paleozoic basement.

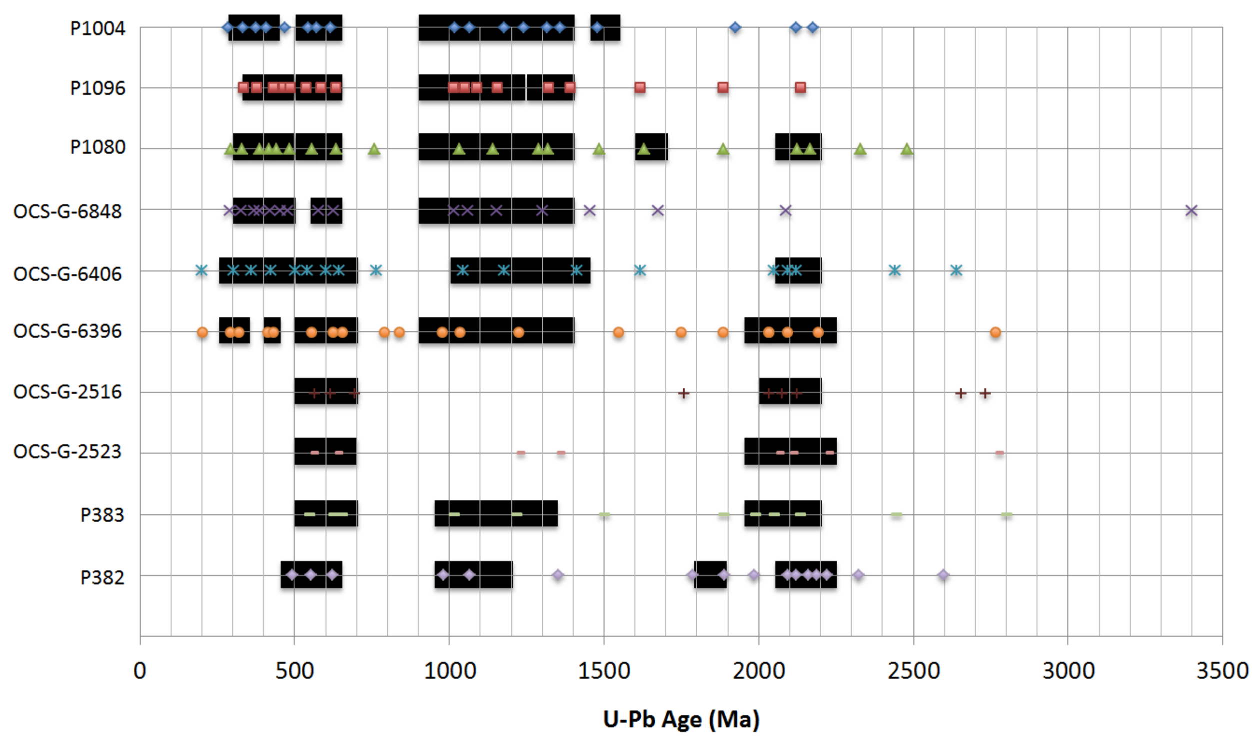

Figure 32. Prominent U-Pb age populations for each sample (black box) with age peaks that occur within relative probability curves.

and overall increases in abundance southward. Age group 900-1400 Ma is particularly abundant in the northern study area and is shared by all samples with the exception of the Florida Middle Ground (FMG, OCS-G-2516) and St. Petersburg (STPB, OCS-G-2523) samples.

Table 2. Table of the four most abundant U-Pb age populations and samples that contain those populations.

U-Pb Age Population	Samples
250-500 Ma	P1004 (12%), P1096 (26%), P1080 (33%), MO (30%), DD (19%), PE (19%)
500-700 Ma	P1004 (15%), P1096 (13%), P1080 (13%), MO (7%), DD (35%), PE (37%), FMG (72%), STPB (73%), P383 (50%), P382 (47%)
900-1400 Ma	P1004 (60%), P1096 (53%), P1080 (38%), MO (56%), DD (23%), PE (22%), P383 (28%), P382 (15%)
1950-2250 Ma	P1080 (6%), DD (13%), PE (9%), FMG (9%), STPB (13%), P383 (7%), P382 (18%)

The oldest age group, 1950-2250 Ma, is overall the least abundant and exists in all samples except P1004, 1096, and MO (Table 2). Overlaying the age populations in figure 24 are the age peaks that occur within the samples. The U-Pb age peaks within a single sample often overlap with peaks in other samples likely indicating a similar provenance. The peaks between samples are identified as overlapping if they are within 5 Ma of each other.

Figure 33 shows the various U-Pb age peaks from 200-800 Ma. The orange rectangles group together age peaks within 5 Ma of each other. Between 200 and 500 Ma, samples P1004, P1096, P1080, OCS-G-6848, OCS-G-6406, and OCS-G-6396 have 12 correlatable peaks. However, samples OCS-G-2516, OSC-G-2523, P383, and P382 lack any correlative age peaks younger than 500 Ma. In fact, only one age peak at 493 Ma from sample P382 is younger than 500 Ma. The youngest correlative age peaks are Triassic (201-202 Ma) and occur in the Destin Dome and Pensacola samples which lie within the Apalachicola Embayment. Other correlative peaks that occur between 250-500 Ma include 292-295 Ma (P1080, OCS-G-6848, and OCS-G-6396), 325-328 Ma (P1080 and OCS-G-6848), 328-332 Ma (P1096 and P1080), 332-334 Ma

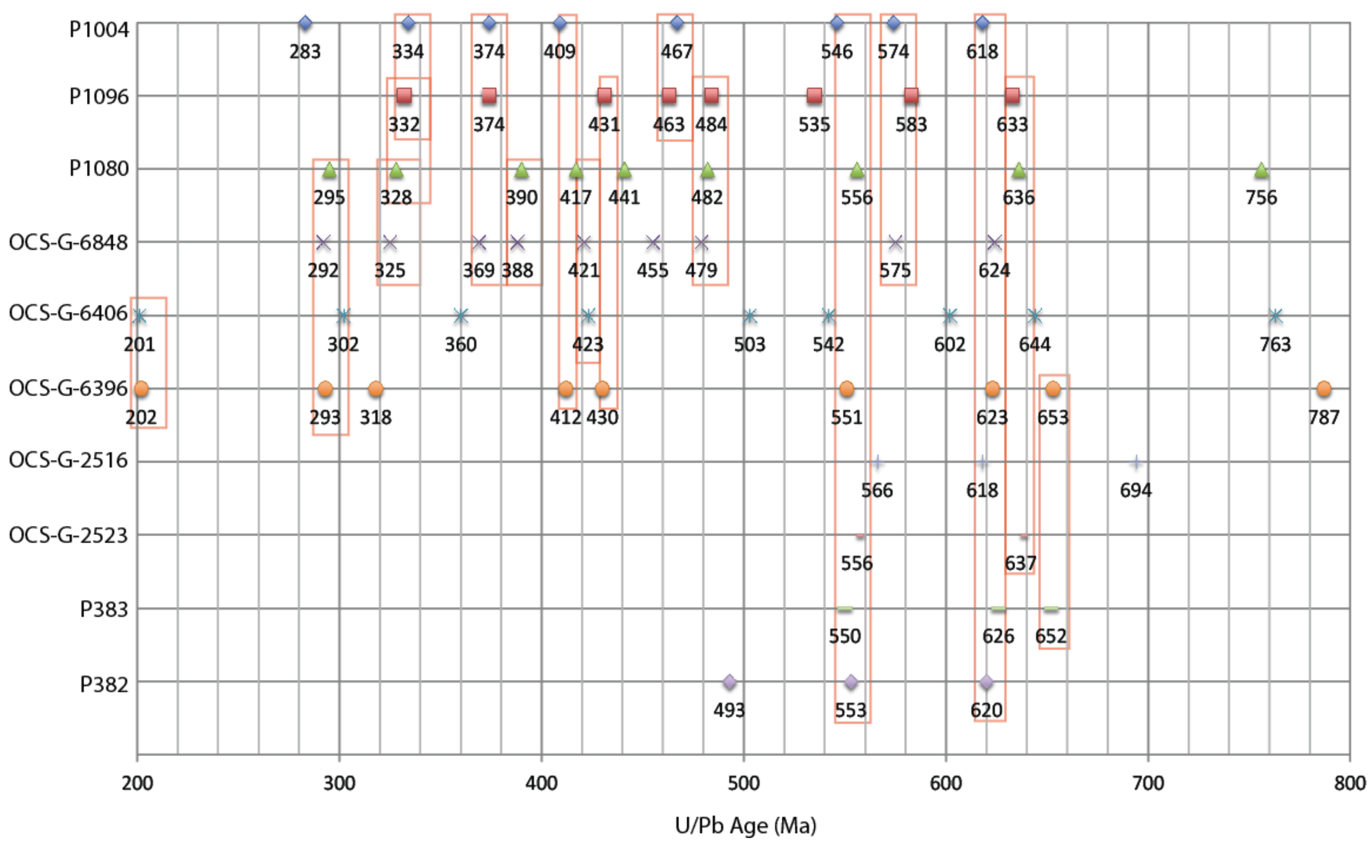

Figure 33. U-Pb age population peaks from 200-800 Ma that occur within the samples. Orange boxes show overlapping peaks within 5 Ma of each other that occur across samples.

(P1004 and P1096), 369-374 Ma (P1004, P1096, and OCS-G-6848), 388-390 (P1080 and OCS-G-6848), 409-412 Ma (P1004 and OCS-G-6396), 417-423 Ma (P1080, OCS-G-6846, and OCS-G-6406), 430-431 Ma (P1096 and OCS-G-6396), 463-467 Ma (P1004 and P1096), and 479-484 Ma (P1096, P1080, and OCS-G-6848).

Several ages peaks within the 500-700 Ma age population are correlatable between samples. These include 546-556 Ma (P1004, P1080, OCS-G-6396, OCS-G-2523, P383, and P382), 574-575 Ma (P1004 and OCS-G-6848), 618-626 Ma (P1004, OCS-G-6848, OCS-G-6396, OCS-G-2516, P383, and P382), 633-637 Ma (P1096, P1080, and OCS-G-2523), and 652-653 Ma (OCS-G-6396 and P383). The age peaks with the greatest number of correlative samples are 546-556 Ma and 618-626 Ma which each contain six samples.

The age population 900-1400 Ma contains eight correlatable age peaks (Fig. 34). These include 1011-1013 Ma (P1096, OCS-G-6848, and P383), 1030-1031 Ma (P1080 and OCS-G-6396, 1060-1065 Ma (P1004 and OCS-G-6848), 1152-1154 Ma (P1096 and OCS-G-6848), 1177 Ma (P1004 and OCS-G-6404), 1221-1223 Ma (OCS-G-6396 and OCS-G-2523), 1315-1320 Ma (P1004, P1096, and P1080), and 1350-1352 Ma (OCS-G-2523 and P382).

The oldest age population 1950-2250 Ma contains nine correlatable age peaks (Fig. 35). These include 1988-1990 Ma (P383 and P382), 2032-2037 Ma (OCS-G-6396 and OCS-G-2516), 2050 Ma (OCS-G-6406 and P383), 2088-2092 Ma (OCS-G-6848 and OCS-G-6396), 2092-2095 Ma (OCS-G-6406, OCS-G-6396, P382), 2121-2125 Ma (P1004, P1080, OCS-G-6406, OCS-G-2516, and P382), 2133-2134 Ma (P1096 and P383), 2188-2192 Ma (OCS-G-6396 and P382), and 2218 Ma (OCS-G-2523 and P382). The age peak at 2121-2125 Ma has the greatest abundance of

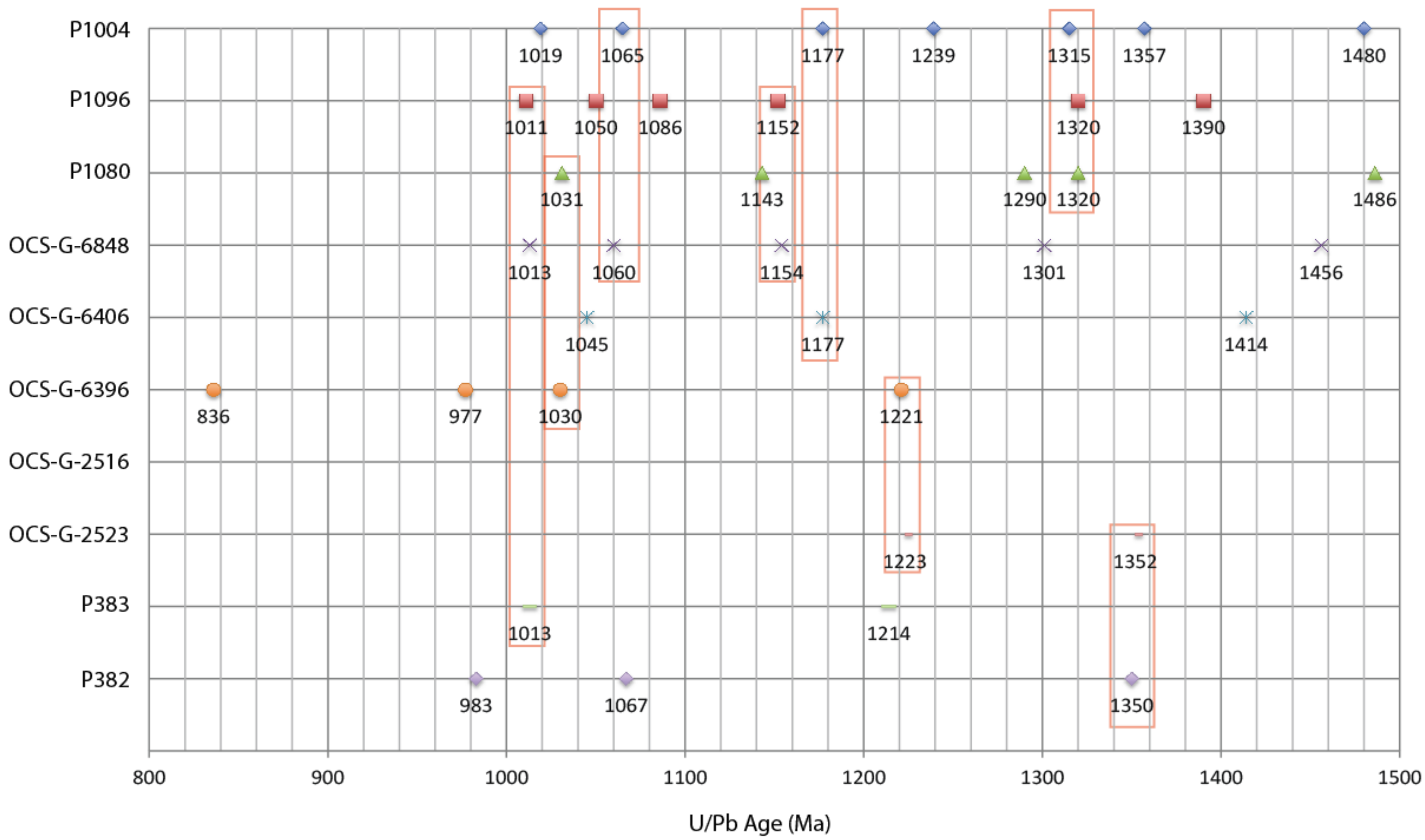

Figure 34. U-Pb age population peaks from 800-1500 Ma that occur within the samples. Orange boxes show overlapping peaks within 5 Ma of each other that occur across samples.

correlative samples with five samples containing this age peak that span the Florida Panhandle, Destin Dome, Florida Middle Ground, and offshore Florida peninsula samples.

Other correlatable age peaks that occur outside of the major age populations include 1616-1620 Ma (P1096 and OCS-G-6406); 1881-1889 Ma (P1096, P1080, OCS-G-6396, P383, and P382), 2443-2445 Ma (OCS-G-6406 and P383), and 2766-2770 Ma (OCS-G-6396 and OCS-G-2523). The 1881-1889 Ma age peak occurs in five samples which include P1096, P1080, Pensacola, and offshore Florida peninsula.

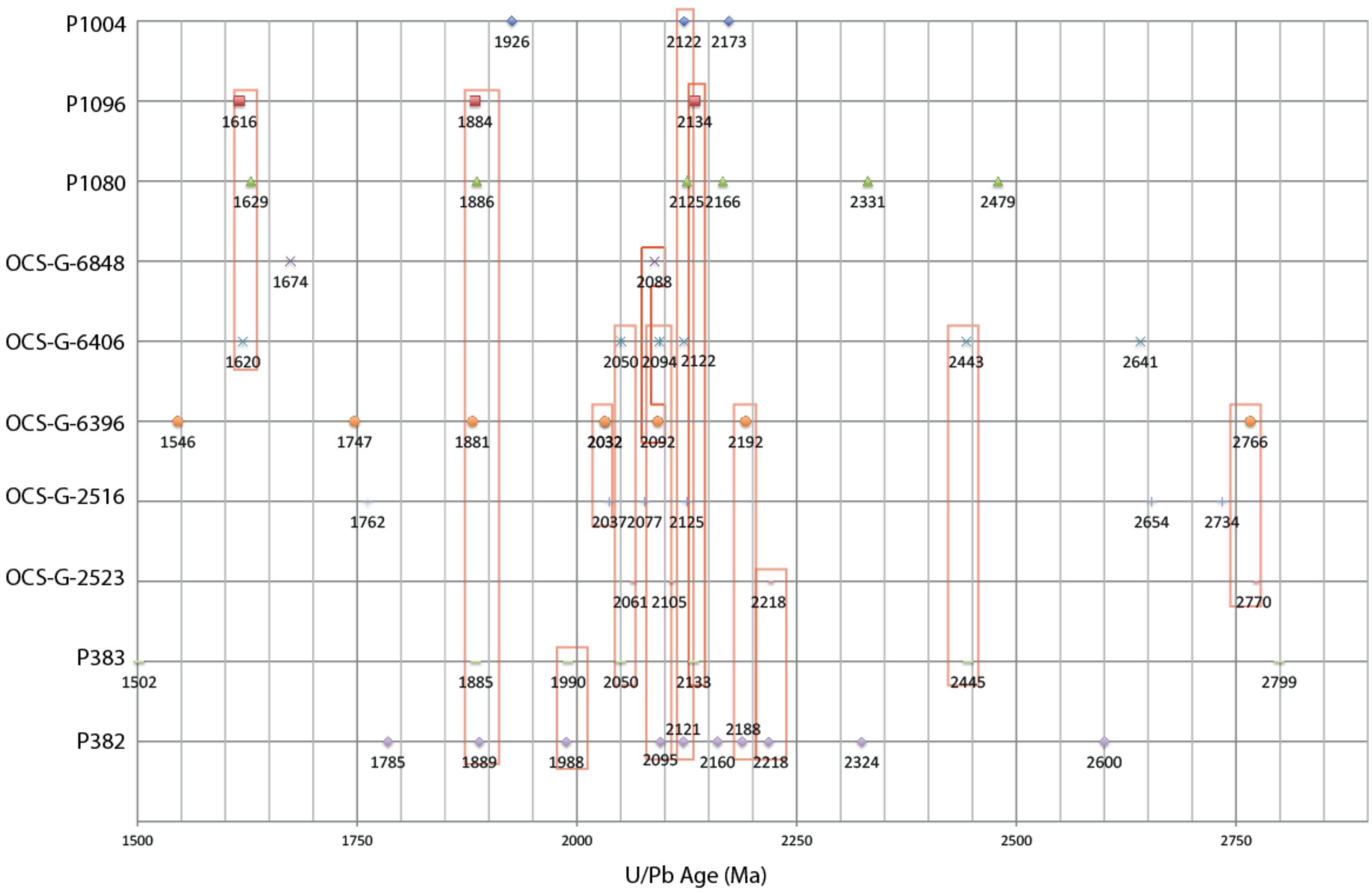

Figure 35. U-Pb age population peaks from 1500-2900 Ma that occur within the samples. Orange boxes show overlapping peaks within 5 Ma of each other that occur across samples.

4.3 Metamorphic Zircon Populations

Several metamorphic zircon age populations were identified based on U/Th ratios of zircon greater than four (Fig. 36). Sample P1004 had a single metamorphic zircon at 411 Ma and 1913 Ma as well as a group of metamorphic zircon between 989 Ma and 1256 Ma. Sample P1096 similarly has a group of metamorphic zircon ages between 1010 Ma and 1157 Ma but also a group at 375-377 Ma. Single metamorphic zircons occur at 629 Ma and 1310 Ma. Sample P1080 has one group of metamorphic zircons between 327 Ma and 457 Ma and a single metamorphic zircon at 584 Ma. Sample OCS-G-6848 from Mobile Bay has two populations of metamorphic zircon at 390– 439 Ma and 978-1189 Ma. The Destin Dome sample OCS-G-6406 has two groups of metamorphic zircons that occur at 533-615 Ma and 2050-2093 Ma. Single metamorphic zircons occur at 767 Ma, 1006 Ma, 1179 Ma, and 2443 Ma.

The Pensacola sample, OCS-G-6396, has only two single metamorphic zircon at 1031 Ma and 561 Ma. The sample from the Florida Middle Ground, OCS-G-2516, has two metamorphic zircon populations at 567-623 Ma and 2038-2084 Ma. It also has two single metamorphic zircons at 1066 Ma and 2735 Ma. Sample OCS-G-2523 from St. Petersburg has one metamorphic zircon population from 529-645 Ma and a single metamorphic zircon at 2063 Ma. Sample P382 from offshore Florida has three single metamorphic zircon at 633 Ma, 1392 Ma, and 2067 Ma. The other offshore Florida sample, P383, has a single metamorphic zircon at 1035 Ma and a metamorphic population from 526-550 Ma.

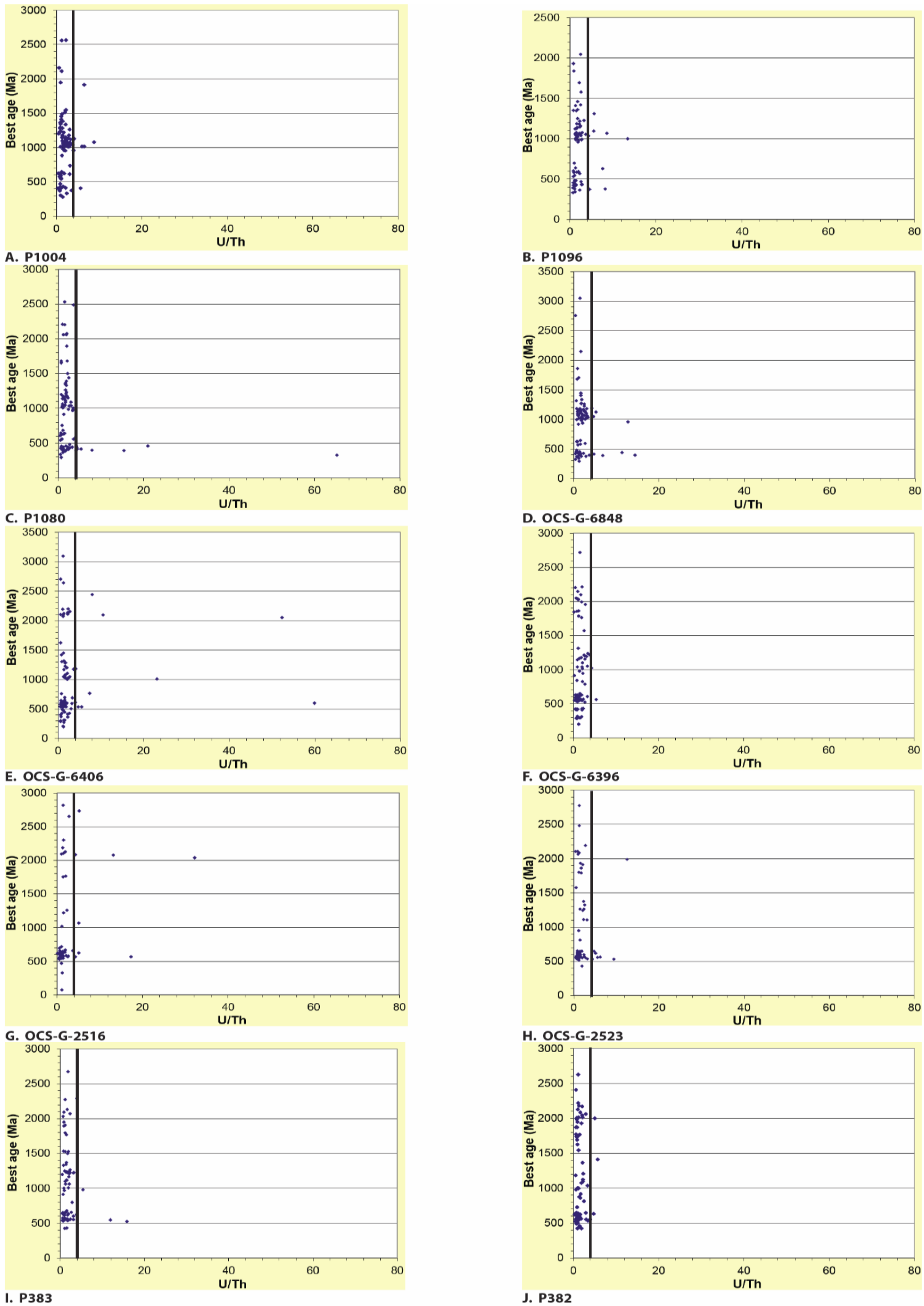

Figure 36. U-Pb age vs. U/Th plots. Black line indicates a U/Th ratio of 4. A ratio greater than 4 indicates a metamorphic zircon.

Several samples share similar metamorphic zircon populations. Four distinct metamorphic populations occur throughout the samples. The youngest metamorphic zircon population is between 327-460 Ma and includes P1004, P1096, P1080, and OCS-G-6848. Samples P1096, P1080, OCS-G-6406, OCS-G-6396, OCS-G-2516, OCS-G-2523, P382, and P383 share a population between 526-645 Ma. Samples P1004, P1096, OCS-G-6848, OCS-G-6406, OCS-G-6396, OCS-G-2516, and P383 share metamorphic zircons from 978-1256 Ma. The oldest metamorphic zircon population occurs from 2038-2093 Ma and includes samples OCS-G-6406, OCS-G-2516, OCS-G-2523, and P382 (Fig. 37).

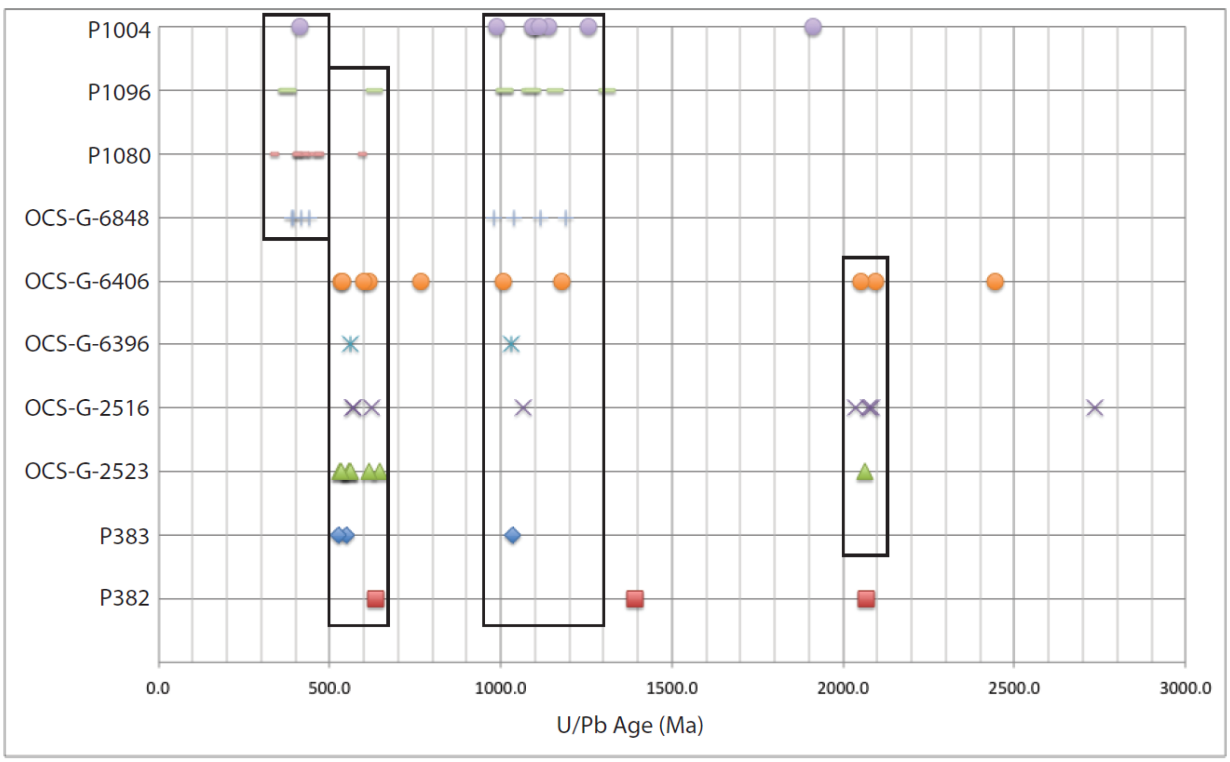

Figure 37. Ages of metamorphic zircons for all samples. Boxes group metamorphic zircons into age populations (300-500 Ma, 500-680 Ma, 950-1300 Ma, and 2000-2125 Ma).

4.4 Regions of Similar U-Pb Age Distribution

Samples are grouped based on similarity in grain age abundances, age peaks, and metamorphic zircon populations. From these attributes, four groups were identified, the Florida Panhandle samples, Mobile Bay sample, Apalachicola Embayment samples, and the southeastern GOM samples. Figure 38 shows the spatial distribution of the wells with similar age distribution.

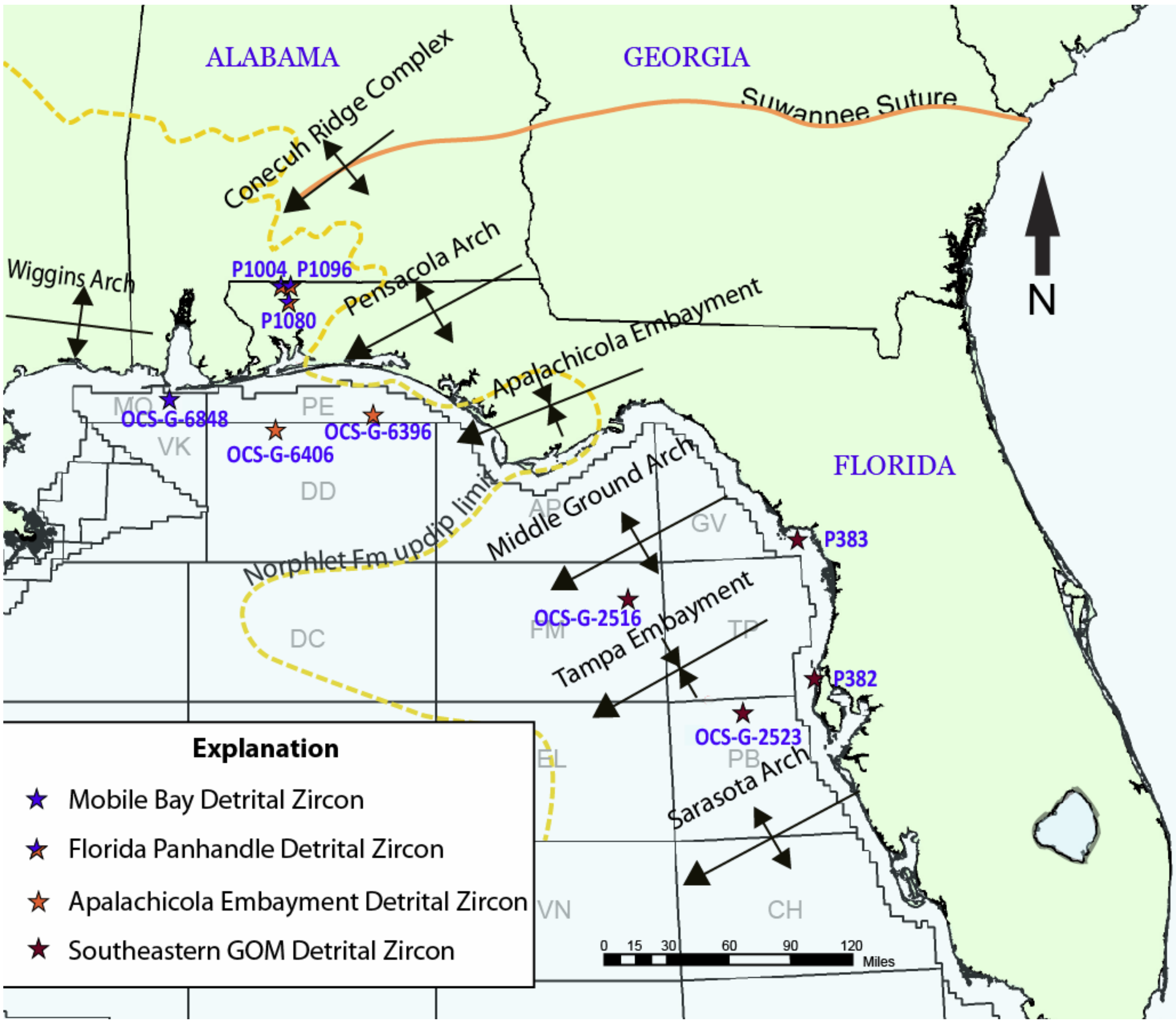

Figure 38. Samples with similar detrital zircon U-Pb age distributions. Four areas were identified including those in the Florida Panhandle (blue/purple), Mobile Bay (blue), Apalachicola Embayment (purple), and southeastern Gulf of Mexico (red).

4.4.1 Florida Panhandle

The U-Pb ages from the Florida Panhandle samples (P1004, P1096, and P1080) all share similar characteristics. The majority of all zircon ages fall between 250-650 Ma (26-45%) and 900-1550 Ma (40-66%). The samples also share similar zircon abundances between 500-700 Ma (11-15%) as well as between 1900-2250 Ma (0-1%). Samples P1004 and P1080 share peaks at 374 Ma and 463-467 Ma. Samples P1096 and P1080 share peaks at 633 Ma and 1884-1886 Ma. Samples P1004 and P1080 share an age peak at 2122-2125 Ma. All samples share an age peak at 1315-1320 Ma. These samples also share metamorphic zircon populations between 300-500 Ma and P1004 and P1096 share metamorphic zircons between 950-1300 Ma.

4.4.2 Mobile Bay

Well OCS-G-6848 differs from many of the other samples due to the large amount of grains within 900-1400 Ma (56%) and small abundance of grains between 500-700 Ma (7%) and 1900-2250 Ma (1%). However, this sample shares several of its major age peaks with other samples, predominantly those from the Florida Panhandle. These include: 367-374 Ma with P1004 and P1096, 417-423 Ma with P1080 and OCS-G-6406, 1011-1013 Ma with P1096 and OCS-G-2523, and 1152-1154 Ma with P1096. This sample also shares a metamorphic zircon population with the Florida Panhandle wells between 300-500 Ma as well as between 950-1300 Ma.

4.4.3 Apalachicola Embayment

Zircon age populations are also similar for wells OCS-G-6406 and OCS-G-6396. These two wells have the youngest aged zircons (3 grains) with a shared peak at 201-202 Ma. They also have a larger abundance of grains between 500-700 Ma (33-37%) than the previously mentioned samples. These two samples only share one age peak (2092-2094 Ma) but share three metamorphic zircon age populations, 500-700 Ma, 950-1300 Ma, and 2000-2150 Ma.

4.4.4 Southeastern Gulf of Mexico

The southeastern samples are the wells that do not contain Norphlet but contain collectively the Jurassic Cotton Valley Group, Haynesville Formation, and the Paleozoic basement. These samples are also drastically different from the previous samples and quite similar to each other. The greatest abundances of grains for these samples occur between 500-700 Ma (45-72%). Within this range, samples OCS-G-2523, P383, and P382 share the 550-551 age peak and OCS-G-2516, P383, and P382 share the 618-626 age peak. These samples also share a smaller age population between 1900-2250 Ma (7-20%). Shared metamorphic zircon populations include 500-700 Ma and 2000-2150 Ma.

4.5 Grain Size Analysis

The result of Evan Knight's detrital zircon grain size analysis showed little correlation between a particular grain size and U-Pb age. Figure 39 shows the results of this work with histograms of grain size distribution for each sample and age vs. grain size plots for each sample. The highlighted section on the age vs. grain size plot is meant to represent the Grenville mountain building event (900-1400 Ma). It has been speculated that Grenville-aged zircons are generally larger, however, this analysis does not show a correlation.

Similarities seen in the various samples include the Florida Panhandle wells (P1004, P1096, and P1080) which have similar tri-modal zircon size distributions and zircon grain-size range. Samples OCS-G-6406 (DD) and OCS-G-6396 (PE) also have similar bimodal distributions with two peaks occurring at 15 and 17-18 mm. Sample OCS-G-2516 (FMG) and P382 both have a uni-modal distribution and have a smaller overall grains size (mean of 10-11mm).

Histogram

Age vs. Grain Size

P1004

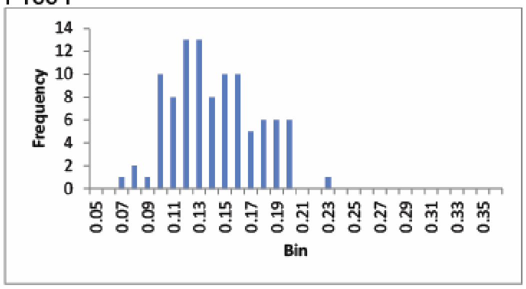

Mean: 0.14
Median:0.14
Standard Dev.:0.03
Kurtosis -0.32
Skewness:0.26

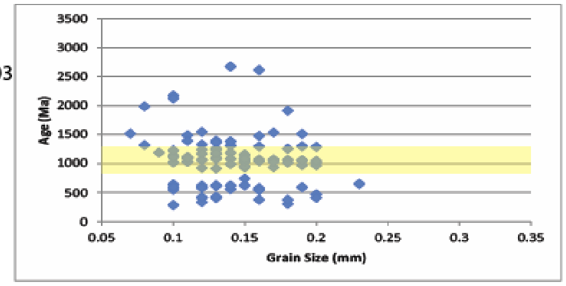

P1096

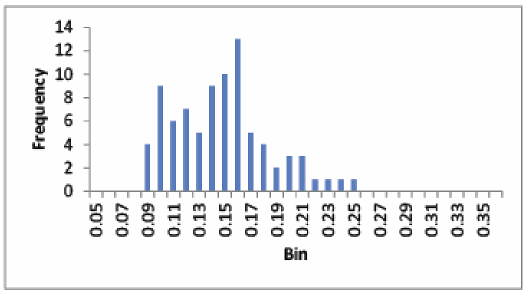

Mean: 0.13
Median:0.13
Standard Dev.:0.03
Kurtosis :-0.62
Skewness:0.45

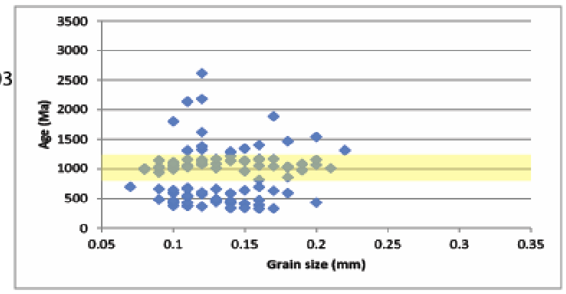

P1080

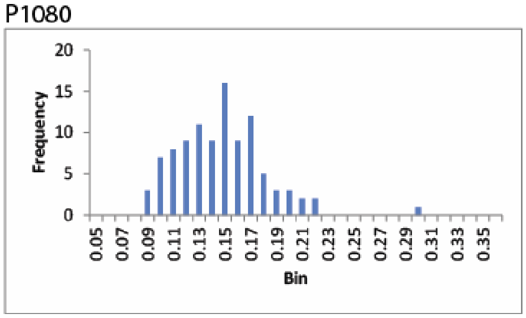

Mean: 0.15
Median:0.15
Standard Dev.:0.04
Kurtosis :0.02
Skewness:0.54

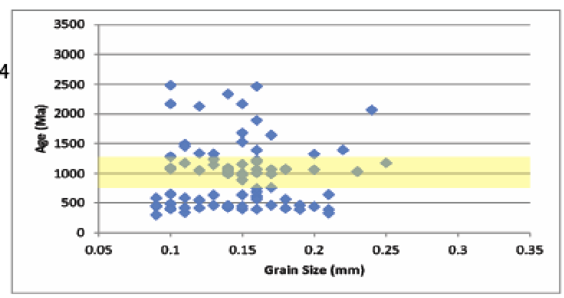

OCS-G-6406

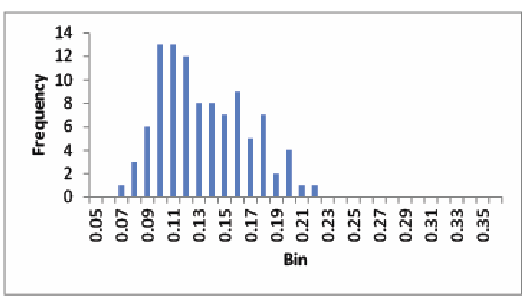

Mean: 0.14
Median:0.15
Standard Dev.:0.03
Kurtosis :2.88
Skewness:0.99

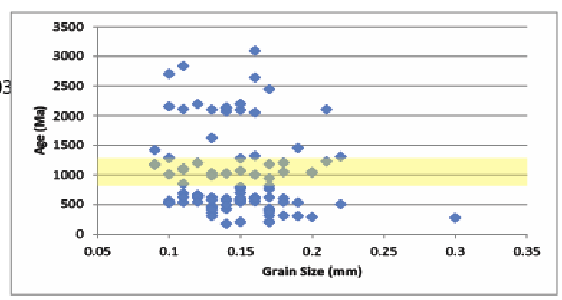

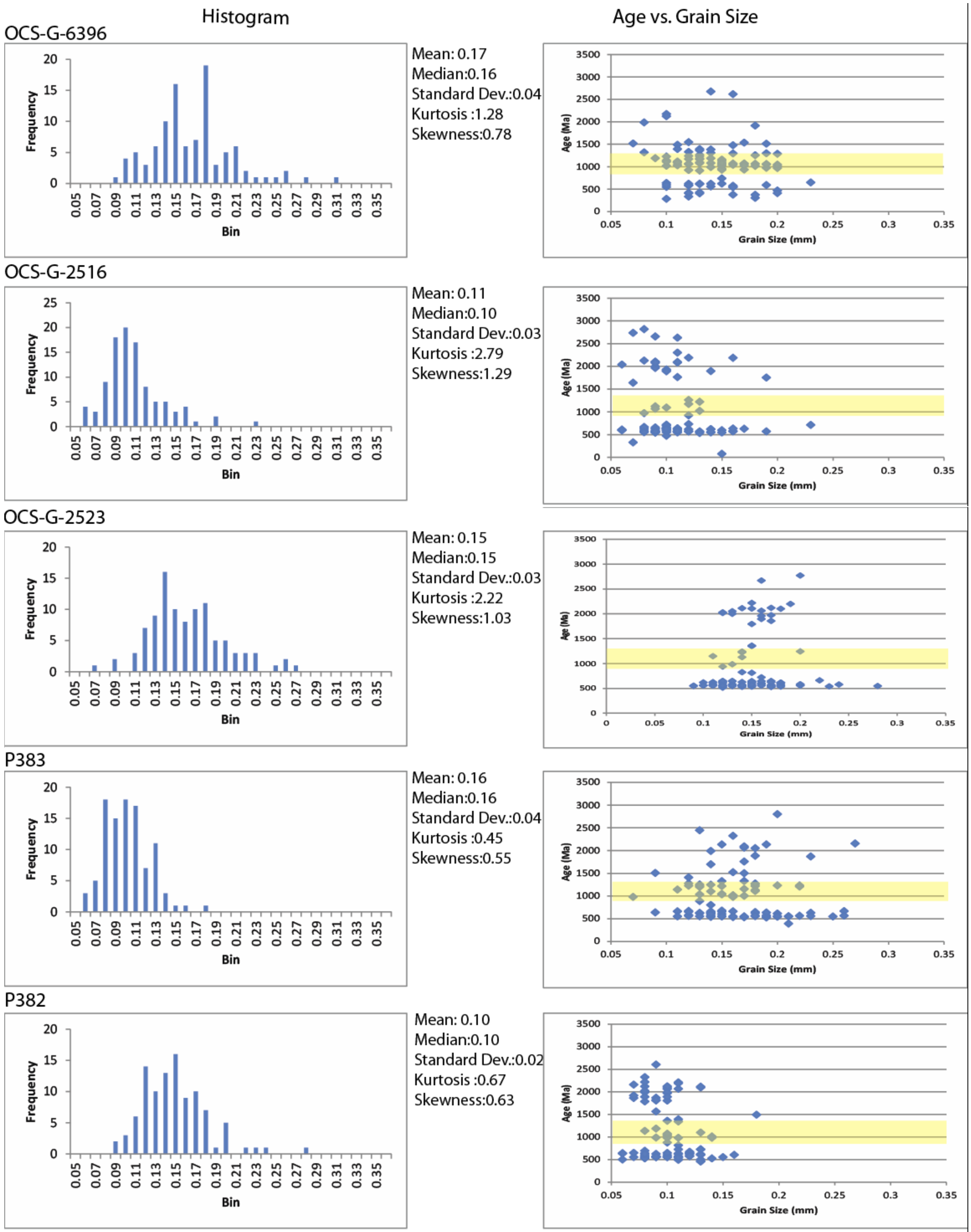

Figure 39. Detrital zircon grain size analysis. Histogram of grain sizes for each sample is on the left. Age vs. grain size plots are on the right. Yellow area highlights the Grenville-age zircon population (900-1400 Ma) which illustrates the low correlation of the Grenville event to a specific size.

4.6 Norphlet Sandstone Composition

The results from point counting eleven thin-sections from five wells shows a range of sandstone compositions that include subarkose, arkose, and lithic arkose (Fig. 40; Folk, 1980). Subarkose is the most abundant sandstone composition which is represented by seven samples classified. Three samples are classified as arkose and only one sample is classified as lithic arkose. The framework grains identified in the eolian facies of the Norphlet Formation include quartz (monocrystalline, undulose and non-undulose, and polycrystalline), feldspar (orthoclase, un-twinned plagioclase, and twinned plagioclase), and lithic grain fragments (sedimentary, metamorphic, and volcanic; Fig. 41).

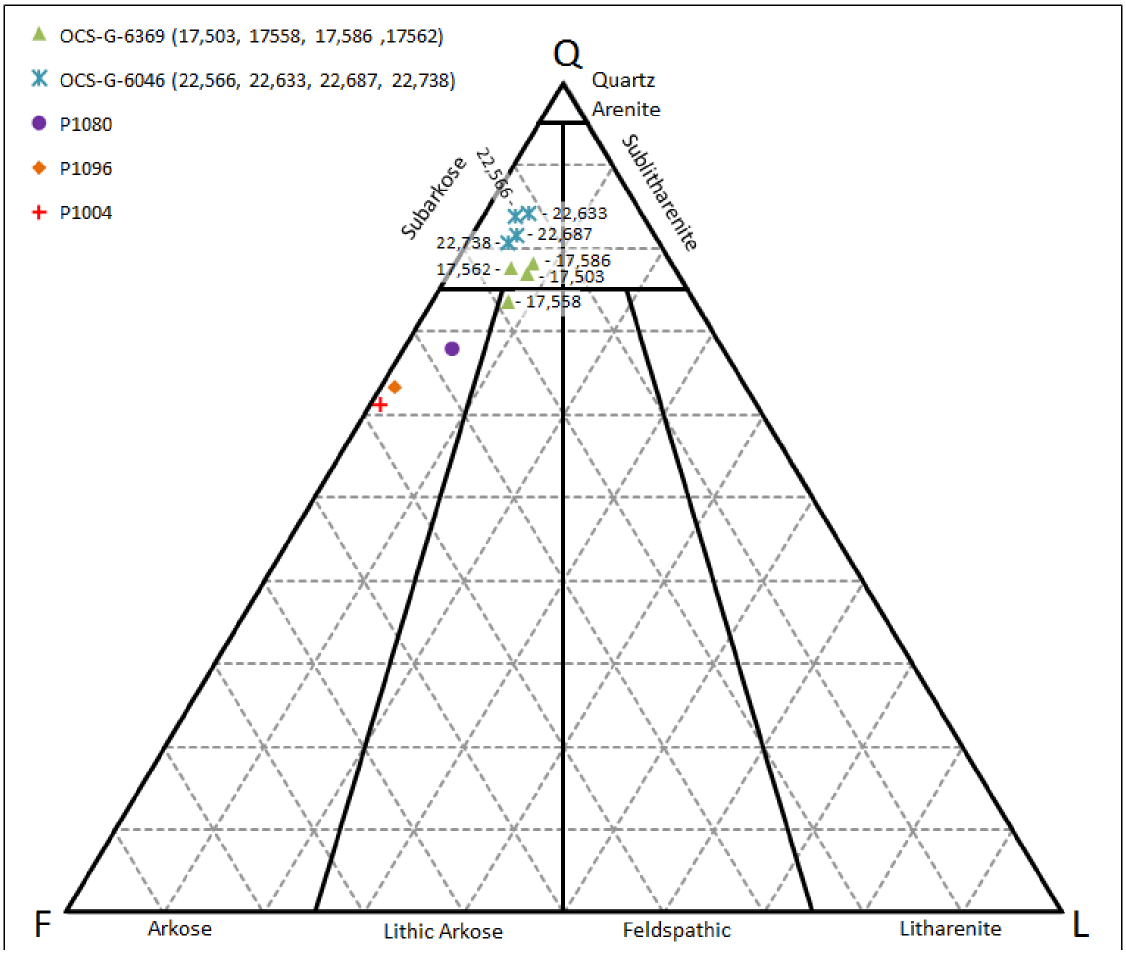

Figure 40. QFL plot of the eolian facies of the Norphlet Formation. Samples are predominantly subarkose with some arkose and one lithic arkose (Folk, 1980).

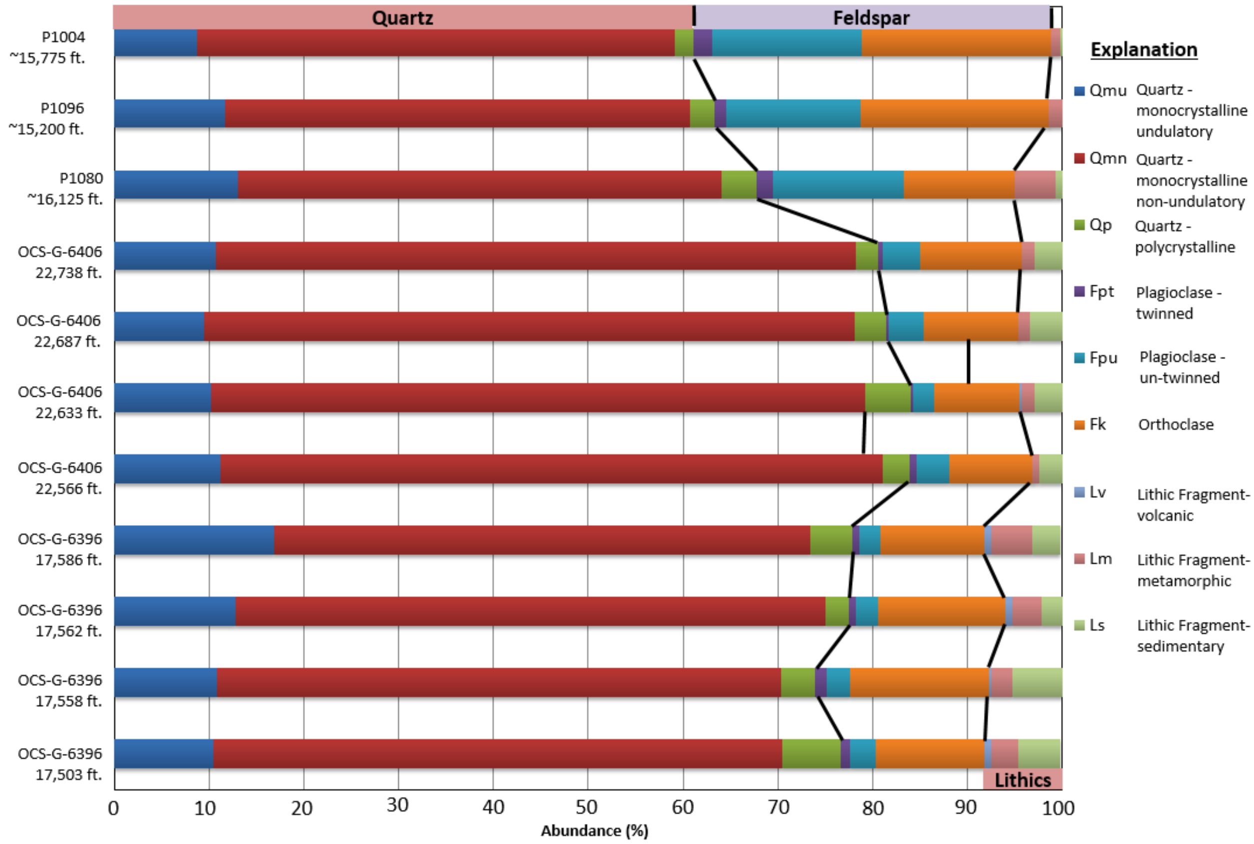

Figure 41. Relative abundances of framework grains for the eolian facies of the Norphlet Formation from modal analysis. Quartz grains include monocrystalline, undulatory (Qmu) and non-undulatory (Qmn), and polycrystalline (Qp). Feldspar grains include plagioclase, twinned (Fpt) and un-twinned (Fpu), and orthoclase (Fk). Lithic rock fragments include volcanic (Lv), metamorphic (Lm), and sedimentary (Ls). Exact depths for samples P1004, P1096, and P1080 are unknown but core chips throughout each sample interval remained lithologically similar.

The most abundant framework-grain type in the eolian facies of the Norphlet Formation is quartz and ranges from 61% (P1004) to 84% (OCS-G-6406). The most common type of quartz is monocrystalline with little to no undulatory extinction (Qmn) and it makes up 73% (OCS-G-6396) to 84% (OCS-G-6406) of the quartz grain population and averages 80%. Several of the quartz grains are heavily vacuolized and contain mineral inclusions (Fig. 42 and 43). The second most common quartz type is undulatory, monocrystalline quartz (Qmu). This type ranges from 12% (OCS-G-6406) to 23% (OCS-G-6396) and averages 15%. The least abundant quartz type is polycrystalline (Qp) which ranges from 3% to 8% averaging 4.6%.

The second most abundant framework grain in the eolian facies is feldspar. Feldspars identified include orthoclase (Fk), un-twinned plagioclase (Fpu), and twinned plagioclase (Fpt). For the two wells in Destin Dome and Pensacolsa (OCS-G-6406 and OSC-G-6396), orthoclase is the most abundant feldspar ranging from 67% (OSC-G-6406) to 81% (OSC-G-6396) and averages 75%. The second most common feldspar for the two samples is un-twinned plagioclase and varies from 14% (OCS-G-6396) to 27% (OCS-G-6046) averaging 20%. The least abundant feldspar is twinned plagioclase which averages 5%. For the three wells in the Florida Panhandle, the amount of orthoclase, averaging 51%, is roughly equal to that of plagioclase, averaging 49%. Of the plagioclase population, approximately 90% is made up of un-twinned plagioclase and 10% twinned plagioclase.

The third most abundant framework grains are lithic fragments and include sedimentary lithic fragments (Ls), metamorphic lithic fragments (Lm), and volcanic lithic fragments (Lv). Abundances of the three types of lithic fragments vary from well locations. The most common lithic fragment in the Destin Dome sample (OCS-G-6046) is sedimentary (silty mudstone) averaging 50% followed by metamorphic averaging 42%. The least abundant is volcanic (plagioclase laths in a groundmass) averaging 9%. The Pensacola sample (OCS-G-6396) has similar types of lithic clasts as the Destin Dome sample and is predominantly sedimentary lithic averaging 72% of the lithic population. The metamorphic lithics average 27% while the volcanics only represent 1%. The most abundant lithic grain in the Florida Panhandle is metamorphic and averages 88%. The dominant type of metamorphic rock fragment found in

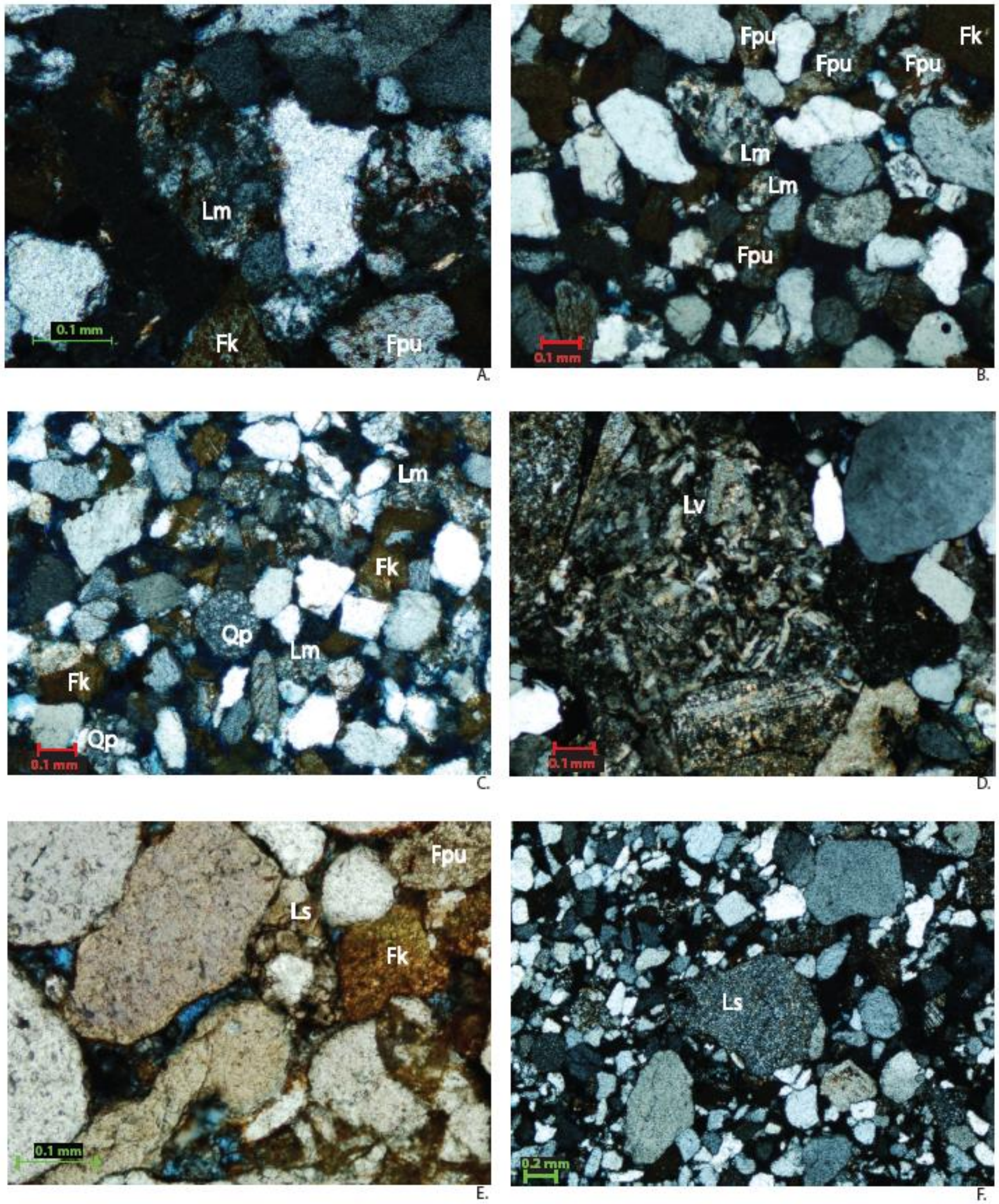

Figure 42. Framework grains in transmitted plane crossed-polarizer light (except E). All thin sections were stained for plagioclase (tinted pink) and orthoclase (tinted yellowish-brown). A) Metamorphic rock fragment surrounded by quartz, plagioclase, and orthoclase (P1004). B) Metamorphic rock fragment surrounded by quartz, plagioclase, and orthoclase (P1080). C) Polycrystalline quartz and metamorphic rock fragments surrounded by quartz, plagioclase, and orthoclase (P1096). D) Volcanic rock fragment of plagioclase laths in a fine grained matrix (OCS-G-6396-17,503 ft). E) Sedimentary rock fragment surrounded by quartz and orthoclase in plane polarized light (OCS-G-6406-22,687 ft). F) Silty mudstone lithic fragment (OCS-G-6396-17,503 ft).

the Florida Panhandle consists of quartz with minor amounts of aligned phyllosilicate minerals (Fig. 42A and 42B). The sedimentary lithics in the Florida wells average 12% and there is no evidence of any volcanic lithics.

A grain texture found in all thin-sections was heavily included quartz. While several different types of inclusion were observed such as feldspar, biotite, and rutile, the most common inclusion is zircon (Fig. 43). Distinct zircon grain boundaries are difficult to observe due to radiation damage however, the radiation damage creates a distinct distortion within the quartz grain. Another common texture includes the alteration of the feldspar grains, predominately sericitization and vacuolization. Alteration is much more common in the plagioclase grains than the orthoclase. In the three Florida samples, a common feldspar form consist of plagioclase rimmed with orthoclase. This is also observed in the Destin Dome and Pensacola samples but is far less prevalent with only a few orthoclase rimmed plagioclase grains.

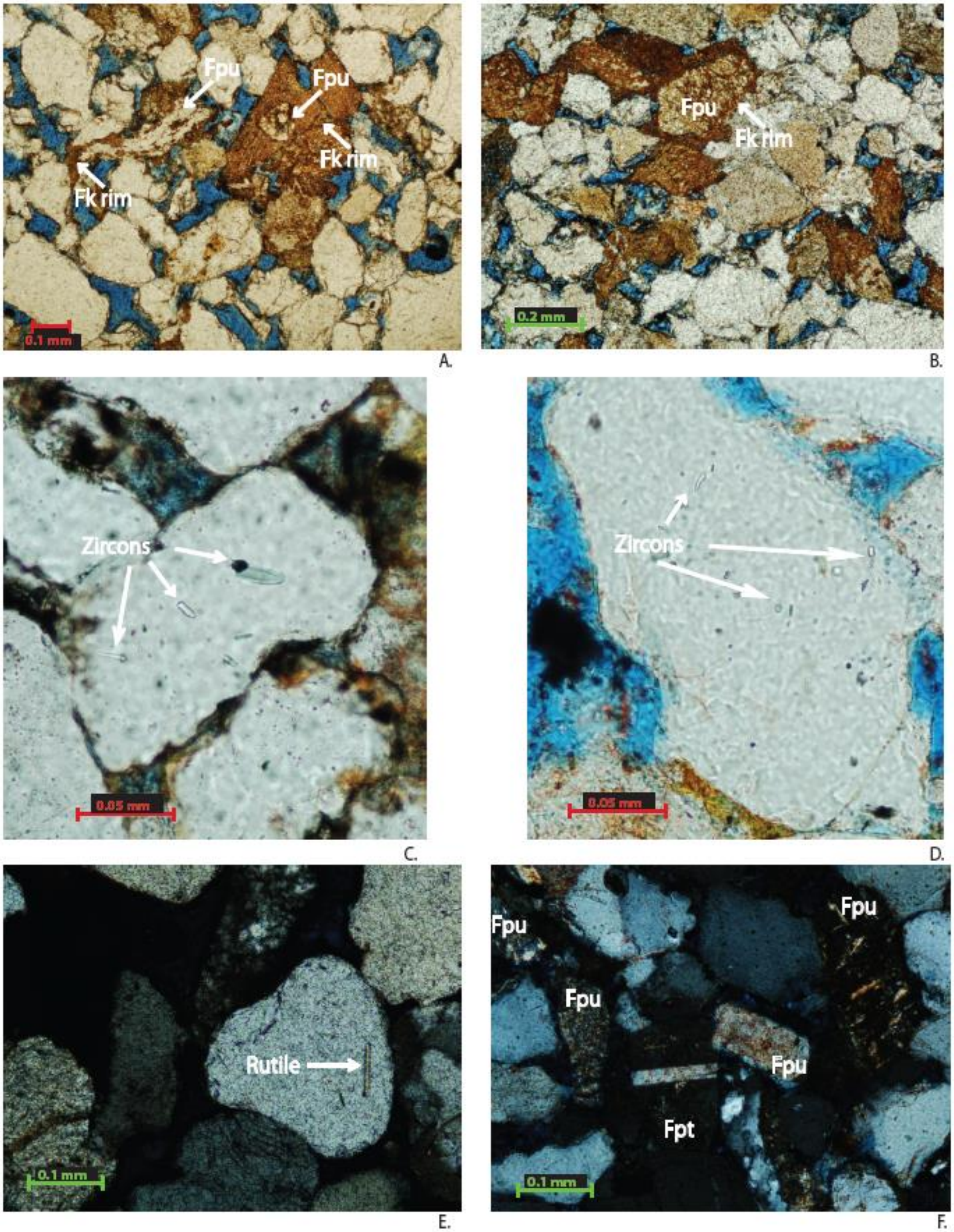

Figure 43. Framework grains textures in thin-section. All thin-sections were stained for plagioclase (tinted pink) and orthoclase (tinted brown). A) Plagioclase grains with orthoclase rims in plane polarized light (PPL; P1080). B) Plagioclase grains with orthoclase rims in PPL (P1004). C) Quartz with zircon inclusions (OCS-G-6406, 22,633 ft) in PPL. D) Quartz with zircon and other various minerals (P1096) in PPL. E) Quartz with rutile inclusion (OSC-G-6406, 22,633 ft) in cross-polarized light (XPL). F) Alteration of feldspar grains, predominantly sericitization (P1004) in XPL.

4.7 Dense Mineral Composition

Dense minerals were counted for all ten samples. The results showed a range of heavy mineral abundances from predominantly phyllosilicate to mostly pyroxene and epidote (Fig. 44). Figure 45 shows examples of various heavy mineral identified in the samples.

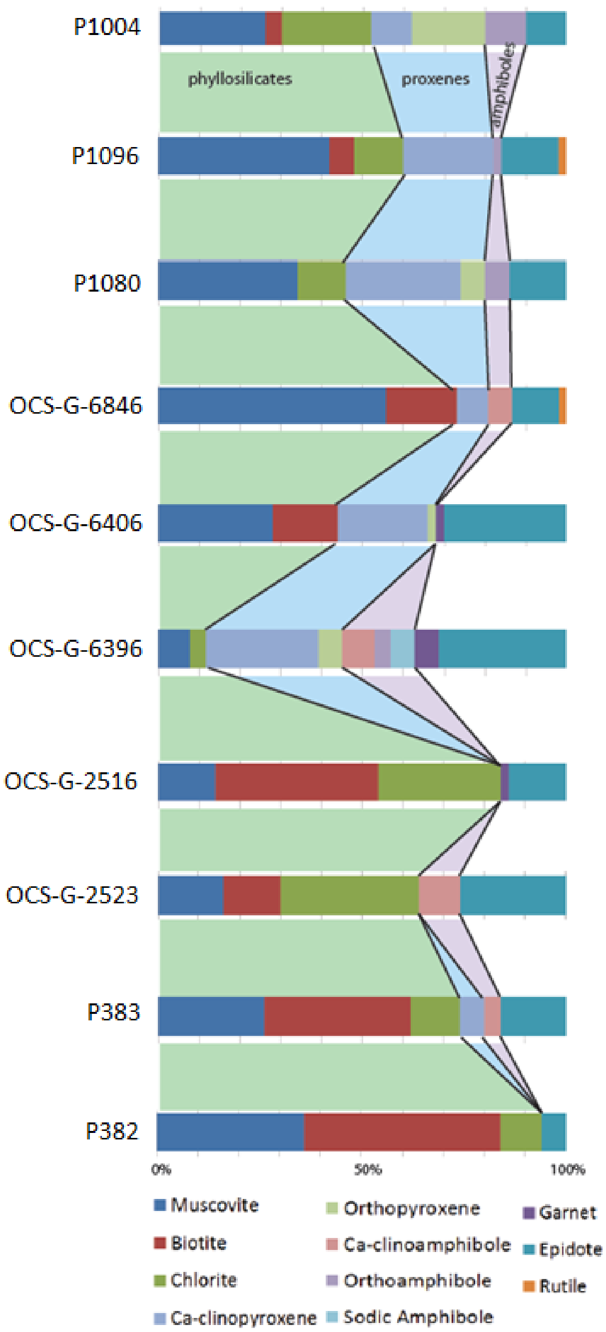

Figure 44. Abundances of dense minerals per sample.

The Florida Panhandle samples are fairly similar with regards to phylosilicates, pyroxenes, amphiboles, and epidote. Phyllosilicates make up 46-60% (26-42% muscovite, 0-6% biotite, and 12-22% chlorite). The ca-clinopyroxenes in these samples (augite and aegirine-augite) range from 10 to 28%. Orthopyroxene is missing from well P1096 but ranges from 6-18% in P1080 and P1004, respectively. The epidote in the Florida Panhandle samples range from 10-14%.

The Mobile Bay well (OCS-G-6848) is mostly phyllosilicates (73%) with 58% muscovite and 17% biotite. The only pyroxene present is ca-clinopyroxene (augite and aegirine-augite) which makes up 8% and the only amphibole present is hornblende making up 6%. Epidote makes up 12% of the sample and rutile makes up the last 2 %.

Sample OCS-G-6406 from Destin Dome consists of 44% phyllosilicates (28% muscovite and 16% biotite). Epidote is the second must abundant dense mineral making up 30%. The predominant chain-silicate is ca-clinopyroxene (aegirine-augite) at 22% while orthopyroxene makes up only 2%. Garnet is also rare making up 2% of the heavy minerals.

Sample OCS-G-6396 varies from the other samples as it has the largest amount of chain silicates and epidote. The most abundant dense mineral is epidote (31%). The second most abundant mineral is pyroxene where ca-clinopyroxene (aegirine-augite) makes up 27% and orthopyroxene makes up 6%. The amphiboles in this sample make up 18%; 8% hornblende, 4% orthoamphibole (anthophyllite-gederite), and 7% sodic amphibole (glaucophane). This sample has the lowest abundance of phyllosilicates at 12 % (8% muscovite and 4% chlorite). Garnet is the most abundant in this sample yet still rare making up only 6%.

Samples OCS-G-2516, OCS-G-2523, P383, and P382 are similar as they all have large abundances of phyllosilicates at 64-94% (14-36% muscovite, 14-48% biotite, and 10-30% chlorite). The second largest dense mineral abundance in these samples is epidote ranging from 6-26%. Pyroxene and amphiboles make up a smaller portions of samples OCS-G-2523 (10% hornblende) and P383 (6% augite and augite-aegirine and 4% hornblende). Sample OCS-G-2516 has minor amounts of garnet making up 2%.

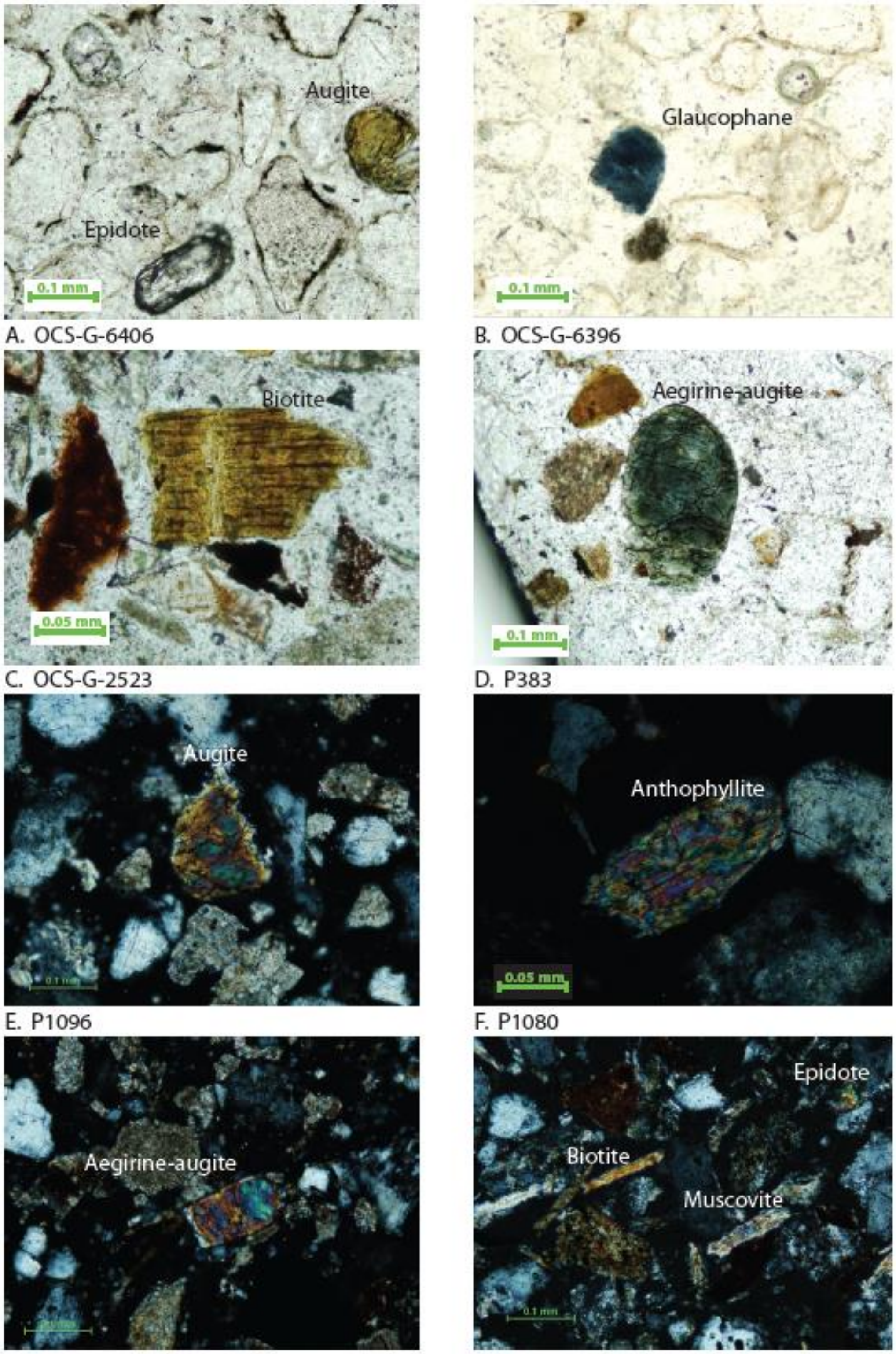

Figure 45. Examples of dense minerals found within the samples. A) Augite and epidote detrital grains in sample OCS-G-6406 (PPL). B) Glaucophane in sample OCS-G-6396 (PPL). C) Biotite in sample OCS-G-2523 (PPL). D) Aegirine-augite in sample P383 (PPL). E) Augite in sample P1096 (XPL). F) Anthophyllite in sample P1080 (XPL). G) Aegirine-augite in sample OCS-G-6848 (XPL). H) Biotite, muscovite, and epidote in sample OCS-G-2516 (XPL).

4.8 Well Log Analysis

Log analysis was done using GeoGraphix 10.2 with 32 wells that drilled into the Norphlet Formation from the Florida Panhandle and offshore federal lease blocks Destin Dome, Pensacola, and Mobile Bay. Figure 46 is an isopach map of the Norphlet Formation in this area. Unfortunately, many wells do not penetrate the entirety of the Norphlet so only ten wells were able to be used for the isopach. In GeoGraphix, the isopach was created using minimum curvature and a geologic bias of 55° at a magnitude of four to account for the trend of the paleo-highs and lows. The isopach shows that the thickest deposits of the Norhplet occur in Mobile Bay and western Pensacola and Destin Dome.

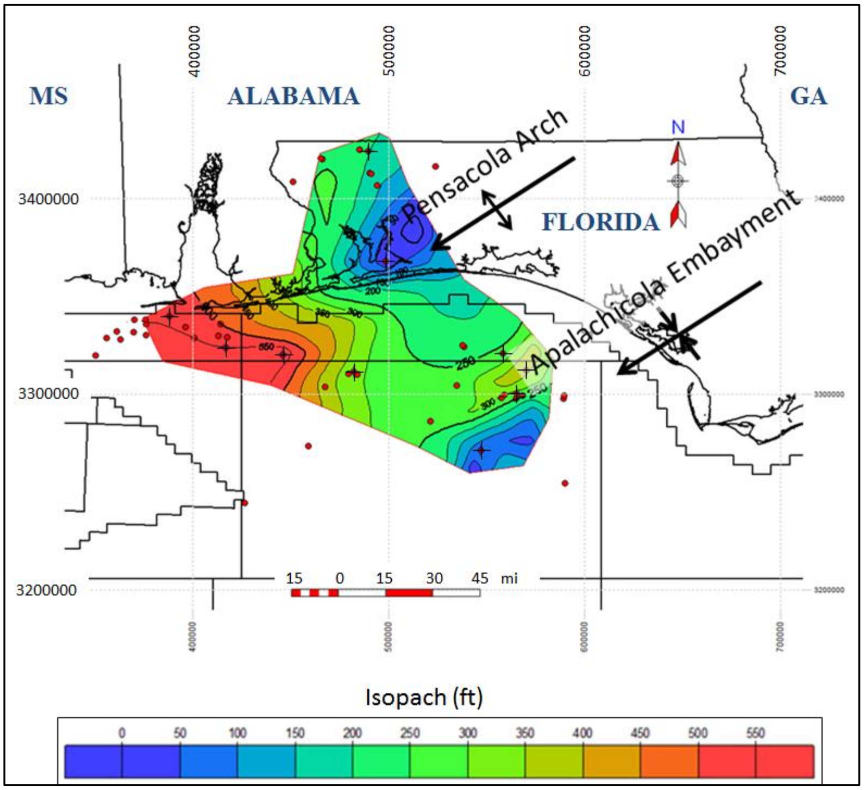

Figure 46. Isopach map of the Norphlet Formation (10 wells used, marked with cross symbol).

Analysis of the v-shale was done using the following equation; shale volume: Vshl[] = min(1, max(0, (GR[]-GRcln) / (GRshl-GRcln))). Similar to the isopach map, v-shale contours were created using minimum curvature and a geologic bias of 55° at a magnitude of four as well as hand edited where needed. The distribution of v-shale showed that a lower (>0.6) v-shale correlates to areas of predominantly eolian facies (Fig. 47). Regions with high v-shale correlate to either wadi or proximal alluvial facies. Unfortunatly, these two facies can not be distinguished by log data in the study area as there is only one well that intersects the alluvial fan facies and the log data is not well defined (facies known from Scott, 1991). The region of wadi facies within the Apalachicola Embayment is in agreement with Hunt (2012) who identified several wadi and shale facies from 61 wells throughout this area.

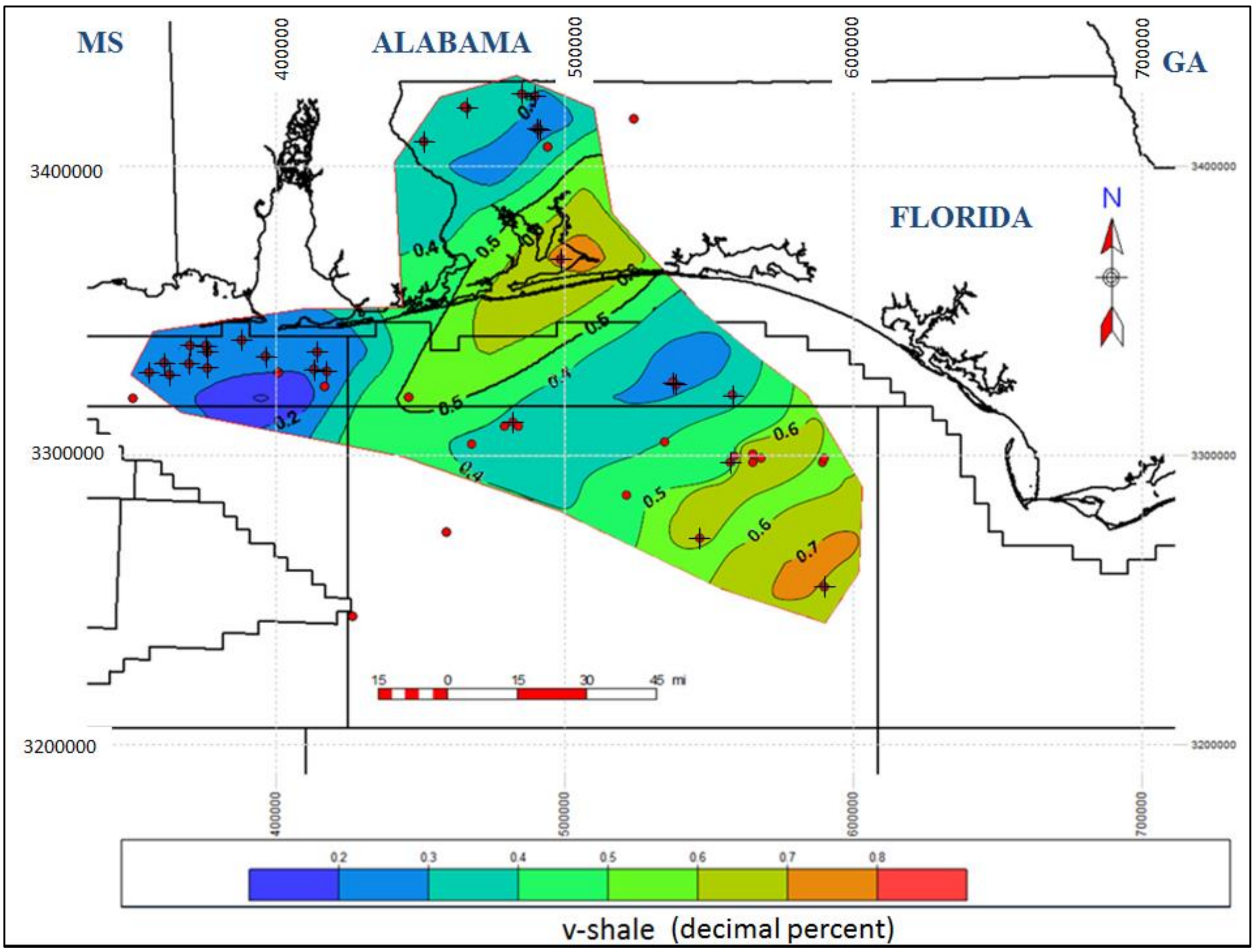

Figure 47. Average shale volume distribution (28 wells used, marked with cross symbol).

5. Discussion

5.1 Possible Source Areas

The rifting of Pangea is thought to have left a remnant of Gondwana, the Suwannee Terrane, attached to the Laurentian Craton (Chowns and Williams, 1983; Dallmeyer, 1987). Deposition of the Norphlet and surrounding formations during the rifting of Pangea could have resulted from sediment input from either or both of these two land masses. To distinguish between Gondwanan- or Laurentian-derived zircon, various source terranes and tectonic events within them are defined. Gondwanan sources include zircon within age ranges that correlate to the Pan-African event (500-680 Ma) and Trans-Amazonian/Eburnean event (1900-2250 Ma) (Mueller et al., 1994;). Laurentian sources include zircon derived from the Laurentian craton (Granite-Rhyolite, Yavapai-Mazatzal, Mid-continent, and Wyoming/Superior provinces), Grenville basement, the Appalachian mountain building events (Taconic, Acadian, and Alleghanian orogenies), and rifting events including Pangea, Rodinia, and Mt. Rogers (Becker et al., 2005; Park et al., 2010).

Figure 48 shows the relative probability plot of all ten samples, 867 zircon dates, and the possible source terranes and tectonic events from which zircon could be derived. Due to the potential for a recycled origin of many of the zircon grains in the Norphlet, it is difficult to interpret provenance. In order to evaluate sediment source within the study area, geochronologic source terranes are identified based on the suites of U-Pb age distributions. This study identified the same four source areas as Lovell (2013) based on the U-Pb detrital

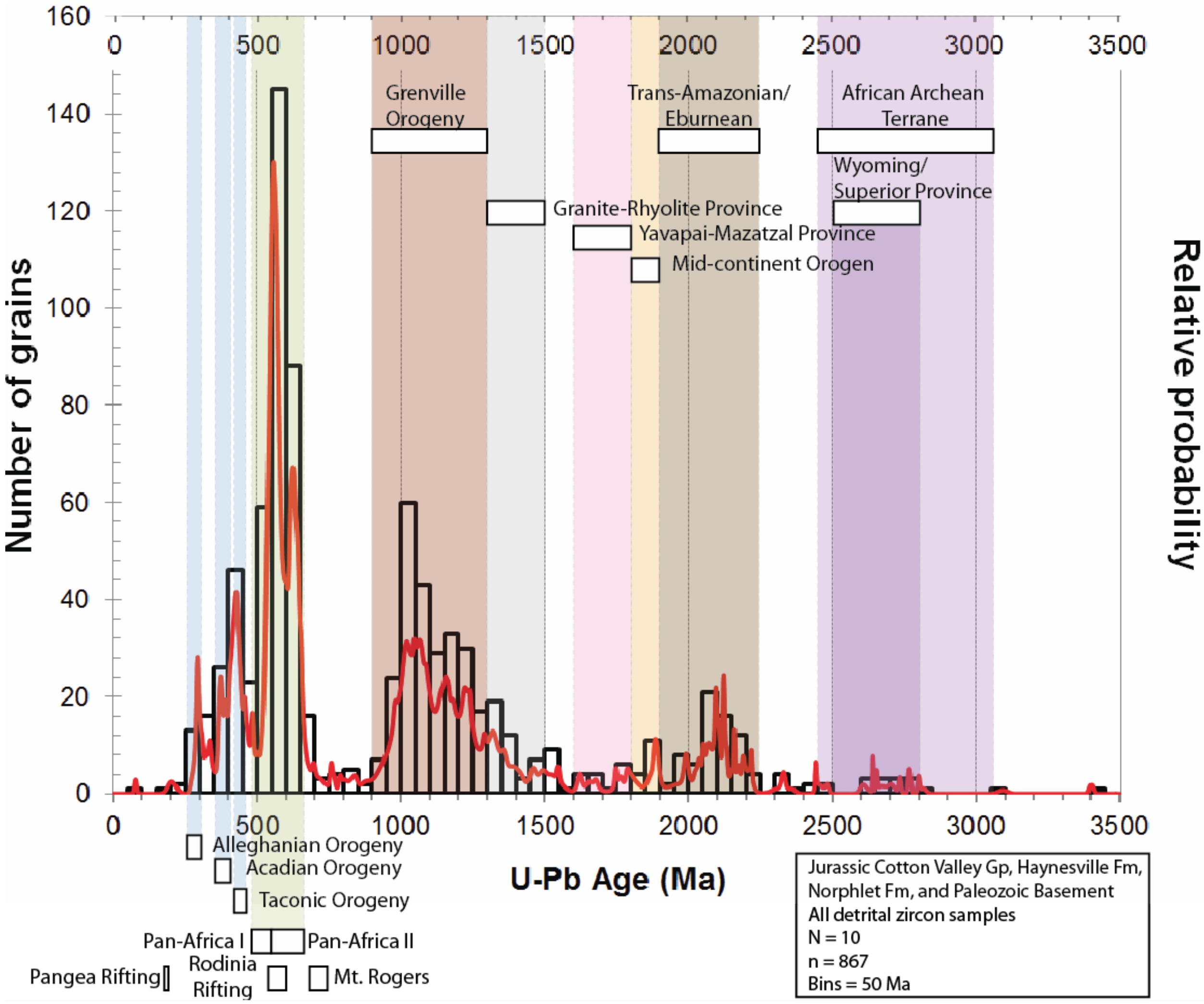

Figure 48. Relative probability plot of all ten samples, 867 zircon. Appalachian mountain building events include Alleghanian, Acadian, Taconic, and Grenville. Laurentian Craton includes Granite-Rhyolite, Yavapai-Mazatzal, Mid-continent, and Wyoming-Superior Provinces. Gondwanan events include Pan-African, Trans-Amazonian /Eburnean, and Archean African Terrane. Rifting events include Pangea, Rodinia, and Mt. Rogers. Red line is the relative probability of all 867 detrital zircons. Black boxes are number of grains with bins set at 50 Ma.

zircon age distributions; the Suwannee Terrane, the Mesozoic rift basin, the Appalachian hinterland and related Wiggins Arch, and Appalachian foreland basin (Fig. 49). Each geochronologic source terrane and their various provenance components are discussed below.

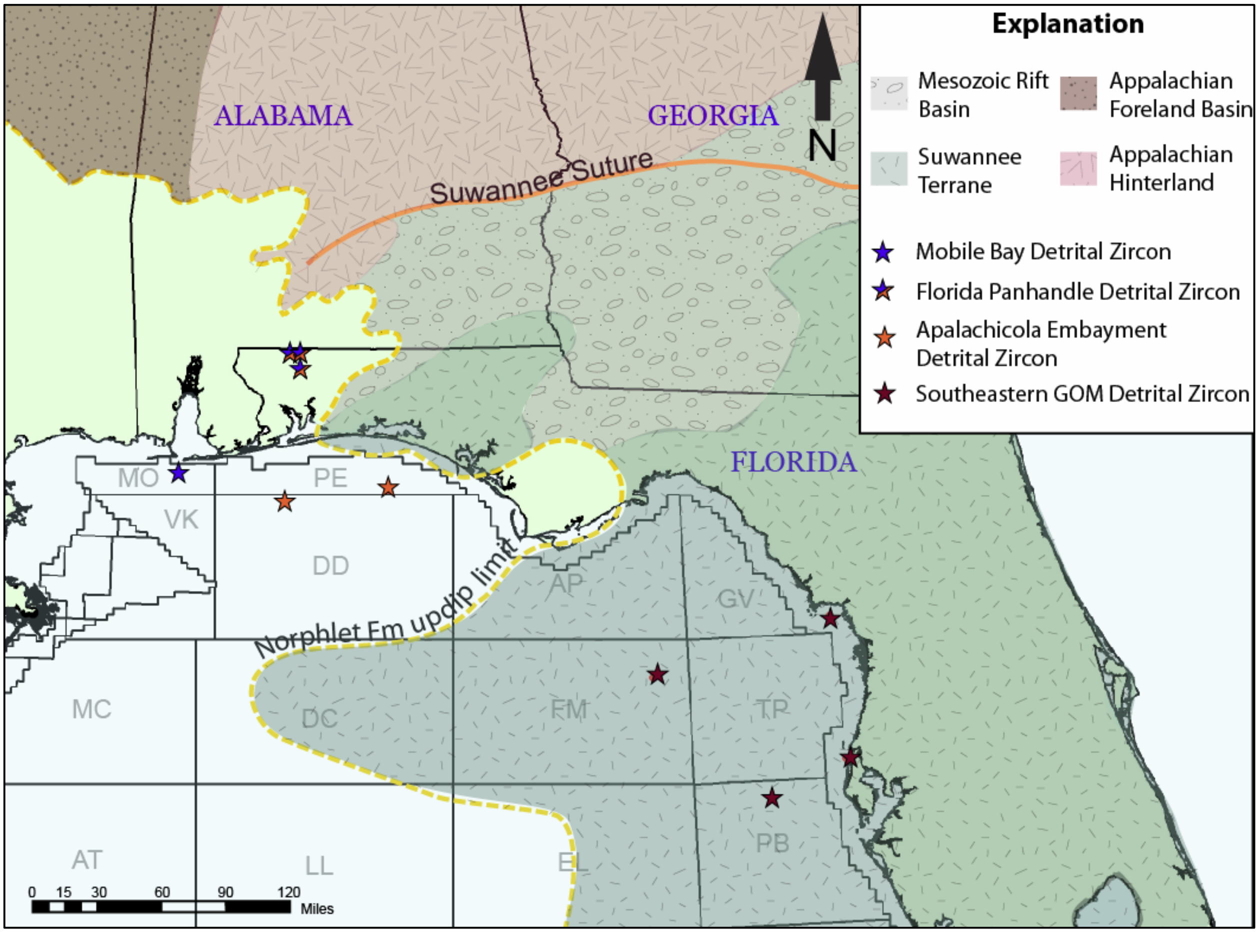

Figure 49. Four geochronologic source terranes identified include Appalachian hinterland, Appalachian foreland basin, Mesozoic rift basin, and the Suwannee Terrane. Stars represent samples with similar U-Pb age distributions.

5.1.1 Suwannee Terrane

The Suwannee Terrane is exotic with respect to Laurentia and is thought to be Gondwanan (Chowns and Williams, 1983; Dallmeyer, 1987; Arthur, 1988). The terrane was sutured to the southeastern margin of Laurentia during the Alleghanian orogeny (315-285 Ma; Dallmeyer, 1989; Hibbard et al., 2002) and consists of six pre-Middle Jurassic (basement) provinces: Late Precambrian to Early Cambrian felsic intrusive and extrusive rocks, Osceola Granite, St. Lucie metamorphic complex, Ordovician to Devonian sedimentary rocks, and early to middle Mesozoic hypabyssal and extrusive mafic rocks (Fig. 50; Arthur, 1988; Dallmeyer, 1989). It has been proposed that underlying these provinces is granitic and metamorphic basement from the African Craton (Chowns and Williams, 1983; Dallmeyer, 1989).

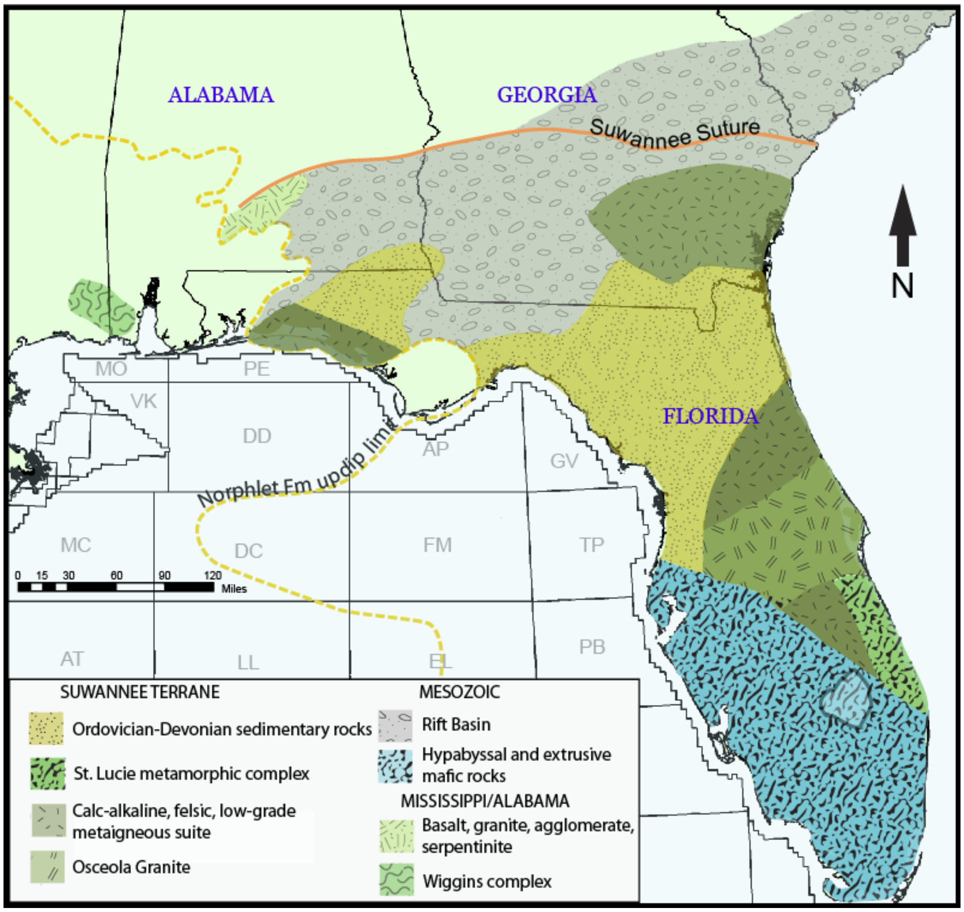

Figure 50. Lithology of the Florida basement (after Dallmeyer, 1989; Chowns and Williams, 1983; Arthur, 1988).

The Late Precambrian to Early Cambrian felsic intrusive and extrusive rocks in the Florida Panhandle are separated by a nonconformity from the overlying Ordovician to Devonian sedimentary strata in the Florida peninsula. The igneous rocks are all considered to be from the same province due to the similarity in lithology (Chowns and Williams, 1983). Radiometric ages have varied significantly for this province with an unpublished age of 709 +/- 25 Ma from K-Ar (feldspar) obtained from a granodiorite from the coastal, central Florida Panhandle (Arthur, 1988) to a plateau age of ~375 Ma (Dallmeyer, 1989). It has been proposed that

Devonian ages likely represent a low-grade metamorphic overprinting as opposed to cooling during the initial magmatism (Chowns and Williams, 1983; Dallmeyer, 1989).

The Osceola Granite is an undeformed granite composed primarily of oligoclase, quartz, perthitic feldspar, and biotite. $^{40}Ar/^{39}Ar$ isotopes from biotite have produced an age plateau ranging from 535 to 527 Ma (Chowns and Williams, 1983; Dallmeyer, 1989). Cooling of the pluton is thought to have occurred relatively quickly and at shallow crustal depths due to the lack of exsolution and/or recrystallization of feldspar grains (Dallmeyer, 1989).

The St. Lucie metamorphic complex consists of high grade metamorphic rocks including dioritic gneiss, amphibolite, and biotite-muscovite schist (Arthur, 1988; Dallmeyer, 1989). Isotopic ages range from 530 Ma (Rb-Sr, biotite) to 503 Ma (K-Ar, hornblende). $^{40}Ar/^{39}Ar$ isotopes identified plateau ages of 513 and 511 Ma which has been interpreted to represent post-metamorphic cooling (Dallmeyer, 1989).

Overlying the Late Precambrian to Early Cambrian felsic intrusive and extrusive rocks are sedimentary rocks from the Ordovician to Devonian. These consist of Lower Ordovician quartz arenites and Ordovician to Middle Devonian shales and siltstones (Chowns and Williams, 1983; Arthur, 1988; Dallmeyer, 1989). Detrital zircon age populations previously found in these sediments include a dominance of 515-635 Ma and 1967-2250 Ma (Mueller, 1994; Heatherington and Mueller, 1999). This correlates with the Trans-Amazoninan/Eburnean Orogens dated from 1900-2250 Ma (Hartmann, 2002; Schofield and Gillespie, 2007; Park et al., 2010) and the Pan-African/Brasiliano Orogens dated from 530-680 Ma (Hoffman, 1999; Park et al., 2010). Other less abundant age populations identified include 2433 Ma and 2700 Ma (Heatherington and Mueller, 1999). These ages are coeval with ages 2450-3040 Ma for metamorphic and igneous rocks of the Archean Terrane (U-Pb; Schofield and Gillespie, 2007). Ages obtained from this study also include a "Grenville" age population for these sediments (samples P383 and P382). Likely sources for these zircon include the South American Sunsas belt dated from 1000-1560 Ma (U-Pb zircon; Bettencourt et al., 2010) and various central and southern African orogenic belts (e.g. Namaqua and Mozambique) that range from 900-1300 Ma with U-Pb detrital zircon age peaks at 1,000 and 1170 Ma (Condie et al., 2009).

5.1.1.a. Rokelide Fold Belt

It has been proposed that the Suwannee Terrane is part of the Rokelide Fold Belt from the western side of the West African Craton (Fig. 51; Chowns and Williams, 1983; Arthur, 1988; Dallmeyer, 1989). The Rokelide orogeny along with the Bassaride-Mauritanide orogenic events are part of the Pan-African tectonothermal event. Evidence for this is supported by geochronology, paleontology, petrography, and stratigraphy. Similar petrography and crystallization ages (~530 Ma) exist for both the Osceola Granite in Florida and the Coya Granite in the Northern Rokelide Orogeny (Dallmeyer, 1989). Similarities have also been found between the Ordovician-Devonian stratigraphy and paleonology of the Suwannee Terrane and the Bove Basin of West Africa. Lastly, the St. Lucie metamorphic complex has yielded similar ages as those from post metamorphic cooling in the Rokelide belt (Chowns and Williams, 1983; Dallmeyer, 1989).

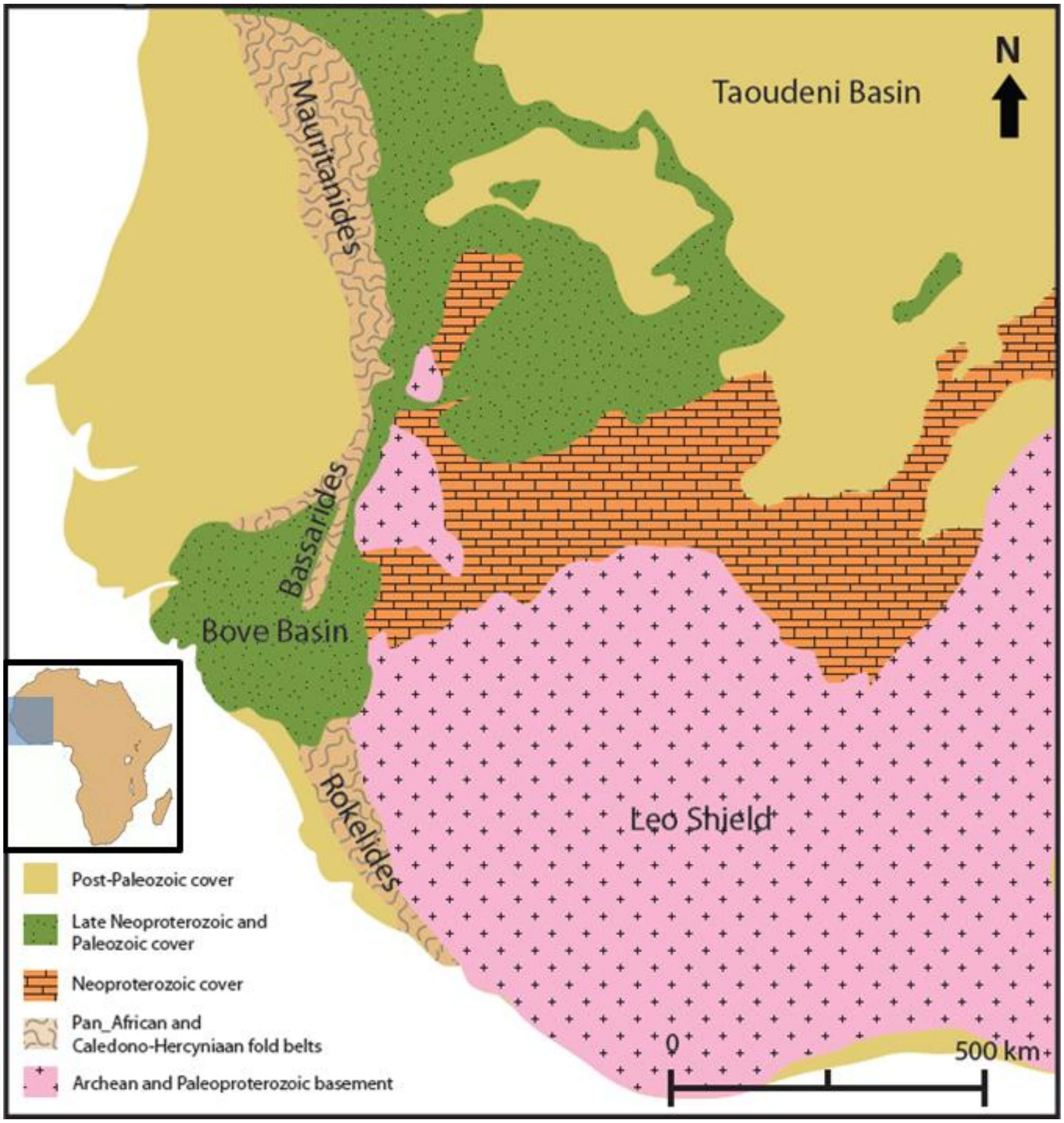

Figure 51. West African Mauritanides, Bassarides, and Rokelides orogenies (modified from Deynoux et al., 2006).

The Pan-African event is separated into two phases, Pan-Africa I that includes the Bassaride-Mauritanide orogenies, which have developed from 650-680 Ma ($^{40}Ar/^{39}Ar$ micaschist; Dallmeyer and Villeneuve, 1987; U-Pb zircon; Dallmeyer, 1989), and Pan-Africa II that includes the Rokelide orogeny (Culver et al., 1991; Veevers, 2007; Villeneuve, 2008), which formed at ~550 Ma (U-Pb zircon; Delor et al., 2002 and K/Ar schists and granitoids; Hurley et al., 1971). These two Pan-African events were followed by post-collisional intrusions from 550-660

Ma (Pan Africa I) and 533-500 Ma (Pan Africa II; Culver et al., 1991; Veevers, 2007; Villeneuve, 2008).

The basement rock beneath the West African orogenies is another component of the Suwannee Terrane which includes a Liberian province (~2700 Ma; Culver et al., 1991; Dallmeyer, 1989), Eburnean province (2050-2150; Park et al., 2009; Schofield and Gillespie, 2007; Culver et al., 1991;), granitic plutonism (1800 Ma; Dallmeyer, 1989), and Pan-African (550 Ma; Villeneuve, 2008; Veevers, 2007; and Culver et al., 1991). The Liberian Province consists of metamorphic rock of high-grade amphibolite gneisses (Dallmeyer, 1989 and Culver et al., 1991). The Eburnean rocks also consist of amphibolite-grade migmatic gneiss as well as metamorphosed shelf sediments to form quartzite and marble (Schofield and Gillepie, 2007; Culver et al., 1991; and Dallmeyer, 1989). At around 1800 Ma, widespread intrusions of granitic plutons occurred (Dallmeyer, 1989). The Pan-African basement rocks, which consist of reworked Archean rocks, are separated into the Kasila Group and the Kenema Assemblage. The Kasila Group consists of high-grade metamorphic rock of granulite facies. The Kenema Assemblage consists of lower-grade greenstone and migmatic granites and gneisses (Culver et al., 1991).

5.1.2 Mesozoic Rift Basin

The Mesozoic Rift Basin of the southeast U.S. subsurface has been interpreted to be a Triassic graben filled with redbeds and associated basalts, diabases, and dacitic ash fall tuffs (Heatherington and Mueller, 1999; Arthur, 1988; and Chowns and Williams, 1983). These rift related rocks are dated from Late Triassic, 203 +/- 12 Ma to Early Jurassic, 182 +/- 11 Ma (K-Ar whole rock; Heatherington and Mueller, 1999). Ages of volcanic rocks in the Mesozoic Rift

Basin are similar to the hypabyssal and extrusive mafic rocks in the South Florida Basin which have a 189 +/- 5 Ma Rb-Sr whole rock age (Arthur, 1988). However, the two regions of extrusive rocks are not thought to be genetically related. The basalts of the South Florida Basin range from tholeiitic to alkaline with associated alkaline rhyolites whereas the Mesozoic Rift Basin basalts are solely tholeiitic in composition. Heatherington and Mueller (1999) preformed trace element and isotopic analysis on the two mafic volcanic suites. They found that the northern Florida basalts were derived from continental lithosphere and that the basalts from the South Florida Basin show evidence for the presence of a mantle plume below.

During Triassic rifting, this basin likely acted as a depocenter for both Laurentian and Gondwanan sediment. The rift basin trends east-northeast and west-southwest from the Florida Panhandle to southern Georgia and cuts across both the Appalachain Mountains and the Suwanne Terrane. Thus rifting could have exposed both Grenville and African Suwannee basement from which zircon could be derived and deposited in the Norphlet Formation.

5.1.3 Appalachian Mountains

The Appalachian orogen contain both Laurentian- and Gondwanan-affinity rocks. Previous studies by Park et al. (2010) and Becker et al. (2005) have identified several Laurentian sediment sources based on U-Pb detrital zircon geochronology. These include sediments shed from the Grenville basement rocks, Rodina rift rocks, Taconic orogen, Acadian orogen, and the Alleghanian orogen. The Grenville basement rocks are predominantly gneiss and provides the most abundant detrital zircon age group in Appalachian foreland basin deposits (900-1300 Ma). Rodinia rifting consists of two age groups, 700-760 Ma from the Mt. Rogers volcanics which represents failed rifting, and 550-620 Ma from the Catoctin Greenstones representing the opening of the Iapetus Ocean. The Taconic Orogeny, ~430-480 Ma, is represented by granulite facies and kyanite grade metamorphic rocks that have been dated ~465 Ma. The Acadian Orogeny produced rocks of two distinct ages: plutonism and low to high-grade metamorphic rocks from a northern deformational front (384-425 Ma) and southern granitoid plutonism (374-382 Ma). The Alleghanian Orogeny consists of magmatism from subduction and regional metamorphism of the green schist and amphibolite facies dating 300-325 Ma (Park et al., 2010). It also consists of a foreland fold and thrust belt that migrated from north to south during approximately 280-300 Ma in the southern Appalachians (Becker et al., 2005; Park et al., 2010).

The Gondwanan component of the Appalachian orogen is the Carolina Terrane which is made up of several exotic Neoproterozoic to early Paleozoic terranes of the southern Appalachians that are thought to be part of Gondwana accreted along the eastern margin of Laurentia. The history of terrane accretion and associated magmatism occurred in three stages, pre 600 Ma, 590-530 Ma, and younger than 530 Ma (Hibbard et al., 2002). Terranes in this zone include the Roanoke Rapids Terrane, Spring Hope Terrane, Uchee Terrane, Pine Mountain Terrane, Savannah River Terrane, and Charlotte Terrane. These terranes consist primarily of metamorphic rocks with very minor undeformed igneous rocks.

The oldest terrane in the Carolina Terrane is the 607-672 Ma (U-Pb zircon) Roanoke Rapids Terrane and consists of low-grade mafic-ultramafic (ophiolitic) rocks, tonalite to quartz-diorite and metavolcanics, felsic volcanic and phyllitic volcaniclastics (Hibbard et al., 2002). The 620-640 Ma (U-Pb zircon) Uchee Terrane is made up of gneiss, schist, and amphibolite (Steltenpohl et al., 2008). The Savannah River Terrane consists of 620 Ma (U-Pb zircon) migmatitic gneiss and schist as well as Carboniferous ($^{40}Ar/^{39}Ar$) underformed granite plutons (Hibbard et al., 2002).

The 544-590 Ma (U-Pb zircon) Spring Hope Terrane consists of greenschist facies, including metavolcanics with metaplutonic and metasedimentary rocks (Hibbard et al., 2002). The Charlotte Terrane is predominantly 538-579 Ma (U-Pb zircon) metaigneous rocks that date with intruded plutonic rocks that formed from 570-580 Ma and 530-540 Ma (U-Pb; Hibbard et al., 2002).

The Pine Mountain Terrane consists of quartzite, marble, and schist. This terrane has been interpreted to be metamorphosed Grenville basement and bears 270-295 Ma U-Pb ages from Rutile (Steltenpohl et al., 2008). Also called the Pine Mountain Window, this region is an exposure of the North American Grenvillian crust (Steltenpohl et al., 2008).

5.1.4 Appalachian Foreland Basin

Sediments shed into the Appalachian foreland basin could have originated from several Laurentian Provinces as well as from the Appalachian hinterland. Park et al. (2010) summarized the various Laurentian provinces, including the Superior Province (2700-2800 Ma), Wyoming Province (2500-2700 and 1600-1800 Ma), Trans-Hudson Province (1800-1900 Ma), Yavapai Province (1700-1760 Ma), Mazatzal (1700-1800 and 1600-1660 Ma), and the Granite and Rhyolite Province (1300-1500 Ma; Fig. 52).

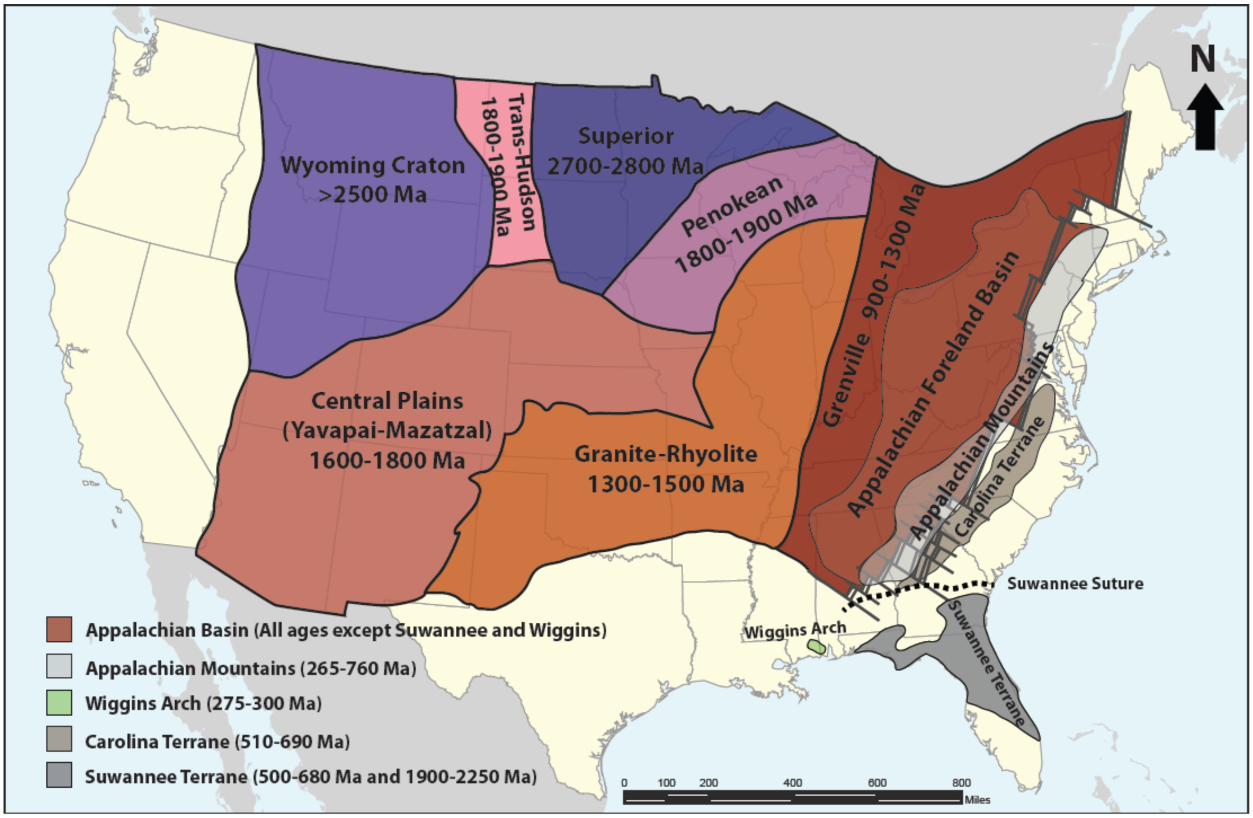

Figure 52. Laurentian basement provinces (modified from Park et al., 2010), Appalachian Mountains and associated foreland basin (Lovell, 2013), Wiggins Arch (Dallmeyer, 1989; Arthur, 1988), and accreted terranes including the Carolina (Hibbard et al., 2002) and Suwannee terrane (Dallmeyer, 1989). Suwanne suture from Steltenpohl et al. (2008).

5.1.4.a Wiggins Arch

The Wiggins Arch is an uplifted block of metamorphic rocks in southwestern Alabama and southeastern Mississippi. It consists predominantly of phyllite, schist, quartzite, qneiss, amphibolite, and deformed granite that formed between 275 and 300 Ma (K-Ar whole Rock; Dallmeyer, 1989; Tew et al., 1991). The Wiggins Arch sits between two Mesozoic faults and lies next to the southwestern extension of the Appalachian piedmont (Tew et al., 1991). The geologic evolution of the Wiggins Arch is still poorly known but is not considered part of the Suwannee Terrane as it records Paleozoic metamorphism whereas the Suwannee Terrane doesn not (Dallmeyer, 1989).

5.2 U-Pb Ages within known Provenance Range

The degree to which these previously discussed sources contributed sediment to the Norphlet and surrounding formations varies across the study area. Of the 867 zircons with useable dates, 777 fit into known source regions discussed above (Fig. 53; See Appendix 3). The following discussion will assess the various provenance contributions to the ten detrital samples as well as the decision process for assigning U-Pb ages to a particular provenance, especially for source areas that overlap in age.

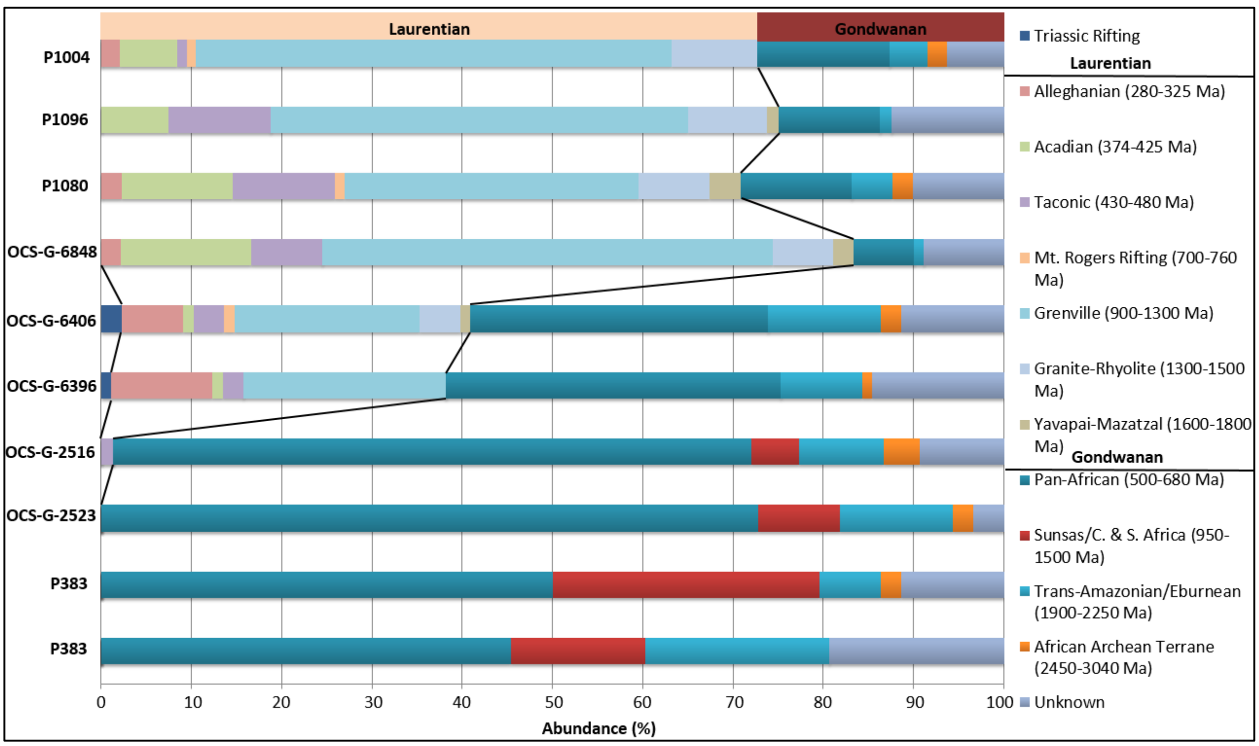

Figure 53. Normalized abundance of detrital zircon U-Pb grouped according to potential source terranes.

5.2.1 Triassic Rifting

The Destin Dome and Pensacola offshore lease block samples contain zircons produced from Triassic rift volcanism. Both of these samples are located within the Apalachicola Embayment and are proximal to known volcanism during this time. Figure 6 shows the location of volcanism during the Triassic in and around the study area (Chowns and Williams, 1983; Arthur, 1988; Heatherington and Mueller, 2003).

5.2.2 Appalachian Orogen Source

Samples P1004, P1080, OCS-G-6848 (MO), OCS-G-6406 (DD), and OCS-G-6396 (PE) have Alleghanian-aged zircons (Fig. 53). However, in samples P1004, P1080, and OCS-G-6848, this population only makes up 2%. For the Destin Dome and Pensacola samples, this population is a lot larger from 7% to 11%, respectively. The samples that contain Acadian-aged zircons include the Florida Panhandle samples (P1004, P1096, and P1080), Apalachicola Embayment samples (OCS-G-6406 and OCS-G-6396), and Mobile Bay sample (OCS-G-6848). This population ranges from 1% (OCS-G-6406 and OCS-G-6396) to 14% (OCS-G-6848). Taconic-aged zircons are found in the Florida Panhandle wells (1-11%) as well as Mobile Bay (8%), Destin Dome (3%), Pensacola (2%), and Florida Middle Ground (1%). Overall, there is a southwestward increase in Appalachian orogen-aged zircon abundance from the Florida Panhandle samples to the Mobile Bay sample. There is also a southward decrease in Appalachian orogen-aged zircon from the Florida Panhandle samples to the Apalachicola Embayment samples which are separated by the Pensacola Arch.

5.2.3 Pan-African Source

Pan-African-aged zircons exist in all samples (Fig. 53). The population is the smallest in the Mobile Bay sample at 7%. The proportion of these Pan-African-sourced zircon in the Florida Panhandle samples are similar ranging from 11-15%. The Destin Dome and Pensacola samples have a higher proportion at 33% to 37%, respectively. For the southeastern samples (OCS-G-2516, OCS-G-2523, P383, and P382), this population makes up the largest portion of zircon ages. For samples OCS-G-2523 and OCS-G-2516, it makes up 71% to 73%, respectively. For samples P383 and P382 this population makes up 50%. Geographically, the abundance of Pan-African-aged zircon increases to the southeast and is the smallest in the Mobile Bay sample and largest in the Florida Middle Ground and St. Petersburg samples (OCS-G-2516 and OCS-G-2523).

5.2.4 Grenville and the Gondwanan Sunsas and South and Central African Orogenies

Previous studies have shown that within the Appalachian foreland basin, Grenville-aged zircons are the most pervasive, found throughout the Paleozoic basin fill (Park et al., 2010; Becker at al., 2005). Park et al. (2010) performed U-Pb detrital zircon geochronology on Appalachian basin sediments from the Taconic, Acadian, and Alleghanian clastic wedges, all of which showed a Grenville-aged population that composed from 40-80% of the total sample, averaging about 61%. The Grenville population for this study ranges from 20- 53% of those samples that contain it (Table 3). The largest portion of Grenville-aged zircon occur in samples P1004 (53%), Mobile Bay (50%), and P1096 (46%). P1080 has a smaller portion at 33% while Pensacola and Destin Dome are even smaller at 20 and 22%, respectively. Figure 54 shows a comparison between the normalized relative probability plot of Park's cumulative data set which illustrates the large Grenville influence on the Appalachian foreland basin sediments. In comparison, the Grenville influence on the Norphlet Formation appears to be smaller, especially in the Apalachicola Embayment samples (OCS-G-6406 and OCS-G-6396).

Table 3. Comparison of Grenville-aged zircon between Park et al. (2010) and this study.

Park et al., 2010	Grenville Population	This Study	Grenville Population
Bluestone Formation, ~330Ma (McCreery, West Virginia)	78%	*Norphlet Formation, ~157 Ma (P1004)*	53%
Princeton Formation, ~335 Ma (Kegley, West Virginia)	73%	*Norphlet Formation, ~157 Ma (P1096)*	46%
Hinton Formation, ~340 Ma (Stony Gap, West Virginia)	44%	*Norphlet Formation, ~157 Ma (P1080)*	33%
Mauch Chunk Formation, ~330-340 Ma (120, Pennslyvania)	57%	*Norphlet Formation, ~157 Ma (OCS-G-6848)*	50%
Grainger Formation, ~ (Rutledge 2, Tennessee)	80%	*Norphlet Formation, ~157 Ma (OCS-G-6406)*	20%
Price Sandstone, ~350 Ma (Caldwell X, West Virginia)	53%	*Norphlet Formation, ~157 Ma (OCS-G-6396)*	22%
Hampshire Formation, ~360 Ma (Onego, West Virginia)	60%	*Haynesville Formation, ~153 Ma (OCS-G-2516)* *Paleozoic Basement, (Ord-Dev)*	0%
Chemung Formation, ~365 Ma (Brandywine, West Virginia)	49%	*Cotton Valley Group, ~140 Ma (OCS-G-2523)* *Haynesville Formation, ~153* *Paleozoic Basement, Ord-Dev*	0%
Foreknobs Formation, ~365 Ma (Kelly Mt. 2, West Virginia)	43%	*Paleozoic Basement, Ord-Dev (P383)*	0%
Oriskany Formation, ~385 Ma (Minnehaha, West Virginia)	77%	*Paleozoic Basement, Ord-Dev (P382)*	0%
Keefer Formation, ~430 Ma (Knapps Creek, West Virginia)	64%		
Rose Hill Formation, ~435 Ma (Eagle Rock B, Virginia)	75%	**AVERAGE (of samples with Grenville)**	**37.33%**
Tuscarora Formation, ~440 (Little Arch, West Virginia)	58%		
Oswego Formation, ~445 Ma (North Fork 1, West Virginia)	44%		
Fincstle Member, Martinsburg Formation, ~ 450 Ma (Fincastle, Virginia)	62%		
AVERAGE	**61.13%**		

The four southeastern samples of this study (OCS-G-2516, OCS-G-2523, P383, and P382) also contain zircon populations that reside within the Grenville age but were not classified as such. This is because the Grenville population of these four samples is largest in the Gondwanan, Paleozoic basement samples (P383-P382) which consist of sediments deposited during the Ordovician-Devonian when Gondwana was not attached to the Laurentian craton and there could be no Laurentian influence (e.g. Grenville). Other potential sources for these Grenville-aged zircon can be inferred from Condie et al. (2009) who compared detrital and igneous zircon data across continents. Condie's study shows Grenville-age peaks in both South America and Africa (Fig. 55) that are attributed to the Sunsas belt in South America and various orogenies in South and Central Africa (Condie et al., 2009). Therefore, "Grenville-

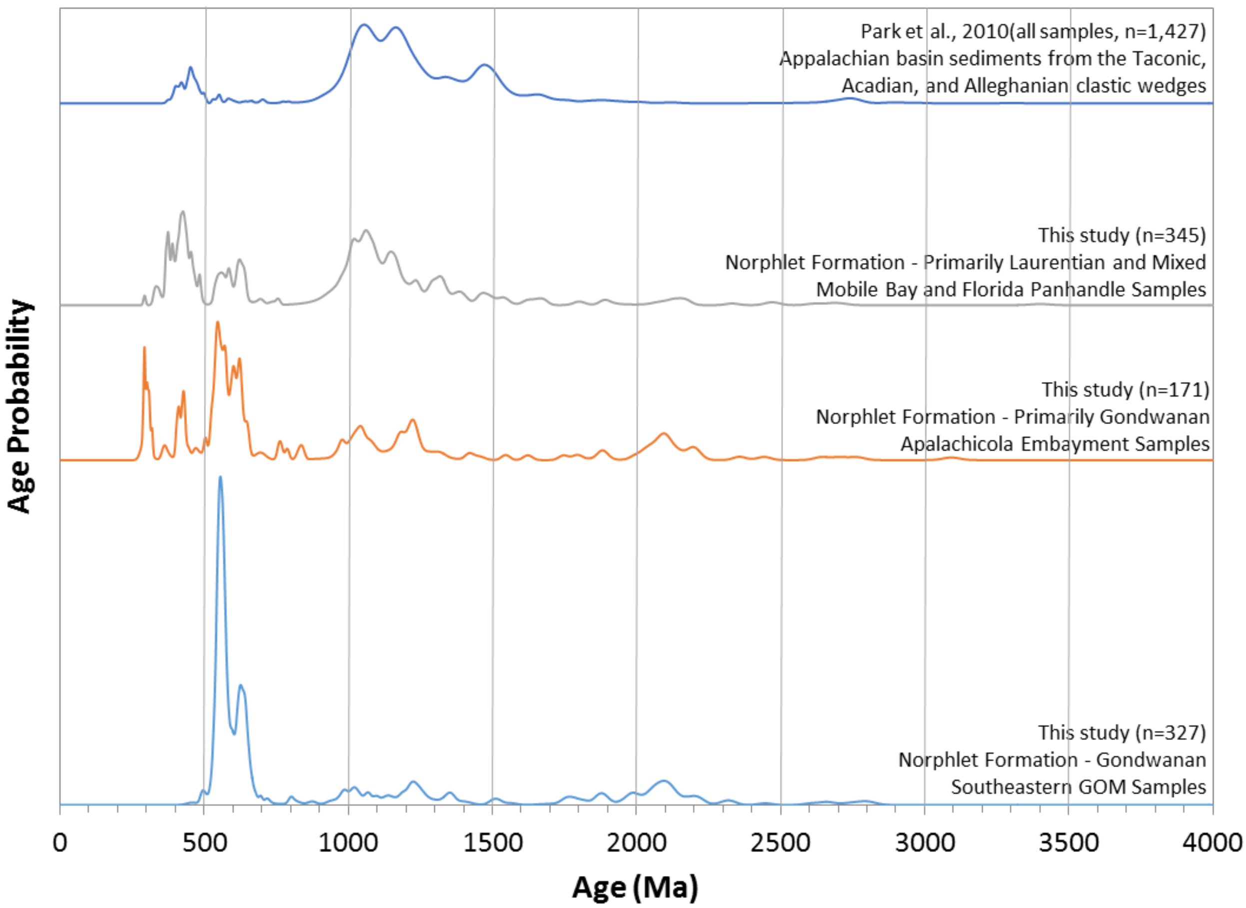

Figure 54. Normalized relative probability curves for cumulative data of the Mobile Bay and Florida Panhandle samples (grey), Apalachicola Embayment samples (orange), and southeastern GOM samples (light blue) of this study and and Park et al. (2010; blue). As opposed to this study which focuses on Jurassic sediment and Paleozoic basement in the eastern Gulf of Mexico, Park et al. (2010) focused on Appalachian foreland basin sediments.

aged" zircon in the Gondwanan basement samples P383 and P382 and proximal OCS-G-2516 and OCS-G-2523 samples, are classified as South America/African and not as Grenville. The portion of South American/African zircon in the Jurassic and basement samples OCS-G-2523 and OCS-G-2516 is much lower (5-9%, respectively) than they are for the basement samples P382 and P383 (15-30%, respectively).

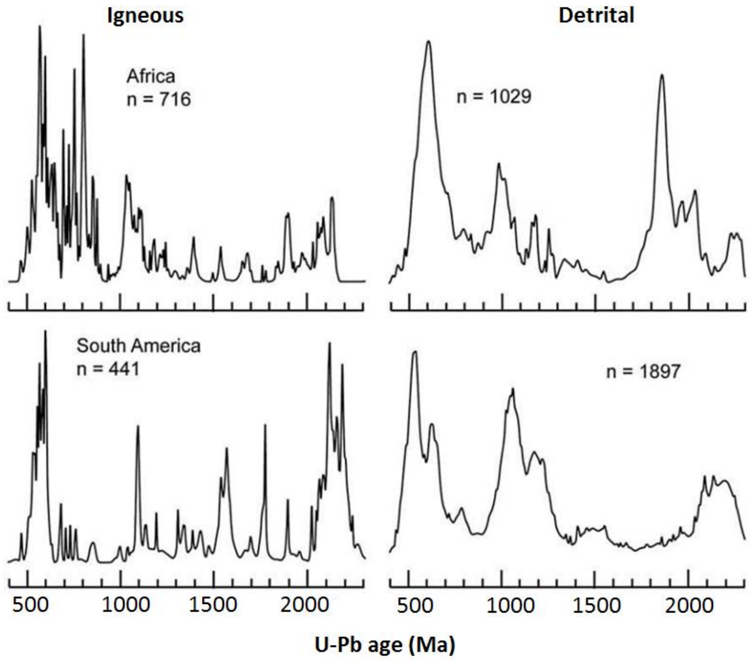

Figure 55. Probability density plots of igneous and detrital U-Pb age distributions between 400-2300 Ma from Africa and South America (Condie et al., 2009)

5.2.5 Laurentian Craton Source

Zircon sourced from the Granite-Rhyolite Province are present in the Florida Panhandle and Mobile Bay samples (7-9%) and less abundant in the Destin Dome sample (5%). Yavapai-Mazatzal-aged zircon are present in the P1096, P1080, Mobile Bay, and Destin Dome samples ranging from 1-3%. While the Pensacola sample has 2 ages (1747 and 1749 Ma) that coincide with the Yavapai-Mazatzal time range, they were not considered so. The Pensacola sample shows a much smaller influence from Laurentia and the Appalachian orogen in other age populations. These two ages more likely correlate to the suturing of the Birimian Basement of West Africa that occurred during the Eburnean Orogen with ages that range from 1700-2000

Ma (Villeneuve, 2008). This event was also likely the source for the small group of 1700-1800 Ma zircon ages in the Paleozoic basement.

5.2.6 Trans-Amazonian/Eburnean Orogenies

Trans-Amazonian/Eburnean-aged zircon are present in all samples in varying abundances. This age population is the smallest in the P1080 and Mobile Bay samples at 1%. The other Florida Panhandle samples (P1004 and P1096) have only 4% of this age population. The Destin Dome, Pensacola, Florida Middle Ground, St. Petersburg, and P383 samples have larger abundances ranging from 7-13%. Florida basement samples P382 has the largest abundance of this population at 20%.

5.2.7 African Archean Terrane

The P1004, P1080, Destin Dome, Pensacola, Florida Middle Ground, St. Petersburg, and P383 samples all have a small portion of this age population (1-4%). These portions were classified as African Archean Terrain (2450-3040 Ma) even though there is some overlap with the Wyoming (>2500 Ma) and Superior (2700-2800 Ma) Provinces. The four southeastern samples (OCS-G-2516, OCS-G-2523, P383, and P382) had zircon ages between 2600-2700 Ma that occur with predominantly other Gondwanan derived grains. The Pensacola sample had one age at 2766 Ma that was classified as African in origin rather than Superior Province due to the smaller influence from Laurentia in the other age populations.

5.2.8 Ambiguous U-Pb Ages

Table 4 summarizes the ambiguous ages and potential origins for this study. Only one U-Pb age date was found that was younger than the Triassic rifting event and the depositional age of the Norphlet in the Florida Middle Ground sample at 77 (+/- 4.2) Ma. Part of the sample was obtained from cuttings, which suggests that the 77 Ma date is due to mixing that occurred during the drilling process and does not belong to the actual formations targeted. Lovell (2013) summarized the potential origins of ambiguous U-Pb ages he observed in the Norphlet Formation from the Mobile Bay and Destin Dome offshore lease blocks (Table 4). However, because the southeastern Gulf of Mexico samples of this study are composed almost entirely Gondwanan-derived zircon, Lovell's possible Laurentian sources for 680-700 Ma, 760-900 Ma, and 1500-1900 Ma do not apply. Instead, U-Pb ages for 680-700 and 760-900 Ma likely belong to early and late phases of the Pan-African Orogeny (Condi et al., 2009; Lovell, 2013). Gondwanan sources experienced long periods of episodic granitoid plutonism that began with the Tran-Amazonian/Eburnean (2200 Ma) events and continued through 1500 Ma (U-Pb; Condi et al., 2009). Condi et al. (2009) attribute the U-Pb ages found in South America and West Africa between 1500-1900 Ma to the accretion of land masses on the western margin of Amazonia. Also, the Birimian Basement of West Africa was sutured together during the Eburnean Orogen with dates that range from 1700-2000 Ma (Villeneuve, 2008).

Table 4. Samples with ambiguous U-Pb ages and their potential origin

Ambiguous Age Range	Sample (# of grains)	Potential Origin
325-374 Ma	P1004 (2), P1096 (3), P1080 (3), MO (4), DD (2), FMG (1)	Continued plutonism between Alleghanian and Acadian orogenies (Lovell, 2013)
425-430 Ma	P1080 (2)	Continued plutonism between the Acadian and Taconic orogenies, likely northern Appalachians (Lovell, 2013).
480-500 Ma	P1096 (3), P1080 (1), DD (1), P382 (2)	Pan-African material including volcanic arcs of the Carolina Terrane.
680-700 Ma	P1080 (1), DD (2), FMG (1)	Pan-African (Lovell, 2013)
760-900 Ma	PE (3), DD (1), STPB (1) P383 (2), P382 (2)	Pan-African (Condi et al., 2009)

1500-1600 Ma	P1004 (4), P1096 (1), PE (1)	Pennsylvanian Hammond Fm., Marathon-Ouachita Orogey (Lovell, 2013)
1800-1900 Ma	P1096 (2), P1080 (1) MO (1), PE (3)	Mid-continent orogenies (Lovell ,2013; Park et al., 2010)
Older than 2250 Ma	P1080 (1), MO (2) DD (2), FMG (1), P383 (1)	Undectected provinces of the Canadian Shield (Lovell, 2013); African Archean Terrane (Heatherington and Mueller, 1999; Schofield and Gullespie, 2007)
African 1500-1900 Ma	P382 (8), P383 (7) FMG (2), STPB (1)	Birimian Basement of the West African Craton (1700-2000 Ma; Villeneuve, 2008). Amazonian granitoid production 1500-1900 Ma (Condi et al., 2009)

5.3 Geospatial Trends in Norphlet Composition

From the five samples (11 thin-sections from various depths) point-counted, several trends are observed. There are few to no volcanic rock fragments within the samples, the amount of plagioclase is largest within the Florida Panhandle and decreases to the south/southeast, and there is little to no sedimentary lithics in the Florida Panhandle but sedimentary lithic abundance increases to the south/southeast.

On the QtFL and QmFLt diagrams (Fig. 56) all samples plot either as craton interior, transitional continental, and quartzose recycled provenance and show no evidence of magmatic arc. Minor amounts of volcanic rock fragments in the Apalachicola Embayment samples coincides with previous interpretations of this region as an area of extension and rifted basement (Salvador, 1987; Dobson and Buffler, 1997). The few volcanic grains in samples OSC-G-6396 and OCS-G-6406 are due to rift-related magmatism that was occurring in Florida and Georgia during the Mesozoic (Fig 6; Chowns and Williams, 1983; Arthur, 1988; Heatherington and Mueller, 2003).

Figures 57 and 58 illustrate the change in the abundance of plagioclase from the Florida Panhandle (P1096 and P1080) to Destin Dome (OCS-G-6406) and Pensacola (OCS-G-6396), from the north side of the Pensacola Arch around the west to the south side of the arch, respectively. The Destin Dome and Pensacola samples have a high quartz content and a high ratio of orthoclase to plagioclase (3:1 on average). This is indicative of a cratonic source with low relief, long-term weathering and transport (Dickinson and Suczek, 1979). The Florida Panhandle samples have a lower quartz content with greater amounts of total feldspar characterized by roughly equal orthoclase and plagioclase. The arkosic (e.g. Folk, 1980) nature and proximal position to the Pensacola Arch of these samples indicate an uplifted basement source where relief is high and erosion is rapid (Dickinson and Suczek, 1979). Sample P1080 which is more proximal to the Pensacola Arch has a more immature texture than the other Florida samples, P1096 and P1004, having coarser, less well sorted, and more angular grains.

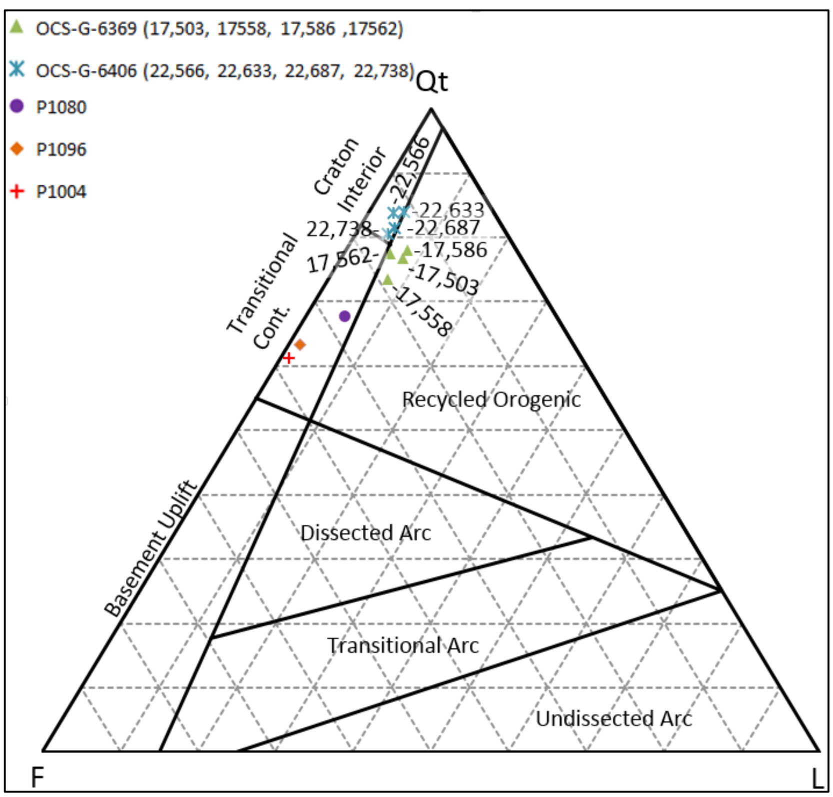

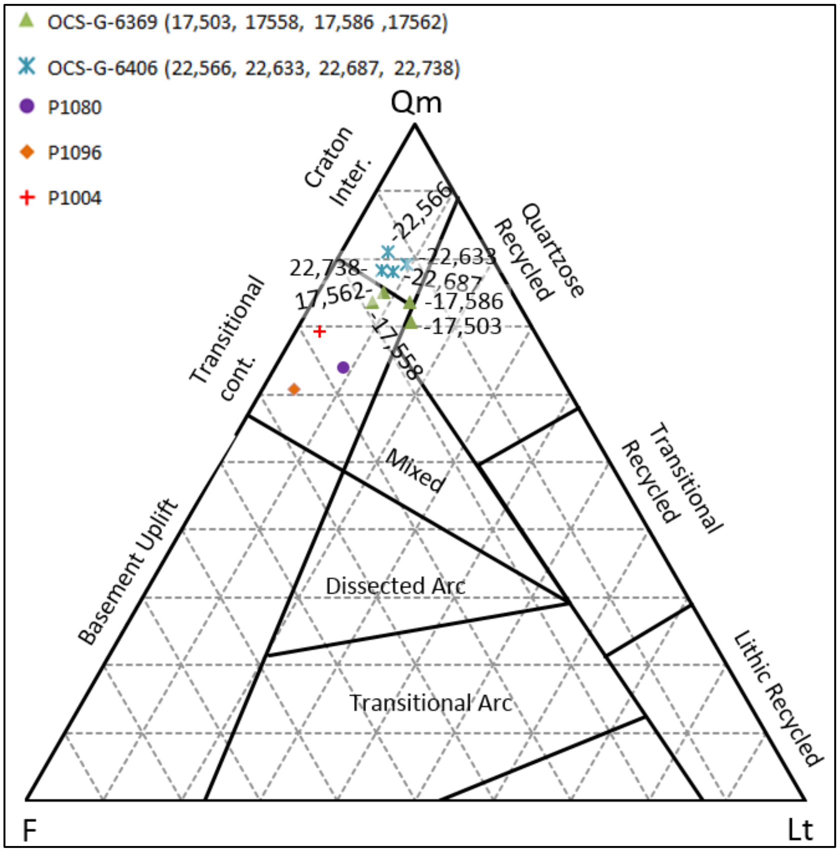

Figure 56. QtFL and QmFLt plots of the eolian facies of the Norphlet Formation after Dickinson, 1979. The ternary plots are used to determine the tectonic setting from which the sediments were derived. All samples plot as continental block and recycled orogenies.

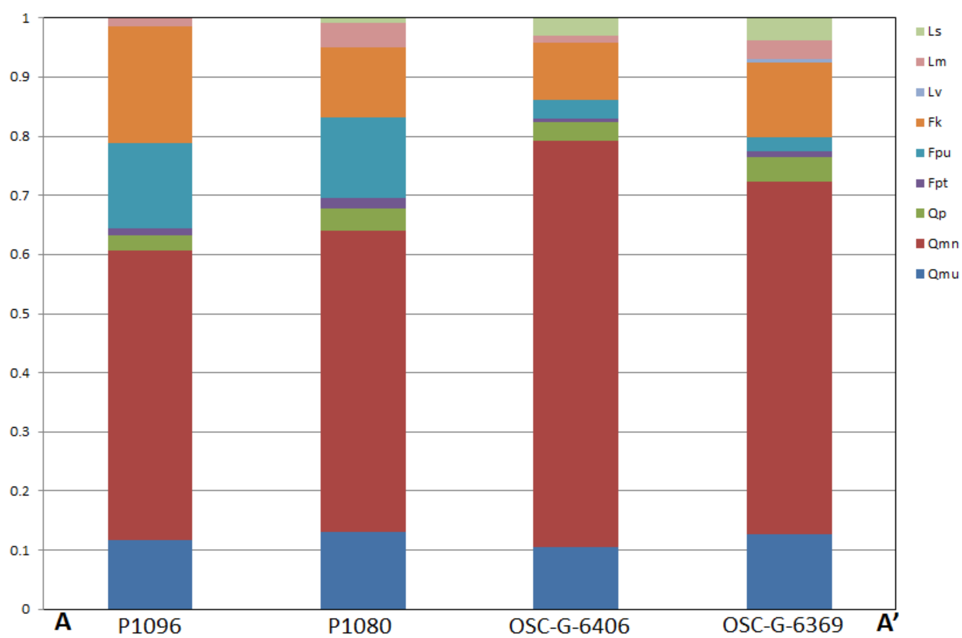

Figure 57. Relative abundances of framework grains for the eolian facies of the

Figure 58. Location of cross-section for Figure 47.

There is a shift within the samples from predominantly metamorphic rock fragments in the Florida Panhandle (P1004, P1096, and P1080) to predominantly sedimentary rock fragments in the Destin Dome sample (OCS-G-6406) to roughly equal metamorphic and sedimentary rock fragments in the Pensacola sample (OCS-G-6396; Fig. 59). This could show a difference in provenance of the Destin Dome and Pensacola samples as opposed to the Florida samples. Possible sources for sedimentary rock fragments in the Destin Dome sample (OCS-G-6406) include both Laurentia and Gondwana based on the U-Pb detrital zircon data. However, due to the larger percentage of sedimentary rock fragments updip in the Pensacola sample (OCS-G-6396), it is possible that more sedimentary rock fragments are being input from Gondwana then Laurentia.

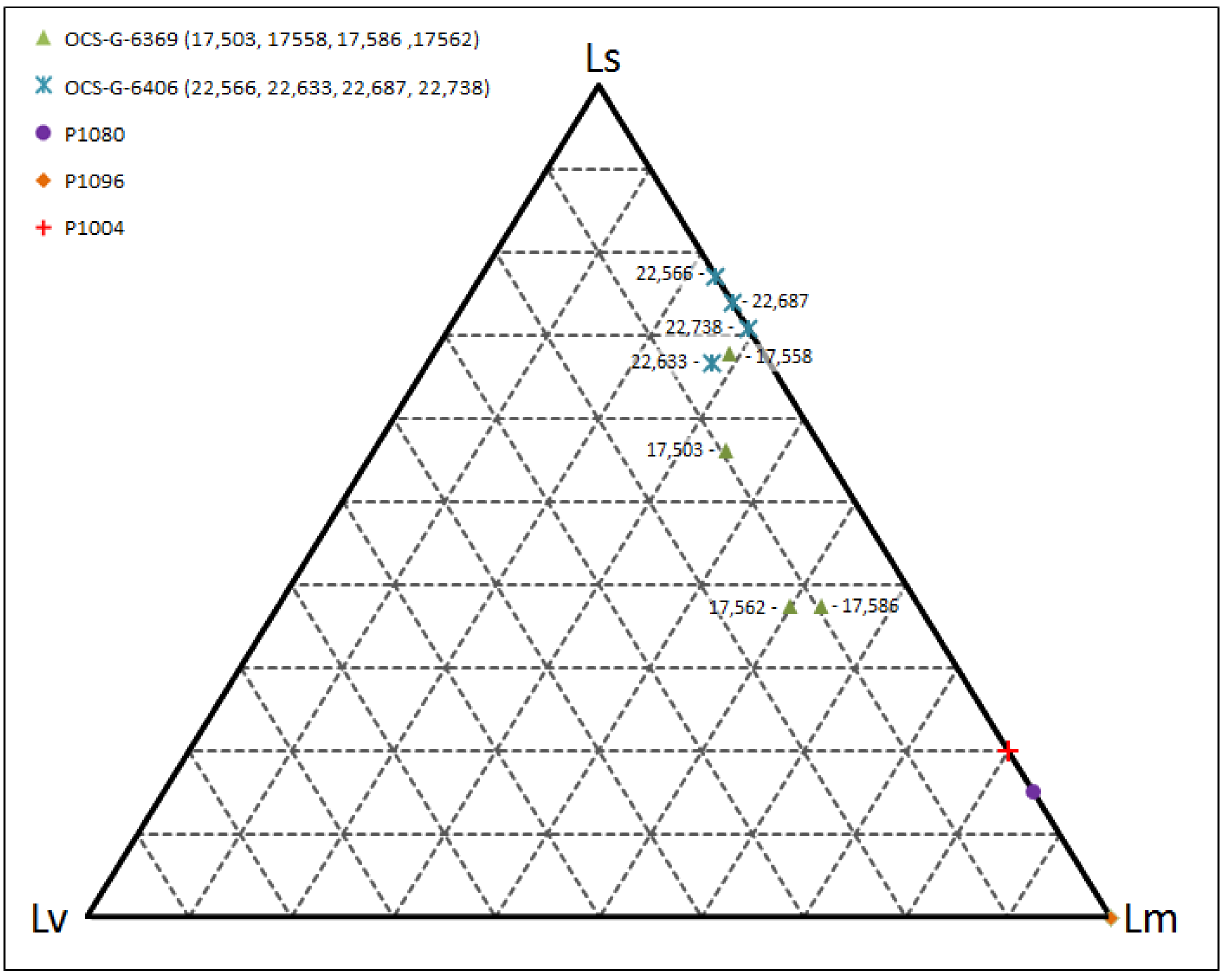

Figure 59. LsLmLv plot showing the relative abundances of lithic rock fragments (sedimentary, metamorphic, and volcanic) of the eolian facies of the Norphlet Formation.

5.4 Geospatial Trends in Dense Mineral Abundances

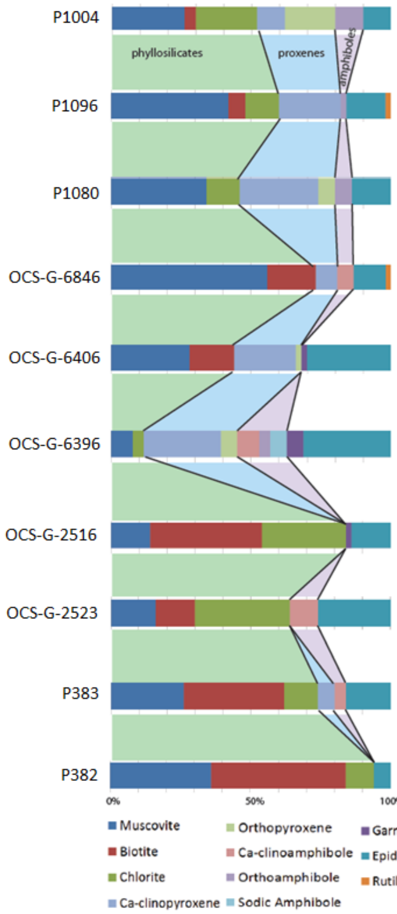

Figure 61. Abundances of dense minerals within the samples.

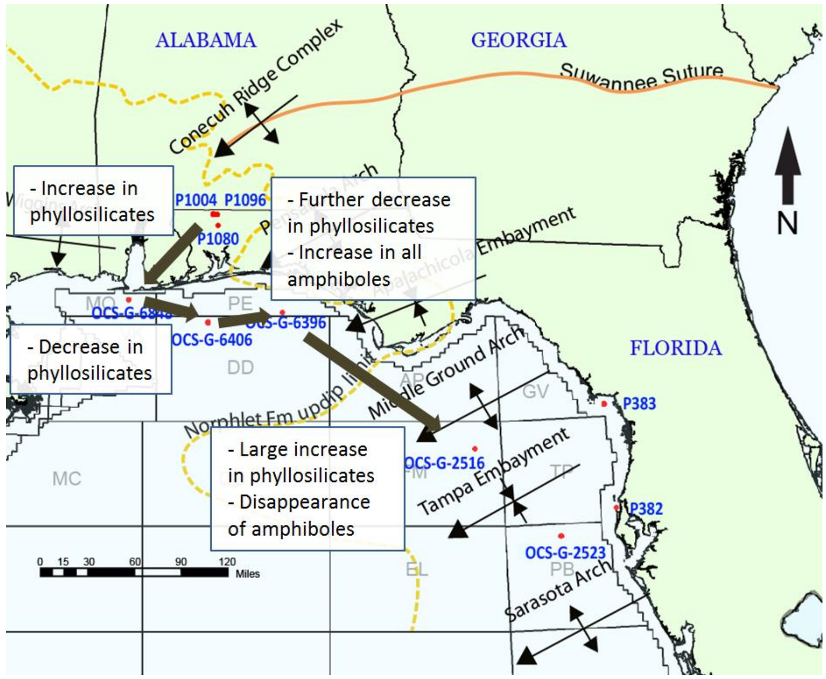

Figure 60. Geospatial trends in dense mineral abundances within the study.

Geospatial trends in dense mineral abundances can be observed from the north side of the Pensacola Arch, around the west to the southern side of the arch and down to the southeastern GOM samples (Fig. 60 and 61). The dense minerals in the Florida Panhandle are predominantly phyllosilicates, averaging 53% and an average of 25% pyroxene and 6% amphibole. Moving westward away from the arch to the Mobile Bay sample there is an increase in phyllosilicates to 73% and a decrease in pyroxenes. This is likely due to the proximity of the Wiggins Arch which consists largely of phyllite. Moving toward the southern side of the arch at sample OCS-G-6406 there is decrease in phyllosilicates and again a slight increase in pyroxenes. Further into the Apalachicola Embayment at sample OCS-G-6396 there is a further drop in phyllosilicates and major increase in chain silicates. This likely coincides with the proximity to volcanic activity occurring during the Triassic. Lastly, shifting toward the southeastern samples there is another increase in phyllosilicates and drop in chain silicates.

6. Provenance Scenario

Geospatial trends in U-Pb detrital zircon geochronology, sandstone composition, and heavy mineral abundances have allowed for the identification of four petrofacies. These petrofacies of similar source affinity have been identified based on similar U-Pb age populations, petrology, and dense mineral abundances and include primarily Laurentian-sourced, mixed Laurentian- and Gondwanan-sourced, primarily Gondwanan-sourced, and entirely Gondwanan-sourced (Fig. 62).

6.1 Primarily Laurentian Affinity: Mobile Bay

Only the Mobile Bay sample (OCS-G-6848) was primarily sourced by Laurentia. The largest U-Pb population in this sample is Grenville (900-1300 Ma), similar to what was seen in the Park et al. (2010) data from the Appalachian foreland basin. The second largest zircon population is coeval with the Appalachain Mountain building events (Taconic, 430-480 Ma, Acadian, 374-425 Ma, and Alleghanian, 280-325 Ma). These ages make up the majority (74%) of this sample. Other Laurentian sources identified in this sample of lower abundance include the Granite-Rhyolite (1300-1500 Ma) and Yavapai-Mazatzal (1600-1800 Ma) Provinces. The smallest population in this sample is Gondwanan with very few U-Pb dates that indicate Pan-African (6 ages; 500-680 Ma) and Trans-Amazonian/Eburnean (1 age; 1900-2250 Ma) sources. Because of the large contribution from the Appalachian hinterland and foreland basin and the near lack of Gondwanan ages, this sample is considered to be sourced primarily from Laurentia.

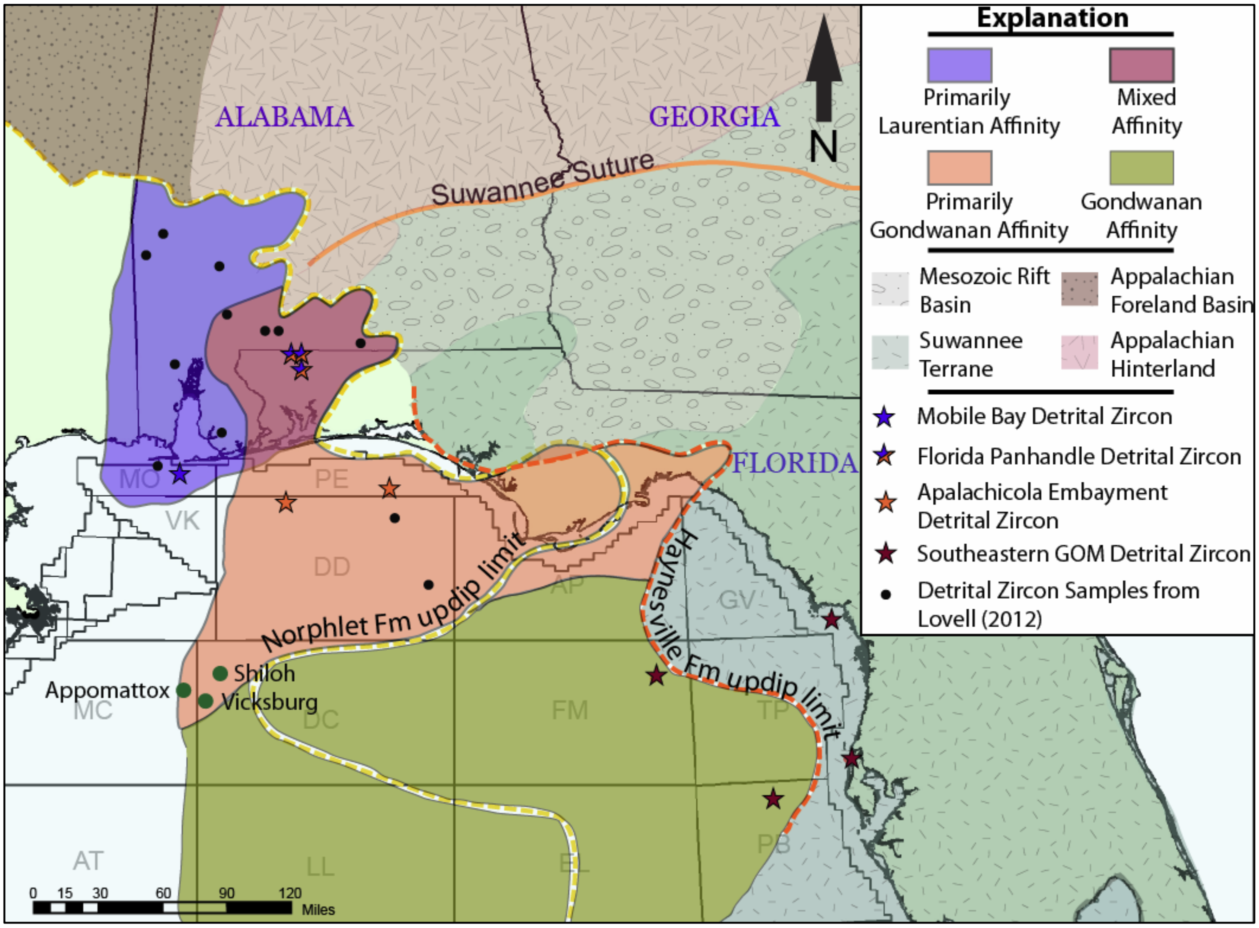

Figure 62. Petrofacies within the study area based on U-Pb detrital zircon age distributions, thin-section petrography, and dense mineral analysis from this study as well as Lovell (2013). Primarily Laurentian-affinity indicated in blue have the largest Laurentian coeval U-Pb age distribution. Gondwanan-affinity indicated in green have near entirely Gondwanan coeval U-Pb age distributions. Primarily Gondwanan-affinity indicated in orange have a larger amount of Gondwanan coeval U-Pb age distributions than Laurentian. Mixed affinity indicated in maroon have the larger Laurentian coeval U-Pb age distributions but distinct Gondwanan coeval U-Pb age distributions as well.

6.2 Gondwanan Affinity: Southeastern Gulf of Mexico

The samples from wells OCS-G-2516, OCS-G-2523, P383, and P382 have distinctly different U-Pb age distributions than the Mobile Bay sample. The two major age populations in these samples correlate to the Pan-African (500-680 Ma) and Trans-Amazonian/Eburnean events (1900-2250 Ma). Major peaks in these samples occur around 550 Ma and 620 Ma. These samples also lack any age population that correlate to Appalachian mountain building (Taconic, Acadian, Alleghanian), Grenville, or the Laurentian Craton (with the exception of two grains in sample OCS-G-2516). Less influential sources in these samples include the Gondwanan Sunsas/Central and South Africa orogenies which occurred between 950-1500 Ma and the African Archaen Terrane. Due to the lack of any Appalachian populations and large influence of the Pan-African and Trans-Amazonian/Eburnean events, these samples are considered to be sourced nearly entirely from Gondwana.

6.3 Mixed Affinity: Florida Panhandle

Samples P1004, P1096, and P1080 show an influence of both Laurentian and Gondwanan sources. The Laurentian influence appears stronger with the largest U-Pb age density belonging to the Grenville event (900-1300 Ma) in all three samples. However, due to the proximity of the sample location to the Carolina Terrane (Peri-Gondwana), some of the dates may actually belong to the Gondwanan Sunsas/Central and South Africa orogenies (900-1500 Ma). Because the Gondwanan Sunsas/Central and South Africa orogenies are a small signature in even the Gonwanan basement, it is likely that most of the 900-1300 Ma ages in samples P1004, P1096, and P1080 were derived from the Grenville rocks of Laurentia. Other Laurentian events identified in these samples include the Appalachain orogen, Granite-Ryholite Province (1300-1500 Ma), and the Yavapai-Mazatzal (1600-1800 Ma) Province. The Gondwanan source includes age populations that correlate with the Pan-African (500-680 Ma) and Trans-Amazonian/Eburnean (1900-2250 Ma) events. These two sources are much more apparent in samples P1004, P1096, and P1080 than compared to the Mobile Bay sample.

6.4 Primarily Gondwanan Affinity: Apalachicola Embayment

Samples OCS-G-6406 and OCS-G-6396 have a large Gondwanan signature in their U-Pb age populations. The Pan-African (500-680 Ma) event has the greatest abundance of U-Pb ages and have peaks near 550 Ma and 620 Ma similar to the southeastern Gulf of Mexico wells (OCS-G-2516, OCS-G-2523, P383, and P382). These samples also have a greater Trans-Amazonian/Eburnean (1900-2250 Ma) signature compared to the Mobile Bay and Florida Panhandle samples. However, some Laurentian influence is still apparent in age populations that correlate to the Alleghanian (280-325 Ma) and Taconic Orogeny (430-480 Ma). The Granite-Rhyolite (1300-1500 Ma) and Yavapai-Mazatzal (1600-1800 Ma) Province appear only in the Destin Dome well (OCS-G-6406). These two samples are also the only two samples that recorded the Triassic rifting event which correlates to the location of volcanism occurring along the Tallahasse graben (which created the Apalachicola Embayment). Only a few ages (1-2%) belong to the African Archean Terrane (2450-3050 Ma).

6.5 Geographic Extent of Petrofacies

The extent of these petrofacies have been based upon the previous U-Pb detrital zircon geochronology study by Lovell (2013) and by transport pathways identified through the correlation between source area from U-Pb ages and lithology. Transport modes include fluvial, based on facies distribution (Hunt, 2012) and the location of Jurassic paleo-highs, and wind, based on vector resultants of Norphlet Formation dune dip meter data (Hunt, 2012) and regional paleo-wind studies (Parrish and Peterson, 1988). Figure 63 shows the primary fluvial transport pathways which are slightly modified from Hunt (2013) based on the larger shale volume (>0.6) identified within the Apalachicola Embayment from this study.

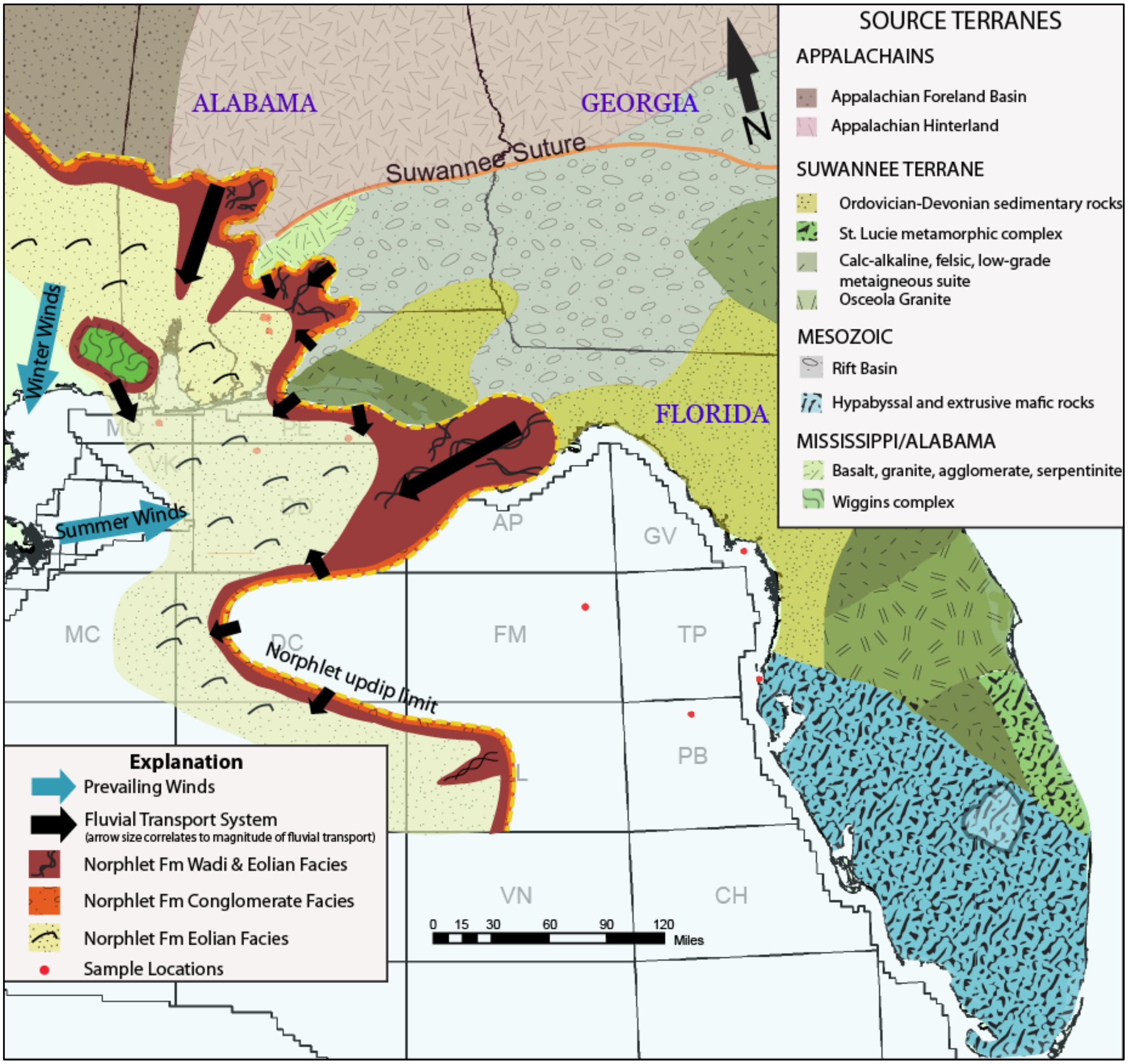

Figure 63. Paleogeographic map from provenance scenario that identifies four areas of similar sourcing. Extent of the conglomerate and wadi facies modified from Hunt (2012) based on U-Pb data and log-analysis. Prevailing winds from Parrish and Peterson (1988).

Figure 64 shows the predicted wind patterns for North American during the latest Jurassic. In the study area, the late Jurassic summer winds were directed east and winter winds directed southwest (east-northeast and south-southwest presently). The influence of these winds on the Norphlet eolian facies is apparent in the vector resultants of the dune dip meter data (Fig. 65).

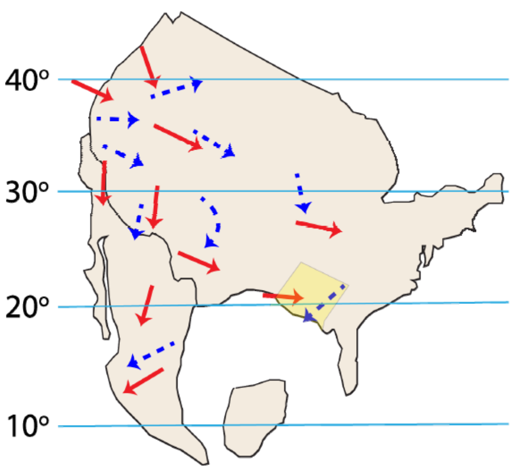

Figure 64. Paleo-wind patterns in North America in the latest Jurassic (Hunt, 2012 modified from Parrish and Peterson, 1988).

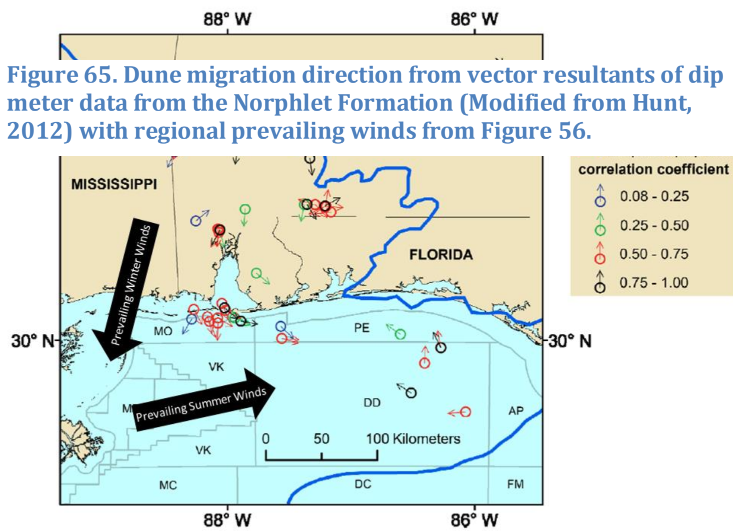

Figure 65. Dune migration direction from vector resultants of dip meter data from the Norphlet Formation (Modified from Hunt, 2012) with regional prevailing winds from Figure 56.

7. Implications for Paleogeography

Provenance data from this study along with previous paleogeographic studies of the Norphlet Formation show that the Norphlet was sourced from proximal paleo-highs and transported into the eolian system via alluvial fans and wadis.   Changes in provenance are apparent in the U-Pb data, sandstone composition, and dense mineral analysis. These proxies show a change in source from north of the Pensacola Arch (mixed affinity) around the west (Laurentian-affinity) and into the Apalachicola Embayment (Gondwanan-affinity). This supports the idea of a nearby source supplying sand to the Norphlet Formation. It also supports the idea that the paleo-highs acted as sediment barriers between the paleo-low depocenters as the Gondwanan-affinity signature is exclusively found to the south of the Pensacola Arch.

The magnitude of fluvial transport of the Norphlet Formation from the paleo-highs is interpreted from the lateral extent of the wadi facies. Hunt (2012) used well logs to determine the extent of wadi facies within the study area (Fig. 63). Certain geographic areas show a greater influence of fluvial transport via wadis such as in the Apalachicola Embayment. This region has the highest shale volume within the study area correlating to a greater amount of clay produced from water transport. Another area of abundant fluvial facies includes the north to south tract of wadi facies in southwestern Alabama. The length of the wadi facies tract in these two areas indicate that the source for sediment within the Apalachicola Embayment as well as Mobile Bay could be from much greater distances than surrounding areas such as the Conecuh Embayment.

The development of a large Norphlet erg system shows that this area was arid during the deposition of the Norphlet Formation. Once sediment entered the eolian system the prevailing wind directions controlled sediment dispersal. Prevailing seasonal wind patterns from Parrish and Peterson (1988) correlate with dip meter data of Norphlet dunes (Hunt, 2012) in southwest Alabama and the Mobile Bay offshore lease blocks (Fig. 64and 65). However, the dune dip meter data does not correlate with the prevailing winds within the Apalachicola Embayment. Because the dip meter data implies a west-northwest migration pattern, this could imply that the Apalachicola Embayment paleo-low channeled winter winds along the axis of the paleo-low. This occurrence is often seen in modern setting such as the Dead Sea wadis which channel east-southeast winds to the south along the axis of the valley (Shafir et al., 2008).

The combination of the overall fluvial and eolian transport direction and magnitude imply that the majority of the Norphlet Formation sand came from the north (Laurentian) and from the east (Gondwanan, via the Apalachicola Embayment). There is little evidence for a mixing zone similar to that of the Florida Panhandle where these two major sediment transport pathways meet. Samples from Mobile Bay and Destin Dome (OCS-G-6848 and OCS-G-6406) which are relatively close are still quite different from each other with regards to U-Pb distribution and composition. Because of this is it assumed that little mixing occurred between sediment from the north and the east. The lack of mixing is common in present erg systems such as the African Namib Sea where opposing south-southeast and north-northeast sand transport systems lead to deposition where sediments remain (Lancaster, 1995). These regions of converging eolian transport systems often correlate to a thickening of the deposits. This correlates with the greatest thickness of the Norphlet Formation occurring in the eastern Mobile Bay and western Destin Dome and Pensacola offshore lease blocks within the study area (Fig. 37).

The paleogeography for the Norphlet Formation in the EGOM can be used to infer sediment deposition for the clastic Haynesville Formation. Hunt (2012) performed U-Pb detrital zircon geochronology on the Haynesville Formation for four samples from the Mobile Bay, Pensacola, and Destin Dome offshore lease blocks and found similar results as Lovell's (2013) Norphlet study implying that sediment transport pathways remained similar from the deposition of the Norphlet Formation to the deposition of the Haynesville Formation. Similar to the Norphlet Formation, the Haynesville Formation was sourced from proximal paleo-highs creating an updip alluvial fan facies. Sediment was then further distributed along the axis of the paleo-lows. Because the Haynesville Formation lacks eolian sediments, transportation is predominantly fluvial, moving down dip. Downdip, sand facies grades into a shale facies which becomes more predominant (Dobson and Buffler, 1997). While Hunt (2012) found Laurentian-aged zircon in his Haynesville Formation samples, the Haynesville Formation samples from the Florida Middle Ground and St. Petersburg offshore lease blocks, OCS-G-2516 and OCS-G-2523, in the Tampa Embayment, had no Laurentian-aged zircon and are inferred to be entirely sourced by the proximal Suwanne Terrane.

8. Conclusions

1. U-Pb analysis of 867 detrital zircon from 10 samples provided ages that are coeval with several possible source terranes and tectonic events. These include Pangean rifting (>250 Ma), Alleghanian (280-325 Ma), Acadian (374-425 Ma), Taconic (430-480 Ma), Pan-African (500-680 Ma), Mt. Rogers rifting (700-760 Ma), Grenville (900-1300), Sunsas and South and Central African Orogenies (950-1500 Ma), Granite-Rhyolite (1300-1500 Ma), Yavapai-Mazatzal (1600-1800 Ma), Trans-Amazonian/Eburnean (1900-2250), and African Archean Terrane (2450-3040 Ma). The U-Pb age distribution of these events within the samples allowed for the identification of four geochologic sources terranes which provided sediment to the Norphlet and surrounding formations. These include the Appalachian foreland basin, Appalachian hinterland, Mesozoic rift basin, and the Suwannee Terrane.

2. Point counting of 11 thin-sections from the Florida Panhandle (P1004, P1096, and P1080) and Apalachicola Embayment (OCS-G-6406 and OCS-G-6396) samples determined the Norphlet to consist of arkose and subarkose, respectively. The average modal abundance from the Florida Panhandle samples is $Q_{64}F_{33}L_3$. The Apalachicola Embayment samples are more compositionally mature with average modal abundances of $Q_{79}F_{15}L_6$.
3. Four areas of source affinity are identified based on U-Pb detrital zircon geochronology, sandstone petrology, and dense mineral analysis. These include the Mobile Bay offshore lease block which has a primarily Laurentian-affinity, the Apalachicola Embayment which has a primarily Gondwanan-affinity, the western Florida Panhandle which has a mixed affinity, and the southeastern Gulf of Mexico which has an entirely Gondwanan-affinity. The primarily and entirely Gondwanan-affinity regions are projected into the DeSoto and Mississippi Canyon offshore lease blocks indicating that the eolian sediment of the major Norphlet hydrocarbon discoveries, Shiloh, Vicksburg, and Appomatox, were sourced from the Suwannee Terrane.
4. Two major directions of sediment transport pathways are identified in the study area, both fluvial and eolian, were determined from the extent of wadi facies and dune dip data, respectively. In southwestern Alabama the major sediment transport pathway is south into the Mobile Bay offshore lease block. Within the Apalachicola Embayment, the dominant sediment transport pathway is west-northwest. Because the Apalachicola Embayment was a major sediment transport pathway that channeled paleowind during the deposition of the Norphlet Formation, the extent of the primarily Gondwanan-

affinity region reaches into the DeSoto and Mississippi Canyon offshore lease blocks. This is supported by the similarity between the Destin Dome and Pensacola samples which are approximately 60 miles apart. The similarity exists in all provenance data, including U-Pb age distributions, dense mineral analysis, and sandstone petrology.

5. The higher shale volume along with the presence of wadi and shale facies within the Apalachicola Embayment also suggests it was a major fluvial transport pathway during the Norphlet deposition.
6. The difference in provenance data from the north side of the Pensacola Arch around the west to south side of the arch suggests that the arch acted as a barrier to sediment transport. Sediments deposited within the northeast-southwest trending paleo-lows within the study area do not show mixing with each other.
7. The lack of mixing between the Mobile Bay and the western Destin Dome offshore lease block samples imply that when the two major transport pathways (south and west-northwest) converge, sediment deposition occurred rather than mixing between the two areas. This region of convergence correlates to the thickest Norphlet deposition within the study area.
8. Paleogeography of the Haynesville Formation within the Tampa Embayment can be inferred from Norphlet Formation paleogeography. Similar to Norphlet Formation, the Haynesville Formation is sourced from proximal paleo-highs which, in the Tampa Embayment, is the Suwannee Terrane. Updip is an alluvial facies which grade into a fluvial facies channeled to the east-southeast by the Tampa Embayment which becomes more shaley downdip.

References

Ajdukiewicz, J. M., P. H. Nicholson, and W. L. Esch, 2010, Prediction of deep reservoir quality using early diagenetic process models in the Jurassic Norphlet Formation, Gulf of Mexico: AAPG Bulletin, v. 94, no. 8, p. 1189–1227.

Andersen, T., 2005, Detrital zircons as tracers of sedimentary provenance: limiting conditions from statistics and numerical simulation: Chemical Geology, v. 216, no. 3-4, p. 249–270.

Arthur, J. D., 1988, Petrogenesis of Early Mesozoic Tholeiite in the Florida Basement and an Overview of Florida Basement Geology: Tallahssee, 40 p.

Becker, T. P., W. A. Thomas, S. D. Samson, and G. E. Gehrels, 2005, Detrital zircon evidence of Laurentian crustal dominance in the lower Pennsylvanian deposits of the Alleghanian clastic wedge in eastern North America: Sedimentary Geology, v. 182, no. 1-4, p. 59–86.

Bettencourt, J. S., W. B. Leite, A. S. Ruiz, R. Matos, B. L. Payolla, and R. M. Tosdal, 2010, The Rondonian-San Ignacio Province in the SW Amazonian Craton: An overview: Journal of South American Earth Sciences, v. 29, no. 1, p. 28–46.

Bureau of Ocean Energy Management, 2012a, Assessment of Technically Recoverable Hydrocarbon Resources of the Gulf of Mexico Outer Continental Shelf as of January 2009: <http://www.data.boem.gov/homepg/data_center/paleo/paleo.asp> (accessed September 1, 2012).

Bureau of Ocean Energy Management, 2012b, Paleontologic Information: <http://www.data.boem.gov/homepg/data_center/paleo/paleo.asp> (accessed September 1, 2012).

Chowns, T. M., and C. T. Williams, 1983, Pre-Cretaceous rocks beneath the Georgia coastal plain - regional implications, *in* G. S. Gohn, ed., Studies related to the Charleston, South Carolina, earthquake of 1886 - tectonics and seismicity: USGS Professional Paper 1313 L, p. 42.

Claypool, G. E., and E. A. Mancinl, 1989, Geochemical Relationships of Petroleum in Mesozoic Reservoirs to Carbonate Source Rocks of Jurassic Smackover Formation , Southwestern Alabama ’: AAPG Bulletin, v. 1, no. 1, p. 904–924.

Condie, K. C., E. Belousova, W. L. Griffin, and K. N. Sircombe, 2009, Granitoid events in space and time: Constraints from igneous and detrital zircon age spectra: Gondwana Research, v. 15, no. 3-4, p. 228–242.

Culver, S. J., H. . Williams, and R. Venkatakrishnan, 1991, The Rokelide Orogen, *in* R. D. Dallmeyer, and J. P. Lecorche, eds., The West African Orogens and Circum-Atlantic Correlatives: Berlin, Springer, p. 124–150.

Dallmeyer, R. D., 1987, 40Ar/39Ar age in detrital muscovite within Lower Ordovician sandstone in the coastal plain basement of Florida: Implications for west Africa terrane linkages: Geology, v. 15, p. 998–1001.

Dallmeyer, R. D., 1989, Contrasting accreted terranes in the southern Appalachian Orogen, basement beneath the Atlantic and Gulf Coastal Plains and West African orogens: Precambrian Research, v. 42, no. 3-4, p. 387–409.

Department of the Interior, 2008, Reasonably Foreseeable Development Scenario for Fluid Minerals: Florida: 43 p.

Dickinson, W. R., and C. A. Suczek, 1979, Plate Tectonics and Sandstone Compositions: AAPG Bulletin, v. 12, no. 12, p. 2164–2182.

Dobson, L. M., and R. T. Buffler, 1997, Seismic Stratigraphy and Geologic History of Jurassic Rocks , Northeastern Gulf of Mexico 1: AAPG Bulletin, v. 1, no. 1, p. 100–120.

Fedo, C. M., T. George, K. N. Sircombe, R. H. Rainbird, and B. Street, 2003, Detrital Zircon Analysis of the Sedimentary Record, *in* J. M. Hancher, and P. W. . Hoskin, eds., Zircon: Reviews in Mineralogy and Geochemistry: p. 277–303.

Folk, R. L., 1980, Petrology of Sedimentary Rocks: Austin, Hamilton Publishing, p. 184.

Gehrels, G., V. Valencia, and A. Pullen, 2006, NoDetrital Zircon Geochronology by Laser Ablation Multicollector ICPMS at the Arizona LaserChron Center, *in* T. Olszewski, ed., Geochronology: Emerging Opportunities: Paleontology Society Papers: p. 67–76.

Hartmann, L. A., 2002, The Mesoproterozoic Supercontinent Atlantica in the Brazilian Shield - Review of Geological and U-Pb Zircon and Sm-Nd Isotopic Evidence: Gondwana Research, v. 5, p. 157–163.

Heatherington, A.L, and P. A. Mueller, 1999, Lithospheric sources of North Florida, USA tholeiites and implications for the origin of the Suwannee terrane: Lithos, v. 46, no. 2, p. 215–233.

Heatherington, A.L., and P. A. Mueller, 2003, Mesozoic Igneous Activity in the Suwannee Terrane, Southeastern USA: Petrogenesis and Gondwanan Affinities: Gondwana Research, v. 6, no. 2, p. 296–311.

Hibbard, J. P., E. F. Stoddard, D. T. Secor, and A. J. Dennis, 2002, The Carolina Zone : overview of Neoproterozoic to Early Paleozoic peri-Gondwanan terranes along the eastern Flank of the southern Appalachians: Earth-Science Reviews, v. 57, p. 299–339.

Hoffman, P. F., 1999, The break-up of Rodinia, birth of Gondwana, true polar wander and the snowball Earth: Journal of African Earth Sciences, v. 28, no. 1, p. 17–33.

Hoskin, P. W. O., and U. Schaltegger, 2003, The Composition of Zircon and Igneous and Metamorphic Petrogenesis, *in* J. M. Hancher, and P. W. . Hoskin, eds., Zircon: Reviews in Mineralogy and Geochemistry: p. 27–62.

Hunt, B. W., 2012, Regional Norphlet Facies Correlation, Analysis and Implications for Paleostructure and Provenance, Eastern Gulf of Mexico: The University of Alabama, p. 112.

Ingersoll, R. V., T. F. Bullard, R. L. Ford, J. P. Grimm, and J. D. Pickle, 1984, The effect of grain size on detrital modes: a testof the Gazzi-Dickinson point-counting method: Journal of Sedimentary Petrology, v. 54, p. 103–116.

Lancaster, N., 1995, The geomorphology of desert dunes: New York, Routledge, p. 290.

Lovell, T., and A. Weislogel, 2010, Detrital Zircon U-Pb Age Constraints on the Provenance of the Late Jurassic Norphlet Formation, Eastern Gulf of Mexico : Implications for Paleogeography: Gulf Coast Association of Geological Societies Transactions, v. 60, p. 443–460.

Lovell, T., 2013, Detrital Zircon U-Pb Age Constraints on the Provenance of the Upper Jurassic Norphlet Formation, Eastern Gulf of Mexico : The University of Alabama, p. 173.

Ludwig, K. R., 2012, A Geochronological Toolkit for Microsoft Excel Berkeley Geochronology Center Special Publication No. 5: p. 75.

Mancini, E. A., R. M. Mink, B. L. Bearden, and R. P. Wilkerson, 1985, Norphlet Formation (Upper Jurassic) of Southwestern and Offshore Alabama : Environments of Deposition and Petroleum Geology: AAPG Bulletin, v. 69, p. 881–898.

Mancini, E. A., B. H. Tew, and R. M. Mink, 1990, Jurassic Sequence Stratigraphy in the Mississippi Interior Salt Basin of Alabama: Gulf Coast Association of Geological Societies Transactions, v. 40, p. 521–530.

Marton, G. L., and R. T. Buffler, 1999, Jurassic—early cretaceous tectono-paleogeographic evolution of the southeastern gulf of Mexico basin, *in* A. D. Miall, ed., Sedimentary Basins of the World: Elsevier, p. 63–91.

MMS, 2001, The Promise of Deep Gas in the Gulf of Mexico: U.S. Department of the Interior: OCS Report, MMS 2001–037 p.

Mueller, P. A., A.L. Heatherington, J.L. Wooden, R. D. Shuster, A. P. Nutman, and I. S. Williams, 1994, Precambrian zircons from the Florida basement : A Gondwanan connection: Geology, v. 22, p. 119–122.

Oil & Gas Journal, 2012, Shell, Nexen locate more oil in gulf Norphlet trend: <http://www.ogj.com/articles/print/vol-110/issue-4a/general-interest/shell-nexen-locate-more.html> (accessed October 21, 2012).

Park, H., D. L. Barbeau Jr., A. Rickenbaker, D. Bachmann-Krug, and George Gehrels, 2010, Application of Foreland Basin Detrital-Zircon Geochronology to the Reconstruction of the Southern and Central Appalachian Orogen: The Journal of Geology, v. 118, no. 1, p. 23–44.

Parrish, J. T., and F. Peterson, 1988, Wind directions predicted from global circulation models and wind directions determined from eolian sandstones of the western United States—A comparison: Sedimentary Geology, v. 56, no. 1-4, p. 261–282.

Pearson, O. N., 2011, Undiscovered Hydrocarbon Resources in the U.S. Gulf Coast Jurassic Norphlet and Smackover Formations: Gulf Coast Association of Geological Societies Transactions, v. 61, p. 329–340.

Van Der Plas, L., and A. C. Tobi, 1965, Point Counting prob.pdf: American Journal of Science, v. 263, p. 87–90.

Ridgway, J. G., 2010, Upper Jurassic (Oxfordian) Smackover Facies characterization at Little Cedar Creek Field, Conecuh County, Alabama: The University of Alabama, p. 129.

Salvador, A., 1987, Late Triassic-Jurassic Paleogeography and Origin of Gulf of Mexico Basin: AAPG Bulletin, v. 71, no. 4, p. 419–451.

Sassen, R., C. H. Moore, J. A. Nunn, F. C. Meendsen, and E. Heydari, 1987, Geochemical Studies of Crude Oil Generation, Migration, and Destruction in the Mississippi Salt Basin: Gulf Coast Association of Geological Societies Transactions, v. 37, p. 217–224.

Schofield, D. I., and M. R. Gillespie, 2007, A tectonic interpretation of “Eburnean terrane” outliers in the Reguibat Shield, Mauritania: Journal of African Earth Sciences, v. 49, no. 4-5, p. 179–186.

Scott, G. W., 1991, Petrology and provenance of the Norphlet Formation, Panhandle, Florida, *in* Florida Geological Survey, Information Circular no. 107: p. 89–121.

Shafir, H., F. J. Jin, Y. Lati, M. Cohen, and P. Alpert, 2008, Wind Channeling by the Dead-Sea Wadis: The Open Atmospheric Science Journal, v. 2, no. 1, p. 139–152.

Steltenpohl, M. G., P. M. Mueller, Ann L. Heatherington, T. B. Hanley, and Joseph L. Wooden, 2008, Gondwanan/peri-Gondwanan origin for the Uchee terrane, Alabama and Georgia: Carolina zone or Suwannee terrane(?) and its suture with Grenvillian basement of the Pine Mountain window: Geosphere, v. 4, no. 1, p. 131.

Tew, B. H., R. M. Mink, S. D. Mann, B. L. Bearden, and E. A. Mancini, 1991, Geologic Framework of Norphlet and pre-Norphlet strata of the onshore and offshore eastern Gulf of Mexico area: Gulf Coast Association of Geological Societies Transactions, v. 41, p. 590–600.

Veevers, J. J., 2007, Pan-Gondwanaland post-collisional extension marked by 650–500 Ma alkaline rocks and carbonatites and related detrital zircons: A review: Earth-Science Reviews, v. 83, no. 1-2, p. 1–47.

Vermeesch, P., 2004, How many grains are needed for a provenance study?: Earth and Planetary Science Letters, v. 224, no. 3-4, p. 441–451.

Villeneuve, M., 2008, Review of the orogenic belts on the western side of the West African Craton: the Bassarides, Rokelides and Mauritanides: The boundaries of the West African Craton, v. Special Pu, p. 169–201.

Walls, I. A., 1985, Provenance of the Jurassic Norphlet Formation in southwestern Alabama: The University of Alabama, p. 143.

Wilson, L. K., 2011 , The origin and development of the Tampa Embayment: Implications for the tectonic evolution of the eastern Gulf of Mexico: The University of Alabama, p. 63.

Appendices

Appendix 1: Detrital Zircon U-Pb Isotopic Analysis

Analysis	U (ppm)	206Pb 204Pb	U/Th	206Pb* 207Pb*	± (%)	207Pb* 235U*	± (%)	206Pb* 238U	± (%)	error corr.	206Pb* 238U*	± (Ma)	207Pb* 235U	± (Ma)	206Pb* 207Pb*	± (Ma)	Best age (Ma)	± (Ma)	Conc (%)
1096-17	95	17593	0.7	20.0251	10.2	0.3626	10.4	0.0527	2.2	0.21	330.9	6.9	314.2	28.2	192.1	238.2	330.9	6.9	NA
1096-14	404	60903	1.2	19.0582	1.5	0.3943	2.7	0.0545	2.3	0.85	342.1	7.7	337.5	7.8	306.0	33.1	342.1	7.7	NA
1096-75	321	34760	2.3	18.3570	1.5	0.4394	1.7	0.0585	1.0	0.55	366.5	3.4	369.8	5.4	390.7	32.6	366.5	3.4	NA
1096-30	429	98507	4.5	18.6564	1.0	0.4433	1.6	0.0600	1.2	0.77	375.5	4.4	372.6	4.9	354.3	22.5	375.5	4.4	NA
1096-91	357	62899	8.1	18.7980	2.7	0.4421	3.7	0.0603	2.5	0.67	377.3	9.1	371.7	11.5	337.2	62.1	377.3	9.1	NA
1096-84	254	26167	1.1	18.4851	1.7	0.4527	2.7	0.0607	2.0	0.75	379.8	7.4	379.2	8.4	375.1	39.3	379.8	7.4	NA
1096-65	68	17723	0.7	18.4785	14.6	0.4656	17.1	0.0624	9.0	0.53	390.2	34.2	388.1	55.3	375.9	329.2	390.2	34.2	NA
1096-4	206	116467	1.2	18.0571	1.5	0.5050	5.0	0.0661	4.7	0.95	412.8	19.0	415.1	16.9	427.6	32.9	412.8	19.0	96.6
1096-43	168	55424	1.4	17.8156	2.8	0.5270	3.1	0.0681	1.2	0.40	424.7	5.0	429.8	10.7	457.6	62.1	424.7	5.0	92.8
1096-29	128	40267	1.5	18.3011	3.8	0.5205	4.1	0.0691	1.6	0.39	430.6	6.7	425.5	14.3	397.6	84.8	430.6	6.7	108.3
1096-49	705	181051	2.9	18.0433	1.0	0.5295	1.5	0.0693	1.1	0.76	431.9	4.8	431.5	5.3	429.3	21.7	431.9	4.8	100.6
1096-41	308	40466	1.2	18.1439	1.2	0.5278	2.0	0.0695	1.5	0.79	432.9	6.5	430.3	6.9	416.9	27.0	432.9	6.5	103.8
1096-22	258	76449	2.7	18.2841	1.8	0.5242	2.2	0.0695	1.3	0.58	433.2	5.3	428.0	7.7	399.6	40.4	433.2	5.3	108.4
1096-54	98	3276	2.8	17.0409	11.8	0.5679	12.1	0.0702	2.7	0.22	437.3	11.3	456.7	44.6	555.3	258.5	437.3	11.3	78.8
1096-23	94	22841	1.0	18.6579	5.6	0.5208	5.7	0.0705	1.4	0.24	439.0	5.7	425.7	19.9	354.1	125.6	439.0	5.7	124.0
1096-15	77	18733	0.8	17.9306	4.6	0.5665	4.9	0.0737	1.6	0.33	458.3	7.2	455.8	18.0	443.2	103.2	458.3	7.2	103.4
1096-61	254	60146	1.0	17.6687	2.2	0.5818	2.4	0.0746	0.9	0.36	463.5	3.8	465.6	8.9	475.9	49.5	463.5	3.8	97.4
1096-46	204	77026	2.5	17.9228	2.0	0.5833	2.5	0.0758	1.5	0.59	471.1	6.7	466.5	9.4	444.2	45.2	471.1	6.7	106.1
1096-47	98	8764	1.4	18.1907	6.9	0.5893	7.1	0.0778	1.7	0.24	482.7	7.9	470.4	26.7	411.1	154.3	482.7	7.9	117.4
1096-11	393	107377	1.4	17.6799	0.6	0.6097	0.9	0.0782	0.7	0.72	485.3	3.1	483.4	3.5	474.4	14.0	485.3	3.1	102.3
1096-40	100	3009	1.1	17.3739	5.0	0.6227	5.3	0.0785	1.8	0.33	487.0	8.2	491.6	20.8	513.0	110.9	487.0	8.2	94.9
1096-72	283	200505	0.8	17.0321	1.6	0.7019	1.7	0.0867	0.8	0.45	536.0	4.0	539.9	7.3	556.5	33.8	536.0	4.0	96.3
1096-56	298	22095	1.0	17.0740	2.6	0.7147	3.2	0.0885	1.9	0.59	546.7	10.0	547.6	13.6	551.1	56.5	546.7	10.0	99.2
1096-59	122	28911	2.2	16.9732	2.2	0.7505	2.4	0.0924	1.0	0.42	569.6	5.6	568.5	10.5	564.0	47.4	569.6	5.6	101.0
1096-83	215	92329	0.9	16.7671	1.1	0.7797	1.5	0.0948	1.1	0.70	584.0	5.9	585.3	6.8	590.6	23.6	584.0	5.9	98.9
1096-76	81	34313	1.6	16.9732	3.4	0.7776	3.8	0.0957	1.6	0.44	589.3	9.3	584.1	16.8	564.0	74.3	589.3	9.3	104.5
1096-39	16	5920	2.0	16.8745	21.0	0.7849	21.5	0.0961	4.6	0.21	591.3	25.7	588.3	96.3	576.7	461.4	591.3	25.7	102.5
1096-48	55	15248	0.7	15.9830	4.6	0.8468	4.9	0.0982	1.8	0.37	603.6	10.6	622.9	22.9	693.6	97.4	603.6	10.6	87.0
1096-74	192	124314	7.6	16.2328	1.7	0.8711	1.8	0.1026	0.8	0.44	629.3	4.9	636.1	8.7	660.4	35.4	629.3	4.9	95.3
1096-89	144	69993	1.2	16.3589	2.6	0.8753	2.7	0.1039	0.7	0.26	636.9	4.3	638.4	12.7	643.8	55.4	636.9	4.3	98.9
1096-73	106	119748	0.9	16.1278	1.4	0.9768	2.1	0.1143	1.6	0.76	697.4	10.6	692.0	10.5	674.3	28.9	697.4	10.6	103.4
1096-20	38	55495	1.3	14.2072	3.2	1.6015	3.8	0.1650	2.0	0.52	984.6	18.0	970.8	23.5	939.6	65.7	939.6	65.7	104.8
1096-37	39	22325	1.9	14.0530	3.1	1.5758	3.4	0.1606	1.3	0.40	960.1	12.0	960.7	20.9	962.0	62.9	962.0	62.9	99.8
1096-38	61	40675	1.4	13.8913	2.8	1.6545	3.1	0.1667	1.4	0.45	993.9	12.8	991.3	19.6	985.6	56.3	985.6	56.3	100.8
1096-82	72	42116	2.7	13.8465	2.1	1.6635	2.3	0.1671	1.0	0.42	995.9	8.9	994.7	14.6	992.2	42.4	992.2	42.4	100.4

Analysis	U	206Pb	U/Th	206Pb*	±	207Pb*	±	206Pb*	±	error	206Pb*	±	207Pb*	±	206Pb*	±	Best age	±	Conc
	(ppm)	204Pb		207Pb*	(%)	235U*	(%)	238U	(%)	corr.	238U*	(Ma)	235U	(Ma)	207Pb*	(Ma)	(Ma)	(Ma)	(%)
1096-86	43	56143	2.6	13.7603	2.9	1.6529	4.3	0.1650	3.2	0.74	984.3	29.0	990.7	27.2	1004.8	58.9	1004.8	58.9	98.0
1096-63	27	39608	1.8	13.7333	3.3	1.7263	3.5	0.1719	1.2	0.34	1022.8	11.3	1018.4	22.8	1008.8	67.7	1008.8	67.7	101.4
1096-1	246	180208	4.3	13.7250	0.8	1.7540	2.2	0.1746	2.1	0.94	1037.4	20.0	1028.6	14.4	1010.0	15.6	1010.0	15.6	102.7
1096-92	50	110967	2.4	13.7199	2.4	1.7733	3.0	0.1765	1.7	0.58	1047.6	16.7	1035.7	19.3	1010.8	49.2	1010.8	49.2	103.6
1096-97	705	561180	13.3	13.7081	0.5	1.6910	2.7	0.1681	2.6	0.99	1001.8	24.3	1005.1	16.9	1012.5	9.2	1012.5	9.2	98.9
1096-88	83	36779	2.5	13.6943	1.7	1.7679	2.4	0.1756	1.6	0.69	1042.8	15.8	1033.8	15.3	1014.6	34.5	1014.6	34.5	102.8
1096-13	70	77808	1.7	13.6111	1.7	1.7495	3.3	0.1727	2.9	0.87	1027.0	27.1	1027.0	21.3	1026.9	33.4	1026.9	33.4	100.0
1096-50	136	178228	2.4	13.5936	1.4	1.7950	1.6	0.1770	0.8	0.49	1050.4	7.5	1043.6	10.4	1029.5	28.2	1029.5	28.2	102.0
1096-8	105	51376	1.5	13.5892	1.5	1.8495	2.1	0.1823	1.5	0.72	1079.4	15.1	1063.2	13.9	1030.2	29.7	1030.2	29.7	104.8
1096-53	58	47589	1.6	13.5861	3.1	1.7685	3.5	0.1743	1.6	0.45	1035.5	15.1	1034.0	22.6	1030.6	63.0	1030.6	63.0	100.5
1096-79	91	54150	1.9	13.5289	1.2	1.8000	1.5	0.1766	0.9	0.63	1048.5	9.2	1045.5	9.8	1039.2	23.6	1039.2	23.6	100.9
1096-3	65	105612	1.3	13.4956	2.2	1.8427	2.8	0.1804	1.8	0.65	1068.9	18.2	1060.8	18.7	1044.1	43.5	1044.1	43.5	102.4
1096-19	98	119948	1.4	13.4812	1.7	1.7958	2.9	0.1756	2.4	0.82	1042.8	23.0	1043.9	19.0	1046.3	33.5	1046.3	33.5	99.7
1096-6	251	132491	1.2	13.4400	0.7	1.8303	2.0	0.1784	1.9	0.93	1058.3	18.2	1056.4	13.1	1052.5	14.5	1052.5	14.5	100.5
1096-87	261	223626	3.7	13.4390	0.4	1.8264	0.9	0.1780	0.8	0.88	1056.1	7.7	1055.0	5.9	1052.6	8.6	1052.6	8.6	100.3
1096-78	86	41933	2.7	13.3209	1.0	1.8742	1.4	0.1811	1.0	0.72	1072.8	10.1	1072.0	9.5	1070.4	20.0	1070.4	20.0	100.2
1096-52	206	243552	2.9	13.2925	1.1	1.8886	1.9	0.1821	1.6	0.83	1078.3	16.1	1077.1	12.9	1074.7	21.6	1074.7	21.6	100.3
1096-71	100	109556	2.1	13.2429	1.6	1.8764	1.9	0.1802	1.1	0.56	1068.2	10.6	1072.8	12.7	1082.2	31.7	1082.2	31.7	98.7
1096-55	131	87327	1.4	13.2424	1.5	1.7613	4.1	0.1692	3.8	0.93	1007.5	35.2	1031.3	26.2	1082.3	29.5	1082.3	29.5	93.1
1096-12	713	372502	5.5	13.2131	0.2	1.9300	1.5	0.1849	1.5	0.99	1094.0	15.2	1091.5	10.2	1086.7	4.5	1086.7	4.5	100.7
1096-31	630	492740	80.8	13.1709	0.3	1.9777	1.0	0.1889	0.9	0.94	1115.5	9.4	1107.9	6.6	1093.1	6.6	1093.1	6.6	102.1
1096-64	136	150551	1.2	12.9887	1.1	2.0178	1.4	0.1901	0.8	0.59	1121.8	8.4	1121.5	9.4	1121.0	22.2	1121.0	22.2	100.1
1096-95	34	27736	1.6	12.8890	4.5	2.0766	4.6	0.1941	1.0	0.22	1143.6	10.7	1141.1	31.7	1136.3	89.7	1136.3	89.7	100.6
1096-35	193	208041	1.6	12.8708	0.5	2.0512	1.3	0.1915	1.1	0.90	1129.4	11.7	1132.7	8.6	1139.1	10.9	1139.1	10.9	99.1
1096-77	51	45487	2.2	12.8487	2.6	2.1647	4.6	0.2017	3.8	0.82	1184.6	41.2	1169.8	32.1	1142.5	52.0	1142.5	52.0	103.7
1096-42	107	186657	1.6	12.7759	1.2	2.1777	2.3	0.2018	2.0	0.85	1184.9	21.5	1174.0	16.3	1153.8	24.4	1153.8	24.4	102.7
1096-51	512	122011	2.0	12.7650	0.4	1.7769	3.0	0.1645	3.0	0.99	981.8	27.4	1037.1	19.7	1155.5	7.2	1155.5	7.2	85.0
1096-60	16	16093	8.6	12.7517	6.6	1.9519	7.7	0.1805	4.0	0.52	1069.8	39.6	1099.1	52.0	1157.5	131.5	1157.5	131.5	92.4
1096-32	77	103205	2.5	12.6931	1.3	2.1398	3.1	0.1970	2.8	0.91	1159.1	29.5	1161.8	21.2	1166.7	25.3	1166.7	25.3	99.4
1096-57	154	75144	2.3	12.6856	0.7	2.2610	1.6	0.2080	1.4	0.89	1218.3	15.7	1200.2	11.3	1167.8	14.8	1167.8	14.8	104.3
1096-36	43	39270	2.2	12.6644	3.3	2.1215	3.6	0.1949	1.5	0.41	1147.7	15.5	1155.8	25.0	1171.2	65.7	1171.2	65.7	98.0
1096-45	181	158747	1.7	12.3721	0.9	2.3877	1.3	0.2143	1.0	0.74	1251.4	11.3	1238.9	9.7	1217.3	17.9	1217.3	17.9	102.8
1096-98	362	59051	3.3	11.9223	0.6	2.4227	9.6	0.2095	9.6	1.00	1226.1	107.5	1249.3	69.4	1289.7	12.4	1289.7	12.4	95.1
1096-5	304	180550	5.7	11.7953	2.4	2.6348	8.3	0.2254	7.9	0.96	1310.3	94.1	1310.4	61.1	1310.5	46.2	1310.5	46.2	100.0
1096-18	72	37943	1.8	11.7805	1.1	2.7544	1.6	0.2353	1.1	0.72	1362.4	14.1	1343.3	12.0	1312.9	21.8	1312.9	21.8	103.8
1096-100	116	62240	0.8	11.6994	0.6	2.7520	1.0	0.2335	0.9	0.83	1352.9	10.6	1342.6	7.8	1326.3	11.4	1326.3	11.4	102.0
1096-67	68	44205	1.5	11.5873	1.3	2.7607	1.4	0.2320	0.6	0.42	1345.0	7.0	1345.0	10.4	1344.9	24.4	1344.9	24.4	100.0
1096-2	84	49348	1.3	11.3644	0.8	2.9651	1.3	0.2444	1.0	0.79	1409.5	12.6	1398.7	9.6	1382.3	15.1	1382.3	15.1	102.0
1096-21	94	147149	2.4	11.2474	0.6	3.0236	1.1	0.2466	0.9	0.85	1421.2	12.1	1413.6	8.6	1402.2	11.5	1402.2	11.5	101.4

Analysis	U	206Pb	U/Th	206Pb*	±	207Pb*	±	206Pb*	±	error	206Pb*	±	207Pb*	±	206Pb*	±	Best age	±	Conc
	(ppm)	204Pb		207Pb*	(%)	235U*	(%)	238U	(%)	corr.	238U*	(Ma)	235U	(Ma)	207Pb*	(Ma)	(Ma)	(Ma)	(%)
1096-44	79	79067	1.7	10.8745	0.7	3.2265	1.0	0.2545	0.7	0.71	1461.5	9.0	1463.5	7.5	1466.5	13.0	1466.5	13.0	99.7
1096-85	122	183423	2.6	10.4495	0.8	3.6632	3.7	0.2776	3.6	0.98	1579.4	50.5	1563.4	29.4	1541.8	15.1	1541.8	15.1	102.4
1096-16	139	494388	2.2	10.0236	0.5	4.1284	1.0	0.3001	0.8	0.87	1691.9	12.4	1659.9	7.8	1619.7	8.8	1619.7	8.8	104.5
1096-68	54	84753	0.9	9.0787	0.7	5.0109	1.4	0.3299	1.2	0.87	1838.1	19.1	1821.2	11.7	1801.8	12.5	1801.8	12.5	102.0
1096-69	56	50719	0.8	8.6573	0.5	5.5646	0.8	0.3494	0.6	0.76	1931.7	10.3	1910.6	7.0	1887.8	9.6	1887.8	9.6	102.3
1096-80	154	108942	2.4	7.5209	0.6	6.8463	2.6	0.3734	2.6	0.98	2045.6	45.0	2091.7	23.3	2137.4	10.1	2137.4	10.1	95.7

Analysis	U	206Pb	U/Th	206Pb*	±	207Pb*	±	206Pb*	±	error	206Pb*	±	207Pb*	±	206Pb*	±	Best age	±	Conc
	(ppm)	204Pb		207Pb*	(%)	235U*	(%)	238U	(%)	corr.	238U*	(Ma)	235U	(Ma)	207Pb*	(Ma)	(Ma)	(Ma)	(%)
8304-84	372	12015	1.4	16.8432	1.3	0.6006	4.3	0.0734	4.1	0.95	456.4	18.1	477.6	16.4	580.7	28.3	456.4	18.1	78.6
8304-60	531	5095	0.7	16.1467	1.4	0.6779	2.1	0.0794	1.5	0.73	492.5	7.3	525.5	8.6	671.8	30.7	492.5	7.3	73.3
8304-94	431	6472	0.8	16.6083	1.4	0.6684	2.6	0.0805	2.2	0.84	499.2	10.6	519.8	10.7	611.1	30.9	499.2	10.6	81.7
8304-46	307	3762	1.0	16.5010	1.6	0.6763	2.5	0.0809	1.9	0.78	501.7	9.4	524.5	10.3	625.1	33.9	501.7	9.4	80.3
8304-78	54	14553	0.5	16.2758	5.6	0.7197	5.8	0.0850	1.4	0.25	525.6	7.3	550.5	24.7	654.7	120.9	525.6	7.3	80.3
8304-88	414	4447	0.8	16.3898	1.9	0.7154	5.3	0.0850	4.9	0.94	526.2	24.8	548.0	22.2	639.7	40.0	526.2	24.8	82.2
8304-77	397	112622	3.4	16.9903	0.9	0.6984	2.1	0.0861	1.9	0.90	532.2	9.5	537.8	8.6	561.8	19.6	532.2	9.5	94.7
8304-37	84	28541	1.0	17.2454	4.2	0.7047	4.3	0.0881	1.1	0.25	544.6	5.7	541.6	18.0	529.3	91.1	544.6	5.7	102.9
8304-25	112	65473	1.3	17.0500	3.7	0.7138	3.8	0.0883	0.8	0.22	545.3	4.4	547.0	16.1	554.2	80.8	545.3	4.4	98.4
8304-62	130	13461	0.8	17.0912	2.6	0.7157	3.1	0.0887	1.7	0.54	548.0	8.8	548.1	13.2	548.9	57.1	548.0	8.8	99.8
8304-79	118	51364	3.0	16.9985	2.0	0.7264	2.2	0.0896	0.9	0.42	552.9	4.9	554.5	9.4	560.7	43.5	552.9	4.9	98.6
8304-36	145	33964	1.2	17.2216	2.5	0.7171	2.6	0.0896	0.8	0.32	553.0	4.4	549.0	11.0	532.3	53.8	553.0	4.4	103.9
8304-56	483	4843	3.9	16.0507	1.1	0.7695	2.8	0.0896	2.6	0.92	553.0	13.6	579.5	12.3	684.5	23.1	553.0	13.6	80.8
8304-53	301	45711	0.9	17.0724	1.5	0.7257	2.6	0.0899	2.1	0.80	554.7	11.1	554.0	11.1	551.3	33.8	554.7	11.1	100.6
8304-57	75	6663	0.9	16.7210	5.9	0.7412	6.0	0.0899	1.1	0.19	554.8	6.1	563.1	25.9	596.5	127.8	554.8	6.1	93.0
8304-40	140	33557	1.0	17.0357	2.3	0.7289	2.6	0.0901	1.1	0.44	555.9	6.0	555.9	11.0	556.0	50.5	555.9	6.0	100.0
8304-6	400	3930	1.2	16.2159	5.1	0.7660	6.7	0.0901	4.4	0.65	556.1	23.3	577.5	29.6	662.6	109.5	556.1	23.3	83.9
8304-28	105	1472	0.5	14.8887	12.2	0.8347	12.7	0.0901	3.3	0.26	556.3	17.7	616.2	58.5	842.9	255.0	556.3	17.7	66.0
8304-26	453	32087	0.8	16.9634	0.8	0.7333	1.2	0.0902	0.9	0.78	556.9	5.0	558.5	5.2	565.2	16.6	556.9	5.0	98.5
8304-93	125	32878	1.3	17.0230	1.9	0.7355	2.9	0.0908	2.1	0.75	560.3	11.5	559.8	12.3	557.6	41.1	560.3	11.5	100.5
8304-99	201	7543	1.8	16.8691	2.8	0.7453	3.2	0.0912	1.6	0.48	562.5	8.4	565.5	14.0	577.4	61.6	562.5	8.4	97.4
8304-41	58	19297	1.1	17.6841	3.7	0.7125	4.0	0.0914	1.3	0.32	563.7	6.9	546.2	16.7	473.9	82.8	563.7	6.9	118.9
8304-86	258	9378	1.2	16.5073	3.7	0.7683	3.9	0.0920	1.3	0.32	567.2	6.8	578.8	17.3	624.3	80.0	567.2	6.8	90.9
8304-18	244	6636	1.6	16.0667	2.1	0.7915	3.4	0.0922	2.6	0.78	568.7	14.4	592.0	15.1	682.4	44.6	568.7	14.4	83.3
8304-82	496	45253	1.4	17.1084	0.6	0.7455	1.8	0.0925	1.6	0.94	570.3	9.0	565.6	7.6	546.7	13.3	570.3	9.0	104.3
8304-66	133	39983	1.1	16.6715	2.0	0.7658	2.9	0.0926	2.1	0.73	570.8	11.6	577.3	12.8	602.9	43.1	570.8	11.6	94.7
8304-47	37	19780	1.1	16.4443	6.9	0.7828	7.1	0.0934	1.8	0.25	575.4	9.7	587.1	31.7	632.6	148.7	575.4	9.7	91.0
8304-81	88	34828	1.6	16.8906	4.0	0.7732	4.3	0.0947	1.5	0.34	583.3	8.1	581.6	18.9	574.7	87.0	583.3	8.1	101.5
8304-13	70	5284	1.0	16.5038	5.5	0.7953	6.0	0.0952	2.3	0.39	586.2	13.1	594.2	27.0	624.8	119.2	586.2	13.1	93.8
8304-14	221	71392	0.9	16.6453	1.2	0.8071	1.8	0.0974	1.3	0.75	599.3	7.7	600.8	8.2	606.3	25.7	599.3	7.7	98.8

Analysis	U	206Pb	U/Th	206Pb*	±	207Pb*	±	206Pb*	±	error	206Pb*	±	207Pb*	±	206Pb*	±	Best age	±	Conc
	(ppm)	204Pb		207Pb*	(%)	235U*	(%)	238U	(%)	corr.	238U*	(Ma)	235U	(Ma)	207Pb*	(Ma)	(Ma)	(Ma)	(%)
8304-17	110	37127	1.1	16.5692	2.3	0.8168	3.1	0.0982	2.1	0.66	603.6	11.8	606.2	14.1	616.2	50.0	603.6	11.8	97.9
8304-64	38	10311	1.2	16.4210	8.1	0.8260	8.2	0.0984	1.4	0.17	604.9	7.9	611.4	37.6	635.6	173.8	604.9	7.9	95.2
8304-75	127	26377	1.1	16.7481	3.4	0.8104	3.6	0.0984	1.1	0.31	605.2	6.4	602.7	16.2	593.0	73.4	605.2	6.4	102.1
8304-39	240	88078	0.8	16.6029	0.8	0.8367	1.2	0.1008	0.9	0.72	618.8	5.0	617.3	5.5	611.8	17.7	618.8	5.0	101.1
8304-58	83	32904	1.6	16.5725	3.4	0.8459	3.8	0.1017	1.6	0.41	624.2	9.2	622.4	17.5	615.8	74.1	624.2	9.2	101.4
8304-100	411	91611	1.5	16.3400	0.9	0.8592	1.4	0.1018	1.1	0.79	625.1	6.6	629.7	6.6	646.3	18.4	625.1	6.6	96.7
8304-80	113	15462	0.3	16.1824	5.2	0.8681	5.4	0.1019	1.4	0.26	625.5	8.4	634.6	25.5	667.0	111.9	625.5	8.4	93.8
8304-65	558	9712	4.8	15.9897	1.9	0.8908	2.8	0.1033	2.0	0.72	633.7	12.0	646.8	13.3	692.6	41.2	633.7	12.0	91.5
8304-15	241	184076	1.1	16.5760	0.9	0.8655	4.0	0.1041	3.9	0.97	638.1	23.7	633.1	18.8	615.3	19.2	638.1	23.7	103.7
8304-76	151	55972	0.8	16.5488	2.3	0.8705	2.8	0.1045	1.7	0.60	640.6	10.3	635.8	13.4	618.9	49.1	640.6	10.3	103.5
8304-50	233	29573	0.5	16.1271	1.7	0.8952	2.0	0.1047	1.1	0.53	642.0	6.5	649.2	9.6	674.4	36.5	642.0	6.5	95.2
8304-12	89	9805	0.8	15.8886	4.7	0.9146	4.7	0.1054	0.8	0.17	645.9	5.0	659.5	23.0	706.2	99.5	645.9	5.0	91.5
8304-61	293	15650	2.9	16.2702	1.1	0.8966	2.2	0.1058	1.9	0.87	648.3	11.9	649.9	10.7	655.5	23.8	648.3	11.9	98.9
8304-44	253	6531	0.8	15.5477	2.7	1.0566	4.4	0.1191	3.4	0.78	725.6	23.4	732.1	22.7	752.1	57.4	725.6	23.4	96.5
8304-71	152	66392	2.5	15.1144	1.8	1.2292	2.7	0.1347	2.0	0.75	814.9	15.5	814.0	15.1	811.5	37.1	814.9	15.5	100.4
8304-21	45	16105	1.4	14.4870	3.3	1.3847	3.7	0.1455	1.7	0.47	875.6	14.3	882.4	22.0	899.5	67.8	875.6	14.3	97.3
8304-72	257	32516	1.2	13.9156	0.9	1.6577	1.8	0.1673	1.5	0.85	997.2	13.8	992.5	11.1	982.1	18.6	982.1	18.6	101.5
8304-97	294	104699	1.0	13.9066	0.7	1.6730	1.8	0.1687	1.6	0.92	1005.1	15.1	998.3	11.2	983.4	14.1	983.4	14.1	102.2
8304-3	254	41280	1.7	13.8809	0.5	1.5154	1.4	0.1526	1.3	0.94	915.3	11.3	936.6	8.7	987.1	10.0	987.1	10.0	92.7
8304-10	220	11241	0.6	13.7098	0.9	1.6473	1.3	0.1638	1.0	0.72	977.8	8.7	988.5	8.4	1012.3	18.7	1012.3	18.7	96.6
8304-45	195	19219	1.6	13.5922	0.9	1.4464	5.2	0.1426	5.2	0.99	859.3	41.5	908.4	31.4	1029.7	17.9	1029.7	17.9	83.4
8304-43	90	92709	1.9	13.4535	1.5	1.8579	1.9	0.1813	1.2	0.64	1074.0	12.0	1066.3	12.5	1050.5	29.4	1050.5	29.4	102.2
8304-96	422	247971	2.2	13.3106	0.4	1.9099	0.9	0.1844	0.8	0.91	1090.9	7.9	1084.6	5.8	1071.9	7.0	1071.9	7.0	101.8
8304-85	538	109507	3.4	13.1393	0.4	1.8342	2.4	0.1748	2.4	0.99	1038.5	22.9	1057.8	15.9	1097.9	8.2	1097.9	8.2	94.6
8304-24	166	195567	2.3	12.8838	0.7	2.0356	1.0	0.1902	0.7	0.70	1122.5	7.5	1127.5	7.1	1137.1	14.8	1137.1	14.8	98.7
8304-30	190	57948	2.3	12.5623	0.5	2.2581	1.6	0.2057	1.5	0.94	1206.0	16.5	1199.3	11.2	1187.2	10.4	1187.2	10.4	101.6
8304-22	280	8833	0.5	11.6071	0.6	2.3932	5.6	0.2015	5.6	0.99	1183.2	60.3	1240.6	40.2	1341.6	12.0	1341.6	12.0	88.2
8304-83	142	341953	2.2	11.5136	0.4	2.8257	1.9	0.2360	1.9	0.98	1365.7	23.3	1362.4	14.5	1357.2	8.1	1357.2	8.1	100.6
8304-32	62	87470	5.7	11.3047	1.8	2.9808	2.3	0.2444	1.4	0.60	1409.5	17.3	1402.7	17.3	1392.5	34.8	1392.5	34.8	101.2
8304-69	77	56384	1.2	10.3280	1.2	3.6122	1.5	0.2706	0.8	0.58	1543.7	11.5	1552.2	11.6	1563.8	22.3	1563.8	22.3	98.7
8304-5	199	99719	1.5	9.1561	0.3	4.7531	1.8	0.3156	1.8	0.99	1768.4	27.8	1776.7	15.3	1786.4	5.2	1786.4	5.2	99.0
8304-4	186	14176	0.9	9.0609	2.1	5.1315	2.5	0.3372	1.4	0.55	1873.3	23.0	1841.3	21.6	1805.4	38.5	1805.4	38.5	103.8
8304-90	109	65518	0.7	8.9874	0.8	4.8467	1.2	0.3159	0.9	0.75	1769.8	14.2	1793.0	10.3	1820.2	14.8	1820.2	14.8	97.2
8304-35	168	15211	1.0	8.7752	0.7	4.5026	9.0	0.2866	9.0	1.00	1624.3	128.8	1731.5	74.9	1863.5	12.5	1863.5	12.5	87.2
8304-70	103	128471	0.7	8.7412	0.5	5.3237	1.2	0.3375	1.1	0.89	1874.7	17.5	1872.7	10.3	1870.5	9.8	1870.5	9.8	100.2
8304-91	164	244190	1.9	8.6426	0.3	5.5626	1.7	0.3487	1.7	0.99	1928.3	28.6	1910.3	15.0	1890.9	5.0	1890.9	5.0	102.0
8304-51	182	24439	0.8	8.6399	0.5	4.7814	3.5	0.2996	3.5	0.99	1689.4	51.9	1781.6	29.7	1891.4	9.0	1891.4	9.0	89.3
8304-74	73	71164	1.0	8.5063	1.5	5.0313	3.7	0.3104	3.4	0.91	1742.7	52.1	1824.6	31.7	1919.4	27.7	1919.4	27.7	90.8
8304-68	44	46834	0.9	8.2591	1.1	5.8940	1.3	0.3531	0.7	0.56	1949.2	12.4	1960.3	11.5	1972.2	19.6	1972.2	19.6	98.8

Analysis	U	206Pb	U/Th	206Pb*	±	207Pb*	±	206Pb*	±	error	206Pb*	±	207Pb*	±	206Pb*	±	Best age	±	Conc
	(ppm)	204Pb		207Pb*	(%)	235U*	(%)	238U	(%)	corr.	238U*	(Ma)	235U	(Ma)	207Pb*	(Ma)	(Ma)	(Ma)	(%)
8304-87	128	26770	0.8	8.1886	0.5	6.1396	2.6	0.3646	2.5	0.98	2004.1	43.6	1995.9	22.6	1987.4	9.3	1987.4	9.3	100.8
8304-2	82	193593	0.8	8.1726	0.4	6.0924	1.4	0.3611	1.3	0.96	1987.5	22.6	1989.2	12.0	1990.9	6.9	1990.9	6.9	99.8
8304-54	187	131038	2.1	8.0247	0.3	6.2946	1.3	0.3663	1.3	0.97	2012.2	21.7	2017.7	11.3	2023.3	5.7	2023.3	5.7	99.4
8304-19	63	69422	0.6	7.8335	0.9	5.9304	2.8	0.3369	2.7	0.95	1871.9	43.2	1965.7	24.3	2065.9	15.0	2065.9	15.0	90.6
8304-16	246	22079	5.1	7.8266	0.7	6.4111	4.1	0.3639	4.1	0.98	2000.7	69.8	2033.8	36.2	2067.5	12.7	2067.5	12.7	96.8
8304-20	117	370678	1.0	7.7164	0.3	6.9925	1.1	0.3913	1.0	0.96	2129.0	18.5	2110.5	9.5	2092.4	5.5	2092.4	5.5	101.7
8304-1	257	389712	2.9	7.6988	0.2	6.7451	1.5	0.3766	1.5	0.99	2060.5	26.6	2078.6	13.4	2096.5	3.3	2096.5	3.3	98.3
8304-31	127	237520	2.1	7.6168	0.6	6.7576	1.3	0.3733	1.1	0.90	2044.9	19.8	2080.2	11.1	2115.3	9.7	2115.3	9.7	96.7
8304-8	301	20379	0.7	7.5909	0.1	5.6216	2.4	0.3095	2.3	1.00	1738.2	35.8	1919.4	20.3	2121.2	2.3	2121.2	2.3	81.9
8304-98	207	50587	1.2	7.5816	0.4	6.6654	1.3	0.3665	1.2	0.96	2013.0	21.4	2068.0	11.4	2123.4	6.1	2123.4	6.1	94.8
8304-29	358	493781	2.0	7.4244	0.1	7.4293	1.5	0.4000	1.5	1.00	2169.2	27.9	2164.5	13.6	2160.0	1.4	2160.0	1.4	100.4
8304-33	144	162790	1.6	7.3015	0.2	7.2097	1.2	0.3818	1.2	0.98	2084.7	21.5	2137.7	10.9	2189.1	3.8	2189.1	3.8	95.2
8304-9	125	28341	1.3	7.2093	0.3	7.6980	1.9	0.4025	1.9	0.98	2180.6	34.7	2196.4	17.1	2211.1	5.9	2211.1	5.9	98.6
8304-63	317	475966	1.1	7.1788	0.1	7.8980	1.1	0.4112	1.1	0.99	2220.5	20.2	2219.4	9.8	2218.5	2.4	2218.5	2.4	100.1
8304-23	102	25082	0.6	6.7388	0.4	9.2770	1.9	0.4534	1.8	0.98	2410.4	36.5	2365.7	17.0	2327.5	7.0	2327.5	7.0	103.6
8304-42	86	141910	1.1	5.7159	0.6	12.1259	1.5	0.5027	1.4	0.92	2625.3	30.4	2614.2	14.3	2605.5	9.8	2605.5	9.8	100.8

Analysis	U	206Pb	U/Th	206Pb*	±	207Pb*	±	206Pb*	±	error	206Pb*	±	207Pb*	±	206Pb*	±	Best age	±	Conc
	(ppm)	204Pb		207Pb*	(%)	235U*	(%)	238U	(%)	corr.	238U*	(Ma)	235U	(Ma)	207Pb*	(Ma)	(Ma)	(Ma)	(%)
8305-67	181	27826	0.8	16.9543	2.0	0.7114	2.6	0.0875	1.7	0.65	540.6	8.6	545.6	10.9	566.5	42.9	540.6	8.6	95.4
8305-26	44	28063	0.5	17.7966	6.5	0.6781	6.7	0.0875	1.3	0.19	540.9	6.6	525.6	27.4	459.9	145.3	540.9	6.6	117.6
8305-50	32	11588	0.9	17.3773	8.8	0.6960	9.1	0.0877	2.4	0.27	542.1	12.7	536.4	38.1	512.5	193.9	542.1	12.7	105.8
8305-15	294	112644	0.8	17.2513	1.1	0.7016	1.4	0.0878	0.9	0.64	542.4	4.6	539.7	5.8	528.5	23.3	542.4	4.6	102.6
8305-69	146	68347	1.1	17.2510	4.0	0.7082	4.1	0.0886	1.1	0.26	547.3	5.7	543.7	17.4	528.6	87.6	547.3	5.7	103.6
8305-90	216	105594	2.0	17.0193	1.7	0.7189	2.0	0.0887	1.0	0.49	548.1	5.1	550.0	8.3	558.1	37.2	548.1	5.1	98.2
8305-98	91	16136	1.9	17.1480	3.5	0.7156	4.1	0.0890	2.1	0.51	549.6	11.1	548.0	17.4	541.7	77.1	549.6	11.1	101.5
8305-89	198	126594	0.9	17.2041	2.2	0.7137	2.3	0.0891	0.9	0.37	549.9	4.6	546.9	9.9	534.5	47.4	549.9	4.6	102.9
8305-57	177	80536	11.9	17.0034	2.0	0.7222	2.7	0.0891	1.8	0.66	550.0	9.3	552.0	11.4	560.1	43.4	550.0	9.3	98.2
8305-83	190	6198	0.7	15.8462	7.4	0.7753	7.5	0.0891	1.6	0.21	550.2	8.2	582.8	33.5	711.8	157.1	550.2	8.2	77.3
8305-48	177	13079	1.5	16.9802	1.4	0.7253	2.0	0.0893	1.4	0.69	551.5	7.2	553.8	8.5	563.1	31.5	551.5	7.2	97.9
8305-3	66	20022	1.1	17.8163	5.3	0.6941	5.8	0.0897	2.2	0.38	553.7	11.8	535.3	24.1	457.5	118.7	553.7	11.8	121.0
8305-47	265	61600	0.8	17.2019	0.8	0.7192	1.4	0.0897	1.2	0.82	553.9	6.2	550.2	6.0	534.8	17.6	553.9	6.2	103.6
8305-91	72	29342	3.1	17.5379	7.3	0.7064	7.4	0.0899	1.2	0.17	554.7	6.5	542.6	31.2	492.3	161.4	554.7	6.5	112.7
8305-49	57	22339	0.9	17.0135	7.8	0.7294	7.9	0.0900	1.5	0.19	555.5	7.8	556.2	34.0	558.8	170.2	555.5	7.8	99.4
8305-63	345	44904	0.9	16.9610	1.0	0.7339	2.3	0.0903	2.1	0.90	557.2	11.0	558.8	9.8	565.6	21.5	557.2	11.0	98.5
8305-97	410	25903	0.9	17.0436	1.1	0.7327	2.5	0.0906	2.2	0.90	558.9	11.9	558.1	10.6	555.0	23.9	558.9	11.9	100.7
8305-58	58	15053	1.2	16.4929	5.3	0.7572	5.4	0.0906	1.2	0.23	558.9	6.7	572.4	23.7	626.2	113.8	558.9	6.7	89.3
8305-43	274	12055	1.3	16.7059	4.2	0.7492	5.2	0.0908	3.1	0.59	560.1	16.4	567.8	22.6	598.5	91.2	560.1	16.4	93.6
8305-8	100	5817	2.5	15.7739	5.8	0.7941	6.0	0.0908	1.4	0.24	560.6	7.8	593.5	27.0	721.5	123.8	560.6	7.8	77.7

Analysis	U	206Pb	U/Th	206Pb*	±	207Pb*	±	206Pb*	±	error	206Pb*	±	207Pb*	±	206Pb*	±	Best age	±	Conc
	(ppm)	204Pb		207Pb*	(%)	235U*	(%)	238U	(%)	corr.	238U*	(Ma)	235U	(Ma)	207Pb*	(Ma)	(Ma)	(Ma)	(%)
8305-30	92	38111	1.0	16.3798	2.7	0.7660	3.4	0.0910	2.1	0.60	561.5	11.1	577.5	15.0	641.1	58.5	561.5	11.1	87.6
8305-37	96	68453	0.8	17.3014	3.2	0.7279	3.5	0.0913	1.6	0.45	563.5	8.6	555.3	15.1	522.1	69.5	563.5	8.6	107.9
8305-94	33	18813	1.7	17.7635	13.6	0.7105	13.8	0.0915	2.6	0.19	564.6	13.8	545.0	58.4	464.0	302.4	564.6	13.8	121.7
8305-56	120	30261	1.2	17.1147	3.6	0.7417	4.4	0.0921	2.4	0.56	567.7	13.2	563.4	18.9	545.9	79.2	567.7	13.2	104.0
8305-61	35	15198	0.7	16.5285	11.8	0.7737	11.9	0.0927	1.3	0.11	571.8	7.3	581.9	52.5	621.5	254.8	571.8	7.3	92.0
8305-4	48	20766	1.1	17.5009	4.5	0.7376	5.6	0.0936	3.2	0.58	576.9	17.9	561.0	24.1	496.9	100.1	576.9	17.9	116.1
8305-99	137	13628	3.1	16.1787	5.5	0.8318	5.8	0.0976	1.9	0.34	600.3	11.2	614.6	26.7	667.5	116.9	600.3	11.2	89.9
8305-28	73	31985	1.0	16.8002	3.4	0.8188	3.6	0.0998	1.0	0.28	613.0	6.0	607.4	16.4	586.3	74.6	613.0	6.0	104.6
8305-86	100	18367	1.8	16.3352	3.6	0.8499	3.8	0.1007	1.1	0.28	618.5	6.3	624.6	17.6	646.9	77.7	618.5	6.3	95.6
8305-35	94	25907	3.8	16.5977	3.3	0.8429	3.6	0.1015	1.2	0.34	623.0	7.3	620.7	16.5	612.5	72.3	623.0	7.3	101.7
8305-88	104	14882	0.8	16.3850	1.7	0.8612	1.8	0.1023	0.7	0.38	628.1	4.1	630.8	8.6	640.4	36.3	628.1	4.1	98.1
8305-14	199	76314	0.7	16.4690	1.3	0.8575	1.7	0.1024	1.0	0.62	628.6	6.3	628.8	7.9	629.3	28.6	628.6	6.3	99.9
8305-41	447	127738	2.0	16.4404	0.6	0.8723	1.1	0.1040	0.9	0.84	637.9	5.8	636.8	5.4	633.1	13.3	637.9	5.8	100.7
8305-82	107	46435	0.9	16.5702	3.3	0.8663	4.0	0.1041	2.2	0.56	638.5	13.6	633.6	18.6	616.1	70.5	638.5	13.6	103.6
8305-46	77	5367	0.5	15.8373	4.9	0.9070	5.1	0.1042	1.5	0.30	638.9	9.4	655.5	24.8	713.0	104.1	638.9	9.4	89.6
8305-77	54	23058	0.7	16.5224	7.6	0.8887	7.9	0.1065	2.1	0.26	652.3	12.9	645.6	37.6	622.3	164.0	652.3	12.9	104.8
8305-11	103	33381	0.6	16.3321	2.1	0.9017	2.2	0.1068	0.7	0.33	654.1	4.6	652.6	10.8	647.3	45.6	654.1	4.6	101.1
8305-95	158	66923	2.7	16.2985	1.7	0.9097	2.1	0.1075	1.3	0.59	658.4	8.0	656.9	10.4	651.7	37.2	658.4	8.0	101.0
8305-13	177	100238	1.4	16.1234	1.8	0.9256	2.8	0.1082	2.1	0.76	662.5	13.2	665.3	13.5	674.8	38.5	662.5	13.2	98.2
8305-9	112	37161	1.4	16.1321	1.5	0.9306	1.7	0.1089	0.9	0.51	666.2	5.6	667.9	8.5	673.7	31.9	666.2	5.6	98.9
8305-22	206	53693	1.6	16.0578	0.8	0.9524	1.3	0.1109	1.1	0.83	678.1	7.2	679.4	6.7	683.6	16.0	678.1	7.2	99.2
8305-38	450	53263	2.8	15.2346	0.4	1.1987	1.2	0.1324	1.1	0.93	801.8	8.1	800.0	6.4	794.9	9.1	801.8	8.1	100.9
8305-64	46	24027	0.7	14.5528	4.1	1.4457	4.2	0.1526	1.0	0.24	915.4	8.5	908.1	25.1	890.2	83.9	890.2	83.9	102.8
8305-100	91	23775	2.0	13.9366	2.0	1.6732	2.2	0.1691	0.8	0.35	1007.3	7.0	998.4	13.8	978.9	41.5	978.9	41.5	102.9
8305-78	220	60408	1.0	13.9235	1.1	1.6025	2.0	0.1618	1.7	0.84	966.9	15.5	971.2	12.8	980.9	22.3	980.9	22.3	98.6
8305-12	427	24120	0.9	13.6802	0.5	1.6914	1.4	0.1678	1.3	0.92	1000.1	11.7	1005.3	8.8	1016.7	11.0	1016.7	11.0	98.4
8305-25	108	72553	1.3	13.5567	1.9	1.8265	2.1	0.1796	0.9	0.44	1064.7	8.8	1055.0	13.5	1035.0	37.5	1035.0	37.5	102.9
8305-93	175	61509	5.4	13.5553	0.6	1.6752	1.1	0.1647	0.9	0.82	982.8	8.3	999.2	7.0	1035.2	12.7	1035.2	12.7	94.9
8305-73	142	41108	2.1	13.4895	1.3	1.8268	4.8	0.1787	4.6	0.96	1060.0	44.9	1055.1	31.3	1045.1	26.0	1045.1	26.0	101.4
8305-51	106	69800	1.2	13.1124	1.2	1.9614	1.7	0.1865	1.1	0.67	1102.6	11.3	1102.4	11.2	1102.0	24.5	1102.0	24.5	100.0
8305-27	185	175326	1.6	12.9214	1.7	2.0149	3.0	0.1888	2.5	0.83	1115.0	25.1	1120.6	20.1	1131.3	33.1	1131.3	33.1	98.6
8305-80	72	24781	1.5	12.8602	1.9	2.0331	3.4	0.1896	2.8	0.84	1119.4	29.1	1126.7	23.1	1140.7	37.0	1140.7	37.0	98.1
8305-16	74	35833	2.0	12.7698	2.0	2.1444	2.8	0.1986	2.0	0.72	1167.8	21.4	1163.2	19.3	1154.7	38.7	1154.7	38.7	101.1
8305-2	111	89754	2.2	12.4879	1.5	2.2819	2.9	0.2067	2.5	0.85	1211.1	27.5	1206.7	20.7	1198.9	30.4	1198.9	30.4	101.0
8305-85	143	70918	2.3	12.4305	1.0	2.4058	4.1	0.2169	4.0	0.97	1265.4	45.9	1244.3	29.6	1208.0	20.4	1208.0	20.4	104.8
8305-19	62	50700	2.3	12.3671	1.9	2.3354	3.1	0.2095	2.5	0.79	1226.0	27.4	1223.1	22.1	1218.1	37.7	1218.1	37.7	100.7
8305-92	269	206524	1.8	12.3637	0.4	2.3315	0.7	0.2091	0.5	0.74	1223.8	5.5	1221.9	4.7	1218.6	8.8	1218.6	8.8	100.4
8305-87	68	47096	2.0	12.3362	1.3	2.3629	1.8	0.2114	1.2	0.68	1236.3	13.5	1231.4	12.6	1222.9	25.7	1222.9	25.7	101.1
8305-23	92	66115	1.1	12.3099	1.3	2.3901	2.5	0.2134	2.1	0.86	1246.8	24.0	1239.6	17.7	1227.1	25.0	1227.1	25.0	101.6

Analysis	U	206Pb	U/Th	206Pb*	±	207Pb*	±	206Pb*	±	error	206Pb*	±	207Pb*	±	206Pb*	±	Best age	±	Conc
	(ppm)	204Pb		207Pb*	(%)	235U*	(%)	238U	(%)	corr.	238U*	(Ma)	235U	(Ma)	207Pb*	(Ma)	(Ma)	(Ma)	(%)
8305-60	147	174733	1.6	12.2807	0.9	2.3760	1.4	0.2116	1.0	0.72	1237.5	11.1	1235.4	9.8	1231.8	18.5	1231.8	18.5	100.5
8305-65	29	29511	2.0	12.2784	4.6	2.3534	4.8	0.2096	1.5	0.31	1226.5	16.4	1228.6	34.1	1232.2	89.5	1232.2	89.5	99.5
8305-45	34	26468	0.5	12.1868	2.1	2.3164	2.7	0.2047	1.7	0.64	1200.7	19.1	1217.3	19.3	1246.9	41.0	1246.9	41.0	96.3
8305-81	62	70276	1.5	12.1514	2.0	2.3893	2.3	0.2106	1.1	0.49	1231.8	12.7	1239.4	16.4	1252.5	38.9	1252.5	38.9	98.3
8305-20	180	113309	1.4	12.1248	0.9	2.3923	1.6	0.2104	1.3	0.83	1230.8	14.6	1240.3	11.2	1256.9	17.1	1256.9	17.1	97.9
8305-55	103	35865	3.2	12.0226	1.3	2.3988	2.6	0.2092	2.2	0.87	1224.4	24.9	1242.2	18.4	1273.4	24.9	1273.4	24.9	96.2
8305-5	227	55574	3.2	12.0001	3.8	2.4076	4.8	0.2095	2.9	0.60	1226.4	32.2	1244.9	34.3	1277.0	74.5	1277.0	74.5	96.0
8305-70	100	98134	1.4	11.7002	1.6	2.7242	1.9	0.2312	0.9	0.48	1340.6	10.9	1335.1	13.9	1326.2	31.7	1326.2	31.7	101.1
8305-52	54	40809	0.8	11.6831	2.1	2.7040	2.3	0.2291	1.0	0.45	1329.9	12.6	1329.5	17.2	1329.0	40.0	1329.0	40.0	100.1
8305-79	87	49341	1.5	11.2106	1.3	2.9126	1.9	0.2368	1.5	0.75	1370.1	17.9	1385.2	14.6	1408.5	24.4	1408.5	24.4	97.3
8305-54	125	67594	1.8	10.6719	0.5	3.3943	1.2	0.2627	1.1	0.92	1503.7	14.9	1503.1	9.5	1502.1	9.2	1502.1	9.2	100.1
8305-72	92	58251	1.2	10.6412	1.2	3.4666	1.4	0.2675	0.7	0.52	1528.3	9.5	1519.6	10.6	1507.6	21.9	1507.6	21.9	101.4
8305-34	204	238667	2.0	10.5566	0.6	3.4892	0.9	0.2671	0.6	0.73	1526.3	8.6	1524.8	6.9	1522.6	11.2	1522.6	11.2	100.2
8305-44	39	37465	0.8	9.6114	2.2	3.8607	6.1	0.2691	5.7	0.93	1536.4	77.7	1605.5	49.1	1697.4	40.2	1697.4	40.2	90.5
8305-77	56	43946	1.4	9.3026	1.6	4.6893	1.8	0.3164	0.8	0.46	1772.0	12.4	1765.3	14.7	1757.4	28.7	1757.4	28.7	100.8
8305-53	71	86851	0.9	8.7490	1.0	5.3961	1.4	0.3424	0.9	0.67	1898.2	15.2	1884.2	11.8	1868.8	18.3	1868.8	18.3	101.6
8305-75	180	368828	1.1	8.6674	0.3	5.4780	0.7	0.3444	0.6	0.87	1907.6	9.5	1897.2	5.7	1885.7	6.0	1885.7	6.0	101.2
8305-84	165	135602	0.7	8.1730	0.3	6.2462	0.8	0.3702	0.7	0.91	2030.6	11.9	2010.9	6.6	1990.8	5.6	1990.8	5.6	102.0
8305-40	197	36081	1.2	7.8954	0.5	5.6079	2.9	0.3211	2.9	0.99	1795.2	45.2	1917.3	25.2	2052.1	8.4	2052.1	8.4	87.5
8305-24	103	95704	2.3	7.8369	0.5	6.6700	1.3	0.3791	1.2	0.91	2072.1	21.4	2068.7	11.7	2065.2	9.7	2065.2	9.7	100.3
8305-59	78	89689	0.9	7.7233	0.6	6.8482	0.9	0.3836	0.7	0.77	2093.1	12.8	2092.0	8.3	2090.9	10.5	2090.9	10.5	100.1
8305-6	153	19797	0.9	7.5393	0.2	6.4560	2.1	0.3530	2.0	1.00	1949.0	34.4	2039.9	18.0	2133.2	2.8	2133.2	2.8	91.4
8305-42	104	128229	1.6	7.4415	0.3	7.2622	6.1	0.3919	6.1	1.00	2131.8	110.1	2144.2	54.3	2156.0	5.8	2156.0	5.8	98.9
8305-17	43	39728	1.1	6.7472	1.2	8.6538	1.8	0.4235	1.3	0.74	2276.3	25.3	2302.2	16.3	2325.3	20.8	2325.3	20.8	97.9
8305-21	99	185863	3.9	6.2818	0.4	9.3673	1.1	0.4268	1.0	0.91	2291.1	19.2	2374.6	10.0	2447.1	7.5	2447.1	7.5	93.6
8305-66	137	27550	1.9	5.0813	0.2	13.9422	0.8	0.5138	0.8	0.96	2672.9	16.7	2745.8	7.6	2799.8	3.7	2799.8	3.7	95.5

Analysis	U	206Pb	U/Th	206Pb*	±	207Pb*	±	206Pb*	±	error	206Pb*	±	207Pb*	±	206Pb*	±	Best age	±	Conc
	(ppm)	204Pb		207Pb*	(%)	235U*	(%)	238U	(%)	corr.	238U*	(Ma)	235U	(Ma)	207Pb*	(Ma)	(Ma)	(Ma)	(%)
FMG-90	242	52659	0.6	16.9488	1.4	0.7021	1.7	0.0863	0.9	0.57	533.6	4.8	540.0	6.9	567.2	29.6	533.6	4.8	94.1
FMG-78	236	22796	0.5	17.0842	1.9	0.7087	3.7	0.0878	3.2	0.86	542.6	16.6	543.9	15.7	549.8	42.1	542.6	16.6	98.7
FMG-75	299	40193	0.7	17.1317	2.2	0.7112	2.6	0.0884	1.5	0.57	545.8	7.8	545.4	11.1	543.7	47.1	545.8	7.8	100.4
FMG-46	94	36771	1.0	17.3762	5.4	0.7028	5.6	0.0886	1.3	0.24	547.1	7.1	540.4	23.4	512.6	119.0	547.1	7.1	106.7
FMG-79	297	136858	1.2	17.1320	1.2	0.7134	2.6	0.0886	2.3	0.88	547.5	11.9	546.8	11.0	543.7	27.3	547.5	11.9	100.7
FMG-26	544	68216	1.4	16.8280	0.8	0.7266	1.6	0.0887	1.4	0.86	547.7	7.5	554.6	7.0	582.7	18.0	547.7	7.5	94.0
FMG-64	168	46527	0.7	17.1386	2.9	0.7180	3.1	0.0892	1.2	0.39	551.1	6.4	549.5	13.1	542.8	62.3	551.1	6.4	101.5
FMG-89	80	18376	1.1	16.9235	2.5	0.7283	2.7	0.0894	0.8	0.32	552.0	4.5	555.6	11.4	570.4	55.0	552.0	4.5	96.8
FMG-96	100	24635	0.6	17.4060	3.1	0.7134	3.4	0.0901	1.4	0.42	555.9	7.5	546.7	14.4	508.9	68.0	555.9	7.5	109.2
FMG-73	330	148036	0.9	17.1135	1.6	0.7283	2.1	0.0904	1.4	0.64	557.9	7.3	555.6	9.2	546.0	35.9	557.9	7.3	102.2

Analysis	U	206Pb	U/Th	206Pb*	±	207Pb*	±	206Pb*	±	error	206Pb*	±	207Pb*	±	206Pb*	±	Best age	±	Conc
	(ppm)	204Pb		207Pb*	(%)	235U*	(%)	238U	(%)	corr.	238U*	(Ma)	235U	(Ma)	207Pb*	(Ma)	(Ma)	(Ma)	(%)
FMG-84	435	151308	0.7	17.1301	1.2	0.7326	1.4	0.0910	0.8	0.55	561.6	4.3	558.1	6.2	543.9	26.3	561.6	4.3	103.2
FMG-58	205	23760	0.7	16.8002	3.4	0.7518	3.7	0.0916	1.4	0.38	565.0	7.7	569.3	16.2	586.3	74.7	565.0	7.7	96.4
FMG-27	297	75812	0.9	17.1320	0.9	0.7375	1.2	0.0916	0.7	0.61	565.2	3.9	560.9	5.0	543.7	20.1	565.2	3.9	104.0
FMG-82	335	25760	1.1	17.1261	0.8	0.7399	1.4	0.0919	1.2	0.82	566.8	6.5	562.4	6.2	544.5	18.0	566.8	6.5	104.1
FMG-57	158	66271	0.9	17.0156	1.6	0.7451	1.9	0.0920	1.0	0.53	567.1	5.6	565.4	8.4	558.6	35.8	567.1	5.6	101.5
FMG-51	185	98578	4.3	17.2978	1.3	0.7335	1.5	0.0920	0.7	0.49	567.5	3.9	558.6	6.3	522.6	28.2	567.5	3.9	108.6
FMG-65	55	113782	1.0	16.6417	5.4	0.7639	5.6	0.0922	1.5	0.28	568.5	8.4	576.2	24.6	606.8	116.5	568.5	8.4	93.7
FMG-70	254	55386	2.5	16.8336	1.9	0.7564	2.4	0.0923	1.6	0.64	569.4	8.5	571.9	10.6	582.0	40.3	569.4	8.5	97.8
FMG-25	217	70910	1.2	17.0902	1.1	0.7454	1.6	0.0924	1.2	0.76	569.7	6.7	565.6	7.1	549.0	23.3	569.7	6.7	103.8
FMG-36	382	105099	17.3	17.0166	0.9	0.7489	1.5	0.0924	1.1	0.77	569.9	6.1	567.6	6.3	558.5	20.1	569.9	6.1	102.0
FMG-87	55	12477	0.8	16.6767	7.4	0.7647	7.6	0.0925	1.7	0.23	570.2	9.3	576.7	33.4	602.3	160.2	570.2	9.3	94.7
FMG-28	330	90821	1.1	16.9276	0.8	0.7534	1.3	0.0925	1.0	0.80	570.3	5.5	570.2	5.5	569.9	16.7	570.3	5.5	100.1
FMG-6	190	34783	1.0	17.0373	2.2	0.7502	2.9	0.0927	1.9	0.65	571.4	10.2	568.3	12.5	555.8	47.7	571.4	10.2	102.8
FMG-42	77	42065	1.2	17.5251	7.3	0.7298	7.5	0.0928	1.5	0.20	571.8	8.2	556.4	32.0	493.9	161.6	571.8	8.2	115.8
FMG-21	146	35741	1.0	16.9177	2.4	0.7575	2.7	0.0929	1.2	0.44	572.9	6.4	572.6	11.7	571.1	52.4	572.9	6.4	100.3
FMG-37	315	60949	1.3	16.9828	1.4	0.7556	2.9	0.0931	2.5	0.88	573.7	14.0	571.5	12.6	562.8	29.7	573.7	14.0	101.9
FMG-12	431	37869	0.9	16.9831	0.9	0.7589	3.5	0.0935	3.4	0.97	576.1	18.8	573.4	15.5	562.7	19.0	576.1	18.8	102.4
FMG-14	127	16794	1.3	17.0860	2.3	0.7576	2.9	0.0939	1.8	0.60	578.5	9.8	572.6	12.8	549.6	50.7	578.5	9.8	105.3
FMG-76	439	10090	1.6	16.5471	1.4	0.7824	2.3	0.0939	1.8	0.80	578.6	9.9	586.9	10.1	619.1	29.5	578.6	9.9	93.4
FMG-93	87	35901	2.6	17.3003	4.7	0.7520	5.0	0.0944	1.6	0.33	581.3	9.1	569.4	21.8	522.3	103.7	581.3	9.1	111.3
FMG-67	404	5478	2.2	16.1635	1.5	0.8076	2.2	0.0947	1.6	0.73	583.1	9.2	601.1	10.2	669.5	32.7	583.1	9.2	87.1
FMG-22	93	24154	0.9	17.1813	5.7	0.7652	6.2	0.0954	2.5	0.40	587.1	13.9	577.0	27.3	537.4	124.8	587.1	13.9	109.2
FMG-11	104	38008	0.9	16.5513	2.4	0.8058	2.6	0.0967	0.9	0.36	595.2	5.3	600.1	11.9	618.6	52.8	595.2	5.3	96.2
FMG-34	115	45030	1.1	16.4786	3.0	0.8109	3.2	0.0969	1.1	0.35	596.3	6.4	603.0	14.7	628.1	65.6	596.3	6.4	94.9
FMG-69	42	13841	0.7	17.9968	6.1	0.7426	6.3	0.0969	1.7	0.27	596.4	9.7	563.9	27.3	435.0	135.2	596.4	9.7	137.1
FMG-44	773	5981	0.8	16.1954	1.5	0.8461	2.9	0.0994	2.4	0.85	610.8	14.1	622.5	13.3	665.3	32.2	610.8	14.1	91.8
FMG-86	58	20876	0.5	16.7626	7.3	0.8269	7.5	0.1005	1.6	0.21	617.5	9.3	611.9	34.3	591.2	158.5	617.5	9.3	104.5
FMG-72	263	161337	1.4	16.4435	1.5	0.8433	1.7	0.1006	0.6	0.38	617.8	3.7	621.0	7.7	632.7	33.2	617.8	3.7	97.6
FMG-40	431	215213	0.2	16.6244	0.8	0.8361	1.9	0.1008	1.7	0.91	619.2	10.3	617.0	8.8	609.0	17.1	619.2	10.3	101.7
FMG-9	344	2312	0.9	16.5298	2.1	0.8431	4.7	0.1011	4.2	0.89	620.7	24.7	620.9	21.7	621.4	45.6	620.7	24.7	99.9
FMG-15	112	26625	0.7	16.6093	1.7	0.8418	2.3	0.1014	1.6	0.68	622.6	9.4	620.1	10.8	611.0	36.6	622.6	9.4	101.9
FMG-39	249	19097	5.1	16.7340	1.7	0.8367	5.1	0.1015	4.8	0.94	623.5	28.2	617.3	23.4	594.9	37.2	623.5	28.2	104.8
FMG-97	510	28425	0.6	16.5095	1.0	0.8517	2.0	0.1020	1.7	0.87	626.0	10.2	625.6	9.2	624.0	21.2	626.0	10.2	100.3
FMG-99	298	61562	0.9	16.6145	1.2	0.8482	1.5	0.1022	0.9	0.62	627.4	5.6	623.7	7.1	610.3	25.8	627.4	5.6	102.8
FMG-35	82	24653	1.0	16.2539	2.6	0.8704	3.1	0.1026	1.6	0.52	629.6	9.4	635.8	14.4	657.6	56.1	629.6	9.4	95.7
FMG-16	50	9815	1.2	16.3681	8.8	0.8657	9.0	0.1028	1.6	0.17	630.6	9.4	633.2	42.2	642.6	189.8	630.6	9.4	98.1
FMG-61	161	73680	1.6	16.4748	1.8	0.8636	2.4	0.1032	1.5	0.64	633.0	9.1	632.1	11.2	628.6	39.6	633.0	9.1	100.7
FMG-85	214	72942	1.5	16.3140	1.3	0.8724	2.0	0.1032	1.6	0.77	633.3	9.4	636.9	9.6	649.7	27.8	633.3	9.4	97.5
FMG-33	189	42642	1.9	16.5846	1.4	0.8647	1.6	0.1040	0.8	0.48	637.9	4.7	632.7	7.5	614.2	30.4	637.9	4.7	103.9

Analysis	U (ppm)	206Pb 204Pb	U/Th	206Pb* 207Pb*	± (%)	207Pb* 235U*	± (%)	206Pb* 238U	± (%)	error corr.	206Pb* 238U*	± (Ma)	207Pb* 235U	± (Ma)	206Pb* 207Pb*	± (Ma)	Best age (Ma)	± (Ma)	Conc (%)
FMG-29	362	101766	1.3	16.4794	0.5	0.8801	1.2	0.1052	1.0	0.91	644.8	6.4	641.0	5.5	628.0	10.5	644.8	6.4	102.7
FMG-24	235	28937	3.7	15.8670	2.2	0.9313	6.5	0.1072	6.1	0.94	656.3	38.1	668.3	31.7	709.0	46.7	656.3	38.1	92.6
FMG-50	226	74772	0.7	16.3758	0.9	0.9047	1.1	0.1074	0.7	0.65	657.9	4.6	654.2	5.4	641.6	18.4	657.9	4.6	102.5
FMG-19	63	42622	2.0	16.0323	4.6	0.9362	5.3	0.1089	2.6	0.49	666.1	16.5	670.9	25.9	687.0	97.8	666.1	16.5	97.0
FMG-38	264	112691	0.5	16.0441	1.4	0.9811	1.6	0.1142	0.7	0.47	696.9	4.9	694.2	7.9	685.4	29.6	696.9	4.9	101.7
FMG-7	131	43101	1.1	15.7635	2.2	1.0310	2.6	0.1179	1.4	0.54	718.3	9.5	719.4	13.2	722.9	45.7	718.3	9.5	99.4
FMG-32	276	166584	1.1	13.6506	0.6	1.7161	1.8	0.1699	1.7	0.95	1011.6	15.8	1014.6	11.4	1021.0	11.2	1021.0	11.2	99.1
FMG-2	336	114316	5.1	13.3441	0.3	1.9058	0.8	0.1844	0.7	0.90	1091.2	7.2	1083.1	5.3	1066.9	7.0	1066.9	7.0	102.3
FMG-98	79	36433	1.6	12.3450	1.1	2.4269	1.4	0.2173	0.8	0.61	1267.6	9.8	1250.6	10.1	1221.6	21.9	1221.6	21.9	103.8
FMG-80	107	31608	2.4	12.1111	3.0	2.4742	5.4	0.2173	4.5	0.83	1267.7	51.8	1264.5	39.3	1259.1	59.5	1259.1	59.5	100.7
FMG-100	156	103458	1.5	9.3280	0.7	4.4927	1.1	0.3039	0.8	0.79	1710.8	12.6	1729.6	8.8	1752.4	11.9	1752.4	11.9	97.6
FMG-88	202	232980	2.1	9.2668	0.4	4.7493	0.9	0.3192	0.9	0.92	1785.8	13.3	1776.0	7.8	1764.5	6.8	1764.5	6.8	101.2
FMG-20	837	26429	32.1	7.9585	0.3	5.3249	2.6	0.3074	2.6	1.00	1727.7	39.7	1872.9	22.5	2038.0	4.6	2038.0	4.6	84.8
FMG-66	196	301796	13.2	7.7877	0.4	5.8155	1.9	0.3285	1.8	0.98	1830.9	29.1	1948.7	16.1	2076.3	6.5	2076.3	6.5	88.2
FMG-71	234	218907	4.3	7.7530	0.7	6.8524	0.9	0.3853	0.5	0.62	2101.1	9.6	2092.5	7.6	2084.1	11.9	2084.1	11.9	100.8
FMG-91	78	127730	1.1	7.7135	0.6	6.8290	1.0	0.3820	0.8	0.79	2085.8	13.4	2089.5	8.4	2093.1	10.2	2093.1	10.2	99.7
FMG-31	84	63439	1.6	7.6686	0.5	7.1802	0.7	0.3993	0.5	0.72	2166.0	9.7	2134.0	6.5	2103.4	8.9	2103.4	8.9	103.0
FMG-74	302	390274	1.9	7.5686	0.3	7.1428	1.4	0.3921	1.4	0.98	2132.5	25.6	2129.4	12.8	2126.4	4.9	2126.4	4.9	100.3
FMG-47	60	64050	1.4	7.3031	0.6	7.1760	1.4	0.3801	1.3	0.89	2076.7	22.6	2133.5	12.7	2188.7	11.2	2188.7	11.2	94.9
FMG-8	36	18123	1.5	6.8442	1.1	9.0467	1.5	0.4491	1.1	0.72	2391.1	22.0	2342.7	14.0	2300.9	18.2	2300.9	18.2	103.9
FMG-41	350	28370	2.8	5.5501	0.2	11.0458	2.1	0.4446	2.1	1.00	2371.3	42.4	2527.0	20.0	2654.5	3.0	2654.5	3.0	89.3
FMG-17	561	482799	5.2	5.2857	0.2	13.2335	1.3	0.5073	1.3	0.98	2645.2	27.7	2696.4	12.3	2735.1	3.9	2735.1	3.9	96.7
FMG-62	448	107210	1.5	5.0315	0.7	13.3788	1.7	0.4882	1.5	0.92	2562.9	32.6	2706.8	15.9	2815.9	10.9	2815.9	10.9	91.0

Analysis	U (ppm)	206Pb 204Pb	U/Th	206Pb* 207Pb*	± (%)	207Pb* 235U*	± (%)	206Pb* 238U	± (%)	error corr.	206Pb* 238U*	± (Ma)	207Pb* 235U	± (Ma)	206Pb* 207Pb*	± (Ma)	Best age (Ma)	± (Ma)	Conc (%)
MO-4	89	11982	1.1	19.9026	8.1	0.4214	8.4	0.0608	2.0	0.24	380.6	7.3	357.0	25.2	206.3	189.3	380.6	7.3	NA
MO-5	301	78024	0.9	16.6105	1.3	0.8444	1.9	0.1017	1.4	0.72	624.5	8.2	621.6	8.9	610.9	28.5	624.5	8.2	102.2
MO-6	521	300377	1.5	12.7096	0.4	2.1812	1.1	0.2011	1.0	0.94	1181.0	10.7	1175.1	7.4	1164.1	7.2	1164.1	7.2	101.5
MO-7	218	51508	1.5	18.4912	2.4	0.4842	2.5	0.0649	0.9	0.35	405.6	3.4	401.0	8.4	374.4	53.3	405.6	3.4	108.3
MO-8	27	56058	0.4	5.3631	1.2	13.7252	2.0	0.5339	1.6	0.80	2757.7	36.3	2730.9	19.0	2711.2	19.8	2711.2	19.8	101.7
MO-9	49	44779	2.0	14.3194	4.5	1.5056	4.7	0.1564	1.1	0.24	936.5	9.7	932.7	28.4	923.5	92.8	923.5	92.8	101.4
MO-10	65	35674	1.0	13.5039	3.0	1.8372	3.3	0.1799	1.4	0.41	1066.6	13.3	1058.9	21.9	1042.9	61.4	1042.9	61.4	102.3
MO-11	254	33080	1.0	18.6043	2.5	0.4388	2.9	0.0592	1.4	0.50	370.8	5.2	369.4	8.9	360.6	56.4	370.8	5.2	NA
MO-12	131	332438	1.5	3.4852	0.4	23.9260	2.4	0.6048	2.3	0.98	3049.0	56.8	3265.4	23.2	3401.0	6.7	3401.0	6.7	89.7
MO-13	180	78992	1.8	13.9859	1.3	1.6258	1.6	0.1649	1.0	0.63	984.0	9.4	980.2	10.2	971.7	25.6	971.7	25.6	101.3
MO-14	200	84656	1.8	12.3972	0.7	2.4162	1.4	0.2172	1.2	0.88	1267.3	14.4	1247.4	10.2	1213.2	13.2	1213.2	13.2	104.5
MO-15	181	80122	4.8	18.4896	4.7	0.4984	4.9	0.0668	1.6	0.33	417.0	6.6	410.6	16.7	374.5	105.1	417.0	6.6	111.3
MO-16	72	24916	1.6	16.3643	3.2	0.8824	3.4	0.1047	1.1	0.32	642.0	6.7	642.3	16.0	643.1	68.6	642.0	6.7	99.8

Analysis	U (ppm)	206Pb/204Pb	U/Th	206Pb*/207Pb*	± (%)	207Pb*/235U*	± (%)	206Pb*/238U	± (%)	error corr.	206Pb*/238U*	± (Ma)	207Pb*/235U	± (Ma)	206Pb*/207Pb*	± (Ma)	Best age (Ma)	± (Ma)	Conc (%)
MO-17	204	62516	1.7	13.0097	1.1	2.0512	2.1	0.1935	1.8	0.85	1140.5	18.6	1132.7	14.3	1117.7	22.1	1117.7	22.1	102.0
MO-19	159	24009	0.7	13.4988	1.1	1.7057	1.2	0.1670	0.6	0.48	995.5	5.4	1010.7	7.9	1043.7	21.9	1043.7	21.9	95.4
MO-20	450	612605	2.5	13.3938	0.4	1.8534	0.8	0.1800	0.7	0.89	1067.2	7.0	1064.6	5.3	1059.4	7.3	1059.4	7.3	100.7
MO-21	288	243475	1.1	13.3040	0.9	1.8591	1.1	0.1794	0.6	0.52	1063.6	5.7	1066.7	7.3	1072.9	19.0	1072.9	19.0	99.1
MO-22	135	84011	1.7	12.6817	0.7	2.1302	2.3	0.1959	2.2	0.95	1153.4	23.0	1158.6	15.8	1168.5	13.9	1168.5	13.9	98.7
MO-23	64	37774	1.8	12.0127	1.4	2.4998	1.6	0.2178	0.6	0.41	1270.2	7.3	1272.0	11.3	1275.0	27.8	1275.0	27.8	99.6
MO-24	102	22821	1.4	17.9130	4.4	0.5567	4.7	0.0723	1.5	0.32	450.2	6.4	449.4	16.9	445.4	98.1	450.2	6.4	101.1
MO-25	222	34460	6.8	18.6277	2.3	0.4627	2.6	0.0625	1.2	0.47	390.9	4.6	386.1	8.2	357.8	51.1	390.9	4.6	NA
MO-26	57	38640	1.8	12.8739	2.4	2.0002	2.7	0.1868	1.3	0.49	1103.8	13.4	1115.6	18.3	1138.6	46.8	1138.6	46.8	96.9
MO-27	318	128790	2.4	13.3420	0.6	1.8758	1.1	0.1815	1.0	0.85	1075.2	9.6	1072.6	7.5	1067.2	12.0	1067.2	12.0	100.8
MO-28	53	42973	1.7	11.2707	1.8	2.9818	2.1	0.2437	1.1	0.53	1406.1	13.8	1403.0	15.8	1398.2	33.9	1398.2	33.9	100.6
MO-29	26	16392	1.1	13.6100	6.6	1.7268	6.8	0.1705	1.7	0.25	1014.6	15.8	1018.6	43.9	1027.1	134.0	1027.1	134.0	98.8
MO-30	169	134762	4.2	12.5464	1.1	2.2276	1.4	0.2027	0.9	0.62	1189.8	9.8	1189.8	10.1	1189.7	22.3	1189.7	22.3	100.0
MO-31	118	63387	0.7	16.5351	2.7	0.8505	2.8	0.1020	0.8	0.27	626.1	4.5	624.9	13.0	620.7	57.8	626.1	4.5	100.9
MO-33	342	141154	3.1	13.7188	0.5	1.7316	1.1	0.1723	1.0	0.89	1024.7	9.3	1020.3	7.1	1011.0	10.2	1011.0	10.2	101.4
MO-34	53	33380	3.4	13.6858	3.2	1.7547	3.6	0.1742	1.7	0.47	1035.0	16.2	1028.9	23.1	1015.8	63.9	1015.8	63.9	101.9
MO-35	57	33969	1.8	12.0307	3.0	2.5005	3.3	0.2182	1.2	0.38	1272.2	14.4	1272.2	23.8	1272.0	59.2	1272.0	59.2	100.0
MO-37	207	104418	4.6	13.5305	1.1	1.7958	1.8	0.1762	1.5	0.80	1046.3	14.2	1043.9	12.0	1038.9	22.5	1038.9	22.5	100.7
MO-38	180	98701	1.6	16.8094	1.8	0.7750	2.5	0.0945	1.7	0.68	582.0	9.4	582.6	11.0	585.1	39.8	582.0	9.4	99.5
MO-39	164	86817	3.1	13.4848	1.2	1.8341	3.3	0.1794	3.1	0.93	1063.6	30.1	1057.7	21.8	1045.8	25.1	1045.8	25.1	101.7
MO-40	133	106254	1.2	9.7186	0.4	4.2957	1.0	0.3028	0.9	0.93	1705.1	14.2	1692.5	8.4	1677.0	7.1	1677.0	7.1	101.7
MO-41	417	116116	12.7	13.9379	0.6	1.5821	1.6	0.1599	1.5	0.92	956.4	12.9	963.2	9.8	978.7	12.4	978.7	12.4	97.7
MO-43	65	54026	1.8	13.6734	2.6	1.7428	2.9	0.1728	1.3	0.46	1027.7	12.7	1024.5	18.6	1017.7	51.8	1017.7	51.8	101.0
MO-44	93	20207	0.4	19.6445	11.9	0.3653	12.1	0.0520	2.0	0.17	327.1	6.4	316.2	32.9	236.5	276.0	327.1	6.4	NA
MO-46	63	33895	1.1	12.9343	1.1	2.1032	2.7	0.1973	2.4	0.90	1160.8	25.5	1149.8	18.3	1129.3	22.7	1129.3	22.7	102.8
MO-47	115	155671	1.7	10.9178	0.4	3.1645	1.5	0.2506	1.5	0.97	1441.5	18.9	1448.5	11.7	1458.9	7.4	1458.9	7.4	98.8
MO-48	128	46899	0.4	17.8221	4.1	0.5205	4.3	0.0673	1.2	0.27	419.7	4.7	425.5	15.0	456.7	91.9	419.7	4.7	91.9
MO-49	67	40874	2.2	13.3860	2.6	1.7617	7.8	0.1710	7.4	0.94	1017.8	69.4	1031.5	50.6	1060.6	51.8	1060.6	51.8	96.0
MO-51	89	37553	2.7	16.7045	3.0	0.7938	3.3	0.0962	1.4	0.41	591.9	7.8	593.3	15.0	598.7	65.7	591.9	7.8	98.9
MO-52	26	11044	0.9	13.1497	2.9	1.9390	3.5	0.1849	1.9	0.54	1093.8	18.9	1094.7	23.2	1096.3	58.2	1096.3	58.2	99.8
MO-53	108	99124	1.1	13.6647	1.6	1.8038	1.8	0.1788	0.8	0.45	1060.2	7.9	1046.8	11.7	1019.0	32.2	1019.0	32.2	104.0
MO-54	481	366779	2.2	12.7814	0.5	2.1423	2.6	0.1986	2.5	0.98	1167.7	27.0	1162.6	17.9	1152.9	10.8	1152.9	10.8	101.3
MO-56	471	823635	2.5	12.2564	0.4	2.3576	1.8	0.2096	1.7	0.98	1226.5	19.4	1229.9	12.7	1235.7	7.3	1235.7	7.3	99.3
MO-57	352	356292	2.9	13.6645	0.6	1.7490	1.1	0.1733	0.9	0.86	1030.5	8.9	1026.8	7.0	1019.0	11.3	1019.0	11.3	101.1
MO-58	427	92615	0.6	17.9007	1.2	0.5651	1.3	0.0734	0.6	0.48	456.4	2.8	454.9	4.9	446.9	26.1	456.4	2.8	102.1
MO-59	57	26832	1.6	13.6521	3.1	1.7500	3.3	0.1733	1.1	0.33	1030.1	10.2	1027.2	21.2	1020.8	62.7	1020.8	62.7	100.9
MO-60	142	11256	0.7	17.5049	4.4	0.5699	4.8	0.0724	1.9	0.40	450.3	8.4	457.9	17.7	496.4	96.7	450.3	8.4	90.7
MO-61	462	136395	2.9	18.2080	2.1	0.4551	2.7	0.0601	1.7	0.62	376.3	6.3	380.9	8.7	409.0	47.8	376.3	6.3	NA
MO-62	246	293876	0.7	11.8439	0.7	2.3493	1.4	0.2018	1.2	0.86	1185.0	12.6	1227.4	9.6	1302.5	13.2	1302.5	13.2	91.0

Analysis	U (ppm)	206Pb/204Pb	U/Th	206Pb*/207Pb*	± (%)	207Pb*/235U*	± (%)	206Pb*/238U	± (%)	error corr.	206Pb*/238U*	± (Ma)	207Pb*/235U	± (Ma)	206Pb*/207Pb*	± (Ma)	Best age (Ma)	± (Ma)	Conc (%)
MO-63	189	52581	1.3	18.1845	2.9	0.5014	3.2	0.0661	1.4	0.45	412.8	5.7	412.7	10.8	411.9	64.1	412.8	5.7	100.2
MO-64	28	8635	1.7	13.0573	7.0	1.8385	7.3	0.1741	2.0	0.28	1034.7	19.2	1059.3	48.0	1110.4	140.1	1110.4	140.1	93.2
MO-65	76	36602	0.9	12.9486	1.4	2.0381	1.8	0.1914	1.2	0.65	1129.0	12.2	1128.3	12.4	1127.1	27.7	1127.1	27.7	100.2
MO-66	398	48627	1.3	18.9944	1.4	0.3382	2.1	0.0466	1.5	0.72	293.6	4.2	295.8	5.3	313.6	32.7	293.6	4.2	NA
MO-67	123	55969	1.3	18.6290	3.4	0.5179	3.6	0.0700	1.3	0.35	436.0	5.3	423.8	12.4	357.6	75.7	436.0	5.3	121.9
MO-68	77	25055	1.0	16.9318	7.1	0.7479	7.2	0.0918	1.1	0.16	566.4	6.2	567.0	31.3	569.3	155.1	566.4	6.2	99.5
MO-69	412	174020	0.8	18.8959	2.0	0.4297	2.2	0.0589	0.9	0.40	368.8	3.2	362.9	6.7	325.5	46.0	368.8	3.2	NA
MO- 70	35	27135	0.8	9.0702	1.4	5.0863	1.8	0.3346	1.0	0.58	1860.6	16.5	1833.8	14.9	1803.5	26.1	1803.5	26.1	103.2
MO- 71	215	50286	0.9	18.0672	2.4	0.5303	3.0	0.0695	1.8	0.59	433.1	7.5	432.0	10.6	426.3	53.8	433.1	7.5	101.6
MO- 72	136	141153	1.6	7.7238	0.4	7.0636	1.0	0.3957	0.8	0.89	2149.2	15.5	2119.5	8.5	2090.8	7.8	2090.8	7.8	102.8
MO- 73	58	45437	2.1	14.1084	4.8	1.5359	4.9	0.1572	1.2	0.23	941.0	10.1	944.9	30.4	954.0	98.4	954.0	98.4	98.6
MO- 74	101	10779	1.1	14.0201	2.0	1.5087	2.6	0.1534	1.6	0.63	920.1	14.1	933.9	15.8	966.8	40.8	966.8	40.8	95.2
MO- 75	128	56308	5.2	13.0112	1.3	2.0177	3.0	0.1904	2.7	0.90	1123.5	27.9	1121.5	20.5	1117.5	26.8	1117.5	26.8	100.5
MO- 76	261	47017	14.3	18.2674	1.7	0.4764	4.6	0.0631	4.3	0.93	394.5	16.3	395.6	15.0	401.7	38.4	394.5	16.3	NA
MO- 77	698	264489	1.5	12.7125	0.2	2.1271	0.8	0.1961	0.7	0.96	1154.4	7.8	1157.6	5.3	1163.6	4.3	1163.6	4.3	99.2
MO- 78	305	47819	1.1	18.5830	4.2	0.4067	4.9	0.0548	2.5	0.51	344.0	8.4	346.5	14.5	363.2	95.5	344.0	8.4	NA
MO- 79	588	87160	0.7	18.1018	3.0	0.4466	3.6	0.0586	2.0	0.56	367.3	7.1	374.9	11.2	422.1	66.6	367.3	7.1	NA
MO- 80	333	77169	1.2	18.3594	3.0	0.5036	3.3	0.0671	1.2	0.36	418.4	4.7	414.1	11.1	390.4	68.3	418.4	4.7	107.2
MO- 81	148	369200	1.3	13.2732	0.6	1.9278	1.3	0.1856	1.2	0.89	1097.4	11.7	1090.8	8.7	1077.6	12.1	1077.6	12.1	101.8
MO- 82	49	36489	2.0	13.4807	3.4	1.8539	3.9	0.1813	1.7	0.44	1073.8	16.9	1064.8	25.4	1046.4	69.6	1046.4	69.6	102.6
MO- 83	247	110721	2.9	12.9126	0.7	1.9936	1.7	0.1867	1.6	0.92	1103.5	16.1	1113.3	11.7	1132.6	13.8	1132.6	13.8	97.4
MO- 84	78	45570	0.6	11.7142	1.8	2.6711	2.2	0.2269	1.2	0.54	1318.4	13.9	1320.5	16.0	1323.9	35.2	1323.9	35.2	99.6
MO- 85	100	102129	0.8	9.8340	0.5	4.1771	0.9	0.2979	0.8	0.86	1681.0	11.7	1669.5	7.5	1655.1	8.6	1655.1	8.6	101.6
MO- 86	164	18194	2.5	12.6126	1.1	2.1248	4.9	0.1944	4.8	0.98	1145.0	50.0	1156.9	33.7	1179.3	21.3	1179.3	21.3	97.1
MO- 88	138	17367	1.7	18.1043	4.1	0.5155	4.6	0.0677	2.0	0.44	422.2	8.3	422.1	15.9	421.7	92.4	422.2	8.3	100.1
MO- 89	505	63870	11.3	17.0901	1.9	0.5687	3.4	0.0705	2.8	0.83	439.1	11.9	457.2	12.4	549.1	40.6	439.1	11.9	80.0
MO- 90	598	97956	3.7	18.4387	1.2	0.4713	2.0	0.0630	1.6	0.80	394.0	6.1	392.1	6.5	380.8	27.1	394.0	6.1	NA
MO- 92	146	142462	1.9	11.7239	0.7	2.7131	1.2	0.2307	0.9	0.79	1338.1	11.0	1332.1	8.6	1322.3	13.7	1322.3	13.7	101.2
MO- 93	167	52853	2.3	18.0095	2.9	0.5230	3.1	0.0683	0.9	0.31	426.0	3.9	427.2	10.7	433.5	64.8	426.0	3.9	98.3
MO- 95	256	223342	2.5	12.9515	1.2	2.0403	3.3	0.1917	3.0	0.93	1130.3	31.5	1129.1	22.2	1126.6	23.1	1126.6	23.1	100.3
MO- 91	133	30733	1.7	18.5261	5.0	0.4513	5.6	0.0606	2.5	0.45	379.5	9.2	378.2	17.8	370.1	113.6	379.5	9.2	NA
MO- 97	189	104722	2.4	11.8295	1.0	2.5087	1.7	0.2152	1.3	0.80	1256.6	15.4	1274.6	12.2	1304.9	19.4	1304.9	19.4	96.3
MO- 98	217	69956	2.4	12.8399	0.4	1.9318	1.7	0.1799	1.7	0.98	1066.4	16.4	1092.2	11.5	1143.9	7.5	1143.9	7.5	93.2
MO- 99	172	127786	2.6	13.0239	1.2	2.0452	2.6	0.1932	2.3	0.88	1138.6	24.1	1130.7	17.8	1115.5	24.5	1115.5	24.5	102.1
MO- 100	442	144289	1.2	18.1711	1.4	0.5142	1.7	0.0678	1.0	0.61	422.7	4.2	421.3	5.9	413.5	30.4	422.7	4.2	102.2

Analysis	U (ppm)	206Pb/204Pb	U/Th	206Pb*/207Pb*	± (%)	207Pb*/235U*	± (%)	206Pb*/238U	± (%)	error corr.	206Pb*/238U*	± (Ma)	207Pb*/235U	± (Ma)	206Pb*/207Pb*	± (Ma)	Best age (Ma)	± (Ma)	Conc (%)
P1004-68	473	116188	0.8	18.2570	1.1	0.4498	1.4	0.0596	0.9	0.63	373.0	3.2	377.1	4.5	403.0	24.7	373.0	3.2	NA

Analysis	U (ppm)	206Pb / 204Pb	U/Th	206Pb* / 207Pb*	± (%)	207Pb* / 235U*	± (%)	206Pb* / 238U	± (%)	error corr.	206Pb* / 238U*	± (Ma)	207Pb* / 235U	± (Ma)	206Pb* / 207Pb*	± (Ma)	Best age (Ma)	± (Ma)	Conc (%)
P1004-8	1006	191310	3.5	18.2298	0.5	0.4550	1.1	0.0602	1.0	0.87	376.6	3.5	380.7	3.5	406.3	12.2	376.6	3.5	NA
P1004-51	58	12599	1.0	18.2046	8.3	0.4924	8.4	0.0650	1.6	0.19	406.0	6.4	406.5	28.3	409.4	185.7	406.0	6.4	99.2
P1004-33	90	20665	0.4	18.9146	4.1	0.4791	4.3	0.0657	1.2	0.28	410.4	4.7	397.5	14.1	323.2	93.8	410.4	4.7	127.0
P1004-89	155	17115	5.6	17.1769	6.3	0.5291	6.7	0.0659	2.2	0.34	411.5	8.9	431.2	23.4	538.0	137.3	411.5	8.9	76.5
P1004-55	146	17191	2.2	17.8454	5.0	0.5157	5.4	0.0667	2.0	0.38	416.5	8.2	422.3	18.5	453.9	110.1	416.5	8.2	91.8
P1004-74	188	66418	0.9	18.1987	3.4	0.5164	3.7	0.0682	1.3	0.36	425.0	5.5	422.7	12.8	410.1	77.2	425.0	5.5	103.6
P1004-27	92	28832	0.9	18.1616	7.8	0.5730	7.9	0.0755	1.2	0.15	469.0	5.4	459.9	29.1	414.7	173.7	469.0	5.4	113.1
P1004-53	75	30102	1.1	16.4244	4.5	0.7418	4.8	0.0884	1.4	0.30	545.9	7.4	563.5	20.6	635.2	97.8	545.9	7.4	85.9
P1004-48	78	14239	1.1	18.4026	7.6	0.6633	7.7	0.0885	1.4	0.18	546.9	7.2	516.7	31.3	385.2	170.8	546.9	7.2	142.0
P1004-79	33	9872	0.9	16.9480	10.5	0.7346	10.9	0.0903	2.8	0.26	557.3	15.0	559.2	46.8	567.3	229.0	557.3	15.0	98.2
P1004-28	63	19641	1.0	17.4288	6.7	0.7162	7.0	0.0905	2.1	0.30	558.7	11.1	548.4	29.8	506.0	147.8	558.7	11.1	110.4
P1004-4	103	31878	0.8	16.7443	4.2	0.7685	4.5	0.0933	1.5	0.33	575.2	8.2	578.9	19.7	593.5	91.4	575.2	8.2	96.9
P1004-23	65	38751	0.8	17.0655	3.4	0.7598	3.9	0.0940	1.9	0.48	579.4	10.5	573.9	17.2	552.2	75.0	579.4	10.5	104.9
P1004-54	168	65018	1.0	16.2470	1.3	0.8128	1.8	0.0958	1.3	0.70	589.6	7.1	604.0	8.2	658.5	27.8	589.6	7.1	89.5
P1004-47	258	66275	3.1	16.4959	1.0	0.8329	1.4	0.0996	1.0	0.68	612.3	5.6	615.2	6.5	625.8	22.3	612.3	5.6	97.8
P1004-88	75	31688	1.0	16.4091	5.1	0.8466	5.2	0.1008	1.0	0.20	618.8	6.1	622.8	24.3	637.2	110.1	618.8	6.1	97.1
P1004-17	98	4912	0.9	15.6027	8.0	0.8909	8.2	0.1008	1.4	0.17	619.2	8.1	646.9	39.0	744.6	170.1	619.2	8.1	83.2
P1004-42	121	33300	0.4	16.3981	2.1	0.8504	2.3	0.1011	0.9	0.39	621.1	5.2	624.9	10.6	638.6	45.1	621.1	5.2	97.3
P1004-64	187	110379	1.8	16.5242	1.4	0.8449	2.5	0.1013	2.1	0.83	621.7	12.2	621.8	11.6	622.1	30.1	621.7	12.2	99.9
P1004-36	84	41785	1.2	16.2490	5.3	0.8834	5.5	0.1041	1.4	0.26	638.4	8.7	642.8	26.3	658.2	114.4	638.4	8.7	97.0
P1004-45	214	176717	1.2	16.0000	1.4	0.9132	7.1	0.1060	6.9	0.98	649.3	42.8	658.7	34.3	691.2	29.8	649.3	42.8	93.9
P1004-46	49	17192	3.2	14.7310	2.5	1.1348	3.0	0.1212	1.7	0.58	737.7	12.2	770.0	16.4	865.0	51.3	737.7	12.2	85.3
P1004-52	57	15856	1.3	14.3068	2.7	1.4140	3.6	0.1467	2.4	0.66	882.5	19.5	894.8	21.3	925.3	55.1	925.3	55.1	95.4
P1004-67	126	124550	2.0	14.2418	1.2	1.5483	1.5	0.1599	0.9	0.61	956.4	8.0	949.8	9.1	934.7	24.1	934.7	24.1	102.3
P1004-91	72	110551	1.5	14.0934	2.0	1.6053	2.5	0.1641	1.6	0.62	979.4	14.4	972.3	15.9	956.1	40.6	956.1	40.6	102.4
P1004-56	24	15362	1.0	14.0075	4.8	1.6706	5.1	0.1697	1.7	0.34	1010.6	16.3	997.4	32.3	968.6	97.6	968.6	97.6	104.3
P1004-66	61	31546	1.8	13.9630	1.7	1.5890	2.2	0.1609	1.3	0.61	961.9	11.7	965.9	13.4	975.1	34.9	975.1	34.9	98.6
P1004-73	200	94844	4.0	13.8670	0.8	1.5947	1.3	0.1604	1.0	0.79	958.9	9.2	968.2	8.1	989.1	16.2	989.1	16.2	96.9
P1004-1	166	70878	2.0	13.7003	0.9	1.7571	2.0	0.1746	1.8	0.90	1037.3	17.4	1029.8	13.0	1013.7	17.3	1013.7	17.3	102.3
P1004-98	109	61433	3.0	13.6820	1.3	1.7212	1.6	0.1708	1.0	0.58	1016.5	9.0	1016.5	10.6	1016.4	27.3	1016.4	27.3	100.0
P1004-43	436	271823	3.7	13.6632	0.3	1.7717	1.3	0.1756	1.3	0.97	1042.7	12.5	1035.1	8.7	1019.2	7.0	1019.2	7.0	102.3
P1004-22	113	85597	1.6	13.6272	1.9	1.7805	2.3	0.1760	1.4	0.61	1045.0	13.9	1038.4	15.3	1024.5	37.5	1024.5	37.5	102.0
P1004-72	155	132626	1.9	13.6141	0.7	1.7308	1.6	0.1709	1.4	0.89	1017.1	13.3	1020.1	10.2	1026.5	14.8	1026.5	14.8	99.1
P1004-76	138	96679	1.9	13.5741	1.2	1.7887	2.1	0.1761	1.7	0.81	1045.6	16.4	1041.4	13.7	1032.4	25.2	1032.4	25.2	101.3
P1004-58	84	39911	2.3	13.5655	2.3	1.7571	2.8	0.1729	1.6	0.58	1027.9	15.5	1029.8	18.1	1033.7	45.8	1033.7	45.8	99.4
P1004-96	121	45285	1.8	13.5558	1.3	1.7394	1.4	0.1710	0.7	0.47	1017.7	6.4	1023.2	9.3	1035.1	25.8	1035.1	25.8	98.3
P1004-70	108	136372	2.9	13.5232	1.9	1.7779	2.1	0.1744	0.9	0.42	1036.2	8.5	1037.4	13.7	1040.0	38.5	1040.0	38.5	99.6
P1004-60	155	139668	2.8	13.4879	1.4	1.7429	2.4	0.1705	1.9	0.81	1014.8	18.1	1024.5	15.4	1045.3	28.2	1045.3	28.2	97.1
P1004-21	113	65291	2.5	13.4292	1.1	1.8171	1.3	0.1770	0.7	0.53	1050.5	6.7	1051.6	8.5	1054.1	22.0	1054.1	22.0	99.7

Analysis	U (ppm)	206Pb 204Pb	U/Th	206Pb* 207Pb*	± (%)	207Pb* 235U*	± (%)	206Pb* 238U	± (%)	error corr.	206Pb* 238U*	± (Ma)	207Pb* 235U	± (Ma)	206Pb* 207Pb*	± (Ma)	Best age (Ma)	± (Ma)	Conc (%)
P1004-80	133	62002	2.3	13.4107	1.2	1.8369	1.6	0.1787	1.0	0.64	1059.6	9.9	1058.7	10.4	1056.9	24.5	1056.9	24.5	100.3
P1004-92	106	61122	3.1	13.3879	1.6	1.8705	2.2	0.1816	1.6	0.71	1075.8	15.9	1070.7	14.9	1060.3	31.7	1060.3	31.7	101.5
P1004-59	72	50016	1.6	13.3697	2.3	1.7717	2.9	0.1718	1.8	0.62	1022.0	16.7	1035.1	18.6	1063.0	45.4	1063.0	45.4	96.1
P1004-93	157	116069	2.6	13.3678	0.9	1.8569	1.5	0.1800	1.1	0.77	1067.1	11.1	1065.9	9.7	1063.3	18.8	1063.3	18.8	100.4
P1004-9	63	34054	1.4	13.3552	1.9	1.9149	2.1	0.1855	0.9	0.45	1096.8	9.4	1086.3	13.9	1065.2	37.6	1065.2	37.6	103.0
P1004-15	259	176820	3.2	13.3421	0.5	1.8584	0.7	0.1798	0.5	0.74	1066.0	5.3	1066.4	4.8	1067.2	9.9	1067.2	9.9	99.9
P1004-41	142	101142	1.9	13.3254	0.9	1.8456	1.1	0.1784	0.6	0.56	1058.0	5.8	1061.8	6.9	1069.7	17.5	1069.7	17.5	98.9
P1004-61	55	45768	2.2	13.3171	3.9	1.9362	9.9	0.1870	9.1	0.92	1105.2	92.8	1093.7	66.5	1071.0	77.6	1071.0	77.6	103.2
P1004-49	76	47801	1.7	13.2763	2.4	1.8284	2.5	0.1761	0.7	0.26	1045.4	6.4	1055.7	16.4	1077.1	48.3	1077.1	48.3	97.1
P1004-69	181	176140	2.3	13.2508	0.7	1.8490	1.0	0.1777	0.7	0.70	1054.4	6.8	1063.1	6.6	1081.0	14.5	1081.0	14.5	97.5
P1004-100	137	64342	2.6	13.2432	2.0	1.8234	3.3	0.1751	2.6	0.80	1040.4	25.3	1053.9	21.7	1082.1	40.1	1082.1	40.1	96.1
P1004-81	145	82704	2.4	13.1772	0.8	1.9320	1.4	0.1846	1.1	0.80	1092.3	10.8	1092.2	9.0	1092.1	16.3	1092.1	16.3	100.0
P1004-85	248	209556	6.5	13.1708	1.7	1.7921	1.9	0.1712	0.8	0.43	1018.6	7.9	1042.6	12.5	1093.1	34.7	1093.1	34.7	93.2
P1004-16	426	149235	6.0	13.1450	1.4	1.7970	1.8	0.1713	1.1	0.61	1019.4	10.5	1044.4	11.9	1097.0	28.8	1097.0	28.8	92.9
P1004-3	212	3869	1.8	13.0926	1.2	1.9002	1.4	0.1804	0.8	0.53	1069.4	7.4	1081.2	9.5	1105.0	24.2	1105.0	24.2	96.8
P1004-87	286	111612	8.8	13.0583	0.5	1.9270	1.8	0.1825	1.7	0.96	1080.6	17.0	1090.5	11.9	1110.2	10.4	1110.2	10.4	97.3
P1004-82	59	27880	1.9	13.0248	1.1	1.9354	2.0	0.1828	1.7	0.84	1082.4	16.5	1093.4	13.2	1115.4	21.5	1115.4	21.5	97.0
P1004-63	47	31492	2.2	12.9657	2.3	2.0789	2.7	0.1955	1.3	0.50	1151.1	14.1	1141.9	18.3	1124.5	46.2	1124.5	46.2	102.4
P1004-11	685	540799	4.1	12.8695	0.4	2.0328	0.7	0.1897	0.5	0.76	1120.0	5.1	1126.5	4.5	1139.3	8.6	1139.3	8.6	98.3
P1004-40	133	131917	2.0	12.7554	1.1	2.0924	1.8	0.1936	1.4	0.78	1140.7	14.7	1146.3	12.5	1157.0	22.8	1157.0	22.8	98.6
P1004-30	247	145003	1.3	12.7042	0.7	2.1063	5.3	0.1941	5.3	0.99	1143.4	55.3	1150.9	36.6	1164.9	13.3	1164.9	13.3	98.2
P1004-75	29	18858	1.5	12.6776	3.4	2.1453	3.8	0.1973	1.9	0.48	1160.5	19.7	1163.5	26.6	1169.1	66.7	1169.1	66.7	99.3
P1004-95	260	117815	2.9	12.6047	0.3	2.1116	1.0	0.1930	1.0	0.95	1137.8	10.0	1152.6	6.9	1180.5	5.9	1180.5	5.9	96.4
P1004-34	46	26060	1.4	12.5736	4.1	2.2043	4.6	0.2010	2.1	0.46	1180.8	22.8	1182.4	32.3	1185.4	81.1	1185.4	81.1	99.6
P1004-38	75	77397	2.9	12.5484	1.4	2.2034	1.7	0.2005	1.0	0.59	1178.2	10.8	1182.1	11.9	1189.4	27.1	1189.4	27.1	99.1
P1004-97	77	9322	1.6	12.3238	2.9	2.0118	3.1	0.1798	1.1	0.36	1066.0	10.7	1119.5	20.8	1224.9	56.4	1224.9	56.4	87.0
P1004-62	267	196172	0.8	12.2808	0.8	2.3595	1.3	0.2102	1.0	0.79	1229.7	11.3	1230.4	9.2	1231.8	15.7	1231.8	15.7	99.8
P1004-50	372	534392	1.7	12.2346	0.2	2.3500	0.9	0.2085	0.8	0.97	1221.0	9.3	1227.6	6.1	1239.2	4.2	1239.2	4.2	98.5
P1004-12	41	34337	4.2	12.1287	2.1	2.1761	2.6	0.1914	1.6	0.60	1129.1	16.4	1173.4	18.4	1256.2	41.6	1256.2	41.6	89.9
P1004-35	80	84318	3.4	12.0950	1.5	2.1647	3.8	0.1899	3.5	0.93	1120.8	36.4	1169.8	26.6	1261.6	28.4	1261.6	28.4	88.8
P1004-77	140	162400	3.1	11.9429	1.9	2.5042	5.5	0.2169	5.1	0.94	1265.5	59.1	1273.3	39.7	1286.3	36.2	1286.3	36.2	98.4
P1004-14	59	29354	0.9	11.8904	1.1	2.5433	4.5	0.2193	4.4	0.97	1278.3	50.4	1284.5	32.7	1294.9	21.2	1294.9	21.2	98.7
P1004-20	48	53269	0.9	11.8820	2.7	2.5735	6.3	0.2218	5.6	0.90	1291.3	66.0	1293.1	45.7	1296.3	52.5	1296.3	52.5	99.6
P1004-2	36	11811	1.4	11.8103	2.4	2.5712	3.8	0.2202	2.9	0.77	1283.1	34.2	1292.5	27.9	1308.0	47.4	1308.0	47.4	98.1
P1004-31	313	138214	1.1	11.7411	0.4	2.4815	0.9	0.2113	0.8	0.88	1235.8	8.9	1266.7	6.6	1319.4	8.5	1319.4	8.5	93.7
P1004-32	78	50513	2.1	11.6812	1.4	2.7180	2.7	0.2303	2.4	0.86	1335.9	28.4	1333.4	20.4	1329.3	27.3	1329.3	27.3	100.5
P1004-78	13	15683	0.5	11.4768	8.0	2.4679	8.4	0.2054	2.5	0.30	1204.4	27.5	1262.7	60.7	1363.4	154.4	1363.4	154.4	88.3
P1004-5	142	86223	1.2	11.3734	1.0	2.9683	1.2	0.2448	0.7	0.59	1411.9	9.2	1399.5	9.3	1380.8	19.1	1380.8	19.1	102.2
P1004-37	55	36433	0.9	11.3079	1.9	2.8674	2.7	0.2352	1.9	0.70	1361.5	23.0	1373.4	20.2	1391.9	37.1	1391.9	37.1	97.8

Analysis	U	206Pb	U/Th	206Pb*	±	207Pb*	±	206Pb*	±	error	206Pb*	±	207Pb*	±	206Pb*	±	Best age	±	Conc
	(ppm)	204Pb		207Pb*	(%)	235U*	(%)	238U	(%)	corr.	238U*	(Ma)	235U	(Ma)	207Pb*	(Ma)	(Ma)	(Ma)	(%)
P1004-24	40	49383	1.0	11.3040	3.5	2.8297	5.2	0.2320	3.8	0.73	1344.9	46.2	1363.4	38.8	1392.6	67.3	1392.6	67.3	96.6
P1004-71	129	104681	1.3	10.8199	0.7	3.3067	1.2	0.2595	1.0	0.84	1487.2	13.9	1482.6	9.7	1476.1	12.6	1476.1	12.6	100.8
P1004-19	61	68526	2.0	10.7497	1.0	3.3860	1.6	0.2640	1.2	0.76	1510.2	16.3	1501.2	12.5	1488.4	19.6	1488.4	19.6	101.5
P1004-94	132	9235	1.4	10.6186	1.1	3.1008	3.4	0.2388	3.2	0.94	1380.5	39.2	1432.9	25.7	1511.6	21.3	1511.6	21.3	91.3
P1004-39	83	63356	1.1	10.5877	1.6	3.2984	3.2	0.2533	2.7	0.86	1455.4	35.3	1480.7	24.6	1517.1	30.6	1517.1	30.6	95.9
P1004-25	75	41373	2.1	10.4905	1.3	3.5550	2.0	0.2705	1.5	0.76	1543.3	20.3	1539.6	15.5	1534.5	24.1	1534.5	24.1	100.6
P1004-29	83	62142	2.2	10.4230	1.1	3.5943	1.5	0.2717	1.0	0.66	1549.5	13.6	1548.3	11.9	1546.6	21.1	1546.6	21.1	100.2
P1004-84	29	53898	6.5	8.5338	1.5	5.5904	2.3	0.3460	1.8	0.75	1915.5	29.4	1914.6	20.2	1913.7	27.7	1913.7	27.7	100.1
P1004-86	115	6532	1.0	8.1995	3.4	5.9398	4.2	0.3532	2.5	0.59	1950.0	41.2	1967.1	36.2	1985.1	60.0	1985.1	60.0	98.2
P1004-83	261	216679	1.2	7.5837	0.2	7.0504	1.2	0.3878	1.2	0.99	2112.6	21.3	2117.8	10.6	2122.9	2.9	2122.9	2.9	99.5
P1004-7	238	191077	0.6	7.3661	0.3	7.4546	1.0	0.3983	1.0	0.97	2161.0	17.8	2167.6	9.0	2173.7	4.4	2173.7	4.4	99.4
P1004-26	131	237666	1.2	5.6820	1.0	11.8361	2.0	0.4878	1.8	0.88	2561.0	38.3	2591.5	19.2	2615.5	15.9	2615.5	15.9	97.9
P1004-57	26	95627	2.3	5.4876	1.2	12.2903	3.8	0.4892	3.6	0.95	2567.0	76.7	2626.8	35.8	2673.2	19.5	2673.2	19.5	96.0

Analysis	U	206Pb	U/Th	206Pb*	±	207Pb*	±	206Pb*	±	error	206Pb*	±	207Pb*	±	206Pb*	±	Best age	±	Conc
	(ppm)	204Pb		207Pb*	(%)	235U*	(%)	238U	(%)	corr.	238U*	(Ma)	235U	(Ma)	207Pb*	(Ma)	(Ma)	(Ma)	(%)
P1080-33	292	38682	0.5	19.0765	2.1	0.3880	3.1	0.0537	2.3	0.74	337.1	7.6	332.9	8.9	303.8	48.4	337.1	7.6	NA
P1080-93	35	10325	1.1	24.4222	10.6	0.3293	11.5	0.0583	4.5	0.39	365.4	15.9	289.0	29.0	-290.9	271.4	365.4	15.9	NA
P1080-57	172	29054	1.5	18.0153	1.9	0.4747	3.0	0.0620	2.3	0.77	387.9	8.8	394.4	9.9	432.7	43.3	387.9	8.8	NA
P1080-81	50	15454	1.7	17.8811	5.1	0.4799	5.2	0.0622	1.0	0.19	389.2	3.7	398.0	17.2	449.4	113.8	389.2	3.7	NA
P1080-38	270	72321	4.1	18.3420	1.7	0.4715	6.0	0.0627	5.8	0.96	392.2	22.0	392.2	19.6	392.6	38.4	392.2	22.0	NA
P1080-86	547	176247	15.3	18.2266	1.1	0.4767	2.7	0.0630	2.5	0.92	394.0	9.6	395.8	9.0	406.7	23.9	394.0	9.6	NA
P1080-9	92	36130	1.6	18.7788	8.0	0.4644	8.1	0.0633	1.3	0.16	395.4	5.0	387.3	26.0	339.6	180.7	395.4	5.0	NA
P1080-64	434	113732	7.9	18.2661	1.8	0.4802	3.0	0.0636	2.4	0.79	397.6	9.1	398.2	9.9	401.9	41.3	397.6	9.1	NA
P1080-96	221	41516	1.3	18.2939	2.6	0.4799	4.7	0.0637	4.0	0.84	397.9	15.4	398.0	15.6	398.4	57.4	397.9	15.4	NA
P1080-12	217	11336	0.8	16.3727	14.8	0.5432	15.5	0.0645	4.6	0.30	402.9	18.1	440.5	55.3	642.0	318.9	402.9	18.1	62.8
P1080-71	172	52467	2.0	18.4912	2.2	0.4868	2.6	0.0653	1.4	0.55	407.7	5.7	402.8	8.6	374.3	48.4	407.7	5.7	108.9
P1080-84	203	70996	5.3	17.7304	4.4	0.5182	4.6	0.0666	1.2	0.26	415.9	4.7	423.9	15.9	468.2	98.2	415.9	4.7	88.8
P1080-61	622	133858	4.5	18.0969	1.0	0.5108	1.3	0.0670	0.9	0.67	418.3	3.5	419.0	4.5	422.7	21.6	418.3	3.5	99.0
P1080-17	195	32625	2.6	18.1853	3.4	0.5193	3.7	0.0685	1.4	0.37	427.0	5.7	424.7	12.8	411.8	76.2	427.0	5.7	103.7
P1080-15	314	27163	0.5	17.9172	1.5	0.5274	1.7	0.0685	0.9	0.50	427.3	3.6	430.1	6.0	444.9	33.0	427.3	3.6	96.0
P1080-83	59	35642	4.4	18.9343	10.7	0.5101	10.8	0.0701	1.3	0.12	436.5	5.3	418.5	37.1	320.9	244.4	436.5	5.3	136.0
P1080-31	145	57165	2.8	18.1683	1.4	0.5341	1.9	0.0704	1.3	0.67	438.4	5.3	434.5	6.6	413.9	30.8	438.4	5.3	105.9
P1080-98	110	34382	3.2	18.1049	5.3	0.5410	5.4	0.0710	0.9	0.17	442.4	3.8	439.1	19.1	421.7	118.3	442.4	3.8	104.9
P1080-35	74	53188	2.3	17.5482	7.0	0.5588	7.3	0.0711	2.2	0.30	442.9	9.3	450.7	26.7	491.0	154.7	442.9	9.3	90.2
P1080-55	47	17037	1.1	19.3943	9.1	0.5128	9.2	0.0721	1.4	0.16	449.0	6.3	420.3	31.8	266.0	209.9	449.0	6.3	168.8
P1080-70	116	20548	0.7	18.0350	4.7	0.5584	4.8	0.0730	1.0	0.21	454.4	4.3	450.5	17.4	430.3	104.2	454.4	4.3	105.6
P1080-99	277	106381	0.7	17.7101	1.5	0.5700	2.4	0.0732	1.9	0.80	455.5	8.5	458.0	9.0	470.7	32.5	455.5	8.5	96.8
P1080-73	164	49706	20.9	17.4640	3.2	0.5803	7.3	0.0735	6.6	0.90	457.2	29.2	464.7	27.3	501.6	69.4	457.2	29.2	91.2

Analysis	U (ppm)	206Pb 204Pb	U/Th	206Pb* 207Pb*	± (%)	207Pb* 235U*	± (%)	206Pb* 238U	± (%)	error corr.	206Pb* 238U*	± (Ma)	207Pb* 235U	± (Ma)	206Pb* 207Pb*	± (Ma)	Best age (Ma)	± (Ma)	Conc (%)
P1080-54	77	20837	1.8	18.1562	5.7	0.5610	6.0	0.0739	1.9	0.32	459.4	8.4	452.2	21.8	415.4	126.6	459.4	8.4	110.6
P1080-22	174	44266	4.2	15.3173	4.0	0.6668	8.2	0.0741	7.1	0.87	460.7	31.7	518.8	33.1	783.5	83.1	460.7	31.7	58.8
P1080-18	175	55845	2.6	17.1423	3.0	0.6264	3.1	0.0779	0.7	0.23	483.4	3.3	493.8	12.1	542.4	65.8	483.4	3.3	89.1
P1080-41	55	13145	0.5	17.4327	6.9	0.6939	7.5	0.0877	2.8	0.37	542.1	14.6	535.1	31.1	505.5	152.7	542.1	14.6	107.2
P1080-58	90	38635	0.7	17.0807	2.2	0.7201	2.6	0.0892	1.3	0.51	550.9	6.9	550.7	10.9	550.2	48.5	550.9	6.9	100.1
P1080-97	80	15155	3.5	16.6948	4.6	0.7466	4.7	0.0904	1.2	0.26	557.9	6.5	566.2	20.5	599.9	98.8	557.9	6.5	93.0
P1080-43	100	42642	0.9	17.1830	2.9	0.7288	3.0	0.0908	1.0	0.32	560.4	5.3	555.8	13.0	537.2	62.7	560.4	5.3	104.3
P1080-69	156	46211	4.1	17.1536	2.8	0.7622	3.3	0.0948	1.7	0.53	584.0	9.7	575.3	14.3	540.9	60.4	584.0	9.7	108.0
P1080-2	94	38671	0.4	16.4008	3.4	0.8295	3.9	0.0987	1.9	0.47	606.6	10.7	613.3	18.0	638.3	74.3	606.6	10.7	95.0
P1080-59	82	55686	0.7	16.5029	3.6	0.8380	3.9	0.1003	1.3	0.34	616.1	7.8	618.0	17.9	624.9	78.5	616.1	7.8	98.6
P1080-98	336	248906	1.3	16.4519	0.9	0.8659	1.6	0.1033	1.3	0.83	633.8	8.1	633.3	7.6	631.6	19.1	633.8	8.1	100.3
P1080-62	68	25704	0.8	16.5173	3.2	0.8643	3.8	0.1035	1.9	0.52	635.1	11.8	632.5	17.8	623.0	69.7	635.1	11.8	101.9
P1080-42	139	163567	1.4	16.0561	3.5	0.8986	3.6	0.1046	1.1	0.30	641.5	6.7	651.0	17.5	683.8	74.1	641.5	6.7	93.8
P1080-26	95	47781	0.6	16.4906	2.7	0.8848	3.7	0.1058	2.5	0.68	648.4	15.5	643.6	17.6	626.5	58.7	648.4	15.5	103.5
P1080-72	78	31390	1.0	16.0179	2.8	0.9678	4.0	0.1124	2.9	0.72	686.9	18.8	687.3	20.0	688.9	58.9	686.9	18.8	99.7
P1080-23	204	103627	0.9	15.4823	0.9	1.1097	1.0	0.1246	0.5	0.50	757.0	3.6	758.0	5.4	761.0	18.4	757.0	3.6	99.5
P1080-8	51	11365	1.3	14.2014	5.0	1.4787	5.6	0.1523	2.5	0.44	913.9	21.1	921.7	33.9	940.5	103.0	940.5	103.0	97.2
P1080-37	57	43949	3.5	13.8842	2.3	1.6342	3.2	0.1646	2.3	0.71	982.1	20.7	983.5	20.2	986.6	46.1	986.6	46.1	99.5
P1080-56	64	45150	2.6	13.8724	4.1	1.7266	5.0	0.1737	2.9	0.57	1032.6	27.4	1018.5	32.3	988.4	83.9	988.4	83.9	104.5
P1080-1	39	24437	3.4	13.8298	5.9	1.6178	6.2	0.1623	1.9	0.30	969.4	16.9	977.1	39.0	994.6	120.4	994.6	120.4	97.5
P1080-68	162	192064	2.3	13.8016	0.7	1.6481	2.0	0.1650	1.9	0.94	984.3	17.5	988.8	12.9	998.7	14.4	998.7	14.4	98.6
P1080-91	70	64197	1.1	13.7675	2.4	1.6955	2.6	0.1693	0.9	0.33	1008.3	8.0	1006.8	16.6	1003.8	49.7	1003.8	49.7	100.4
P1080-25	35	31010	1.5	13.6561	4.1	1.7904	4.4	0.1773	1.5	0.35	1052.4	14.7	1042.0	28.6	1020.2	83.4	1020.2	83.4	103.2
P1080-40	68	44101	1.0	13.6084	1.9	1.7674	2.2	0.1744	1.1	0.51	1036.5	10.8	1033.6	14.3	1027.3	38.2	1027.3	38.2	100.9
P1080-4	268	117904	0.9	13.5992	0.6	1.7414	1.1	0.1718	1.0	0.85	1021.8	9.1	1024.0	7.3	1028.7	12.0	1028.7	12.0	99.3
P1080-94	44	25577	2.9	13.5351	3.4	1.7806	3.7	0.1748	1.4	0.37	1038.5	13.1	1038.4	23.7	1038.2	68.4	1038.2	68.4	100.0
P1080-46	129	66403	3.5	13.4615	0.9	1.7372	1.6	0.1696	1.3	0.81	1009.9	12.0	1022.4	10.2	1049.3	18.9	1049.3	18.9	96.3
P1080-47	143	79627	0.9	13.3564	1.3	1.7711	2.7	0.1716	2.4	0.88	1020.7	22.6	1034.9	17.7	1065.0	26.2	1065.0	26.2	95.8
P1080-10	34	18458	1.5	13.3547	4.6	1.8150	4.7	0.1758	0.9	0.19	1044.0	8.9	1050.9	30.9	1065.3	93.2	1065.3	93.2	98.0
P1080-49	72	82725	3.0	13.3467	1.4	1.9048	1.8	0.1844	1.1	0.62	1090.9	11.0	1082.8	11.8	1066.5	28.1	1066.5	28.1	102.3
P1080-60	115	154753	1.2	13.3447	1.2	1.8126	1.9	0.1754	1.4	0.76	1042.0	13.7	1050.0	12.3	1066.8	24.5	1066.8	24.5	97.7
P1080-16	51	40784	1.0	13.3113	2.4	1.8560	2.8	0.1792	1.4	0.50	1062.5	13.6	1065.6	18.3	1071.8	48.2	1071.8	48.2	99.1
P1080-34	78	203579	1.6	13.2069	0.7	1.9249	2.0	0.1844	1.8	0.93	1090.9	18.3	1089.8	13.1	1087.6	14.6	1087.6	14.6	100.3
P1080-78	15	26340	1.7	13.1888	7.4	1.9719	7.8	0.1886	2.2	0.28	1113.9	22.6	1106.0	52.3	1090.4	149.2	1090.4	149.2	102.2
P1080 prob 51	124	85621	1.1	12.8652	1.2	2.1525	1.3	0.2008	0.6	0.48	1179.9	6.9	1165.9	9.3	1139.9	23.3	1139.9	23.3	103.5
P1080-21	353	703772	1.5	12.8519	0.6	2.0638	1.5	0.1924	1.4	0.93	1134.2	14.8	1136.9	10.5	1142.0	11.2	1142.0	11.2	99.3
P1080-76	193	160320	1.7	12.7871	0.9	2.1528	2.1	0.1997	1.9	0.90	1173.4	20.5	1165.9	14.7	1152.0	18.4	1152.0	18.4	101.9
P1080-36	202	119357	1.2	12.6771	1.0	2.1496	2.4	0.1976	2.2	0.91	1162.6	23.3	1164.9	16.7	1169.2	20.0	1169.2	20.0	99.4
P1080-63	135	118403	0.7	12.6486	0.9	2.2286	4.2	0.2044	4.1	0.98	1199.2	45.3	1190.1	29.8	1173.7	18.6	1173.7	18.6	102.2

Analysis	U	206Pb	U/Th	206Pb*	±	207Pb*	±	206Pb*	±	error	206Pb*	±	207Pb*	±	206Pb*	±	Best age	±	Conc
	(ppm)	204Pb		207Pb*	(%)	235U*	(%)	238U	(%)	corr.	238U*	(Ma)	235U	(Ma)	207Pb*	(Ma)	(Ma)	(Ma)	(%)
P1080-77	49	51402	1.0	12.5188	2.8	2.1311	2.8	0.1935	0.5	0.19	1140.3	5.5	1158.9	19.4	1194.0	54.4	1194.0	54.4	95.5
P1080-92	142	115168	2.1	12.5037	0.5	2.1953	1.1	0.1991	0.9	0.87	1170.4	10.0	1179.5	7.5	1196.4	10.5	1196.4	10.5	97.8
P1080-74	109	162383	1.9	12.3460	1.2	2.2388	2.2	0.2005	1.9	0.84	1177.8	20.3	1193.3	15.8	1221.4	24.0	1221.4	24.0	96.4
P1080-82	163	104570	1.7	12.2435	0.6	2.3270	0.9	0.2066	0.7	0.73	1210.8	7.6	1220.6	6.7	1237.8	12.6	1237.8	12.6	97.8
P1080-95	63	26281	2.3	12.2417	1.7	2.2016	3.2	0.1955	2.7	0.85	1150.9	28.3	1181.5	22.1	1238.1	32.7	1238.1	32.7	93.0
P1080-3	468	381945	1.6	11.9201	0.2	2.5065	1.1	0.2167	1.0	0.97	1264.4	11.8	1273.9	7.7	1290.0	4.7	1290.0	4.7	98.0
P1080-48	177	99206	1.9	11.7373	0.6	2.6889	1.5	0.2289	1.3	0.91	1328.7	16.1	1325.4	10.9	1320.0	11.9	1320.0	11.9	100.7
P1080-52	57	35515	1.7	11.6906	1.8	2.7799	2.1	0.2357	1.1	0.52	1364.3	13.5	1350.2	15.6	1327.8	34.4	1327.8	34.4	102.8
P1080-14	574	62543	1.8	11.6484	0.7	2.4958	1.3	0.2108	1.1	0.84	1233.3	12.2	1270.8	9.4	1334.8	13.5	1334.8	13.5	92.4
P1080-89	119	72210	1.7	11.3323	0.9	2.8169	2.2	0.2315	2.0	0.91	1342.5	24.1	1360.0	16.3	1387.8	17.2	1387.8	17.2	96.7
P1080-32	55	48675	1.9	11.3213	2.3	2.9335	2.4	0.2409	0.7	0.29	1391.2	8.7	1390.6	18.1	1389.6	44.0	1389.6	44.0	100.1
P1080-50	178	102573	2.5	10.9463	0.5	3.1614	1.2	0.2510	1.1	0.89	1443.5	14.1	1447.8	9.4	1454.0	10.4	1454.0	10.4	99.3
P1080-27	141	295014	2.2	10.7370	0.5	3.3681	1.2	0.2623	1.1	0.92	1501.5	14.9	1497.0	9.4	1490.6	8.7	1490.6	8.7	100.7
P1080-6	53	56364	0.7	9.9902	1.3	4.0412	1.6	0.2928	0.9	0.58	1655.5	13.5	1642.5	12.9	1625.9	24.0	1625.9	24.0	101.8
P1080-87	108	65282	2.0	9.9033	1.2	4.1463	1.5	0.2978	0.9	0.60	1680.4	13.4	1663.5	12.4	1642.1	22.5	1642.1	22.5	102.3
P1080-44	77	55498	0.7	9.7075	0.9	4.2327	1.4	0.2980	1.0	0.74	1681.4	14.8	1680.4	11.1	1679.1	16.9	1679.1	16.9	100.1
P1080-88	110	129211	1.9	8.6467	0.7	5.4553	2.2	0.3421	2.0	0.95	1896.8	33.7	1893.6	18.6	1890.0	12.7	1890.0	12.7	100.4
P1080-11	16	12008	1.2	7.8412	1.4	6.6156	2.0	0.3762	1.5	0.73	2058.6	25.9	2061.4	17.8	2064.2	24.4	2064.2	24.4	99.7
P1080-30	181	312063	1.8	7.5701	0.2	6.8490	1.5	0.3760	1.5	0.99	2057.7	25.9	2092.1	13.1	2126.0	2.9	2126.0	2.9	96.8
P1080-75	41	126131	1.5	7.3963	0.9	7.5951	1.3	0.4074	1.0	0.74	2203.1	17.9	2184.3	11.7	2166.6	15.4	2166.6	15.4	101.7
P1080-65	255	799061	2.0	7.3945	0.4	7.0806	1.6	0.3797	1.5	0.97	2075.0	27.3	2121.6	14.1	2167.0	6.5	2167.0	6.5	95.8
P1080-24	140	165867	0.9	6.7206	0.3	8.3774	0.7	0.4083	0.6	0.87	2207.3	11.3	2272.7	6.3	2332.1	5.8	2332.1	5.8	94.6
P1080-53	36	44381	3.6	6.2277	0.5	10.4143	1.1	0.4704	1.0	0.89	2485.3	19.9	2472.3	10.0	2461.7	8.4	2461.7	8.4	101.0
P1080-13	122	325470	1.4	6.1550	0.4	10.7797	1.1	0.4812	1.0	0.94	2532.5	21.3	2504.3	10.0	2481.5	6.2	2481.5	6.2	102.1

Analysis	U	206Pb	U/Th	206Pb*	±	207Pb*	±	206Pb*	±	error	206Pb*	±	207Pb*	±	206Pb*	±	Best age	±	Conc
	(ppm)	204Pb		207Pb*	(%)	235U*	(%)	238U	(%)	corr.	238U*	(Ma)	235U	(Ma)	207Pb*	(Ma)	(Ma)	(Ma)	(%)
PE-30	284	32353	1.0	19.3038	3.2	0.3302	3.3	0.0462	1.1	0.32	291.4	3.1	289.7	8.4	276.8	72.4	291.4	3.1	NA
PE-73	147	36319	0.8	18.8187	3.4	0.3396	3.7	0.0464	1.4	0.38	292.1	4.0	296.9	9.5	334.7	77.1	292.1	4.0	NA
PE-20	118	18387	1.6	18.7790	5.9	0.3410	6.9	0.0464	3.5	0.51	292.6	10.1	297.9	17.8	339.5	134.2	292.6	10.1	NA
PE-17	110	16815	0.9	19.3562	8.0	0.3322	8.1	0.0466	0.9	0.12	293.9	2.7	291.3	20.4	270.5	183.9	293.9	2.7	NA
PE-47	185	77646	1.5	19.2819	3.7	0.3382	4.1	0.0473	1.9	0.46	297.9	5.6	295.8	10.6	279.4	83.8	297.9	5.6	NA
PE-58	154	33642	1.1	19.0845	3.2	0.3496	3.5	0.0484	1.4	0.41	304.7	4.3	304.4	9.3	302.8	73.4	304.7	4.3	NA
PE-68	40	9403	2.0	19.4752	20.6	0.3480	21.3	0.0492	5.0	0.24	309.3	15.2	303.2	55.8	256.5	479.0	309.3	15.2	NA
PE-93	618	49162	1.0	18.9717	0.9	0.3693	1.4	0.0508	1.1	0.78	319.5	3.4	319.1	3.8	316.3	19.5	319.5	3.4	NA
PE-36	225	37498	2.0	18.0874	2.5	0.5002	2.8	0.0656	1.3	0.46	409.7	5.2	411.9	9.6	423.8	56.4	409.7	5.2	96.7
PE-14	175	30289	0.9	18.3996	2.8	0.4947	2.9	0.0660	0.9	0.31	412.1	3.6	408.1	9.9	385.5	62.8	412.1	3.6	106.9
PE-32	16	3781	0.6	21.4084	55.1	0.4273	55.3	0.0663	4.7	0.08	414.1	18.9	361.2	169.8	34.5	1423.3	414.1	18.9	1201.4
PE-24	112	10754	0.5	18.2579	2.8	0.5152	3.2	0.0682	1.5	0.46	425.4	6.1	421.9	11.0	402.9	63.4	425.4	6.1	105.6

Analysis	U	206Pb	U/Th	206Pb*	±	207Pb*	±	206Pb*	±	error	206Pb*	±	207Pb*	±	206Pb*	±	Best age	±	Conc
	(ppm)	204Pb		207Pb*	(%)	235U*	(%)	238U	(%)	corr.	238U*	(Ma)	235U	(Ma)	207Pb*	(Ma)	(Ma)	(Ma)	(%)
PE-75	133	49525	2.1	17.7109	2.4	0.5370	2.7	0.0690	1.3	0.49	430.0	5.6	436.4	9.7	470.6	52.7	430.0	5.6	91.4
PE-48	390	136482	2.4	18.0351	1.5	0.5298	1.8	0.0693	0.9	0.49	431.9	3.7	431.7	6.2	430.3	34.3	431.9	3.7	100.4
PE-78	373	129448	2.7	17.3077	1.0	0.6767	1.4	0.0849	1.1	0.74	525.6	5.3	524.8	5.9	521.3	21.2	525.6	5.3	100.8
PE-91	100	56238	1.0	17.4302	3.3	0.6794	3.6	0.0859	1.3	0.36	531.2	6.6	526.4	14.7	505.8	73.4	531.2	6.6	105.0
PE-5	57	11090	0.8	16.8476	7.0	0.7067	7.4	0.0863	2.3	0.31	533.9	11.9	542.8	31.1	580.2	152.5	533.9	11.9	92.0
PE-9	47	7358	0.8	17.6062	9.6	0.6887	10.3	0.0879	3.7	0.36	543.3	19.3	532.0	42.5	483.7	211.8	543.3	19.3	112.3
PE-54	55	19511	0.7	17.7460	5.5	0.6869	5.7	0.0884	1.5	0.27	546.1	8.0	530.9	23.6	466.2	121.6	546.1	8.0	117.1
PE-23	81	31830	2.1	17.0591	6.0	0.7185	6.3	0.0889	2.0	0.32	549.0	10.7	549.8	26.8	553.0	130.4	549.0	10.7	99.3
PE-64	39	10015	1.0	16.3627	7.6	0.7517	7.7	0.0892	1.3	0.17	550.8	7.1	569.2	33.6	643.3	163.5	550.8	7.1	85.6
PE-81	81	18253	0.7	17.2267	3.4	0.7143	3.7	0.0892	1.6	0.42	551.1	8.4	547.3	15.8	531.7	74.0	551.1	8.4	103.6
PE-52	86	21911	0.9	17.0565	4.0	0.7222	4.2	0.0893	1.3	0.31	551.6	6.8	552.0	18.0	553.3	87.7	551.6	6.8	99.7
PE-77	86	23678	1.6	17.1612	5.8	0.7197	6.0	0.0896	1.6	0.26	553.1	8.3	550.5	25.6	540.0	127.5	553.1	8.3	102.4
PE-51	40	26050	0.3	16.4300	8.3	0.7530	8.7	0.0897	2.8	0.32	553.9	14.7	570.0	38.0	634.5	177.9	553.9	14.7	87.3
PE-94	179	62374	0.9	16.9749	1.8	0.7341	3.5	0.0904	3.0	0.86	557.7	15.9	558.9	14.9	563.8	38.8	557.7	15.9	98.9
PE-50	151	39021	5.4	17.4151	2.8	0.7210	3.0	0.0911	1.0	0.34	561.8	5.6	551.2	12.8	507.8	62.3	561.8	5.6	110.6
PE-71	41	9276	1.2	17.4174	7.3	0.7267	7.5	0.0918	1.8	0.24	566.2	9.8	554.6	32.2	507.4	161.1	566.2	9.8	111.6
PE-56	65	16847	1.8	17.0001	5.0	0.7459	5.2	0.0920	1.4	0.26	567.2	7.4	565.8	22.5	560.6	109.0	567.2	7.4	101.2
PE-53	118	32347	2.3	17.2406	3.0	0.7395	4.9	0.0925	3.8	0.78	570.1	20.8	562.1	21.0	529.9	66.1	570.1	20.8	107.6
PE-46	102	31053	1.0	16.8994	5.4	0.7569	5.6	0.0928	1.2	0.22	571.9	6.7	572.2	24.3	573.5	117.9	571.9	6.7	99.7
PE-74	111	34451	0.8	16.8228	3.1	0.7610	3.3	0.0929	1.0	0.31	572.4	5.5	574.6	14.4	583.3	67.6	572.4	5.5	98.1
PE-60	93	29626	1.0	16.7186	4.5	0.7703	4.6	0.0934	1.1	0.23	575.7	5.8	580.0	20.4	596.9	97.2	575.7	5.8	96.4
PE-39	26	5341	1.2	17.5901	15.4	0.7518	15.6	0.0959	2.8	0.18	590.4	15.6	569.3	68.2	485.7	341.0	590.4	15.6	121.5
PE-43	22	9896	1.1	17.1430	19.5	0.7730	19.8	0.0961	3.7	0.19	591.6	21.2	581.5	88.0	542.3	429.6	591.6	21.2	109.1
PE-59	92	31540	0.5	17.1051	4.8	0.7758	5.0	0.0962	1.1	0.22	592.3	6.2	583.1	22.0	547.1	105.9	592.3	6.2	108.3
PE-44	39	12950	3.3	16.7936	7.3	0.8121	7.6	0.0989	2.3	0.30	608.1	13.4	603.7	34.8	587.1	158.2	608.1	13.4	103.6
PE-70	252	18645	1.2	16.2058	1.0	0.8438	1.8	0.0992	1.5	0.84	609.6	8.7	621.2	8.3	664.0	20.7	609.6	8.7	91.8
PE-84	90	19527	1.7	16.3852	5.2	0.8496	5.5	0.1010	1.5	0.28	620.1	8.9	624.4	25.4	640.3	112.7	620.1	8.9	96.8
PE-83	108	44310	1.5	16.5995	2.4	0.8441	2.5	0.1016	0.8	0.31	623.9	4.5	621.4	11.5	612.3	51.1	623.9	4.5	101.9
PE-8	171	47697	0.9	16.5423	2.1	0.8472	3.4	0.1016	2.7	0.78	624.0	15.9	623.1	15.9	619.7	45.9	624.0	15.9	100.7
PE-45	99	40524	1.5	16.2320	2.2	0.8640	2.7	0.1017	1.7	0.61	624.4	9.9	632.3	12.8	660.5	46.4	624.4	9.9	94.5
PE-21	96	44118	0.8	16.5796	3.1	0.8476	3.3	0.1019	0.9	0.27	625.6	5.3	623.3	15.2	614.9	67.6	625.6	5.3	101.7
PE-6	145	36758	2.0	16.6896	1.7	0.8456	2.2	0.1024	1.4	0.61	628.2	8.1	622.3	10.3	600.6	37.9	628.2	8.1	104.6
PE-25	43	12605	0.5	16.5653	9.6	0.8521	9.8	0.1024	2.1	0.21	628.3	12.6	625.8	45.8	616.7	206.9	628.3	12.6	101.9
PE-66	69	63527	1.0	15.8288	4.2	0.8973	4.4	0.1030	1.2	0.27	632.1	7.0	650.3	20.9	714.2	89.1	632.1	7.0	88.5
PE-34	168	85447	1.5	16.3230	1.0	0.9004	1.1	0.1066	0.4	0.37	652.9	2.5	651.9	5.2	648.5	21.7	652.9	2.5	100.7
PE-19	217	98276	2.7	15.2747	0.8	1.1741	1.0	0.1301	0.6	0.63	788.2	4.7	788.5	5.5	789.4	16.3	788.2	4.7	99.9
PE-90	117	37415	2.2	15.2498	1.5	1.2411	2.0	0.1373	1.3	0.64	829.2	9.8	819.4	11.0	792.8	31.5	829.2	9.8	104.6
PE-38	166	82275	0.9	14.9770	1.3	1.2839	1.5	0.1395	0.9	0.57	841.6	7.0	838.6	8.8	830.6	26.2	841.6	7.0	101.3
PE-11	55	33828	0.3	14.3197	4.4	1.4710	4.6	0.1528	1.3	0.28	916.5	11.0	918.5	27.9	923.5	91.1	923.5	91.1	99.2

Analysis	U	206Pb	U/Th	206Pb*	±	207Pb*	±	206Pb*	±	error	206Pb*	±	207Pb*	±	206Pb*	±	Best age	±	Conc
	(ppm)	204Pb		207Pb*	(%)	235U*	(%)	238U	(%)	corr.	238U*	(Ma)	235U	(Ma)	207Pb*	(Ma)	(Ma)	(Ma)	(%)
PE-10	202	235460	1.4	14.0134	0.8	1.6144	1.4	0.1641	1.2	0.84	979.4	10.7	975.8	8.8	967.7	15.4	967.7	15.4	101.2
PE-18	429	262494	2.2	13.9379	0.2	1.5680	0.7	0.1585	0.7	0.95	948.4	5.8	957.6	4.3	978.7	4.5	978.7	4.5	96.9
PE-65	163	137406	2.2	13.7172	1.1	1.7094	1.9	0.1701	1.5	0.80	1012.5	14.1	1012.1	12.1	1011.2	22.8	1011.2	22.8	100.1
PE-22	76	59854	3.4	13.5954	1.8	1.8017	2.3	0.1777	1.4	0.60	1054.1	13.3	1046.1	15.0	1029.2	37.2	1029.2	37.2	102.4
PE-27	102	49454	4.3	13.5815	1.5	1.7447	3.1	0.1719	2.7	0.87	1022.3	25.8	1025.2	20.2	1031.3	31.0	1031.3	31.0	99.1
PE-87	76	172889	2.0	13.5447	1.7	1.7795	2.0	0.1748	1.1	0.56	1038.5	10.8	1038.0	13.1	1036.8	34.0	1036.8	34.0	100.2
PE-40	70	40980	1.0	13.4768	3.0	1.7929	3.3	0.1752	1.2	0.38	1040.9	11.9	1042.9	21.4	1047.0	61.3	1047.0	61.3	99.4
PE-85	145	86386	2.1	13.3426	0.9	1.9275	1.1	0.1865	0.7	0.62	1102.5	6.9	1090.7	7.3	1067.1	17.2	1067.1	17.2	103.3
PE-98	93	102378	2.7	12.8476	1.7	2.1042	2.0	0.1961	1.0	0.50	1154.2	10.3	1150.2	13.6	1142.7	34.1	1142.7	34.1	101.0
PE-2	130	68126	1.5	12.6204	0.9	2.1653	1.6	0.1982	1.3	0.81	1165.6	14.2	1170.0	11.4	1178.1	18.8	1178.1	18.8	98.9
PE-1	71	3561	1.0	12.5697	2.5	2.1273	3.0	0.1939	1.8	0.58	1142.6	18.4	1157.7	20.9	1186.0	48.7	1186.0	48.7	96.3
PE-15	91	96461	1.8	12.5012	1.8	2.2152	1.9	0.2008	0.5	0.28	1179.8	5.9	1185.8	13.5	1196.8	36.5	1196.8	36.5	98.6
PE-100	70	37320	1.9	12.4556	1.8	2.2239	3.0	0.2009	2.4	0.80	1180.2	25.7	1188.6	21.0	1204.0	35.7	1204.0	35.7	98.0
PE-49	215	115408	2.7	12.3904	1.0	2.2822	1.2	0.2051	0.7	0.56	1202.6	7.7	1206.8	8.8	1214.3	20.2	1214.3	20.2	99.0
PE-69	442	236589	2.5	12.3472	0.3	2.3192	1.3	0.2077	1.2	0.97	1216.5	13.5	1218.2	8.9	1221.2	5.9	1221.2	5.9	99.6
PE-62	326	169869	3.1	12.3378	0.4	2.2791	1.0	0.2039	0.9	0.92	1196.4	10.1	1205.8	7.1	1222.7	8.0	1222.7	8.0	97.9
PE-3	263	131211	3.8	12.2851	0.4	2.3434	0.9	0.2088	0.8	0.87	1222.4	8.5	1225.6	6.2	1231.1	8.5	1231.1	8.5	99.3
PE-80	193	196639	3.4	12.2150	0.5	2.3900	1.0	0.2117	0.8	0.87	1238.0	9.4	1239.6	6.9	1242.3	9.5	1242.3	9.5	99.7
PE-76	59	35396	1.2	11.9489	2.2	2.6085	2.4	0.2261	1.0	0.43	1313.8	12.2	1303.0	17.6	1285.3	42.1	1285.3	42.1	102.2
PE-31	668	510470	2.5	10.4217	0.2	3.6504	2.5	0.2759	2.5	1.00	1570.8	34.8	1560.6	20.0	1546.8	4.5	1546.8	4.5	101.5
PE-35	344	423610	2.0	9.3526	0.2	4.6335	1.1	0.3143	1.1	0.99	1761.8	17.4	1755.3	9.6	1747.6	3.5	1747.6	3.5	100.8
PE-67	69	159889	1.2	9.1112	0.5	4.8261	0.9	0.3189	0.7	0.82	1784.4	11.4	1789.5	7.5	1795.3	9.2	1795.3	9.2	99.4
PE-33	16	15989	0.1	8.7923	3.2	5.2037	4.5	0.3318	3.2	0.72	1847.3	52.0	1853.2	38.5	1859.9	57.0	1859.9	57.0	99.3
PE-16	268	219225	1.2	8.6889	0.2	5.3250	0.8	0.3356	0.8	0.96	1865.3	13.2	1872.9	7.2	1881.3	4.1	1881.3	4.1	99.2
PE-13	102	164022	0.9	8.6732	0.7	5.3116	1.0	0.3341	0.8	0.76	1858.3	12.5	1870.7	8.6	1884.5	11.7	1884.5	11.7	98.6
PE-89	80	57093	1.1	8.1504	0.6	6.2530	0.9	0.3696	0.7	0.75	2027.7	11.7	2011.9	7.9	1995.7	10.6	1995.7	10.6	101.6
PE-28	31	37503	0.7	7.9959	1.0	6.4478	1.4	0.3739	1.0	0.72	2047.8	17.6	2038.8	12.2	2029.7	17.0	2029.7	17.0	100.9
PE-37	145	45716	1.1	7.9775	0.4	6.4327	0.8	0.3722	0.7	0.89	2039.7	12.0	2036.7	6.8	2033.8	6.2	2033.8	6.2	100.3
PE-99	89	90491	1.9	7.8389	0.9	6.3689	2.4	0.3621	2.2	0.93	1992.1	38.2	2028.0	21.0	2064.7	15.5	2064.7	15.5	96.5
PE-41	58	53738	1.7	7.7564	0.9	6.8400	1.2	0.3848	0.8	0.67	2098.6	14.5	2090.9	10.7	2083.3	15.8	2083.3	15.8	100.7
PE-72	101	162923	2.8	7.6989	0.5	6.3506	1.4	0.3546	1.3	0.94	1956.5	21.8	2025.5	12.0	2096.4	8.0	2096.4	8.0	93.3
PE-7	282	390390	2.1	7.2872	0.5	7.7485	3.1	0.4095	3.0	0.99	2212.7	56.8	2202.2	27.7	2192.5	9.1	2192.5	9.1	100.9
PE-92	70	12226	1.1	7.2187	0.9	7.5501	8.6	0.3953	8.5	0.99	2147.3	155.4	2179.0	76.8	2208.9	14.9	2208.9	14.9	97.2
PE-86	33	58693	0.5	6.6184	0.8	8.4925	1.5	0.4076	1.3	0.86	2204.2	24.6	2285.1	14.0	2358.3	13.6	2358.3	13.6	93.5
PE-96	209	297467	1.5	5.1854	0.2	13.9501	1.7	0.5246	1.7	0.99	2718.8	37.9	2746.3	16.3	2766.6	3.7	2766.6	3.7	98.3

Analysis	U	206Pb	U/Th	206Pb*	±	207Pb*	±	206Pb*	±	error	206Pb*	±	207Pb*	±	206Pb*	±	Best age	±	Conc
	(ppm)	204Pb		207Pb*	(%)	235U*	(%)	238U	(%)	corr.	238U*	(Ma)	235U	(Ma)	207Pb*	(Ma)	(Ma)	(Ma)	(%)
DD-71	41	7168	0.6	22.8864	39.2	0.2728	39.3	0.0453	3.6	0.09	285.5	10.0	244.9	85.8	-127.9	1001.0	285.5	10.0	NA

Analysis	U	206Pb	U/Th	206Pb*	±	207Pb*	±	206Pb*	±	error	206Pb*	±	207Pb*	±	206Pb*	±	Best age	±	Conc
	(ppm)	204Pb		207Pb*	(%)	235U*	(%)	238U	(%)	corr.	238U*	(Ma)	235U	(Ma)	207Pb*	(Ma)	(Ma)	(Ma)	(%)
DD-89	128	17515	0.6	19.3546	8.4	0.3402	8.8	0.0478	2.6	0.30	300.7	7.7	297.3	22.7	270.7	193.2	300.7	7.7	NA
DD-84	192	36528	0.6	19.3366	4.0	0.3412	4.1	0.0478	1.0	0.23	301.3	2.8	298.1	10.6	272.8	91.2	301.3	2.8	NA
DD-29	876	216414	1.6	18.9510	0.7	0.3579	1.3	0.0492	1.1	0.87	309.6	3.4	310.7	3.5	318.8	15.0	309.6	3.4	NA
DD-98	93	2102	1.3	18.2696	9.3	0.3722	9.4	0.0493	1.6	0.17	310.4	4.7	321.3	26.0	401.4	208.5	310.4	4.7	NA
DD-28	234	48520	2.2	17.7086	2.5	0.4480	3.5	0.0575	2.4	0.69	360.6	8.4	375.9	10.9	470.9	55.4	360.6	8.4	NA
DD-88	987	7196	0.7	17.1311	0.5	0.4761	3.2	0.0591	3.1	0.99	370.4	11.2	395.4	10.3	543.8	10.1	370.4	11.2	NA
DD-10	213	37680	0.6	17.9444	3.2	0.4972	3.3	0.0647	0.8	0.24	404.2	3.1	409.8	11.1	441.5	70.9	404.2	3.1	91.6
DD-83	351	92505	2.3	17.9881	1.1	0.5109	1.7	0.0667	1.2	0.75	415.9	5.0	419.0	5.7	436.1	24.7	415.9	5.0	95.4
DD-49	224	45096	2.6	18.0678	3.4	0.5197	3.5	0.0681	1.1	0.30	424.7	4.4	425.0	12.3	426.3	75.4	424.7	4.4	99.6
DD-11	320	84454	0.8	17.9401	1.7	0.5298	2.3	0.0689	1.5	0.66	429.7	6.2	431.6	7.9	442.1	38.0	429.7	6.2	97.2
DD-39	152	30750	1.6	17.7843	3.1	0.5531	3.5	0.0713	1.7	0.47	444.2	7.1	447.0	12.8	461.4	69.4	444.2	7.1	96.3
DD-1	236	63026	1.3	17.5845	1.8	0.5924	2.8	0.0756	2.1	0.76	469.5	9.6	472.4	10.5	486.4	39.4	469.5	9.6	96.5
DD-58	811	42897	1.0	16.5659	0.9	0.6566	3.9	0.0789	3.8	0.97	489.5	17.8	512.6	15.6	616.7	19.1	489.5	17.8	79.4
DD-86	281	90647	3.0	17.0234	1.8	0.6589	2.1	0.0814	0.9	0.46	504.2	4.6	514.0	8.3	557.6	39.8	504.2	4.6	90.4
DD-73	104	44675	1.1	13.8205	2.7	0.8419	10.3	0.0844	10.0	0.97	522.3	50.0	620.2	48.0	996.0	54.9	522.3	50.0	52.4
DD-14	195	96557	4.7	17.0133	2.5	0.6988	3.2	0.0862	2.0	0.62	533.2	10.1	538.1	13.5	558.8	55.4	533.2	10.1	95.4
DD-33	733	313104	1.9	16.9888	0.6	0.7037	2.9	0.0867	2.8	0.98	536.0	14.5	541.0	12.1	562.0	14.0	536.0	14.5	95.4
DD-75	80	19454	0.6	16.6331	4.9	0.7211	8.1	0.0870	6.5	0.80	537.7	33.6	551.3	34.7	607.9	105.6	537.7	33.6	88.5
DD-3	201	133302	5.5	17.2829	1.7	0.6959	2.0	0.0872	1.1	0.52	539.1	5.4	536.3	8.3	524.5	37.4	539.1	5.4	102.8
DD-74	393	235962	1.3	16.9842	1.2	0.7111	2.4	0.0876	2.1	0.88	541.3	11.1	545.4	10.3	562.6	25.5	541.3	11.1	96.2
DD-79	70	28148	0.5	16.6713	5.0	0.7279	5.2	0.0880	1.2	0.23	543.8	6.1	555.3	22.1	603.0	109.1	543.8	6.1	90.2
DD-46	461	114315	0.7	17.1631	1.1	0.7077	1.4	0.0881	0.8	0.60	544.2	4.4	543.4	5.9	539.7	24.6	544.2	4.4	100.8
DD-69	153	73244	1.1	17.1201	2.1	0.7147	2.5	0.0887	1.4	0.54	548.1	7.2	547.5	10.8	545.2	46.9	548.1	7.2	100.5
DD-34	382	80902	0.8	17.0560	0.9	0.7329	2.1	0.0907	1.9	0.89	559.5	10.0	558.3	9.0	553.4	20.6	559.5	10.0	101.1
DD-70	89	33089	0.9	16.7560	4.2	0.7507	4.9	0.0912	2.5	0.51	562.8	13.3	568.7	21.2	592.0	91.1	562.8	13.3	95.1
DD-50	148	31900	1.7	17.3645	2.2	0.7256	3.0	0.0914	2.1	0.68	563.7	11.2	554.0	13.0	514.1	48.7	563.7	11.2	109.6
DD-76	52	15358	1.1	16.3785	5.7	0.7820	6.0	0.0929	1.8	0.29	572.6	9.6	586.6	26.6	641.2	122.8	572.6	9.6	89.3
DD-64	148	49837	1.5	16.7064	3.1	0.7680	3.7	0.0931	2.1	0.55	573.6	11.3	578.6	16.4	598.4	67.2	573.6	11.3	95.9
DD-56	511	147827	0.6	16.8231	0.6	0.7740	1.5	0.0944	1.4	0.91	581.8	7.6	582.1	6.7	583.3	13.8	581.8	7.6	99.7
DD-42	29	13768	1.1	17.4524	10.8	0.7596	11.1	0.0962	2.4	0.22	591.8	13.7	573.8	48.8	503.0	239.3	591.8	13.7	117.6
DD-37	98	18920	3.2	16.6851	4.5	0.7952	4.9	0.0962	1.8	0.38	592.2	10.4	594.1	21.8	601.2	97.2	592.2	10.4	98.5
DD-55	226	57045	1.2	16.8117	1.6	0.7967	2.4	0.0971	1.8	0.76	597.6	10.4	595.0	10.8	584.8	34.1	597.6	10.4	102.2
DD-66	289	145976	2.0	16.5852	1.1	0.8086	1.9	0.0973	1.5	0.81	598.4	8.7	601.7	8.5	614.2	23.9	598.4	8.7	97.4
DD-81	110	38699	59.9	16.3914	3.4	0.8210	3.5	0.0976	0.8	0.22	600.3	4.4	608.6	16.1	639.5	73.7	600.3	4.4	93.9
DD-96	176	58002	1.9	16.8795	1.6	0.8027	1.7	0.0983	0.7	0.39	604.3	3.9	598.4	7.9	576.0	35.0	604.3	3.9	104.9
DD-43	150	42963	1.4	16.5721	1.9	0.8182	2.3	0.0983	1.2	0.53	604.7	6.9	607.1	10.3	615.9	41.5	604.7	6.9	98.2
DD-67	255	165153	0.7	16.4367	1.0	0.8393	2.9	0.1001	2.7	0.93	614.7	15.9	618.8	13.5	633.6	22.6	614.7	15.9	97.0
DD-8	274	106513	4.0	16.5783	1.1	0.8336	1.3	0.1002	0.7	0.51	615.8	4.0	615.6	6.1	615.0	24.7	615.8	4.0	100.1
DD-95	165	63311	0.8	16.7185	1.0	0.8363	1.3	0.1014	0.9	0.63	622.6	5.0	617.1	6.2	596.9	22.5	622.6	5.0	104.3

Analysis	U	206Pb	U/Th	206Pb*	±	207Pb*	±	206Pb*	±	error	206Pb*	±	207Pb*	±	206Pb*	±	Best age	±	Conc
	(ppm)	204Pb		207Pb*	(%)	235U*	(%)	238U	(%)	corr.	238U*	(Ma)	235U	(Ma)	207Pb*	(Ma)	(Ma)	(Ma)	(%)
DD-62	48	17963	1.4	16.5088	6.7	0.8583	7.1	0.1028	2.4	0.34	630.6	14.2	629.2	33.2	624.1	143.7	630.6	14.2	101.0
DD-23	77	48850	0.6	16.1323	3.9	0.9008	4.0	0.1054	0.9	0.24	646.0	5.8	652.2	19.2	673.7	83.0	646.0	5.8	95.9
DD-22	110	24128	1.5	16.2632	2.4	0.8981	3.0	0.1059	1.7	0.57	649.1	10.3	650.7	14.2	656.4	52.5	649.1	10.3	98.9
DD-19	240	78437	3.3	15.4158	1.5	1.0092	4.4	0.1128	4.1	0.94	689.2	27.0	708.5	22.4	770.1	31.0	689.2	27.0	89.5
DD-52	32	9639	1.6	14.9843	7.8	1.0505	8.2	0.1142	2.5	0.30	696.9	16.4	729.1	42.8	829.6	163.6	696.9	16.4	84.0
DD-85	174	159299	0.8	15.5884	1.4	1.1052	1.7	0.1250	1.0	0.57	759.0	6.9	755.9	9.1	746.6	29.7	759.0	6.9	101.7
DD-45	990	27550	7.3	14.4636	0.5	1.2046	0.9	0.1264	0.8	0.81	767.1	5.4	802.7	5.2	902.9	11.3	767.1	5.4	85.0
DD-78	29	50943	2.2	13.7862	5.7	1.6225	6.2	0.1622	2.4	0.39	969.2	21.6	979.0	38.9	1001.0	116.1	1001.0	116.1	96.8
DD-20	778	40302	23.1	13.7478	2.2	1.4859	2.9	0.1482	1.9	0.66	890.6	15.7	924.6	17.5	1006.7	44.1	1006.7	44.1	88.5
DD-44	162	79842	1.7	13.6372	1.0	1.8215	1.3	0.1802	0.9	0.65	1067.8	8.4	1053.2	8.6	1023.0	20.0	1023.0	20.0	104.4
DD-59	120	49864	2.4	13.6151	1.2	1.7194	2.7	0.1698	2.4	0.89	1010.9	22.1	1015.8	17.1	1026.3	24.8	1026.3	24.8	98.5
DD-5	161	42846	2.5	13.5551	0.8	1.7117	1.3	0.1683	1.0	0.78	1002.6	9.1	1012.9	8.0	1035.3	15.9	1035.3	15.9	96.8
DD-47	84	32932	1.3	13.4857	1.9	1.8125	2.6	0.1773	1.7	0.65	1052.1	16.2	1050.0	16.7	1045.6	38.9	1045.6	38.9	100.6
DD-15	769	535982	2.7	13.4822	0.2	1.7894	1.0	0.1750	1.0	0.98	1039.4	9.3	1041.6	6.4	1046.2	3.6	1046.2	3.6	99.4
DD-7	71	45403	1.7	13.3506	2.1	1.9042	2.4	0.1844	1.2	0.48	1090.9	11.6	1082.6	16.0	1065.9	42.3	1065.9	42.3	102.3
DD-65	143	76138	1.7	13.2405	0.8	1.8946	1.7	0.1819	1.5	0.89	1077.6	15.1	1079.2	11.3	1082.5	15.5	1082.5	15.5	99.5
DD-91	43	53625	2.1	13.0694	2.1	1.9951	2.8	0.1891	1.9	0.67	1116.6	19.5	1113.9	19.3	1108.5	42.2	1108.5	42.2	100.7
DD-4	55	19301	1.4	12.6878	3.0	2.1362	3.4	0.1966	1.6	0.46	1156.9	16.6	1160.6	23.6	1167.5	59.9	1167.5	59.9	99.1
DD-36	143	39020	3.6	12.6168	1.5	2.0136	2.2	0.1843	1.6	0.72	1090.2	15.8	1120.1	14.9	1178.6	30.3	1178.6	30.3	92.5
DD-17	343	139597	4.1	12.6136	0.4	2.1709	1.2	0.1986	1.1	0.93	1167.8	11.6	1171.8	8.1	1179.1	8.5	1179.1	8.5	99.0
DD-38	69	32181	2.0	12.4632	1.4	2.3202	2.6	0.2097	2.1	0.83	1227.4	23.8	1218.5	18.1	1202.8	27.8	1202.8	27.8	102.0
DD-25	160	119392	2.0	12.4523	0.9	2.2297	2.5	0.2014	2.4	0.94	1182.7	25.6	1190.4	17.7	1204.5	17.5	1204.5	17.5	98.2
DD-99	140	80858	1.6	12.3129	1.0	2.3817	1.3	0.2127	0.8	0.63	1243.1	9.5	1237.1	9.5	1226.6	20.2	1226.6	20.2	101.3
DD-31	356	18366	1.7	12.0095	1.2	2.0939	2.2	0.1824	1.9	0.85	1080.0	18.8	1146.8	15.4	1275.5	23.1	1275.5	23.1	84.7
DD-48	46	48195	1.7	11.9608	3.7	2.4681	8.6	0.2141	7.7	0.90	1250.6	88.0	1262.7	62.1	1283.4	72.1	1283.4	72.1	97.4
DD-97	28	92310	0.9	11.8223	3.6	2.6638	3.8	0.2284	1.2	0.31	1326.1	14.2	1318.5	28.3	1306.0	70.8	1306.0	70.8	101.5
DD-82	77	63196	1.4	11.7424	1.0	2.6982	2.1	0.2298	1.9	0.89	1333.4	22.9	1328.0	15.9	1319.2	19.1	1319.2	19.1	101.1
DD-54	193	181092	0.8	11.1493	0.5	3.1056	1.6	0.2511	1.5	0.94	1444.3	18.9	1434.1	12.0	1419.0	10.2	1419.0	10.2	101.8
DD-24	91	168723	1.3	10.9524	1.1	3.1942	1.7	0.2537	1.3	0.75	1457.7	16.5	1455.8	13.2	1452.9	21.6	1452.9	21.6	100.3
DD-90	120	139617	0.6	10.0036	0.4	3.9762	1.4	0.2885	1.4	0.97	1633.9	19.5	1629.3	11.3	1623.4	6.6	1623.4	6.6	100.7
DD-94	670	688529	52.4	7.9022	0.2	5.8370	1.5	0.3345	1.5	0.99	1860.3	23.4	1951.9	12.6	2050.5	2.8	2050.5	2.8	90.7
DD-61	152	41558	1.1	7.8128	0.4	5.7212	0.8	0.3242	0.7	0.89	1810.2	11.3	1934.6	6.9	2070.6	6.4	2070.6	6.4	87.4
DD-6	506	801176	10.5	7.7113	0.1	6.4277	1.1	0.3595	1.1	0.99	1979.7	18.4	2036.1	9.6	2093.6	2.2	2093.6	2.2	94.6
DD-32	79	94808	1.1	7.6867	0.5	7.0060	2.9	0.3906	2.8	0.98	2125.5	50.9	2112.2	25.4	2099.2	8.8	2099.2	8.8	101.3
DD-80	163	207072	0.5	7.6714	0.4	6.7214	0.9	0.3740	0.8	0.92	2048.0	14.8	2075.4	8.1	2102.7	6.5	2102.7	6.5	97.4
DD-12	228	230212	2.2	7.6480	0.6	6.5485	4.8	0.3632	4.8	0.99	1997.5	82.5	2052.4	42.7	2108.1	10.5	2108.1	10.5	94.8
DD-63	379	403355	1.4	7.5855	0.1	6.8853	1.8	0.3788	1.8	1.00	2070.7	32.0	2096.8	16.0	2122.5	2.4	2122.5	2.4	97.6
DD-77	88	239720	2.2	7.5258	0.4	7.4213	1.4	0.4051	1.3	0.95	2192.3	23.9	2163.5	12.1	2136.3	7.3	2136.3	7.3	102.6
DD-53	190	238212	2.8	7.4582	0.4	6.7809	1.2	0.3668	1.2	0.95	2014.3	20.0	2083.2	10.8	2152.1	6.7	2152.1	6.7	93.6

Analysis	U	206Pb	U/Th	206Pb*	±	207Pb*	±	206Pb*	±	error	206Pb*	±	207Pb*	±	206Pb*	±	Best age	±	Conc
	(ppm)	204Pb		207Pb*	(%)	235U*	(%)	238U	(%)	corr.	238U*	(Ma)	235U	(Ma)	207Pb*	(Ma)	(Ma)	(Ma)	(%)
DD-68	46	156380	1.1	7.2768	1.9	6.9429	5.5	0.3664	5.2	0.94	2012.5	89.4	2104.2	48.9	2195.0	32.8	2195.0	32.8	91.7
DD-16	110	83122	2.3	7.2672	0.4	7.5221	1.6	0.3965	1.6	0.97	2152.7	28.7	2175.6	14.5	2197.3	7.3	2197.3	7.3	98.0
DD-41	121	93308	8.0	6.2948	0.1	9.7730	1.3	0.4462	1.3	0.99	2378.3	26.3	2413.6	12.3	2443.6	2.4	2443.6	2.4	97.3
DD-92	368	388199	1.2	5.5942	0.1	11.8988	1.7	0.4828	1.7	1.00	2539.3	36.1	2596.5	16.1	2641.3	1.6	2641.3	1.6	96.1
DD-13	32	63846	0.6	5.3856	0.6	13.1981	1.4	0.5155	1.3	0.90	2680.1	28.6	2693.9	13.7	2704.3	10.4	2704.3	10.4	99.1
DD-35	795	823656	1.1	4.2373	1.0	16.4210	2.5	0.5046	2.2	0.91	2633.7	48.1	2901.6	23.5	3093.2	16.6	3093.2	16.6	85.1

Analysis	U	206Pb	U/Th	206Pb*	±	207Pb*	±	206Pb*	±	error	206Pb*	±	207Pb*	±	206Pb*	±	Best age	±	Conc
	(ppm)	204Pb		207Pb*	(%)	235U*	(%)	238U	(%)	corr.	238U*	(Ma)	235U	(Ma)	207Pb*	(Ma)	(Ma)	(Ma)	(%)
STPB-57	859	188233	3.2	17.1581	0.6	0.6948	1.1	0.0865	1.0	0.87	534.6	5.0	535.7	4.7	540.4	12.3	534.6	5.0	98.9
STPB-11	29	6798	0.8	16.8295	15.4	0.7103	17.1	0.0867	7.6	0.44	536.0	39.1	544.9	72.4	582.5	335.5	536.0	39.1	92.0
STPB-61	73	16375	0.9	16.9853	5.8	0.7047	6.3	0.0868	2.3	0.37	536.6	12.0	541.6	26.4	562.4	127.1	536.6	12.0	95.4
STPB-69	239	71580	0.9	16.9106	2.1	0.7080	3.0	0.0868	2.1	0.71	536.8	11.0	543.5	12.7	572.0	46.2	536.8	11.0	93.8
STPB-72	47	19400	0.8	18.2862	10.1	0.6571	10.2	0.0871	1.7	0.17	538.6	9.0	512.8	41.1	399.4	226.1	538.6	9.0	134.9
STPB-83	76	38499	0.7	17.2558	7.4	0.6985	7.6	0.0874	1.8	0.23	540.3	9.2	537.9	31.7	528.0	162.2	540.3	9.2	102.3
STPB-49	205	33362	1.2	16.5403	6.5	0.7349	6.6	0.0882	1.0	0.16	544.6	5.4	559.4	28.3	620.0	140.1	544.6	5.4	87.8
STPB-2	16	5063	0.6	17.6239	19.2	0.6912	20.0	0.0884	5.6	0.28	545.8	29.3	533.5	83.2	481.5	428.0	545.8	29.3	113.4
STPB-5	303	48215	0.9	17.0183	1.1	0.7169	1.8	0.0885	1.4	0.78	546.6	7.4	548.8	7.7	558.2	24.6	546.6	7.4	97.9
STPB-44	267	57936	1.3	17.3495	1.8	0.7040	2.1	0.0886	1.2	0.54	547.1	6.1	541.2	9.0	516.0	39.4	547.1	6.1	106.0
STPB-39	120	37656	0.7	16.9720	5.6	0.7230	5.8	0.0890	1.8	0.31	549.6	9.5	552.4	24.9	564.1	121.1	549.6	9.5	97.4
STPB-80	90	19603	2.8	17.5723	4.9	0.6994	5.0	0.0891	1.3	0.26	550.5	7.0	538.5	21.1	487.9	107.4	550.5	7.0	112.8
STPB-67	129	23076	0.6	16.3324	10.9	0.7552	11.8	0.0895	4.6	0.39	552.3	24.2	571.2	51.6	647.3	234.3	552.3	24.2	85.3
STPB-79	30	8049	2.0	16.8551	16.3	0.7333	16.4	0.0896	1.9	0.11	553.4	9.8	558.5	70.6	579.2	356.2	553.4	9.8	95.5
STPB-74	252	23809	1.1	16.3466	4.3	0.7568	4.6	0.0897	1.6	0.35	553.9	8.6	572.2	20.3	645.4	93.2	553.9	8.6	85.8
STPB-65	167	77434	1.1	17.4227	2.3	0.7108	2.4	0.0898	0.6	0.24	554.5	3.0	545.2	10.0	506.8	50.3	554.5	3.0	109.4
STPB-34	99	71106	5.6	17.2791	5.4	0.7176	5.6	0.0899	1.5	0.27	555.2	8.0	549.3	23.6	525.0	117.7	555.2	8.0	105.8
STPB-35	120	49539	5.6	17.1007	4.0	0.7274	4.1	0.0902	0.9	0.22	556.8	4.8	555.0	17.6	547.7	87.8	556.8	4.8	101.7
STPB-1	132	24426	1.8	17.0305	1.9	0.7309	2.5	0.0903	1.6	0.63	557.2	8.3	557.1	10.6	556.6	41.8	557.2	8.3	100.1
STPB-91	40	8883	0.8	16.7837	8.3	0.7417	8.7	0.0903	2.6	0.30	557.2	13.9	563.4	37.7	588.4	180.6	557.2	13.9	94.7
STPB-55	87	24889	1.5	17.2849	2.9	0.7203	3.2	0.0903	1.3	0.41	557.3	7.0	550.9	13.5	524.2	63.6	557.3	7.0	106.3
STPB-89	43	8828	1.2	17.1970	10.8	0.7242	10.9	0.0903	1.3	0.12	557.4	6.8	553.1	46.4	535.4	236.7	557.4	6.8	104.1
STPB-62	147	121474	0.7	16.9447	3.1	0.7352	3.2	0.0904	0.6	0.18	557.6	3.1	559.6	13.7	567.7	68.2	557.6	3.1	98.2
STPB-86	218	105775	0.8	17.3109	1.6	0.7213	2.7	0.0906	2.1	0.80	558.8	11.4	551.4	11.3	520.9	35.0	558.8	11.4	107.3
STPB-47	45	9519	1.3	17.4736	5.9	0.7149	7.0	0.0906	3.7	0.53	559.1	19.8	547.6	29.5	500.4	130.3	559.1	19.8	111.7
STPB-78	133	39681	1.4	16.7973	2.1	0.7453	2.6	0.0908	1.5	0.58	560.2	8.3	565.5	11.4	586.7	46.4	560.2	8.3	95.5
STPB-10	162	44647	0.9	16.8139	2.4	0.7461	3.1	0.0910	2.0	0.65	561.3	10.9	566.0	13.5	584.5	51.2	561.3	10.9	96.0
STPB-85	112	33585	6.3	17.1494	4.3	0.7320	4.6	0.0910	1.6	0.34	561.7	8.5	557.7	19.8	541.5	94.9	561.7	8.5	103.7
STPB-27	145	31154	1.0	17.5396	2.8	0.7158	3.0	0.0911	1.1	0.35	561.8	5.8	548.2	12.9	492.1	62.7	561.8	5.8	114.2
STPB-52	127	33111	1.5	17.4831	4.2	0.7189	4.4	0.0912	1.3	0.30	562.4	7.1	550.0	18.7	499.2	92.7	562.4	7.1	112.7

Analysis	U	206Pb	U/Th	206Pb*	±	207Pb*	±	206Pb*	±	error	206Pb*	±	207Pb*	±	206Pb*	±	Best age	±	Conc
	(ppm)	204Pb		207Pb*	(%)	235U*	(%)	238U	(%)	corr.	238U*	(Ma)	235U	(Ma)	207Pb*	(Ma)	(Ma)	(Ma)	(%)
STPB-62	140	32753	1.2	17.2315	2.1	0.7303	2.2	0.0913	0.8	0.34	563.1	4.1	556.8	9.6	531.0	46.1	563.1	4.1	106.0
STPB-76	22	6183	0.6	19.9712	17.4	0.6310	17.9	0.0914	3.9	0.22	563.8	20.8	496.7	70.3	198.3	407.7	563.8	20.8	284.3
STPB-21	574	18591	2.5	16.0143	0.6	0.7873	1.9	0.0914	1.8	0.95	564.1	9.8	589.7	8.6	689.3	13.0	564.1	9.8	81.8
STPB-45	147	29967	0.7	17.1322	2.5	0.7370	2.7	0.0916	1.0	0.38	564.8	5.5	560.6	11.5	543.7	53.9	564.8	5.5	103.9
STPB-68	47	11136	1.4	17.9856	9.9	0.7046	10.1	0.0919	2.3	0.22	566.8	12.2	541.5	42.5	436.4	220.0	566.8	12.2	129.9
STPB-38	94	32698	0.9	16.5661	2.3	0.7664	2.9	0.0921	1.8	0.61	567.9	9.7	577.7	12.8	616.6	49.6	567.9	9.7	92.1
STPB-100	25	5478	1.2	15.8417	10.7	0.8037	11.4	0.0923	4.0	0.35	569.4	21.6	598.9	51.7	712.4	228.0	569.4	21.6	79.9
STPB-99	192	108527	0.9	16.7272	1.3	0.7656	1.8	0.0929	1.3	0.71	572.6	7.1	577.3	8.1	595.7	28.2	572.6	7.1	96.1
STPB-22	35	9359	1.2	16.7356	7.8	0.7686	8.5	0.0933	3.4	0.40	575.0	18.6	579.0	37.4	594.6	168.6	575.0	18.6	96.7
STPB-64	137	23444	1.5	16.8654	2.5	0.7631	4.1	0.0933	3.3	0.79	575.2	18.0	575.8	18.1	577.9	54.3	575.2	18.0	99.5
STPB-51	164	42004	0.8	17.1681	2.4	0.7529	2.6	0.0937	1.2	0.45	577.6	6.6	569.9	11.5	539.1	51.6	577.6	6.6	107.2
STPB-7	78	42709	0.7	16.6035	3.8	0.7800	4.8	0.0939	3.0	0.62	578.7	16.7	585.5	21.6	611.8	82.1	578.7	16.7	94.6
STPB-31	84	27001	1.2	17.4940	2.4	0.7449	2.7	0.0945	1.3	0.47	582.1	7.0	565.2	11.6	497.8	52.2	582.1	7.0	116.9
STPB-29	93	17670	1.5	17.3735	4.6	0.7500	4.8	0.0945	1.3	0.28	582.1	7.4	568.2	20.9	513.0	101.3	582.1	7.4	113.5
STPB-90	89	29610	1.5	16.6100	2.9	0.7863	3.3	0.0947	1.6	0.49	583.4	9.2	589.1	15.0	610.9	62.9	583.4	9.2	95.5
STPB-23	103	33778	2.3	16.5949	3.0	0.8075	8.3	0.0972	7.7	0.93	597.9	44.2	601.1	37.6	612.9	63.9	597.9	44.2	97.6
STPB-71	172	24830	1.5	16.7153	1.4	0.8043	2.2	0.0975	1.7	0.77	599.7	9.7	599.2	9.9	597.3	30.4	599.7	9.7	100.4
STPB-43	82	52577	0.9	16.6554	4.9	0.8117	5.1	0.0981	1.4	0.28	603.0	8.1	603.4	23.0	605.0	105.1	603.0	8.1	99.7
STPB-12	381	132660	5.1	16.5901	0.9	0.8323	1.2	0.1001	0.7	0.61	615.3	4.1	614.9	5.3	613.5	19.9	615.3	4.1	100.3
STPB-59	168	62328	0.9	16.7489	1.5	0.8264	2.2	0.1004	1.6	0.73	616.7	9.4	611.6	10.0	592.9	32.3	616.7	9.4	104.0
STPB-50	50	12566	1.0	16.4845	5.6	0.8440	6.1	0.1009	2.3	0.38	619.7	13.7	621.4	28.2	627.3	120.6	619.7	13.7	98.8
STPB-93	188	27590	0.8	15.5818	8.1	0.9004	8.3	0.1018	2.0	0.24	624.7	11.8	651.9	40.1	747.5	171.2	624.7	11.8	83.6
STPB-75	65	32507	1.4	16.6710	4.6	0.8452	5.0	0.1022	1.9	0.39	627.2	11.6	622.0	23.0	603.0	98.6	627.2	11.6	104.0
STPB-42	61	19309	1.1	16.4966	4.3	0.8591	4.5	0.1028	1.3	0.29	630.8	8.0	629.7	21.3	625.7	93.6	630.8	8.0	100.8
STPB-14	209	81187	1.3	16.2312	1.4	0.8838	1.6	0.1040	0.8	0.47	638.0	4.6	643.0	7.7	660.6	30.7	638.0	4.6	96.6
STPB-41	236	55651	1.3	16.4466	1.6	0.8755	2.1	0.1044	1.4	0.65	640.3	8.4	638.5	10.0	632.3	34.3	640.3	8.4	101.3
STPB-9	148	62693	1.5	16.3257	2.0	0.8860	2.3	0.1049	1.1	0.47	643.1	6.5	644.2	10.8	648.2	43.0	643.1	6.5	99.2
STPB-82	393	100906	4.8	16.5200	0.9	0.8791	1.8	0.1053	1.6	0.88	645.6	9.9	640.5	8.6	622.6	18.4	645.6	9.9	103.7
STPB-37	101	29970	1.9	16.4784	3.4	0.8813	3.7	0.1053	1.4	0.38	645.6	8.6	641.7	17.4	628.1	72.9	645.6	8.6	102.8
STPB-94	368	83233	1.8	16.3585	1.4	0.8929	1.7	0.1059	1.1	0.60	649.1	6.5	647.9	8.4	643.8	30.0	649.1	6.5	100.8
STPB-87	135	42631	0.8	16.1630	3.3	0.9061	3.8	0.1062	1.9	0.50	650.8	12.0	655.0	18.5	669.6	71.0	650.8	12.0	97.2
STPB-6	169	23443	1.5	15.0745	2.1	1.2284	4.8	0.1343	4.4	0.90	812.3	33.4	813.6	27.1	817.1	43.0	812.3	33.4	99.4
STPB-17	154	103469	1.2	14.2051	0.8	1.5351	1.1	0.1582	0.7	0.66	946.5	6.2	944.6	6.6	939.9	16.5	939.9	16.5	100.7
STPB-46	138	136035	1.1	13.8932	1.3	1.5668	1.6	0.1579	0.9	0.56	945.0	7.8	957.2	9.9	985.3	26.9	985.3	26.9	95.9
STPB-36	53	47293	2.3	12.9352	3.7	1.9988	7.8	0.1875	6.9	0.88	1107.9	70.2	1115.1	53.0	1129.1	73.3	1129.1	73.3	98.1
STPB-56	124	79273	3.1	12.8092	1.2	2.0141	2.2	0.1871	1.8	0.83	1105.7	18.3	1120.3	14.7	1148.6	23.9	1148.6	23.9	96.3
STPB-28	122	93506	1.5	12.3220	0.8	2.4223	1.9	0.2165	1.7	0.90	1263.2	19.5	1249.2	13.5	1225.2	15.7	1225.2	15.7	103.1
STPB-95	164	96791	2.1	12.2323	1.0	2.3937	1.3	0.2124	0.8	0.60	1241.4	8.6	1240.7	9.1	1239.5	19.9	1239.5	19.9	100.1
STPB-40	88	70169	2.4	12.2098	1.0	2.4476	2.1	0.2167	1.9	0.89	1264.6	21.9	1256.7	15.4	1243.2	18.7	1243.2	18.7	101.7

Analysis	U	206Pb	U/Th	206Pb*	±	207Pb*	±	206Pb*	±	error	206Pb*	±	207Pb*	±	206Pb*	±	Best age	±	Conc
	(ppm)	204Pb		207Pb*	(%)	235U*	(%)	238U	(%)	corr.	238U*	(Ma)	235U	(Ma)	207Pb*	(Ma)	(Ma)	(Ma)	(%)
STPB-66	60	40051	2.6	11.5465	1.6	2.7218	3.3	0.2279	2.9	0.87	1323.6	34.2	1334.4	24.4	1351.7	31.2	1351.7	31.2	97.9
STPB-97	254	252052	2.3	11.5061	0.4	2.8467	0.9	0.2376	0.8	0.89	1374.0	9.6	1367.9	6.5	1358.5	7.6	1358.5	7.6	101.1
STPB-84	47	32945	1.2	9.1082	1.5	4.8731	1.7	0.3219	0.9	0.51	1799.1	13.6	1797.6	14.4	1795.9	26.8	1795.9	26.8	100.2
STPB-58	49	25171	0.6	8.3177	1.2	4.5911	2.5	0.2770	2.2	0.88	1576.1	31.2	1747.7	21.1	1959.6	21.1	1959.6	21.1	80.4
STPB-25	46	65375	1.8	8.2535	1.7	5.5930	3.4	0.3348	2.9	0.87	1861.6	47.6	1915.0	29.2	1973.4	29.8	1973.4	29.8	94.3
STPB-81	102	147715	1.6	8.1217	0.8	5.9412	1.4	0.3500	1.2	0.85	1934.4	20.5	1967.3	12.5	2002.0	13.5	2002.0	13.5	96.6
STPB-58	183	125631	2.1	7.9903	1.3	5.9625	3.9	0.3455	3.6	0.94	1913.2	59.9	1970.4	33.5	2030.9	23.3	2030.9	23.3	94.2
STPB-3	108	70956	1.7	7.8960	0.9	5.5940	2.5	0.3204	2.3	0.93	1791.5	36.0	1915.2	21.3	2051.9	16.0	2051.9	16.0	87.3
STPB-70	249	213413	12.5	7.8446	0.4	6.3598	2.9	0.3618	2.9	0.99	1990.9	49.9	2026.7	25.8	2063.4	6.6	2063.4	6.6	96.5
STPB-32	201	101678	0.9	7.6703	0.3	6.9457	1.0	0.3864	0.9	0.94	2106.1	16.0	2104.5	8.5	2103.0	5.9	2103.0	5.9	100.1
STPB-96	187	303619	1.0	7.6536	0.3	6.7918	2.0	0.3770	1.9	0.99	2062.3	34.4	2084.7	17.4	2106.8	4.6	2106.8	4.6	97.9
STPB-63	117	115482	0.5	7.5947	0.3	7.0083	1.0	0.3860	0.9	0.96	2104.4	16.8	2112.5	8.6	2120.3	4.6	2120.3	4.6	99.2
STPB-73	19	25149	2.8	7.2577	2.3	7.6876	2.5	0.4047	1.0	0.40	2190.5	18.2	2195.2	22.1	2199.5	39.1	2199.5	39.1	99.6
STPB-53	129	67229	1.3	7.1739	0.4	7.3389	2.8	0.3818	2.7	0.99	2084.9	48.6	2153.6	24.6	2219.7	7.0	2219.7	7.0	93.9
STPB-74	58	174990	1.3	5.4962	0.8	11.7789	2.5	0.4695	2.3	0.94	2481.5	48.0	2587.0	23.1	2670.7	13.6	2670.7	13.6	92.9
STPB-15	265	422944	1.3	5.1712	0.3	14.3367	2.0	0.5377	1.9	0.99	2773.8	43.6	2772.2	18.6	2771.1	4.8	2771.1	4.8	100.1

Appendix 2. Norphlet Formation Sandstone Composition

	Qt	F	L	Qm	F	Lt	Qp	Fpt	Fpu	Fk	Ls	Lv	Lm
P1004													
Total	245	151	5	237	151	13	8	8	63	80	1	0	4
Total/401	0.611	0.377	0.012	0.591	0.377	0.032	0.020	0.020	0.157	0.200	0.002	0.000	0.010
relative %	61.1	37.7	1.2	59.1	37.7	3.2	2.0	2.0	15.7	20.0	0.2	0.0	1.0
P1096													
Total	253	141	6	243	141	16	10	5	57	79	0	0	6
Total/400	0.633	0.353	0.015	0.608	0.353	0.040	0.025	0.013	0.143	0.198	0.000	0.000	0.015
relative %	63.3	35.3	1.5	60.8	35.3	4.0	2.5	1.3	14.3	19.8	0.0	0.0	1.5
P1080													
Total	271	109	20	256	109	35	15	7	55	47	3	0	17
Total/400	0.678	0.273	0.050	0.640	0.273	0.088	0.038	0.018	0.138	0.118	0.008	0.000	0.043
relative %	67.8	27.3	5.0	64.0	27.3	8.8	3.8	1.8	13.8	11.8	0.8	0.0	4.3
OCS-G-6396 17,503 ft.													
Total	308	61	32	283	61	57	25	4	11	46	18	3	11
Total/401	0.768	0.152	0.080	0.706	0.152	0.142	0.062	0.010	0.027	0.115	0.045	0.007	0.027
relative %	76.8	15.2	8.0	70.6	15.2	14.2	6.2	1.0	2.7	11.5	4.5	0.7	2.7
OCS-G-6396 17,586 ft.													
Total	313	56	32	295	56	50	18	3	9	44	12	3	17
Total/401	0.781	0.140	0.080	0.736	0.140	0.125	0.045	0.007	0.022	0.110	0.030	0.007	0.042
relative %	78.1	14.0	8.0	73.6	14.0	12.5	4.5	0.7	2.2	11.0	3.0	0.7	4.2
OCS-G-6396 17,559 ft.													
Total	296	73	31	282	73	45	14	5	10	58	21	1	9
Total/400	0.740	0.183	0.078	0.705	0.183	0.113	0.035	0.013	0.025	0.145	0.053	0.003	0.023
relative %	74.0	18.3	7.8	70.5	18.3	11.3	3.5	1.3	2.5	14.5	5.3	0.3	2.3
OCS-G-6396 17,562 ft.													
Total	310	66	24	300	66	34	10	3	9	54	9	3	12
Total/400	0.775	0.165	0.060	0.750	0.165	0.085	0.025	0.008	0.023	0.135	0.023	0.008	0.030
relative %	77.5	16.5	6.0	75.0	16.5	8.5	2.5	0.8	2.3	13.5	2.3	0.8	3.0

	Qt	F	L	Qm	F	Lt	Qp	Fpt	Fpu	Fk	Ls	Lv	Lm
OCS-G-6406 22,566 ft.													
Total	337	52	13	326	52	24	11	3	14	35	10	0	3
Total/402	0.838	0.129	0.032	0.811	0.129	0.060	0.027	0.007	0.035	0.087	0.025	0.000	0.007
relative %	83.8	12.9	3.2	81.1	12.9	6.0	2.7	0.7	3.5	8.7	2.5	0.0	0.7
OCS-G-6406 22,633 ft.													
Total	336	46	18	317	46	37	19	1	9	36	12	1	5
Total/400	0.840	0.115	0.045	0.793	0.115	0.093	0.048	0.003	0.023	0.090	0.030	0.003	0.013
relative %	84.0	11.5	4.5	79.3	11.5	9.3	4.8	0.3	2.3	9.0	3.0	0.3	1.3
OCS-G-6406 22,687 ft.													
Total	334	57	19	320	57	33	14	1	15	41	14	0	5
Total/410	0.815	0.139	0.046	0.780	0.139	0.080	0.034	0.002	0.037	0.100	0.034	0.000	0.012
relative %	81.5	13.9	4.6	78.0	13.9	8.0	3.4	0.2	3.7	10.0	3.4	0.0	1.2
OCS-G-6406 22,738 ft.													
Total	322	61	17	313	61	26	9	2	16	43	12	0	5
Total/400	0.805	0.153	0.043	0.783	0.153	0.065	0.023	0.005	0.040	0.108	0.030	0.000	0.013
relative %	80.5	15.3	4.3	78.3	15.3	6.5	2.3	0.5	4.0	10.8	3.0	0.0	1.3

Appendix 3. U-Pb Ages within Known Coeval Source Terranes.

Triassic Rifting

Analysis	Best age (Ma)	± (Ma)
PE-57	202.1	16.7
DD-57	199.1	10.7
DD-26	212.1	14.1

Alleghanian (280-325 Ma)

Analysis	Best age (Ma)	± (Ma)
MO-66	293.6	4.2
MO-44	327.1	6.4
P1004-44	283.5	4.2
P1004-10	305.7	8.2
P1080-20	295.7	3.8
P1080-7	296.0	3.2
PE-79	286.4	9.4
PE-55	289.8	4.0
PE-30	291.4	3.1
PE-73	292.1	4.0
PE-20	292.6	10.1
PE-17	293.9	2.7
PE-47	297.9	5.6
PE-58	304.7	4.3
PE-68	309.3	15.2
PE-93	319.5	3.4
DD-51	273.8	5.8
DD-71	285.5	10.0
DD-89	300.7	7.7
DD-84	301.3	2.8
DD-29	309.6	3.4
DD-98	310.4	4.7

Acadian (374-425)

Analysis	Best age (Ma)	± (Ma)	Analysis	Best age (Ma)	± (Ma)
1096-30	375.5	4.4	P1080-57	387.9	8.8
1096-91	377.3	9.1	P1080-81	389.2	3.7
1096-84	379.8	7.4	P1080-38	392.2	22.0
1096-65	390.2	34.2	P1080-86	394.0	9.6
1096-4	412.8	19.0	P1080-9	395.4	5.0
1096-43	424.7	5.0	P1080-64	397.6	9.1
			P1080-96	397.9	15.4
			P1080-12	402.9	18.1
			P1080-71	407.7	5.7
MO-61	376.3	6.3	P1080-84	415.9	4.7
MO- 91	379.5	9.2	P1080-61	418.3	3.5
MO-4	380.6	7.3			
MO-25	390.9	4.6	PE-24	425.4	6.1
MO- 90	394.0	6.1			
MO- 76	394.5	16.3	DD-49	424.7	4.4
MO-7	405.6	3.4			
MO-63	412.8	5.7	P1004-8	376.6	3.5
MO-15	417.0	6.6	P1004-51	406.0	6.4
MO- 80	418.4	4.7	P1004-33	410.4	4.7
MO-48	419.7	4.7	P1004-89	411.5	8.9
MO- 88	422.2	8.3	P1004-55	416.5	8.2
MO- 100	422.7	4.2	P1004-74	425.0	5.5

Taconic (430-480 Ma)

Analysis	Best age (Ma)	± (Ma)	Analysis	Best age (Ma)	± (Ma)
1096-29	430.6	6.7	P1004-27	469.0	5.4
1096-49	431.9	4.8			
1096-41	432.9	6.5			
1096-22	433.2	5.3			
1096-54	437.3	11.3	P1080-83	436.5	5.3
1096-23	439.0	5.7	P1080-31	438.4	5.3
1096-15	458.3	7.2	P1080-98	442.4	3.8
1096-61	463.5	3.8	P1080-35	442.9	9.3
1096-46	471.1	6.7	P1080-55	449.0	6.3
			P1080-70	454.4	4.3
MO- 71	433.1	7.5	P1080-99	455.5	8.5
MO-67	436.0	5.3	P1080-73	457.2	29.2
MO- 89	439.1	11.9	P1080-54	459.4	8.4
MO-24	450.2	6.4	P1080-22	460.7	31.7
MO-60	450.3	8.4			
MO-58	456.4	2.8	FMG-92	473.4	30.9
MO-1	480.2	4.1			
			DD-11	429.7	6.2
PE-75	430.0	5.6	DD-39	444.2	7.1
PE-48	431.9	3.7	DD-1	469.5	9.6

Pan-African (500-680 Ma)

Analysis	Best age	±	Analysis	Best age	±	Analysis	Best age	±	Analysis	Best age	±	Analysis	Best age	±	Analysis	Best age	±
	(Ma)	(Ma)		(Ma)	(Ma)		(Ma)	(Ma)		(Ma)	(Ma)		(Ma)	(Ma)		(Ma)	(Ma)
8304-46	501.7	9.4	8304-81	583.3	8.1	1096-72	536.0	4.0	P1004-79	557.3	15.0	8305-57	550.0	9.3	8305-41	637.9	5.8
8304-78	525.6	7.3	8304-13	586.2	13.1	1096-56	546.7	10.0	P1004-28	558.7	11.1	8305-83	550.2	8.2	8305-82	638.5	13.6
8304-88	526.2	24.8	8304-14	599.3	7.7	1096-59	569.6	5.6	P1004-4	575.2	8.2	8305-48	551.5	7.2	8305-46	638.9	9.4
8304-77	532.2	9.5	8304-17	603.6	11.8	1096-83	584.0	5.9	P1004-23	579.4	10.5	8305-3	553.7	11.8	8305-77	652.3	12.9
8304-37	544.6	5.7	8304-64	604.9	7.9	1096-76	589.3	9.3	P1004-54	589.6	7.1	8305-47	553.9	6.2	8305-11	654.1	4.6
8304-25	545.3	4.4	8304-75	605.2	6.4	1096-39	591.3	25.7	P1004-47	612.3	5.6	8305-91	554.7	6.5	8305-95	658.4	8.0
8304-62	548.0	8.8	8304-39	618.8	5.0	1096-48	603.6	10.6	P1004-88	618.8	6.1	8305-49	555.5	7.8	8305-13	662.5	13.2
8304-79	552.9	4.9	8304-58	624.2	9.2	1096-74	629.3	4.9	P1004-17	619.2	8.1	8305-63	557.2	11.0	8305-9	666.2	5.6
8304-36	553.0	4.4	8304-100	625.1	6.6	1096-89	636.9	4.3	P1004-42	621.1	5.2	8305-97	558.9	11.9	8305-22	678.1	7.2
8304-56	553.0	13.6	8304-80	625.5	8.4				P1004-64	621.7	12.2	8305-58	558.9	6.7			
8304-53	554.7	11.1	8304-65	633.7	12.0	P1080-41	542.1	14.6	P1004-36	638.4	8.7	8305-43	560.1	16.4	FMG-90	533.6	4.8
8304-57	554.8	6.1	8304-15	638.1	23.7	P1080-58	550.9	6.9	P1004-45	649.3	42.8	8305-8	560.6	7.8	FMG-78	542.6	16.6
8304-40	555.9	6.0	8304-76	640.6	10.3	P1080-97	557.9	6.5				8305-30	561.5	11.1	FMG-75	545.8	7.8
8304-6	556.1	23.3	8304-50	642.0	6.5	P1080-43	560.4	5.3	8305-18	526.2	4.9	8305-37	563.5	8.6	FMG-46	547.1	7.1
8304-28	556.3	17.7	8304-12	645.9	5.0	P1080-69	584.0	9.7	8305-7	531.1	11.7	8305-94	564.6	13.8	FMG-79	547.5	11.9
8304-26	556.9	5.0	8304-61	648.3	11.9	P1080-2	606.6	10.7	8305-39	535.8	3.4	8305-56	567.7	13.2	FMG-26	547.7	7.5
8304-93	560.3	11.5				P1080-59	616.1	7.8	8305-67	540.6	8.6	8305-61	571.8	7.3	FMG-64	551.1	6.4
8304-99	562.5	8.4				P1080-98	633.8	8.1	8305-26	540.9	6.6	8305-4	576.9	17.9	FMG-89	552.0	4.5
8304-41	563.7	6.9	MO-68	566.4	6.2	P1080-62	635.1	11.8	8305-50	542.1	12.7	8305-99	600.3	11.2	FMG-96	555.9	7.5
8304-86	567.2	6.8	MO-38	582.0	9.4	P1080-42	641.5	6.7	8305-15	542.4	4.6	8305-28	613.0	6.0	FMG-73	557.9	7.3
8304-18	568.7	14.4	MO-51	591.9	7.8	P1080-26	648.4	15.5	8305-69	547.3	5.7	8305-86	618.5	6.3	FMG-84	561.6	4.3
8304-82	570.3	9.0	MO-5	624.5	8.2				8305-90	548.1	5.1	8305-35	623.0	7.3	FMG-58	565.0	7.7
8304-66	570.8	11.6	MO-31	626.1	4.5	P1004-53	545.9	7.4	8305-98	549.6	11.1	8305-88	628.1	4.1	FMG-27	565.2	3.9
8304-47	575.4	9.7	MO-16	642.0	6.7	P1004-48	546.9	7.2	8305-89	549.9	4.6	8305-14	628.6	6.3	FMG-82	566.8	6.5

Pan-African (500-680 Ma)

Analysis	Best age	±	Analysis	Best age	±	Analysis	Best age	±	Analysis	Best age	±	Analysis	Best age	±	Analysis	Best age	±	Analysis	Best age	±
	(Ma)	(Ma)		(Ma)	(Ma)		(Ma)	(Ma)		(Ma)	(Ma)		(Ma)	(Ma)		(Ma)	(Ma)		(Ma)	(Ma)
FMG-57	567.1	5.6	FMG-40	619.2	10.3	PE-52	551.6	6.8	PE-34	652.9	2.5	DD-43	604.7	6.9	STPB-79	553.4	9.8	STPB-99	572.6	7.1
FMG-51	567.5	3.9	FMG-9	620.7	24.7	PE-77	553.1	8.3				DD-67	614.7	15.9	STPB-74	553.9	8.6	STPB-22	575.0	18.6
FMG-65	568.5	8.4	FMG-15	622.6	9.4	PE-51	553.9	14.7	DD-86	504.2	4.6	DD-8	615.8	4.0	STPB-65	554.5	3.0	STPB-64	575.2	18.0
FMG-70	569.4	8.5	FMG-39	623.5	28.2	PE-94	557.7	15.9	DD-73	522.3	50.0	DD-95	622.6	5.0	STPB-34	555.2	8.0	STPB-51	577.6	6.6
FMG-25	569.7	6.7	FMG-97	626.0	10.2	PE-50	561.8	5.6	DD-14	533.2	10.1	DD-62	630.6	14.2	STPB-35	556.8	4.8	STPB-7	578.7	16.7
FMG-36	569.9	6.1	FMG-99	627.4	5.6	PE-71	566.2	9.8	DD-33	536.0	14.5	DD-23	646.0	5.8	STPB-1	557.2	8.3	STPB-31	582.1	7.0
FMG-87	570.2	9.3	FMG-35	629.6	9.4	PE-56	567.2	7.4	DD-75	537.7	33.6	DD-22	649.1	10.3	STPB-91	557.2	13.9	STPB-29	582.1	7.4
FMG-28	570.3	5.5	FMG-16	630.6	9.4	PE-53	570.1	20.8	DD-3	539.1	5.4				STPB-55	557.3	7.0	STPB-90	583.4	9.2
FMG-6	571.4	10.2	FMG-61	633.0	9.1	PE-46	571.9	6.7	DD-74	541.3	11.1	STPB-60	516.0	4.3	STPB-89	557.4	6.8	STPB-23	597.9	44.2
FMG-42	571.8	8.2	FMG-85	633.3	9.4	PE-74	572.4	5.5	DD-79	543.8	6.1	STPB-88	529.2	5.8	STPB-62	557.6	3.1	STPB-71	599.7	9.7
FMG-21	572.9	6.4	FMG-33	637.9	4.7	PE-60	575.7	5.8	DD-46	544.2	4.4	STPB-18	532.4	4.4	STPB-86	558.8	11.4	STPB-43	603.0	8.1
FMG-37	573.7	14.0	FMG-29	644.8	6.4	PE-39	590.4	15.6	DD-69	548.1	7.2	STPB-57	534.6	5.0	STPB-47	559.1	19.8	STPB-12	615.3	4.1
FMG-12	576.1	18.8	FMG-24	656.3	38.1	PE-43	591.6	21.2	DD-34	559.5	10.0	STPB-11	536.0	39.1	STPB-78	560.2	8.3	STPB-59	616.7	9.4
FMG-14	578.5	9.8	FMG-50	657.9	4.6	PE-59	592.3	6.2	DD-70	562.8	13.3	STPB-61	536.6	12.0	STPB-10	561.3	10.9	STPB-50	619.7	13.7
FMG-76	578.6	9.9	FMG-19	666.1	16.5	PE-44	608.1	13.4	DD-50	563.7	11.2	STPB-69	536.8	11.0	STPB-85	561.7	8.5	STPB-93	624.7	11.8
FMG-93	581.3	9.1				PE-70	609.6	8.7	DD-76	572.6	9.6	STPB-72	538.6	9.0	STPB-27	561.8	5.8	STPB-75	627.2	11.6
FMG-67	583.1	9.2	PE-78	525.6	5.3	PE-84	620.1	8.9	DD-64	573.6	11.3	STPB-83	540.3	9.2	STPB-52	562.4	7.1	STPB-42	630.8	8.0
FMG-22	587.1	13.9	PE-91	531.2	6.6	PE-83	623.9	4.5	DD-56	581.8	7.6	STPB-49	544.6	5.4	STPB-62	563.1	4.1	STPB-14	638.0	4.6
FMG-11	595.2	5.3	PE-5	533.9	11.9	PE-8	624.0	15.9	DD-42	591.8	13.7	STPB-2	545.8	29.3	STPB-76	563.8	20.8	STPB-41	640.3	8.4
FMG-34	596.3	6.4	PE-9	543.3	19.3	PE-45	624.4	9.9	DD-37	592.2	10.4	STPB-5	546.6	7.4	STPB-21	564.1	9.8	STPB-9	643.1	6.5
FMG-69	596.4	9.7	PE-54	546.1	8.0	PE-21	625.6	5.3	DD-55	597.6	10.4	STPB-44	547.1	6.1	STPB-45	564.8	5.5	STPB-82	645.6	9.9
FMG-44	610.8	14.1	PE-23	549.0	10.7	PE-6	628.2	8.1	DD-66	598.4	8.7	STPB-39	549.6	9.5	STPB-68	566.8	12.2	STPB-37	645.6	8.6
FMG-86	617.5	9.3	PE-64	550.8	7.1	PE-25	628.3	12.6	DD-81	600.3	4.4	STPB-80	550.5	7.0	STPB-38	567.9	9.7	STPB-94	649.1	6.5
FMG-72	617.8	3.7	PE-81	551.1	8.4	PE-66	632.1	7.0	DD-96	604.3	3.9	STPB-67	552.3	24.2	STPB-100	569.4	21.6	STPB-87	650.8	12.0

Grenville (900-1300 Ma)

Analysis	Best age	±	Analysis	Best age	±	Analysis	Best age	±	Analysis	Best age	±	Analysis	Best age	±	Analysis	Best age	±
	(Ma)	(Ma)		(Ma)	(Ma)		(Ma)	(Ma)		(Ma)	(Ma)		(Ma)	(Ma)		(Ma)	(Ma)
1096-20	939.6	65.7	1096-31	1093.1	6.6	MO-57	1019.0	11.3	MO-54	1152.9	10.8	P1004-58	1033.7	45.8	P1004-40	1157.0	22.8
1096-37	962.0	62.9	1096-64	1121.0	22.2	MO-59	1020.8	62.7	MO-2	1154.4	4.2	P1004-96	1035.1	25.8	P1004-30	1164.9	13.3
1096-38	985.6	56.3	1096-95	1136.3	89.7	MO-29	1027.1	134.0	MO- 77	1163.6	4.3	P1004-70	1040.0	38.5	P1004-75	1169.1	66.7
1096-82	992.2	42.4	1096-35	1139.1	10.9	MO-37	1038.9	22.5	MO-6	1164.1	7.2	P1004-60	1045.3	28.2	P1004-95	1180.5	5.9
1096-86	1004.8	58.9	1096-77	1142.5	52.0	MO-10	1042.9	61.4	MO-22	1168.5	13.9	P1004-21	1054.1	22.0	P1004-34	1185.4	81.1
1096-63	1008.8	67.7	1096-42	1153.8	24.4	MO-19	1043.7	21.9	MO- 86	1179.3	21.3	P1004-80	1056.9	24.5	P1004-38	1189.4	27.1
1096-1	1010.0	15.6	1096-51	1155.5	7.2	MO-39	1045.8	25.1	MO-30	1189.7	22.3	P1004-92	1060.3	31.7	P1004-97	1224.9	56.4
1096-92	1010.8	49.2	1096-60	1157.5	131.5	MO- 82	1046.4	69.6	MO-14	1213.2	13.2	P1004-59	1063.0	45.4	P1004-62	1231.8	15.7
1096-97	1012.5	9.2	1096-32	1166.7	25.3	MO-20	1059.4	7.3	MO-56	1235.7	7.3	P1004-93	1063.3	18.8	P1004-50	1239.2	4.2
1096-88	1014.6	34.5	1096-57	1167.8	14.8	MO-49	1060.6	51.8	MO-35	1272.0	59.2	P1004-9	1065.2	37.6	P1004-12	1256.2	41.6
1096-13	1026.9	33.4	1096-36	1171.2	65.7	MO-27	1067.2	12.0	MO-23	1275.0	27.8	P1004-15	1067.2	9.9	P1004-35	1261.6	28.4
1096-50	1029.5	28.2	1096-45	1217.3	17.9	MO-21	1072.9	19.0				P1004-41	1069.7	17.5	P1004-77	1286.3	36.2
1096-8	1030.2	29.7	1096-98	1289.7	12.4	MO- 81	1077.6	12.1	P1004-52	925.3	55.1	P1004-61	1071.0	77.6	P1004-14	1294.9	21.2
1096-53	1030.6	63.0				MO-52	1096.3	58.2	P1004-67	934.7	24.1	P1004-49	1077.1	48.3	P1004-20	1296.3	52.5
1096-79	1039.2	23.6	MO-9	923.5	92.8	MO-64	1110.4	140.1	P1004-91	956.1	40.6	P1004-69	1081.0	14.5			
1096-3	1044.1	43.5	MO- 73	954.0	98.4	MO- 99	1115.5	24.5	P1004-56	968.6	97.6	P1004-100	1082.1	40.1	P1080-8	940.5	103.0
1096-19	1046.3	33.5	MO-3	961.8	37.9	MO- 75	1117.5	26.8	P1004-66	975.1	34.9	P1004-81	1092.1	16.3	P1080-37	986.6	46.1
1096-6	1052.5	14.5	MO- 74	966.8	40.8	MO-17	1117.7	22.1	P1004-73	989.1	16.2	P1004-85	1093.1	34.7	P1080-56	988.4	83.9
1096-87	1052.6	8.6	MO-13	971.7	25.6	MO- 95	1126.6	23.1	P1004-1	1013.7	17.3	P1004-16	1097.0	28.8	P1080-1	994.6	120.4
1096-78	1070.4	20.0	MO-41	978.7	12.4	MO-65	1127.1	27.7	P1004-98	1016.4	27.3	P1004-3	1105.0	24.2	P1080-68	998.7	14.4
1096-52	1074.7	21.6	MO-33	1011.0	10.2	MO-46	1129.3	22.7	P1004-43	1019.2	7.0	P1004-87	1110.2	10.4	P1080-91	1003.8	49.7
1096-71	1082.2	31.7	MO-34	1015.8	63.9	MO- 83	1132.6	13.8	P1004-22	1024.5	37.5	P1004-82	1115.4	21.5	P1080-25	1020.2	83.4
1096-55	1082.3	29.5	MO-43	1017.7	51.8	MO-26	1138.6	46.8	P1004-72	1026.5	14.8	P1004-63	1124.5	46.2	P1080-40	1027.3	38.2
1096-12	1086.7	4.5	MO-53	1019.0	32.2	MO- 98	1143.9	7.5	P1004-76	1032.4	25.2	P1004-11	1139.3	8.6	P1080-4	1028.7	12.0

Grenville (900-1300 Ma)

Analysis	Best age	±	Analysis	Best age	±	Analysis	Best age	±
	(Ma)	(Ma)		(Ma)	(Ma)		(Ma)	(Ma)
P1080-94	1038.2	68.4	PE-65	1011.2	22.8	DD-15	1046.2	3.6
P1080-46	1049.3	18.9	PE-22	1029.2	37.2	DD-7	1065.9	42.3
P1080-47	1065.0	26.2	PE-27	1031.3	31.0	DD-65	1082.5	15.5
P1080-10	1065.3	93.2	PE-87	1036.8	34.0	DD-91	1108.5	42.2
P1080-49	1066.5	28.1	PE-40	1047.0	61.3	DD-4	1167.5	59.9
P1080-60	1066.8	24.5	PE-85	1067.1	17.2	DD-36	1178.6	30.3
P1080-16	1071.8	48.2	PE-98	1142.7	34.1	DD-17	1179.1	8.5
P1080-34	1087.6	14.6	PE-2	1178.1	18.8	DD-38	1202.8	27.8
P1080-78	1090.4	149.2	PE-1	1186.0	48.7	DD-25	1204.5	17.5
P1080 prob 51	1139.9	23.3	PE-15	1196.8	36.5	DD-99	1226.6	20.2
P1080-21	1142.0	11.2	PE-100	1204.0	35.7	DD-31	1275.5	23.1
P1080-76	1152.0	18.4	PE-49	1214.3	20.2	DD-48	1283.4	72.1
P1080-36	1169.2	20.0	PE-69	1221.2	5.9			
P1080-63	1173.7	18.6	PE-62	1222.7	8.0			
P1080-77	1194.0	54.4	PE-3	1231.1	8.5			
P1080-92	1196.4	10.5	PE-80	1242.3	9.5			
P1080-74	1221.4	24.0	PE-76	1285.3	42.1			
P1080-82	1237.8	12.6						
P1080-95	1238.1	32.7	DD-78	1001.0	116.1			
P1080-3	1290.0	4.7	DD-20	1006.7	44.1			
			DD-44	1023.0	20.0			
PE-11	923.5	91.1	DD-59	1026.3	24.8			
PE-10	967.7	15.4	DD-5	1035.3	15.9			
PE-18	978.7	4.5	DD-47	1045.6	38.9			

Granite-Rhyolite (1300-1500 Ma)

Analysis	Best age (Ma)	± (Ma)	Analysis	Best age (Ma)	± (Ma)
1096-5	1310.5	46.2	P1080-48	1320.0	11.9
1096-18	1312.9	21.8	P1080-52	1327.8	34.4
1096-100	1326.3	11.4	P1080-14	1334.8	13.5
1096-67	1344.9	24.4	P1080-89	1387.8	17.2
1096-2	1382.3	15.1	P1080-32	1389.6	44.0
1096-21	1402.2	11.5	P1080-50	1454.0	10.4
1096-44	1466.5	13.0	P1080-27	1490.6	8.7
			DD-97	1306.0	70.8
			DD-82	1319.2	19.1
P1004-2	1308.0	47.4	DD-54	1419.0	10.2
P1004-31	1319.4	8.5	DD-24	1452.9	21.6
P1004-32	1329.3	27.3			
P1004-78	1363.4	154.4	MO-62	1302.5	13.2
P1004-5	1380.8	19.1	MO- 97	1304.9	19.4
P1004-37	1391.9	37.1	MO- 92	1322.3	13.7
P1004-24	1392.6	67.3	MO- 84	1323.9	35.2
P1004-71	1476.1	12.6	MO-28	1398.2	33.9
P1004-19	1488.4	19.6	MO-47	1458.9	7.4

Gondwanan (Sunsas/C. & S. Africa) 950-1500 Ma

Analysis	Best age (Ma)	± (Ma)	Analysis	Best age (Ma)	± (Ma)	Analysis	Best age (Ma)	± (Ma)
8304-72	982.1	18.6	8305-2	1198.9	30.4	STPB-56	1148.6	23.9
8304-97	983.4	14.1	8305-85	1208.0	20.4	STPB-28	1225.2	15.7
8304-3	987.1	10.0	8305-19	1218.1	37.7	STPB-95	1239.5	19.9
8304-10	1012.3	18.7	8305-92	1218.6	8.8	STPB-40	1243.2	18.7
8304-45	1029.7	17.9	8305-87	1222.9	25.7	STPB-66	1351.7	31.2
8304-43	1050.5	29.4	8305-23	1227.1	25.0	STPB-97	1358.5	7.6
8304-96	1071.9	7.0	8305-60	1231.8	18.5			
8304-85	1097.9	8.2	8305-65	1232.2	89.5			
8304-24	1137.1	14.8	8305-45	1246.9	41.0			
8304-30	1187.2	10.4	8305-81	1252.5	38.9			
8304-22	1341.6	12.0	8305-20	1256.9	17.1			
8304-83	1357.2	8.1	8305-55	1273.4	24.9			
8304-32	1392.5	34.8	8305-5	1277.0	74.5			
			8305-70	1326.2	31.7			
8305-100	978.9	41.5	8305-52	1329.0	40.0			
8305-78	980.9	22.3	8305-79	1408.5	24.4			
8305-12	1016.7	11.0						
8305-25	1035.0	37.5	FMG-32	1021.0	11.2			
8305-93	1035.2	12.7	FMG-2	1066.9	7.0			
8305-73	1045.1	26.0	FMG-98	1221.6	21.9			
8305-51	1102.0	24.5	FMG-80	1259.1	59.5			
8305-27	1131.3	33.1						
8305-80	1140.7	37.0	STPB-46	985.3	26.9			
8305-16	1154.7	38.7	STPB-36	1129.1	73.3			

Yavapai Mazatzal (1600-1800 Ma)

Analysis	Best age (Ma)	± (Ma)
1096-16	1619.7	8.8
MO- 85	1655.1	8.6
MO-40	1677.0	7.1
P1080-6	1625.9	24.0
P1080-87	1642.1	22.5
P1080-44	1679.1	16.9
DD-90	1623.4	6.6

Trans-Amazonian/Eburnean (1900-2250 Ma)

Analysis	Best age (Ma)	± (Ma)	Analysis	Best age (Ma)	± (Ma)	Analysis	Best age (Ma)	± (Ma)	Analysis	Best age (Ma)	± (Ma)
1096-80	2137.4	10.1	8305-59	2090.9	10.5	PE-89	1995.7	10.6	STPB-58	2030.9	23.3
			8305-6	2133.2	2.8	PE-28	2029.7	17.0	STPB-3	2051.9	16.0
8304-74	1919.4	27.7	8305-42	2156.0	5.8	PE-37	2033.8	6.2	STPB-70	2063.4	6.6
8304-68	1972.2	19.6				PE-99	2064.7	15.5	STPB-32	2103.0	5.9
8304-87	1987.4	9.3	FMG-20	2038.0	4.6	PE-41	2083.3	15.8	STPB-96	2106.8	4.6
8304-2	1990.9	6.9	FMG-66	2076.3	6.5	PE-72	2096.4	8.0	STPB-63	2120.3	4.6
8304-54	2023.3	5.7	FMG-71	2084.1	11.9	PE-7	2192.5	9.1	STPB-73	2199.5	39.1
8304-19	2065.9	15.0	FMG-91	2093.1	10.2	PE-92	2208.9	14.9	STPB-53	2219.7	7.0
8304-16	2067.5	12.7	FMG-31	2103.4	8.9						
8304-20	2092.4	5.5	FMG-74	2126.4	4.9	DD-94	2050.5	2.8			
8304-1	2096.5	3.3	FMG-47	2188.7	11.2	DD-61	2070.6	6.4			
8304-31	2115.3	9.7				DD-6	2093.6	2.2			
8304-8	2121.2	2.3	MO- 72	2090.8	7.8	DD-32	2099.2	8.8			
8304-98	2123.4	6.1				DD-80	2102.7	6.5			
8304-29	2160.0	1.4	P1004-84	1913.7	27.7	DD-12	2108.1	10.5			
8304-33	2189.1	3.8	P1004-86	1985.1	60.0	DD-63	2122.5	2.4			
8304-9	2211.1	5.9	P1004-83	2122.9	2.9	DD-77	2136.3	7.3			
8304-63	2218.5	2.4	P1004-7	2173.7	4.4	DD-53	2152.1	6.7			
8304-23	2327.5	7.0				DD-68	2195.0	32.8			
8304-42	2605.5	9.8				DD-16	2197.3	7.3			
			P1080-11	2064.2	24.4						
8305-84	1990.8	5.6	P1080-30	2126.0	2.9	STPB-58	1959.6	21.1			
8305-40	2052.1	8.4	P1080-75	2166.6	15.4	STPB-25	1973.4	29.8			
8305-24	2065.2	9.7	P1080-65	2167.0	6.5	STPB-81	2002.0	13.5			

African Archaen Terrane (2450-3040 Ma)

Analysis	Best age (Ma)	± (Ma)
8305-21	2447.1	7.5
8305-66	2799.8	3.7
P1004-26	2615.5	15.9
P1004-57	2673.2	19.5
P1080-53	2461.7	8.4
P1080-13	2481.5	6.2
PE-96	2766.6	3.7
DD-92	2641.3	1.6
DD-13	2704.3	10.4
STPB-74	2670.7	13.6
STPB-15	2771.1	4.8
FMG-41	2654.5	3.0
FMG-17	2735.1	3.9
FMG-62	2815.9	10.9

Appendix 4. U-Pb Ages with Unknown Source Terranes.

Analysis	Best age	±	Analysis	Best age	±	Analysis	Best age	±	Analysis	Best age	±	Analysis	Best age	±
	(Ma)	(Ma)		(Ma)	(Ma)		(Ma)	(Ma)		(Ma)	(Ma)		(Ma)	(Ma)
1096-17	330.9	6.9	8304-91	1890.9	5.0	MO- 79	367.3	7.1	P1080-24	2332.1	5.8	DD-45	767.1	5.4
1096-14	342.1	7.7	8304-51	1891.4	9.0	MO-69	368.8	3.2				DD-41	2443.6	2.4
1096-75	366.5	3.4				MO-11	370.8	5.2	PE-36	409.7	5.2	DD-35	3093.2	16.6
1096-47	482.7	7.9	8305-38	801.8	8.1	MO- 93	426.0	3.9	PE-14	412.1	3.6			
1096-11	485.3	3.1	8305-64	890.2	83.9	MO- 70	1803.5	26.1	PE-32	414.1	18.9	STPB-6	812.3	33.4
1096-40	487.0	8.2	8305-54	1502.1	9.2	MO-8	2711.2	19.8	PE-19	788.2	4.7	STPB-17	939.9	16.5
1096-73	697.4	10.6	8305-72	1507.6	21.9	MO-12	3401.0	6.7	PE-90	829.2	9.8	STPB-84	1795.9	26.8
1096-85	1541.8	15.1	8305-34	1522.6	11.2				PE-38	841.6	7.0			
1096-68	1801.8	12.5	8305-44	1697.4	40.2	P1004-6	334.9	3.8	PE-31	1546.8	4.5			
1096-69	1887.8	9.6	8305-77	1757.4	28.7	P1004-68	373.0	3.2	PE-33	1859.9	57.0			
			8305-53	1868.8	18.3	P1004-94	1511.6	21.3	PE-16	1881.3	4.1			
8304-84	456.4	18.1	8305-75	1885.7	6.0	P1004-39	1517.1	30.6	PE-13	1884.5	11.7			
8304-60	492.5	7.3	8305-17	2325.3	20.8	P1004-25	1534.5	24.1	PE-86	2358.3	13.6			
8304-94	499.2	10.6				P1004-29	1546.6	21.1	PE-35	1747.6	3.5			
8304-44	725.6	23.4	FMG-77	77.4	4.2				PE-67	1795.3	9.2			
8304-71	814.9	15.5	FMG-52	328.8	20.3	P1080-100	327.0	6.1						
8304-21	875.6	14.3	FMG-38	696.9	4.9	P1080-33	337.1	7.6	DD-28	360.6	8.4			
8304-69	1563.8	22.3	FMG-7	718.3	9.5	P1080-93	365.4	15.9	DD-88	370.4	11.2			
8304-5	1786.4	5.2	FMG-100	1752.4	11.9	P1080-17	427.0	5.7	DD-10	404.2	3.1			
8304-4	1805.4	38.5	FMG-88	1764.5	6.8	P1080-15	427.3	3.6	DD-83	415.9	5.0			
8304-90	1820.2	14.8	FMG-8	2300.9	18.2	P1080-18	483.4	3.3	DD-58	489.5	17.8			
8304-35	1863.5	12.5				P1080-72	686.9	18.8	DD-19	689.2	27.0			
8304-70	1870.5	9.8	MO- 78	344.0	8.4	P1080-88	1890.0	12.7	DD-52	696.9	16.4			